orano

# Safety Analysis Report

## for the

# DN30-X Package

### 0045-BSH-2020-001 Rev. 1

| Prepared | Checked | Released |
|---|---|---|
| S. Fels | Y. van Wijk | F. Hilbert |
| October 6, 2021 | October 7, 2021 | October 7, 2021 |

# Table of Contents

## List of Revisions

| Revision | Date of revision | Modifications |
|---|---|---|
| 0 | June 29, 2021 | Original |
| 1 | October 7, 2021 | • Amended the definition of the permissible content in section 1.3<br>• Amended the material specification for the interior criticality control system in section 1.4.1.1.3<br>• Reorganized the description of the 30B-X cylinder in section 1.4.2.1 and added section 1.4.2.1.4, covering additional provisions to ANSI N14.1<br>• Amended section 1.7.4.1 by also discussing potential impacts on the filling, emptying and washing operations of the 30B-X cylinder because of the presence of the interior criticality control system.<br>• Update of results of dose rate analysis in section 2.5 for permissible content weights of final cylinder designs |

## List of Abbreviations

APDL ........ **A**NSYS **P**arametric **D**esign **L**anguage
BPVC ........ **B**oiler and **P**ressure **V**essel **C**ode
CCR ........ **C**riticality **C**ontrol **R**od
CCS ........ **C**riticality **C**ontrol **S**ystem
CFL ........ **C**ourant-**F**riedrichs-**L**ewy
CSI ........ **C**riticality **S**afety **I**ndex
FEM ........ **F**inite **E**lement **M**ethods
HALEU ........ **H**igh-**A**ssay **L**ow-**E**nriched **U**ranium
IMS ........ **I**ntegrated **M**anagement **S**ystem
MAWP ........ **M**aximum **A**llowable **W**orking **P**ressure
MNOP ........ **M**aximum **N**ormal **O**perating **P**ressure
MTSP ........ **M**anufacturing and **T**est **S**equence **P**lan
ONCS ........ **O**rano **NCS** GmbH
PSP ........ **P**rotective **S**tructural **P**ackaging
QA ........ **Q**uality **A**ssurance
SAR ........ **S**afety **A**nalysis **R**eport
TI ........ **T**ransport **I**ndex

## List of Tables

## List of Figures

## Literature


[10 CFR Part 71] Code of Federal Regulations Title 10 Part 71 "Packaging and Transportation of Radioactive Material"

[49 CFR Part 173] Code of Federal Regulations Title 49 Part 173 "Shippers - General Requirements for Shipments and Packagings"

[ANSI N14.1] Uranium Hexafluoride – Packaging for Transport, ANSI N14.1, 2019

[ANSI N14.5] Radioactive Materials – Leakage Tests on Packages for Shipment, ANSI N14.5, 2014

[ANSYS] ANSYS®, Release 2021 R1, Help System, ANSYS, Inc

[ASME BPVC] ASME Boiler and Pressure Vessel Code, 2019 Edition

[ASTM A106] ASTM A106 / A106M-19a, Standard Specification for Seamless Carbon Steel Pipe for High-Temperature Service, ASTM International, West Conshohocken, PA, 2019, www.astm.org

[ASTM A333] ASTM A333 / A333M-18, Standard Specification for Seamless and Welded Steel Pipe for Low-Temperature Service and Other Applications with Required Notch Toughness, ASTM International, West Conshohocken, PA, 2018, www.astm.org

[ASTM A516] ASTM A516 / A516M-17, Standard Specification for Pressure Vessel Plates, Carbon Steel, for Moderate- and Lower-Temperature Service, ASTM International, West Conshohocken, PA, 2017, www.astm.org

[ASTM C787] ASTM C787-20, Standard Specification for Uranium Hexafluoride for Enrichment, ASTM International, West Conshohocken, PA, 2020, www.astm.org

[ASTM C996] ASTM C996-20, Standard Specification for Uranium Hexafluoride Enriched to Less Than 5 % $^{235}U$, ASTM International, West Conshohocken, PA, 2020, www.astm.org

[CoC 9362] Certificate of Compliance for Radioactive Material Packages, USA/9362/AF-96, Rev. 2, U.S. Nuclear Regulatory Commission, December 2019

[DeWitt 1960] DeWitt, R., Uranium Hexafluoride: A Survey of the Physico-Chemical Properties, Goodyear Atomic Corporation, Portsmouth, Ohio, GAT-280 Chemistry General, 1960

[DIN EN 10028-3] Flat products made of steels for pressure purposes - Part 3: Weldable fine grain steels, normalized, October 2017

[DIN EN 10088-1] Stainless steels - Part 1: List of stainless steels, December 2014

[DIN EN 10088-2] Stainless steels - Part 2: Technical delivery conditions for sheet/plate and strip of corrosion resisting steels for general purposes, December 2014

[DIN EN 10088-3] Stainless steels - Part 3: Technical delivery conditions for semi-finished products, bars, rods, wire, sections and bright products of corrosion resisting steels for general purposes, December 2014

[DIN EN 10216-3] Seamless steel tubes for pressure purposes - Technical delivery conditions - Part 3: Alloy fine grain steel tubes, March 2014

[DNT 2019] DAHER NUCLEAR TECHNOLOGIES, Safety Analysis Report DN30 Package, 0023-BSH-2016-002, Revision 1, Hanau, 2019

[FKM 2012] Rechnerischer Festigkeitsnachweis für Maschinenbauteile aus Stahl, Eisenguss- und Aluminiumwerkstoffen (Translation: Proof of strength by calculation for machine parts made of steel, cast iron and aluminum materials), FKM-Richtline (Guideline), VDAM Verlag, 2012

[ISO 12807] Safe transport of radioactive materials – Leakage testing on packages, ISO 12807, September 2018

[ISO 7195] ISO 7195, Nuclear Energy – Packagings for the transport of uranium hexafluoride ($UF_6$), Third edition, November 2020

[LS-Dyna 2018] LS-DYNA. Keyword User's Manual – Volume I, LS-DYNA R11, 2018

[LS-PrePost] LS-PrePost 4.8.11, http://www.lstc.com/lspp (22.02.2021)

[MILIN 2016] Milin M. et al, Hydration of uranium residues contained in enriched $UF_6$ cylinders, Proceedings PATRAM 2016, Kobe, September 2016

[NEA 2019] International Handbook of Evaluated Criticality Safety Benchmark Experiments, NEA, July 2019 Edition, NEA/NSC/DOC(95)03

[NUREG 2216] Standard Review Plan for Transportation Packages for Spent Fuel and Radioactive Material, U.S. NRC, Office of Nuclear Material Safety and Safeguards, NUREG-2216, August 2020

[SCALE 2011] SCALE 6.1, Comprehensive Modeling and Simulation Suite for Nuclear Safety Analysis and Design ORNL/TM-2005/39, Version 6.1, Oak Ridge National Laboratory, 2011

[SCALE 2020] SCALE 6.2.4, SCALE Code System, ORNL/TM-2005/39, Version 6.2.4, Oak Ridge National Laboratory, 2020

[SSG-26 2012] Advisory Material for the IAEA Regulations for the Safe Transport of Radioactive Material (2012 Edition), Specific Safety Guide No. SSG-26, IAEA, Vienna, 2014

[SSR-6 2018] Regulations for the Safe Transport of Radioactive Material, 2018 Edition, SSR-6 Rev. 1, IAEA, Vienna, 2018

[Swift 1952] Swift, H. W., Plastic instability under plane stress, Journal of Mechanics and Physics of Solids, Volume 1, Issue 1, October 1952

[USEC 651] The $UF_6$ Manual – Good Handling Practices for Uranium Hexafluoride, Rev. 9, USEC, 2006

# PART 1
# GENERAL INFORMATION

## 1.1 List and Status of Documents Pertaining to this SAR

The list of applicable documents and their status pertaining to this safety analysis report (SAR) is included in Appendix 1.1 (List of Applicable Documents).

## 1.2 Administrative Information

### 1.2.1 Name of Package

The package is designated **DN30-X** and consists of the DN30 protective structural packaging (PSP) and the 30B-X cylinder. The “X” in DN30-X and 30B-X is either replaced by “10” or by “20” to refer to a specific design for a maximal enrichment of 10 or 20 wt.-% $^{235}U$ in uranium, respectively.

Since both the 30B-10 and the 30B-20 cylinder are transported in the same DN30 PSP that has been designed in [DNT 2019] for the transport of standard 30B cylinders according to [ANSI N14.1], the following path is taken with respect to licensing of the DN30-X package:

- The designs of the 30B-10 and the 30B-20 cylinder shall be incorporated into a single package approval for the DN30-X package.
- The package approval for the DN30-X package shall incorporate the allowable contents for each cylinder as specified in section 1.3.
- Already existing DN30 PSPs that have been manufactured for the transport of standard 30B cylinders according to [ANSI N14.1] are allowed to be used for the transport of 30B-10 and 30B-20 cylinders as well.



### 1.2.2 Identification of Package Designer

The designer and license holder of the DN30-X package is:

Orano NCS GmbH
Margarete-von-Wrangell-Straße 7
D-63457 Hanau
Germany

The principal contact is:

| | |
|---|---|
| Name: | Mr. Franz Hilbert |
| Tel: | +49 6181 501-232 |
| Fax: | +49 6181 501-266 |
| E-mail: | franz.hilbert@orano-ncs.com |

In this report, Orano NCS GmbH is designated “ONCS”.

### 1.2.3 Type of Package Design

The DN30-X package, loaded with the allowable content as described in section 1.3, fulfils the requirements of [10 CFR Part 71] and [49 CFR Part 173], as well as [SSR-6 2018] for a

**Type AF package for uranium hexafluoride ($UF_6$)**

containing $UF_6$ grade HALEU in less than or equal to $A_2$ quantities:

- For the DN30-10, the maximal allowed enrichment is 10 wt.-% $^{235}U$ in uranium.
- For the DN30-20, the maximal allowed enrichment is 20 wt.-% $^{235}U$ in uranium.

### 1.2.4 Criticality Safety Index

For the DN30-X package, the criticality safety index (CSI) is:

$$\mathrm{CSI} = 0$$

### 1.2.5 Package Design Identification and Restrictions

A unique serial number is assigned to each DN30 PSP valid for its entire operation time. This number is stamped on the nameplate that is used for the already licensed DN30 package under the entry “Serial No.” (see [DNT 2019] and Appendix 1.4.1B (Drawings DN30 PSP), drawing 0023-ZFZ-1000-001).

The serial number has the following pattern:

XX-YYYY-ZZZZ

Where:

| | | |
|---|---|---|
| XX | = | designation of the fabricator (abbreviation assigned by ONCS) |
| YYYY | = | year of manufacturing |
| ZZZZ | = | sequential number |

The list of all serial numbers is managed and filed by ONCS. All users of the DN30-X packaging will be requested to update the status of the individual packaging after completion of the regular periodical inspections. Packagings with overdue periodical inspections (more than 1-year overdue) will be marked in that list as “not in use”.

Each individual DN30 PSP may be marked with an owner serial number different from the manufacturer serial number. This owner serial number may be marked on the nameplate under the entry “Owner’s Serial No.” or on an additional nameplate attached to the DN30 PSP. The owner serial number may change whenever required by the owner.

### 1.2.6 Modes of Transport for which the Package is Designed

- The DN30-X package is designed for transport by road, rail, sea, and inland waterways.
- Transport by air is not permitted.
- Hump shunting of wagons transporting the DN30-X packages is not allowed.

### 1.2.7 Lowest Transport Temperature for which the Package is Designed

The lowest transport temperature allowed for the DN30-X package is -40 °C.

### 1.2.8 Maximum Normal Operating Pressure

The maximum normal operating pressure (MNOP) for the DN30-X package is defined as the pressure at the triple point of $UF_6$ (see table 1-1):

$$\mathrm{MNOP} = 152\,\mathrm{kPa}$$

*Note: the maximum allowable working pressure (MAWP) of the 30B-X cylinder is specified in accordance with [ANSI N14.1] as 1.38 MPa. This definition of the MAWP only applies to the use of the 30B-X cylinder in the enrichment and fuel fabrication process and not for its use as part of the DN30-X package.*

### 1.2.9 Allowable Leakage Rate

With reference to [ANSI N14.1], the allowable leakage rate of the 30B-X cylinder is specified as:

$$L_\mathrm{N} = 1 \cdot 10^{-4}\,\mathrm{Pa} \cdot \mathrm{m}^3/\mathrm{s}$$

### 1.2.10 Reference to Applicable Regulations and Standards

The safety proof of the DN30-X package is based on the following regulations and standards:

- [10 CFR Part 71] Code of Federal Regulations Title 10 Part 71, “Packaging and Transportation of Radioactive Material”
- [49 CFR Part 173] Code of Federal Regulations Title 49 Part 173, “Shippers - General Requirements for Shipments and Packagings”
- [ANSI N14.1] American National Standard, “For Nuclear Materials – Uranium Hexafluoride – Packagings for Transport”, ANSI N14, 2019-12-05
- [ISO 7195] Nuclear Energy – Packagings for the transport of uranium hexafluoride ($UF_6$), Third edition, November 2020
- [SSR-6 2018] “Regulations for the Safe Transport of Radioactive Material”, 2018 Edition, SSR-6, Rev. 1, International Atomic Energy Agency (IAEA), Vienna, 2018

In the remainder of this SAR, reference is only made to [ANSI N14.1]. However, unless stated otherwise, references to [ANSI N14.1] always include [ISO 7195] as well.

## 1.3 Specification of the Radioactive Contents

The allowable content of the DN30-X packaging is uranium in the chemical composition $UF_6$ with maximal enrichments of 10 and 20 wt.-% $^{235}U$ in uranium. In the context of this SAR, the allowable content is designated:

- HALEU 10 for an enrichment of 10 wt.-% $^{235}U$ in uranium
- HALEU 20 for an enrichment of 20 wt.-% $^{235}U$ in uranium

A general specification of HALEU 10 and HALEU 20 defining the impurity and uranium isotope limits is provided in section 1.3.1. Based on this general specification, the permissible contents for the DN30-10 and DN30-20 package are specified in section 1.3.2.

### 1.3.1 General Specification of $UF_6$ grade HALEU 10 and HALEU 20

This general specification of $UF_6$ grade HALEU 10 and HALEU 20 covers nuclear grade $UF_6$ that has been processed through an enrichment plant and that is intended for fuel fabrication. It corresponds to a large extent to [ASTM C996] and the objective of this specification is to define the impurity and uranium isotope limits for HALEU 10 and HALEU 20 that can be transported in the DN30-10 and DN30-20 package, respectively.

#### 1.3.1.1 Terminology

In the following specification of the permissible contents of the DN30-X package, the definitions of terms defined in [ASTM C996], section 3 are used.

#### 1.3.1.2 Origin of Material

HALEU 10 and HALEU 20 shall be enriched from Commercial Natural $UF_6$. Neither Reprocessed nor Derived Enriched $UF_6$ shall be used for HALEU 10 and HALEU 20.

#### 1.3.1.3 Safety, Health Physics and Criticality Requirements

The safety, health and criticality requirements for HALEU 10 and HALEU 20 are identical to the requirements provided in [ASTM C996], section 4 for Enriched Commercial Grade $UF_6$ with a maximal enrichment of 5 wt.-% $^{235}U$ in uranium:

(1) The $UF_6$ concentration shall not be less than 99.5 g $UF_6$ per 100 g of sample in order to limit the potential hydrogen content for nuclear criticality safety.

(2) The total absolute vapor pressure shall not exceed the following values:

- 380 kPa at 80 °C (55 psia at 176 °F), or
- 517 kPa at 93 °C (75 psia at 200 °F), or
- 862 kPa at 112 °C (125 psia at 235 °F)

Additionally, if a measurement is taken over solid $UF_6$, the vapor pressure shall not exceed the following values:

- 50 kPa at 20 °C (7 psia at 68 °F), or
- 69 kPa at 35 °C (10 psia at 95 °F)

The purpose of the pressure check is to limit the hydrogen fluoride, air, or other volatile components that might cause overpressure when heating the 30B-10 or 30B-20 cylinder (see [ASTM C996], section 4.2 for further details).

(3) The total hydrocarbon, chlorocarbon, and partially substituted halohydrocarbon content shall not exceed 0.01 mol % of the $UF_6$. The reason for the exclusion of these materials is to prevent a vigorous reaction with $UF_6$ upon heating (see [ASTM C996], section 4.3 for further details).

(4) For HALEU 10 and HALEU 20 meeting the requirements of section 1.3.1.4, the gamma activity from fission products and the alpha activity from neptunium and plutonium are expected to be below the detection limits (see [ASTM C996], section 4.4 for further details).

#### 1.3.1.4 Chemical, Physical and Isotopic Requirements

Table 1-1 shows the most relevant properties of $UF_6$ extracted from [USEC 651].

**Table 1-1 $UF_6$ properties**

| Property | Metric | | Imperial | |
|---|---|---|---|---|
| | Value | Unit | Value | Unit |
| Density solid at 20 °C (68 °F) | 5.09 | g/cm³ | 317.8 | lb/ft³ |
| Density liquid at 64.1 °C (147.3 °F) | 3.65 | g/cm³ | 227.7 | lb/ft³ |
| Density liquid at 121 °C (250 °F) | 3.26 | g/cm³ | 203.3 | lb/ft³ |
| Sublimation point at 101 kPa (14.7 psia) | 56.6 | °C | 133.8 | °F |
| Triple point at 152 kPa (22 psia) | 64.1 | °C | 147.3 | °F |
| Heat of sublimation at 64.1 °C (147.3 °F) | 135 | kJ/kg | 58.2 | BTU/lb |
| Heat of fusion at 64.1 °C (147.3 °F) | 56 | kJ/kg | 23.5 | BTU/lb |
| Heat of vaporization at 64.1 °C (147.3 °F) | 81 | kJ/kg | 35.1 | BTU/lb |
| Critical pressure | 4610 | kPa | 668.8 | psia |
| Critical temperature | 230.2 | °C | 446.4 | °F |
| Specific heat, solid at 27 °C (81 °F) | 477 | J/(kg K) | 0.114 | BTU/(lb °F) |
| Specific heat, liquid at 72 °C (162 °F) | 544 | J/(kg K) | 0.130 | BTU/(lb °F) |

The chemical, physical and isotopic requirements for HALEU 10 and HALEU 20 are based on [ASTM C996], section 5.

(1) Both HALEU 10 and HALEU 20 must meet the specification criteria. Except for the isotopes given in table 1-2, but including artificially created radioactive species, limits are set so as to have no special impact on the use of this material in existing facilities (see [ASTM C996], section 5.1 for further details).

(2) The following impurities shall not exceed these values:

Boron: 4 µg/gU

Silicon: 250 µg/gU

(3) HALEU 10 and HALEU 20 shall comply with the limits given in table 1-2. For purposes of determining conformance with these limits, the observed values shall be rounded to the nearest significant digit indicated as described in [ASTM C996], section 5.5.

**Table 1-2 Isotopic limits of $UF_6$ grade HALEU 10 and HALEU 20**

| Nuclide | Maximal concentration in wt.-% in uranium | | |
|---|---|---|---|
| | Enriched Commercial Grade[1)] | HALEU 10 | HALEU 20 |
| $^{232}U$ | $1 \cdot 10^{-8}$ | $3 \cdot 10^{-8}$ | $7 \cdot 10^{-8}$ |
| $^{234}U$ | $5.5 \cdot 10^{-2}$ | $1.2 \cdot 10^{-1}$ | $2.6 \cdot 10^{-1}$ |
| $^{235}U$ | 5 | 10 | 20 |
| $^{236}U$ | $2.5 \cdot 10^{-2}$ | $5.0 \cdot 10^{-2}$ | $1.0 \cdot 10^{-1}$ |
| $^{238}U$ | rest | rest | rest |
| $^{99}Tc$ | $1.0 \cdot 10^{-6}$ | $1.0 \cdot 10^{-6}$ | $1.0 \cdot 10^{-6}$ |

1) According to [ASTM C996], provided for information purposes only.

(4) Heels of HALEU 10 and HALEU 20 shall also comply with the limits given in table 1-2. Additionally, the activity limits given in table 1-3 apply for heels of HALEU 10 and HALEU 20.

**Table 1-3 Activity limits for heels of $UF_6$ grade HALEU 10 and HALEU 20**

| Nuclide | Maximal activity in Bq | |
|---|---|---|
| | HALEU 10 | HALEU 20 |
| $^{99}Tc$[1)] | $7.6 \cdot 10^{7}$ | $6.0 \cdot 10^{7}$ |

1) Calculated based on the maximal $A_2$ value for $^{99}Tc$ after a 5-year refilling cycle and 10 years of storage of a filled cylinder (see table 1-8).

## 1.3.2 Permissible Contents for the DN30-X Package

### 1.3.2.1 Permissible Mass of $UF_6$

The permissible mass of $UF_6$ and the maximum heel quantities for each package design are listed in table 1-4.

**Table 1-4 Permissible mass of $UF_6$ for each package design**

| Package design | Enrichment limit in wt.-% $^{235}U$ in U | Permissible mass of $UF_6$ in kg | Maximum heel quantities in kg |
|---|---|---|---|
| DN30-10 | 10 | 1460 | 11.3 |
| DN30-20 | 20 | 1271 | 11.3 |

*Note: Today's cleaning processes for standard 30B cylinders achieve heel quantities below 2 kg on a regular basis, which leaves sufficient margins for the increased free surfaces of the 30B-10 and 30B-20 cylinder in comparison to the standard 30B cylinder. Calculating the ratios of the internal free surfaces of the 30B-X and the 30B cylinder given in table 1-13, heel quantities below $2\ kg \cdot 20.01\ m^2/4.75\ m^2 = 8.5\ kg$ and $2\ kg \cdot 22.89\ m^2/4.75\ m^2 = 9.7\ kg$ are expected for the 30B-10 and the 30B-20 cylinder, respectively. This allows for defining the same maximum heel quantities for the 30B-10 and 30B-20 cylinder as defined in [ANSI N14.1] for the standard 30B cylinder.*

#### 1.3.2.2 Non-Fissile and Fissile Material

The uranium is classified as fissile material enriched from original uranium with natural isotopic composition. The maximal enrichment in $^{235}U$ for each package design is listed in table 1-4.

#### 1.3.2.3 Mass of Fissile Material and Nuclides

The mass of the fissile material for each package design is calculated from the permissible mass of $UF_6$ that is given in table 1-4 and the corresponding maximum enrichment in $^{235}U$ according to the following equation:

$$m_{\text{fiss,X}} = m_{\text{UF}_6\text{,X}} \cdot r_{\text{enrich,X}} \cdot \frac{M_{^{235}\text{U}}}{\left(r_{\text{enrich,X}} \cdot M_{^{235}\text{U}} + \left(1 - r_{\text{enrich,X}}\right) \cdot M_{^{238}\text{U}} + 6 \cdot M_{\text{F}}\right)} \quad (1)$$

In equation (1), $M_{^{235}\text{U}}$, $M_{^{238}\text{U}}$, and $M_{\text{F}}$ are the atomic masses of $^{235}U$, $^{238}U$, and fluorine, respectively. The fissile masses calculated with equation (1) are listed in table 1-5.

**Table 1-5 Mass of fissile material for each DN30-X package design**

| Package design | Enrichment limit in wt.-% $^{235}U$ in U | Mass of $UF_6$ in kg | Fissile material in kg |
|---|---|---|---|
| DN30-10 | 10 | 1460 | 98 |
| DN30-20 | 20 | 1271 | 170 |

#### 1.3.2.4 Special Form or Low Dispersible Radioactive Material

The radioactive content in the DN30-X package is neither in special form nor low dispersible.

#### 1.3.2.5 Total Radioactivity

The radioactive contents have a total radioactivity of less than or equal to 1 $A_2$. For filled cylinders, this is due to the unlimited $A_2$ value of enriched uranium with natural isotopic composition U(enriched to 20 % or less) according to [10 CFR Part 71] Appendix A. Furthermore, the analysis in section 1.3.2.11 shows that the DN30-X also complies with this limit when the 30B-X cylinders are regularly refilled without intermediate washing before loading.

#### 1.3.2.6 Nature and Characteristics of the Radiation Emitted

The radiation emitted by the content of the DN30-X package is mainly gamma radiation with a very small contribution from neutron radiation.

#### 1.3.2.7 Limitation of the Heat Generation Rate of the Content

The heat generation rate for an enrichment limit of 5 wt.-% $^{235}U$ in uranium was determined in [DNT 2019] and is based on a $UF_6$ net weight of $m_{\text{UF}_6\text{,5}} = 2277\ \text{kg}$. Using the isotopic composition given in table 1-2 and the permissible mass of $UF_6$ $m_{\text{UF}_6\text{,X}}$ for the DN30-X as listed in table 1-4,

the heat generation rates for maximum enrichments of "$X$" wt.-% $^{235}$U in uranium are calculated according to equation (2):

$$H_{\mathrm{Gen,X}} = \frac{w_{\%,\mathrm{X}}}{w_{\%,5}} \cdot \frac{m_{\mathrm{UF_6,X}}}{m_{\mathrm{UF_6,5}}} \cdot H_{\mathrm{Gen,5}} \tag{2}$$

In equation (2), $w_{\%,\mathrm{X}}$ refers to the content limit of each uranium isotope for an enrichment of "$X$" wt.-% $^{235}$U in uranium. The corresponding content limit for an enrichment of 5 wt.-% is used as the reference. Table 1-6 shows the resulting heat generation rate of $UF_6$ for maximum enrichments of 5, 10, and 20 wt.-% $^{235}$U in uranium.

For each enrichment limit, the most significant contribution is from $^{234}$U and the contribution to the thermal power from the traces of fission products and other actinides is negligible. For the thermal analysis in section 2.3, a heat generation rate of 3 W is assumed, safely covering the actual heat generation rate of the content of the DN30-X even though higher enrichments up to 20 wt.-% $^{235}$U in uranium are permissible.

**Table 1-6 Heat generation rate of $UF_6$**

| Nuclide | Heat generation rate in W | | |
|---|---|---|---|
| | 5 wt.-% $^{235}$U in U[1)] | 10 wt.-% $^{235}$U in U[1)] | 20 wt.-% $^{235}$U in U[1)] |
| $^{232}$U | $1.0 \cdot 10^{-4}$ | $1.92 \cdot 10^{-4}$ | $3.91 \cdot 10^{-4}$ |
| $^{234}$U | $1.52 \cdot 10^{-1}$ | $2.13 \cdot 10^{-1}$ | $4.01 \cdot 10^{-1}$ |
| $^{235}$U | $4.56 \cdot 10^{-3}$ | $5.85 \cdot 10^{-3}$ | $1.02 \cdot 10^{-2}$ |
| $^{236}$U | $6.73 \cdot 10^{-4}$ | $8.63 \cdot 10^{-4}$ | $1.50 \cdot 10^{-3}$ |
| $^{238}$U | $1.24 \cdot 10^{-2}$ | $7.52 \cdot 10^{-3}$ | $5.81 \cdot 10^{-3}$ |
| Total | $1.70 \cdot 10^{-1}$ | $2.27 \cdot 10^{-1}$ | $4.19 \cdot 10^{-1}$ |

1) The underlying isotopic limits are given in table 1-2.

#### 1.3.2.8 Physical and Chemical State

During transport, the $UF_6$ contained in the DN30-X package is in solid form. $UF_6$ reacts with most metals (nickel, Monel, copper, and aluminum) to create a fluoride of the metal and other uranium compounds. It heavily reacts with hydrocarbons so that the absence of hydrocarbons in empty 30B-X cylinders is essential before those are filled with $UF_6$.

$UF_6$ does not react with nitrogen, oxygen, carbon dioxide or dry air. However, $UF_6$ reacts strongly with water and water vapor in the air producing HF-$H_2O$ fog. If inhaled, this fog is very harmful.

$$\mathrm{UF_6 + 2H_2O \rightarrow UO_2F_2 + 4HF}$$

The $UF_6$ could contain some impurities that are due to chemical reactions. These impurities, like HF or $UO_2F_2 \cdot 5.5\,H_2O$, are also considered in the criticality safety analysis (see section 2.6).

#### 1.3.2.9 Other Dangerous Properties

In accordance with 49 CFR Subpart F - Placarding, § 172.505 (b), $UF_6$ is classified as corrosive and poisonous. Consequently, the CORROSIVE and POISON placard must be used alongside the RADIOACTIVE placard (see figure 1-1).

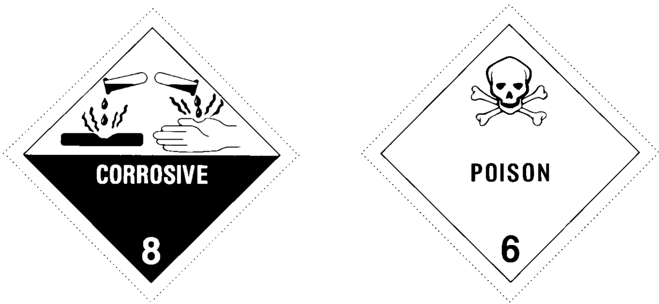


**Figure 1-1 CORROSIVE and POISON placard**

#### 1.3.2.10 Permissible Conditions for Repeated Use

30B-X cylinders complying with their specification in section 1.4.1.1 and within their valid recertification period as specified in section 1.8 may be refilled with content complying with the definitions in section 1.3.1 and 1.3.2. It is shown in section 1.3.2.11 that the DN30-X complies with the limit of 1 $A_2$ for a Type AF package when the 30B-X cylinders are regularly refilled without intermediate washing before loading.

#### 1.3.2.11 Refilling of Cylinders Containing Heel Quantities

After emptying of 30B-X cylinders, heel quantities of $UF_6$ might remain in the cylinder. In table 1-4, the heel quantities of $UF_6$ are specified as maximal 11.3 kg for the 30B-10 and the 30B-20 cylinder. With reference to [ANSI N14.1], a heel is defined as:

| |
|---|
| A heel is a residual amount of $UF_6$ and/or nonvolatile reaction products of uranium |

According to [10 CFR Part 71] Appendix A or [SSR-6 2018] Table 2, the $A_2$ values of natural uranium U(nat), enriched uranium with natural isotopic composition U(enriched to 20 % or less), and depleted uranium U(dep) are unlimited. Hence, all amounts of contents ranging from 0 kg up to the fill limits of the 30B-10 and 30B-20 cylinder specified in table 1-4 that comply with the content specifications in section 1.3 can be transported in the DN30-X package. However, subsequent refilling of 30B-X cylinders without washing before loading may lead to a build-up of decay products that contribute to the radioactivity relevant for the $A_2$ value. This is investigated in the following.

Table 1-7 illustrates the calculation procedure, which is identical to the safety analysis of the DN30 package in [DNT 2019], where a standard 30B cylinder containing Enriched Commercial Grade $UF_6$ specified in [ASTM C996] was investigated. For the investigation of the impact of subsequent refilling of 30B-X cylinders without washing, the covering content masses as listed in table 1-7 are assumed for the 30B-10 and 30B-20 cylinder.

**Table 1-7 Calculation scenario of the radioactivity in 30B-X cylinders for contents complying with HALEU 10 and HALEU 20 for a continuous use without washing**

| Cycle | Time | Cylinder condition | Content mass in kg | |
|---|---|---|---|---|
| | | | 30B-10 | 30B-20 |
| Initial | $0$ | New or empty and washed | 0 | 0 |
| 1 | $t_1$ | Filled and transported to destination | 1460 | 1271 |
| 1 | $t_2$ | Emptied and returned to enrichment facility | 11.3 | 11.3 |
| 2 | $t_3$ | Filled and transported to destination | 1460 | 1271 |
| 2 | $t_4$ | Emptied and returned to enrichment facility | 11.3 | 11.3 |
| 3 | $t_5$ | Filled and transported to destination | 1460 | 1271 |
| 3 | $t_6$ | Emptied and returned to enrichment facility | 11.3 | 11.3 |
| ... | ... | … | … | … |
| $n/2$ | $t_{n-1}$ | Filled and transported to destination | 1460 | 1271 |
| $(n/2)$ | $(t_n)$ | (Emptied and returned to enrichment facility) | (11.3) | (11.3) |
| Final | $t_{n+1}$ | After 5 years refilling is not permissible.[1)] | 11.3 or 1460 | 11.3 or 1271 |

1) Before next use, the cylinder has to be washed and recertified. Transportation of filled or heeled cylinders to the destination is still possible.

First, a new (or emptied and washed) 30B-X cylinder is filled with content as specified in section 1.3. Then, several cycles follow in which the filled cylinder is transported to the destination, emptied, and transported back to the enrichment facility containing the maximum heel quantities of $UF_6$ (see table 1-4). During these cycles, decay products build up that contribute to the radioactivity relevant for the $A_2$ value.

After 5 years, the 30B-X cylinder has to be recertified (see section 1.8), which requires the cylinder to be emptied and washed. However, it is still possible to store a filled or heeled cylinder for a certain time. A final transport to the destination for emptying and/or washing, and recertification is permitted. As in the safety analysis of the DN30 package in [DNT 2019], a storage time of 10 years is considered for the 30B-X cylinder, in which the peak radioactivity of $^{232}U$ and its decay products is reached. For the DN30-X package, only the penalizing 3-month filled/heeled cycle determined in [DNT 2019] is investigated.

Table 1-8 lists the radioactivity of the contributing nuclides for the 3-month cycle in a 30B-10 and 30B-20 cylinder, including a 10-year storage time in filled condition after the 5-year cycle time. A graphical representation of table 1-8 is shown in figure 1-2. This figure also shows the radioactivity of heeled cylinders being stored for 10 years after the 5-year cycle time and a comparison to the standard 30B cylinder loaded with Enriched Commercial Grade $UF_6$ as specified in [ASTM C996].

The results show that the DN30-X complies with the limit of 1 $A_2$ for a Type AF package when the 30B-X cylinders are regularly refilled with the contents specified in table 1-2 and without intermediate washing before loading. Even after a 10-year storage of filled cylinders, a maximal radioactivity of 0.3 $A_2$ and 0.56 $A_2$ is present in the 30B-10 and 30B-20 cylinder, respectively.

**Table 1-8 Radioactivity in 30B-10 and 30B-20 cylinders for a 3-month filled/heeled cycle followed by a 10-year storage of filled cylinders**

| Cycle | Cylinder condition | Radioactivity in $A_2$ | | | | | |
|---|---|---|---|---|---|---|---|
| | | $^{228}$Th | $^{230}$Th | $^{231}$Pa | $^{234}$Th | $^{99}$Tc | Total |
| | | | 30B-10 cylinder | | | | |
| 1 | Filled | $2.09 \cdot 10^{-2}$ | $6.27 \cdot 10^{-4}$ | $1.08 \cdot 10^{-4}$ | $3.80 \cdot 10^{-2}$ | $6.94 \cdot 10^{-6}$ | 0.0597 |
| 1 | Heeled | $1.93 \cdot 10^{-2}$ | $6.32 \cdot 10^{-4}$ | $1.09 \cdot 10^{-4}$ | $3.05 \cdot 10^{-3}$ | $7.00 \cdot 10^{-6}$ | 0.0231 |
| 2 | Filled | $3.85 \cdot 10^{-2}$ | $1.26 \cdot 10^{-3}$ | $2.17 \cdot 10^{-4}$ | $3.82 \cdot 10^{-2}$ | $1.39 \cdot 10^{-5}$ | 0.0782 |
| 2 | Heeled | $3.54 \cdot 10^{-2}$ | $1.26 \cdot 10^{-3}$ | $2.18 \cdot 10^{-4}$ | $3.06 \cdot 10^{-3}$ | $1.40 \cdot 10^{-5}$ | 0.0399 |
| … | … | … | … | … | … | … | … |
| 10 | Filled | $1.06 \cdot 10^{-1}$ | $6.31 \cdot 10^{-3}$ | $1.09 \cdot 10^{-3}$ | $3.82 \cdot 10^{-2}$ | $6.99 \cdot 10^{-5}$ | 0.152 |
| 10 | Heeled | $9.74 \cdot 10^{-2}$ | $6.32 \cdot 10^{-3}$ | $1.09 \cdot 10^{-3}$ | $3.06 \cdot 10^{-3}$ | $7.00 \cdot 10^{-5}$ | 0.108 |
| Final[1)] | Filled | $2.20 \cdot 10^{-1}$ | $3.39 \cdot 10^{-2}$ | $5.75 \cdot 10^{-3}$ | $4.09 \cdot 10^{-2}$ | $7.69 \cdot 10^{-5}$ | 0.30 |
| | | | 30B-20 cylinder | | | | |
| 1 | Filled | $4.25 \cdot 10^{-2}$ | $1.18 \cdot 10^{-3}$ | $1.88 \cdot 10^{-4}$ | $3.31 \cdot 10^{-2}$ | $6.04 \cdot 10^{-6}$ | 0.077 |
| 1 | Heeled | $3.92 \cdot 10^{-2}$ | $1.19 \cdot 10^{-3}$ | $1.90 \cdot 10^{-4}$ | $2.69 \cdot 10^{-3}$ | $6.10 \cdot 10^{-6}$ | 0.0433 |
| 2 | Filled | $7.83 \cdot 10^{-2}$ | $2.37 \cdot 10^{-3}$ | $3.78 \cdot 10^{-4}$ | $3.33 \cdot 10^{-2}$ | $1.21 \cdot 10^{-5}$ | 0.1144 |
| 2 | Heeled | $7.19 \cdot 10^{-2}$ | $2.39 \cdot 10^{-3}$ | $3.79 \cdot 10^{-4}$ | $2.70 \cdot 10^{-3}$ | $1.22 \cdot 10^{-5}$ | 0.0774 |
| … | … | … | … | … | … | … | … |
| 10 | Filled | $2.16 \cdot 10^{-1}$ | $1.19 \cdot 10^{-2}$ | $1.89 \cdot 10^{-3}$ | $3.33 \cdot 10^{-2}$ | $6.09 \cdot 10^{-5}$ | 0.264 |
| 10 | Heeled | $1.98 \cdot 10^{-1}$ | $1.19 \cdot 10^{-2}$ | $1.90 \cdot 10^{-3}$ | $2.70 \cdot 10^{-3}$ | $6.10 \cdot 10^{-5}$ | 0.215 |
| Final[1)] | Filled | $4.47 \cdot 10^{-1}$ | $6.39 \cdot 10^{-2}$ | $1.00 \cdot 10^{-2}$ | $3.56 \cdot 10^{-2}$ | $6.70 \cdot 10^{-5}$ | 0.56 |

1) After 10 years of storage

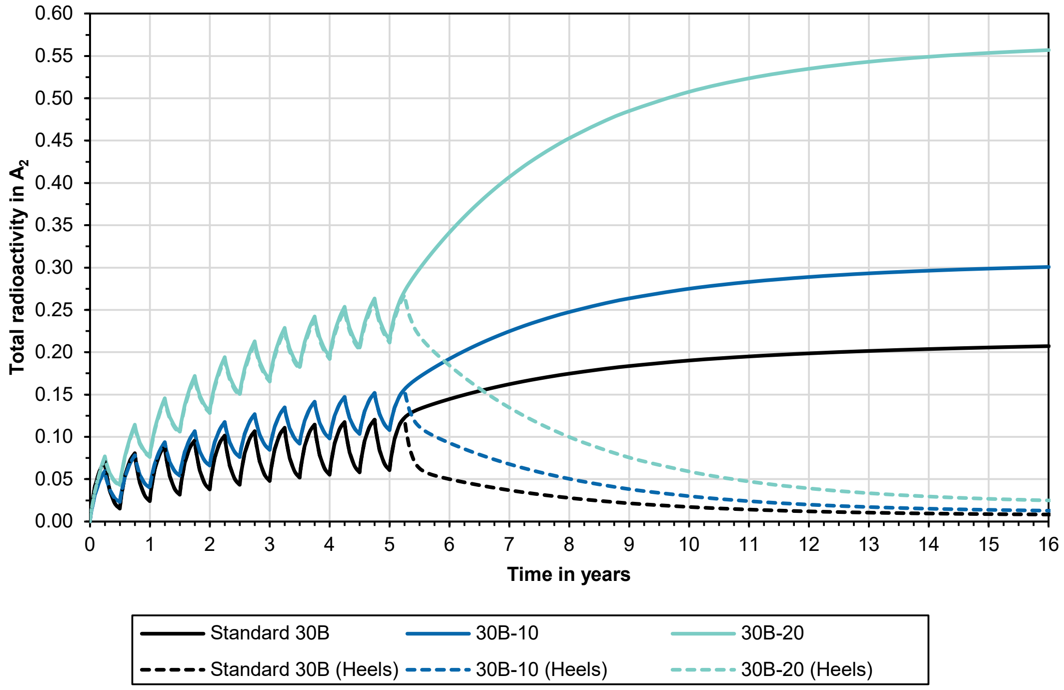


**Figure 1-2 Radioactivity in 30B-10 and 30B-20 cylinders in comparison to 30B cylinders for a 3-month filled/heeled cycle followed by a 10-year storage of filled/heeled cylinders**

## 1.4 Specification of the Packaging

### 1.4.1 List of all Packaging Components and Complete Design Drawings

The DN30-X is a partially new package design, consisting of the new 30B-X cylinder and the already licensed DN30 PSP (see [DNT 2019]). The DN30 PSP provides both the mechanical and thermal protection for the 30B-X cylinder including its radioactive content. The DN30-X packaging is designed to meet RCT, NCT, and HAC as required by [10 CFR Part 71] and [49 CFR Part 173], or [SSR-6 2018].

The main packaging components are:

- The 30B-X cylinder consisting of:
  - The cylinder shell with an ellipsoidal head on each end
  - The valve and plug half coupling
  - The cylinder valve and plug
  - Two skirts being attached to each ellipsoidal head, where the skirt on the valve side has two horizontally aligned holes that are used to prevent the rotation of the cylinder inside the DN30 PSP
  - Two criticality control system (CCS) restraints, each consisting of a backing bar and a rotation preventing device, that maintain the position of the interior CCS within the 30B-X cylinder cavity
  - The interior CCS consisting of criticality control rods (CCRs) containing neutron poison material in the form of boron carbide ($B_4C$), and three lattice holders that keep each CCR in place. The separation of the lattice holders is maintained by 14 longitudinal stiffeners
- The DN30 PSP consisting of:
  - The bottom half with two feet welded to the outer shell for tie-down during transport incorporating four load attachment points to be used for handling the DN30-X package and two forklift pockets for handling the empty and loaded packaging
  - The top half with two load attachment points for handling the top half
  - The valve protecting device that is attached to the bottom half by means of hinges
  - The plug protecting device that is welded to the interior shell of the bottom half
  - The rotation preventing devices consisting of two pins welded to the flange of the bottom half
  - The closure system consisting of six steel blocks welded to the top half and six steel blocks welded to the bottom half forming mortise-and-tenon style joints connected through steel pins
  - Steel blocks welded to the top and bottom half for sealing the DN30-X packaging

Since the DN30-X is only a partially new design, a new set of drawings is only required for the designs of the 30B-10 and the 30B-20 cylinder (see section 1.4.1.1), while the specification and drawings of the DN30 PSP provided in section 1.4.1.2 are identical with those in [DNT 2019]. Furthermore, the following revised and new drawings of the DN30 PSP are required:

- Revised to include the 30B-X:
  - Datasheet 0023-ZDB-1000-000 “DN30 PSP”
  - Drawing 0023-ZFZ-1000-000 “DN30 PSP”
- New to include the 30B-X:
  - Drawing 0023-ZFZ-1000-003 “Additional package nameplate”

### 1.4.1.1 30B-X Cylinder

The DN30 PSP may be loaded with the 30B-10 or the 30B-20 cylinder that both are derived from a standard 30B cylinder as specified in [ANSI N14.1] adding an interior criticality control system (CCS). The CCS consists of criticality control rods (CCRs) containing neutron poison material in the form of boron carbide ($B_4C$), and lattice holders that keep each CCR in place.

The 30B-10 and the 30B-20 cylinders are defined in the following main drawings:

- 30B-10 Cylinder:
  - Parts list 0045-STL-1000-000 “30B-10 Cylinder”
  - Drawing 0045-ZFZ-1000-000 “30B-10 Cylinder”
  - Drawing 0045-ZFZ-1100-000 “30B Cylinder modified”
  - Drawing 0045-ZFZ-1200-000 “CCS”
- 0045-ZFZ-2000-000 “30B-20 Cylinder”
  - Parts list 0045-STL-2000-000 “30B-20 Cylinder”
  - Drawing 0045-ZFZ-2000-000 “30B-20 Cylinder”
  - Drawing 0045-ZFZ-1100-000 “30B Cylinder modified”
  - Drawing 0045-ZFZ-2200-000 “CCS”

Appendix 1.4.1A (Drawings 30B-X Cylinder) contains proprietary drawings and parts lists of the individual parts of the 30B-10 and the 30B-20 cylinder, respectively. The following material specifications for the 30B-X cylinder pressure envelope in section 1.4.1.1.1 as well as the valve and plug in section 1.4.1.1.2 are identical to the material specifications for a standard 30B cylinder and, thus, are adopted from [ANSI N14.1] as they stand. However, additional material specifications are required in case of the CCS, which are given in section 1.4.1.1.3.

#### 1.4.1.1.1 Pressure Envelope and Skirts

The materials of the 30B-X cylinder are specified in table 1-9. They are identical to the material specifications of a standard 30B cylinder and, thus, are adopted from [ANSI N14.1] as they stand.

**Table 1-9 Material specification of the 30B-X cylinder**

| Item | Material specification |
|---|---|
| Cylinder | Cylinder shell, heads, backing bars, and skirts shall conform to [ASTM A516], steel, grade 65 or 70 and shall be normalized.<br>a) All steel shall be Charpy V-notch impact tested and shall meet the Charpy V-notch impact requirements as stated in ASTM A20.<br>b) Steel may be plate or coil form. |
| Couplings | Modified half-coupling per [ANSI N14.1], Figure 14, Forged ASTM A105.<br>*Note: ASTM A106 Grade C may be used in lieu of ASTM A105.* |
| Nameplate | Sheet, ASTM A240, UNS S30400 or S30403. |
| Valve protector (optional) | Plate, weldable carbon steel with a minimum tensile strength of 45000 Psi and a maximum carbon content of 0.26 %, such as ASTM A36. |
| Seal loop(s) | Rod, ASTM A36. |

#### 1.4.1.1.2 Valve and Plug

The materials of the valve and the plug are specified in table 1-10. They are identical to the material specifications of a standard 30B cylinder and, thus, are adopted from [ANSI N14.1] as they stand.

**Table 1-10 Material specification of valve and plug of the 30B-X cylinder**

| Item | Material specification |
|---|---|
| Body | Forging, aluminum bronze (UNS C63600), conforming to [ANSI N14.1], section 7.1.2 and 7.1.4. |
| Stem | Bar, cold drawn, nickel-copper alloy (UNS N04400) ASTM B164 and stress-relieved per [ANSI N14.1], section 7.1.5-2. Certification to include results of testing in accordance with ASTM E2375 over 100 % of stock material. Testing to be per Class AA with straight beam. |
| Packing nut | *Note: Packing nuts require stress-relieving after final machining. Surface hardness measurements of packing nuts after final stress-relieving may be made on the top of the nut.*<br>a) Bar, aluminum bronze (UNS C61300) ASTM B150, stress-relieved per [ANSI N14.1], section 7.1.5-3 or,<br>b) Bar, nickel-copper alloy (UNS N04400) ASTM B164, stress-relieved per [ANSI N14.1], section 7.1.5-2. |
| Port cap | a) Bar, aluminum bronze (UNS C61300) ASTM B150, stress-relieved per [ANSI N14.1], section 7.1.5-3 or,<br>b) Bar, nickel-copper alloy (UNS N04400) ASTM B164, stress-relieved per [ANSI N14.1], section 7.1.5-2, or<br>c) Bar, aluminum bronze (UNS C63600), stress-relieved per [ANSI N14.1], section 7.1.5-1. |
| Packing follower, packing ring | a) Bar, aluminum bronze (UNS C61300) ASTM B150, stress-relieved per [ANSI N14.1], section 7.1.5-3 or,<br>b) Bar, aluminum bronze (UNS C63600), stress-relieved per [ANSI N14.1], section 7.1.5-1. |
| Packing, cap gasket | PTFE |
| Fluorinated lubricant | Compatible for $UF_6$ service. |

| Item | Material specification |
|---|---|
| Solder | Tin-lead alloy, with a minimum tin content of 45 % such as alloy SN50 ASTM B32. |
| Solder flux | Phosphoric acid or approved equivalent. |
| Hex head plug | Bar, upset forged, extruded or extruded and drawn, aluminum bronze (UNS C61300) ASTM B150. |
| Socket head plug | *Note: These plugs may be used in lieu of hex head plugs.*<br>a) Bar, upset forged, extruded or extruded and drawn, aluminum bronze (UNS C61300) ASTM B150 or<br>b) Bar, upset forged, extruded or extruded and drawn, aluminum bronze D (UNS C61400, with a tin content restricted to 0.2-0.5 %) ASTM B150 or<br>c) Plate, chemical composition as specified in a) or b) and conforming to ASTM B171. |

#### 1.4.1.1.3 Criticality Control System

The materials of the interior CCS of the 30B-X cylinder are specified in table 1-11. Except for the neutron poison material in the form of boron carbide ($B_4C$), the same materials as for the pressure-envelope of a standard 30B cylinder are used for the CCS. Consequently, the same standards according to [ANSI N14.1] are applied for these parts.

**Table 1-11 Material specification of interior CCS of the 30B-X cylinder**

| Item | Applicable standards |
|---|---|
| Lattice holders, longitudinal stiffeners, and CCR lids | a) The CCR lids, longitudinal stiffeners, and lattice holders shall conform to [ASTM A516], steel, grade 65 or 70 and shall be normalized.<br>b) All steel shall be Charpy V-notch impact tested per ASTM A20. The test temperature and acceptance criteria shall be as specified in ASTM A20, Table A1.15. Alternatively, the maximum test temperature is specified as -40 °C and the minimum average energy absorption for 3 full-size specimen shall be 27 J. None of the specimen shall have an energy absorption below 22 J.<br>c) Steel may be plate or coil form.<br>*Note: Steel confirming to [DIN EN 10028-3] grade P355NL1 or P355NL2 may be used in lieu of [ASTM A516] grade 65 or 70. In this case, the minimum impact energy requirements of [DIN EN 10028-3] apply.* |
| CCR pipes | a) The CCR pipes shall conform to [ASTM A333] grade 9<br>b) All steel shall be Charpy V-notch impact tested. The impact test temperature and impact requirements shall be as specified in [ASTM A333]. Alternatively, the impact test temperature is specified as -40 °C and the minimum average notched bar impact value of each set of 3 full-size specimen shall be 27 J. None of the specimen shall have a minimum average notched bar impact value below 22 J.<br>*Note: Seamless steel pipes confirming to [DIN EN 10216-3] grade P355NL1 or P355NL2 may be used in lieu of [ASTM A333] grade 9. In this case, the minimum impact energy requirements of [DIN EN 10216-3] apply.* |
| Neutron poison material | Boron carbide ($B_4C$) as specified in Appendix 1.9.2 (Manufacturing Specification 30B-X Cylinder) |

#### 1.4.1.2 DN30 PSP

The design of the DN30 PSP has been established in [DNT 2019] and is defined in the following main drawings:

- 0023-STL-1000-000 “Part list DN30 PSP”
- 0023-ZFZ-1000-100 “Closure device”
- 0023-ZFZ-1100-000 “Bottom half”
- 0023-ZFZ-1200-000 “Top half”

Appendix 1.4.1B (Drawings DN30 PSP) contains proprietary drawings and parts lists of the individual parts of the DN30 PSP. The materials of these parts are specified in [DNT 2019]. For completeness, they are also listed in table 1-12.

**Table 1-12 Material specification of the DN30 PSP**

| Item | Applicable EU standards | Applicable US standards |
|---|---|---|
| Inner / outer steel shells | [DIN EN 10088-2], Grade 1.4301, 1.4307, or 1.4541 | ASME SA-240, Type 304 (UNS S30400) or Type 321 (UNS S32100) |
| Inner structure | [DIN EN 10088-2], Grade 1.4301, 1.4307, or 1.4541 | ASME SA-240, Type 304 (UNS S30400) or Type 321 (UNS S32100) |
| Feet | [DIN EN 10088-2], Grade 1.4301, 1.4307, or 1.4541 | ASME SA-240, Type 304 (UNS S30400) or Type 321 (UNS S32100) |
| Lifting lugs (feet) | [DIN EN 10088-2], Grade 1.4462 | ASME SA-240, Type 2205 (UNS S31803) |
| Steel shells of valve protecting device | [DIN EN 10088-2], Grade 1.4301, 1.4307, or 1.4541 | ASME SA-240, Type 304 (UNS S30400) or Type 321 (UNS S32100) |
| Rotation preventing device | [DIN EN 10088-2], Grade 1.4301, 1.4307, or 1.4541 | ASME SA-240, Type 304 (UNS S30400) or Type 321 (UNS S32100) |
| Plug protecting device | [DIN EN 10088-2], Grade 1.4301, 1.4307, or 1.4541 | ASME SA-240, Type 304 (UNS S30400) or Type 321 (UNS S32100) |
| Closure device | [DIN EN 10088-3] / [DIN EN 10088-2], Grade 1.4541<br>[DIN EN 10088-3] / [DIN EN 10088-2], Grade 1.4571 | ASME SA-479 / ASME SA-240, Type 321 (UNS S32100)<br>ASME SA-479 / ASME SA-240, Type 316Ti (UNS S31635) |
| Body of pin | [DIN EN 10088-3], Grade 1.4542 | ASME SA-564, Type 630 (Alloy 17-4 PH, UNS S17400) |
| Head of pin | [DIN EN 10088-3], Grade 1.4541 or 1.4571 | ASME SA-479, Type 321 (UNS S32100) or Type 316Ti (UNS S31635) |
| Securing bolt | Nitronic 50 | ASME SA-193, Type XM-19 (UNS S20910) |
| Washers | NL16-254SMO ([DIN EN 10088-2], Grade 1.4547) | ASME SA-240M, Alloy 254 (UNS S31254) |
| Gaskets | EPDM | |

| Item | Applicable EU standards | Applicable US standards |
|---|---|---|
| Foam | PIR foam conforming to the specifications RTS 120 and RTS 320 (see [DNT 2019]) | |
| Intumescent material | Intumescent material e.g. conforming to the specifications Promaseal-PL® (see [DNT 2019]) | |
| Thermal insulation | Microporous material e.g. conforming to the specifications MICROTHERM® OVERSTITCHED 1000R HY or WDS® Multiflex® ST 2D50 HY (see [DNT 2019]) | |
| Thermal plugs | Polyamide | |
| Pads | Silicone | |

### 1.4.2 Description of the DN30-X Packaging

The DN30 packaging consists of:

- The 30B-X cylinder
- The DN30 PSP

#### 1.4.2.1 30B-X Cylinder

The 30B-X cylinder is identical to a standard 30B cylinder as specified in [ANSI N14.1], except that an interior criticality control system (CCS) is built into the 30B-X cylinder (see figure 1-3). In the following sections 1.4.2.1.1 to 1.4.2.1.3, a detailed description of 30B-X cylinder is provided. Furthermore, additional provisions to [ANSI N14.1] and their implications on the safety features of the 30B-X cylinder are discussed in section 1.4.2.1.4.

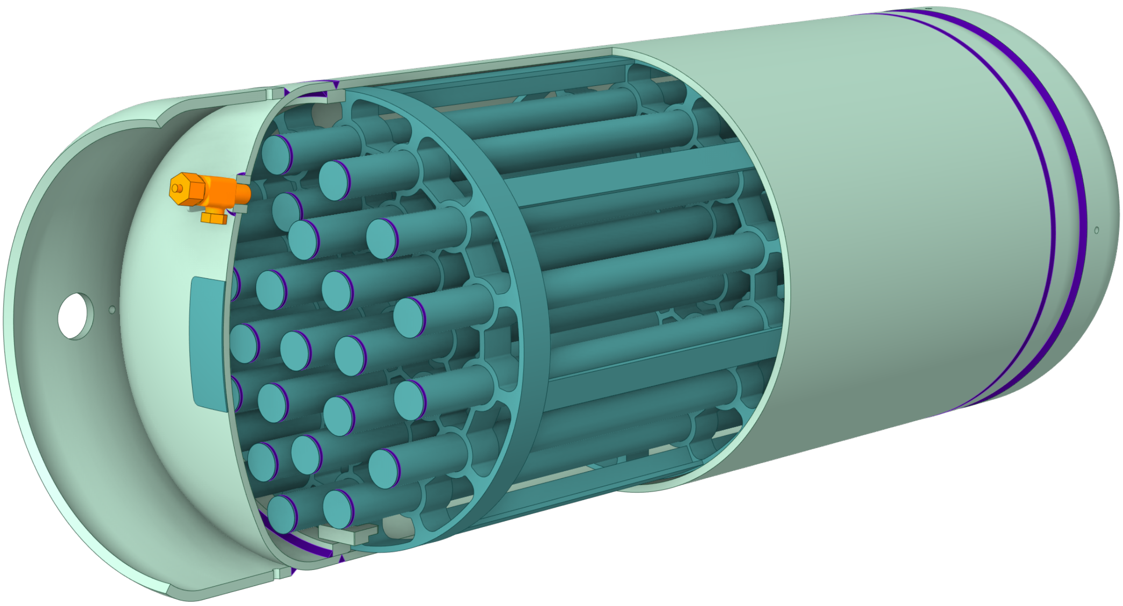

**Figure 1-3 30B-X cylinder – Outside view**

1.4.2.1.1 Criticality Control System

The CCS consists of criticality control rods (CCRs) filled with neutron poison material and lattice holders that retain the CCR positionings. Longitudinal stiffeners between the lattice holders help

to keep the lattice holders separated from each other. The interior CCS of the 30B-X cylinder is shown in figure 1-4.

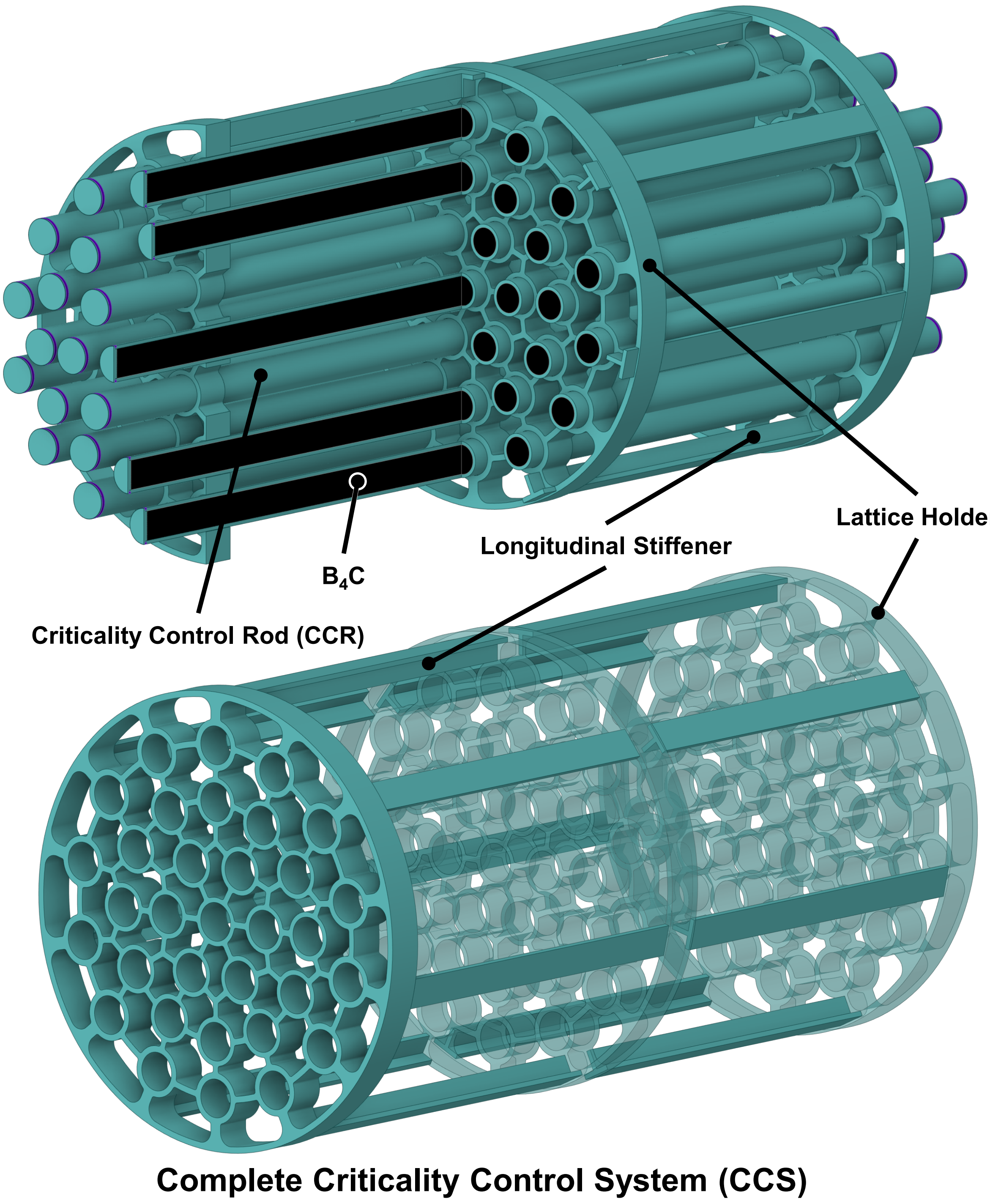


**Figure 1-4 30B-X cylinder – Interior criticality control system**

The CCRs are seamless steel pipes that are filled with boron carbide ($B_4C$) as a neutron absorbing material for criticality control and that are sealed by a welded lid on each end. For the CCRs, standardized seamless pipes are used having an outer diameter of 60.3 mm and a wall thickness of 5.54 mm. Their proper placement, which is crucial for criticality control, is ensured by the three lattice holders. According to the specification in table 1-11, only materials that are

already specified in [ANSI N14.1] are used for the steel pipes and the lattice holders. Hence, compatibility is ensured between the interior CCS, the cylinder material and the $UF_6$ contents.

The cross section through the 30B-X cylinder in figure 1-5 displays the CCS within the cylinder. The length of the CCRs is fitted to the ellipsoidal heads of the 30B-X cylinder. Of special note are the CCRs that end directly in front of the valve and plug – these are shortened by 60 mm to avoid interference with filling and emptying of the cylinder. Shortening these CCRs also helps to ensure that there will be no impact of the CCS on the valve or plug, even under HAC.

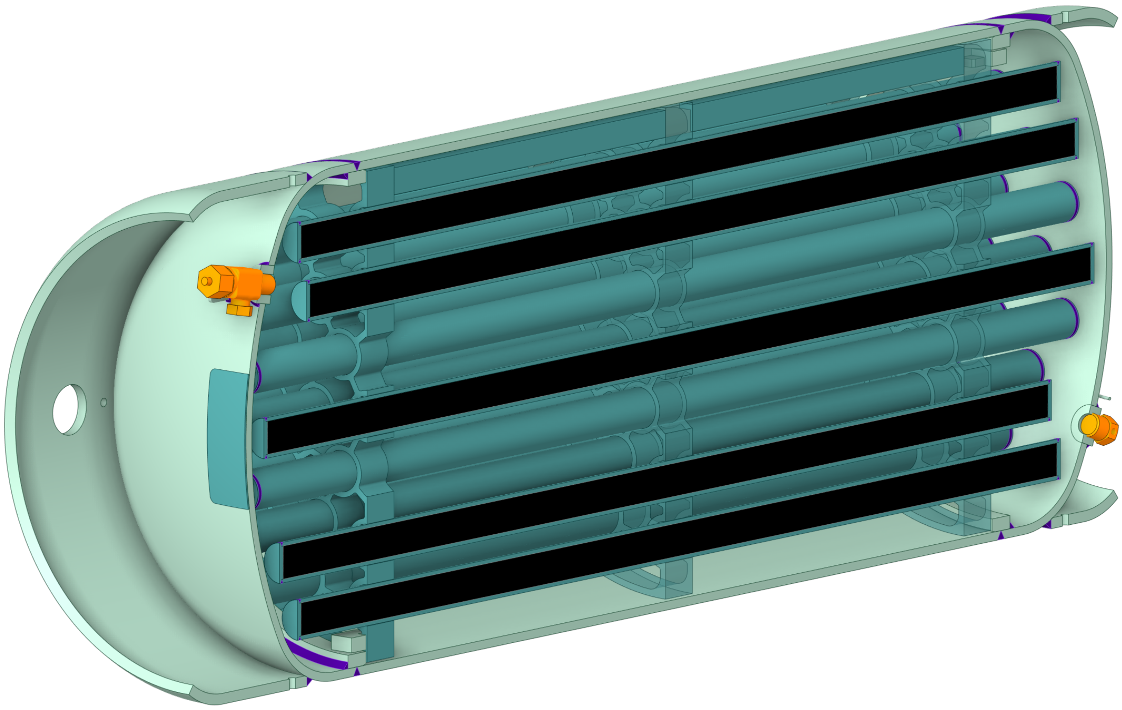

**Figure 1-5 30B-X cylinder – Cross sectional view**

#### 1.4.2.1.2 Pressure Envelope

The pressure envelope of the 30B-X cylinder is identical to the standard 30B cylinder, except for a CCS restraint that is welded to the straight portion of each cylinder head. These inhibit the longitudinal movement and axial rotation of the interior CCS within the 30B-X cylinder, but no fixed connection exists between the CCS and the pressure envelope of the 30B-X cylinder. Simultaneously, the CCS restraints serve as backing bars for the circumferential head welds of the 30B-X cylinder.

The specification of the outer dimensions, the materials as well as the valve and plug of the 30B-X cylinder are identical to the standard 30B cylinder. This ensures that the 30B-X cylinder can be operated and handled in the same way as the standard 30B cylinder. However, deviating from [ANSI N14.1], a minimal wall thickness of 11 mm is specified for the 30B-X cylinder shell and heads.

#### 1.4.2.1.3 Main Characteristics of the 30B-X Cylinder

The main characteristics of the 30B-10 and the 30B-20 cylinder in comparison to the standard 30B cylinder are listed in table 1-13. Only the enrichment limit, nominal tare weight, maximum net weight, minimum volume and minimum ullage differ from a standard 30B cylinder.

**Table 1-13 Main data of the 30B-X cylinder**

| Item | Value | | | Unit |
|---|---|---|---|---|
| | Standard 30B | 30B-10 | 30B-20 | |
| Enrichment limit $^{235}U$ in U | 5 | 10 | 20 | wt.-% |
| Nominal diameter | 760 | 760 | 760 | mm |
| Nominal length | 2060 | 2060 | 2060 | mm |
| Nominal wall thickness | 13 | 13 | 13 | mm |
| Minimum wall thickness | 7.94 | 11 | 11 | mm |
| Nominal tare weight | 635 | 1452 | 1641 | kg |
| Maximum net weight | 2277 | 1460 | 1271 | kg |
| Maximum gross weight | 2912 | 2912 | 2912 | kg |
| Minimum volume | 0.736 | 0.544 | 0.493 | $m^3$ |
| Minimum ullage at 121 °C | 5 | 17.6 | 20.8 | % |
| Nominal internal free surface | 4.75 | 20.01 | 22.89 | $m^2$ |
| Effective cross section of cavity | | | | |
| At lattice holders (minimal) | 0.426 | 0.205 | 0.171 | $m^2$ |
| At CCRs | 0.426 | 0.328 | 0.298 | $m^2$ |

In the determination of the maximum net weight (permissible mass of $UF_6$) listed in table 1-13, two limiting factors are considered. On the one hand, the nominal gross weight of the 30B-10 and 30B-20 cylinder shall be identical to the standard 30B cylinder and, on the other hand, the minimum ullage of 5 % at 121 °C required by [ANSI N14.1] must be complied with. Beside the nominal gross weight, the outer dimensions, the wall thickness and, thus, also the volume of the inner cavity excluding the interior CCS are identical for all cylinder designs. Hence, comparing the density of liquid $UF_6$ at 121 °C and the average density of the internal CCS of the 30B-X cylinder suffices to determine the limiting case.

The lattice holders are entirely made of steel and, for the CCRs consisting of steel rods filled with boron carbide, an average density of about 4.2 g/cm³ is calculated. Consequently, the average density of the CCS is always higher than the density of liquid $UF_6$ at 121 °C of 3.26 g/cm³ (see table 1-1). The limiting case in the determination of the maximum net weight is therefore the gross weight, leading to a minimum ullage for the 30B-10 and the 30B-20 cylinder at 121 °C that is significantly larger than the minimally required 5 % per [ANSI N14.1], respectively.

1.4.2.1.4 Additional provisions to ANSI N14.1

In this section, it is discussed how the safety aspects of the 30B-X cylinder, namely its containment function (see section 1.4.2.3.1), continue to be maintained with the additional provisions to [ANSI N14.1] that are required for the 30B-X cylinder. According to the description of the 30B-X cylinder in the previous sections, these additional provisions and their impact on the safety aspects of the 30B-X cylinder are:

1. Addition of the interior CCS
   - Under normal operating conditions for the 30B-X cylinder (see section 2.1.1.1.1), the presence of the CCS has no impact on the containment function of the 30B-X cylinder. Due to the absence of a fixed connection between the CCS and the 30B-X cylinder pressure envelope, the deformation behavior under internal and external pressure loads is identical to the behavior of a standard 30B cylinder.
   - The interior CCS increases the nominal tare weight of the 30B-10 and 30B-20 cylinder compared to a standard 30B cylinder. Since the maximum gross weight of the 30B-X and standard 30B cylinder are required to be identical (see table 1-13), handling of filled cylinders is not affected. Accordingly, the increased tare weight only needs to be considered with regard to the handling of empty 30B-X cylinder.
   - Another consequence of requiring identical maximum gross weights for the 30B-X and standard 30B cylinder is an increase in the minimum ullages at 121 °C for the 30B-10 and 30B-20 cylinder (see table 1-13). Hence, the risk of a fatal pressure build-up caused by melted $UF_6$ contents is significantly lower for the 30B-X cylinder than for the standard 30B cylinder (see section 2.3.1.4).
2. Incorporation of stronger backing bars in the design of the 30B-X cylinder that also serve as a CCS restraint
   - The incorporation of stronger backing bars has a positive impact on the resulting stresses at the junction of the cylinder shell and heads under normal operating conditions for the 30B-X cylinder.

This shows that all safety aspects of the standard 30B cylinder are at least maintained or even improved with the above-mentioned additional provisions to [ANSI N14.1] that apply to the 30B-X cylinder.

### 1.4.2.2 DN30 PSP

A description of the DN30 PSP is already provided in the safety analysis of the licensed DN30 package. Therefore, the following is a replication of the description in [DNT 2019] to improve the readability of this SAR.

The DN30 PSP consists of:

- The bottom half with integrated feet, load attachment points for handling the loaded package, valve protecting device, plug protecting device, rotation preventing devices and bottom half of the closure devices
- The top half with integrated load attachment points for handling the top half and the top half of the closure devices

The main data of the DN30 PSP are listed in table 1-14.

**Table 1-14 Main data of the DN30 PSP**

| Item | Value | Unit |
| --- | --- | --- |
| Nominal diameter | 1216 | mm |
| Nominal height | 1329 | mm |
| Nominal length | 2437 | mm |
| Nominal tare weight | 1100 | kg |
| Nominal gross weight | 4012 | kg |
| Maximum gross weight | 4100 | kg |

#### 1.4.2.2.1 Bottom Half of the DN30 PSP

The body of the bottom half is made of an inner and outer shell of stainless steel, both in the form of a tub that are connected at the top by a flange. The cavity between the inner and outer shell and flange is filled with the PIR foams RTS 120 and RTS 320. Between the inner shell and the RTS 120 foam, there is also a layer of 10 mm microporous material as thermal insulation. At the side the thickness of the inner shell is 2 mm and of the outer shell 3 mm. At the ends the thickness of the inner shell is 10 mm and of the outer shell 4 mm. All surfaces of the inner shell of the bottom half are covered with a layer of 2.6 mm intumescent material.

At the bottom side there are two feet of stainless-steel welded to the outer shell at each end of the DN30 PSP. The feet have a base plate, made of two 10 mm thick stainless-steel plates welded on top of each other, which contains at each side two holes for tie-down to an adapted flatrack (the arrangement and size of these holes is compatible with existing PSP designs).

At the side of each of the feet there is an eyelet welded to the side plate of the foot. These eyelets are designed to be used for lifting the loaded DN30-X package.

At the top side of the bottom half of the DN30 PSP, the lower halves of the mortise-and-tenon closure system are welded to the outer shell, three per side. Adjacent to one of these parts of the closure system, the sealing block is welded to the outer shell.

At the inside of the bottom half, the valve protecting device is attached to the flange by hinges at one end. The valve protecting device consists of a stainless-steel casing filled with PIR foam RTS 320 and a protecting housing that has its interior surfaces covered with intumescent material.

On the opposite end, there is the plug protecting device in the form of a pot that is welded to the inner shell and that has its interior surfaces covered with intumescent material.

At the inner sides of the flange there are two rotation preventing devices welded to the flange. These devices consist of a pin, which is withdrawn into the flange during loading and inserted during transport into the two holes in the skirt of the 30B-X cylinder.

#### 1.4.2.2.2 Top Half of the DN30 PSP

The body of the top half is similar to the bottom half. It is made of an inner and outer shell of stainless-steel, both in the form of a tub that are connected at the bottom by a flange. The cavity between the inner and outer shell and flange is filled with the PIR foams RTS 120 and RTS 320. Between the inner shell and the RTS 120 foam, there is also a layer of 10 mm microporous material as thermal insulation. At the side, the thickness of the inner shell is 2 mm and of the outer shell 3 mm. At the ends the thickness of the inner shell is 10 mm and of the outer shell 4 mm. All surfaces of the inner shell of the top half are covered with a layer of 2.6 mm intumescent material.

At the top, there are two eyelets welded to the outer shell, one on each side. These eyelets are designed to be used for lifting the top half only.

At the bottom side of the top half of the DN30 PSP, the upper halves of the mortise-and-tenon closure system are welded to the outer shell, three per side. Adjacent to one of these parts of the closure system, the sealing block is welded to the outer shell.

At the inside of the top half there is a recess to accommodate the valve protecting device.

In the flange of the top half, there is an elastomeric gasket to prevent water inleakage under RCT.

#### 1.4.2.3 Design Safety Features of the DN30-X Packaging

The design safety features of the DN30-X packaging are identical to the already licensed DN30 packaging, except for the pressure containment in section 1.4.2.3.1 that is now represented by the 30B-X cylinder instead of the standard 30B cylinder. Therefore, the following is a replication of the description of the design safety features provided in [DNT 2019].

##### 1.4.2.3.1 Pressure Containment of the DN30-X Packaging

The pressure containment consists of:

- The 30B-X cylinder including its valve and plug

##### 1.4.2.3.2 Mechanical Protection System

The mechanical protection system prevents excessive mechanical impacts on the 30B-X cylinder under RCT, NCT and HAC. It consists of:

- The stainless steel and foam structure of the bottom and top half of the DN30 PSP

##### 1.4.2.3.3 Thermal Protection System

The thermal protection system prevents excessive thermal loads on the 30B-X cylinder including its valve and plug under RCT, NCT and HAC. It consists of:

- The stainless steel / foam structure of the bottom and top half of the DN30 PSP (each fitted with nine thermal plugs/valves, screwed into the outer steel shells)
- The microporous thermal insulation layer between the RTS 120 foam and the inner steel shell
- The intumescent material at the inner surfaces of the DN30 PSP

##### 1.4.2.3.4 Closure System

The top and bottom half of the DN30 PSP are connected by the closure system consisting of 6 robust mortise-and-tenon like devices and the flange.

The two parts of each mortise-and-tenon system have four teeth each with a hole in its center. When closed, the two halves are connected by a pin inserted into these holes. This pin is secured by a bolt. The design of the mortise-and-tenon system is such that neither the connecting pin nor the securing bolt are exposed to mechanical impacts but are protected by the massive body of the system. The system prevents excessive relative movements of top and bottom half in vertical direction under RCT, NCT and HAC.

The flange is shaped like an upside-down “U”. It prevents excessive relative movements of the top and bottom half in all horizontal directions under RCT, NCT and HAC. Furthermore, in flat drop orientations the flange will be deformed in such a way that the top and bottom half are clamped together.

##### 1.4.2.3.5 Valve Protecting Device

The valve protecting device consists of a stainless-steel housing filled with PIR foam. It is shaped like a U and encloses the valve of the 30B-X cylinder during transport. It is connected to the bottom half of the DN30 PSP through two hinges. In open condition, it is turned to horizontal position to allow loading and unloading of the cylinder. When the filled cylinder is loaded into the PSP, the device is turned by 90° to vertical orientation so that it is in contact with the cylinder head. The valve protecting device prevents contact of the valve with any part of the DN30 PSP or any other part the 30B-X cylinder except for its original point of contact (thread) under RCT, NCT and HAC.

A protecting housing is placed inside the U-shape of the valve protecting device. This housing is made of thin stainless-steel sheets and its inside is covered with intumescent material.

##### 1.4.2.3.6 Plug Protecting Device

The plug protecting device consists of a pot made of stainless steel welded to the inner shell of the bottom half of the DN30 PSP. This device allows the plug of the 30B-X cylinder to move in axial direction without getting in contact with any part of the DN30 PSP under RCT, NCT and HAC. The inside of the pot is covered with intumescent material.

##### 1.4.2.3.7 Rotation Preventing System

The rotation preventing system consists of two rotation preventing devices installed at the sides of the inner flange of the bottom half of the DN30 PSP. The device consists of a stainless-steel pin accommodated in two sleeves, an internal sleeve in contact with the pin and an external sleeve that is welded to the flange. A lever is welded onto the steel pin to allow turning and lateral movements.

In open condition, the steel pin is withdrawn into the flange so that the cylinder can be loaded or unloaded. In this condition, the top half of the DN30 PSP cannot be put on the bottom half as the position of the lever prevents the correct placement of the top flange onto the bottom flange. The connection of top and bottom half is only possible when the rotation preventing system is properly engaged. This excludes the possibility of the pin being withdrawn while the packaging is closed.

##### 1.4.2.3.8 Sealing System

For sealing of the DN30-X package there are two sealing blocks welded to the top and bottom half adjacent to a closure device. These blocks allow the use of high security seals compliant with ISO 17712 / C-TPAT.

#### 1.4.2.4 Handling Features of the DN30-X Packaging

The handling features of the DN30-X packaging are identical to the already licensed DN30 packaging. Therefore, the following is a replication of the description of the handling features provided in [DNT 2019].

#### 1.4.2.4.1 Lifting of the DN30-X Package, DN30-X Packaging and Empty DN30 PSP

The DN30-X package can be lifted by using:

- The 4 lifting lugs welded to the upper part of the feet
- A forklift
- Handling slings

Handling of the DN30 PSP or empty DN30-X packaging is carried out in the same manner as for the DN30-X package.

##### 1.4.2.4.1.1 Lifting by Using the 4 Lifting Lugs at the Feet

For lifting the DN30-X package by using the 4 lifting lugs welded to the upper part of the feet, shackles must be used and fixed to the lifting lugs. It is preferable to use lifting slings made from Polyester or Nylon. The angle between the vertical axis of the lifting lugs and the slings/chains must not be greater than 30° (see figure 1-6).

**Figure 1-6 Lifting of the DN30-X package by using the 4 lifting lugs**

##### 1.4.2.4.1.2 Lifting by Using a Forklift

The loaded DN30-X package may be handled and lifted by using a forklift. For this purpose, two forklift pockets are welded to the bottom half of the DN30 PSP (see figure 1-7).

**Figure 1-7 Lifting of the DN30-X package by using a forklift**

1.4.2.4.1.3 Lifting by Using Slings (Empty DN30 PSP)

Only the empty DN30 PSP may be handled by slings attached to the bottom half of the DN30 PSP as shown in figure 1-8.

**Figure 1-8 Lifting of the empty DN30 PSP by using slings**

1.4.2.4.2 Lifting of the Top Half of the DN30 PSP

When transported, the loaded DN30-X package or the empty DN30 PSP is usually mounted on dedicated flatracks. At the destination, only the top half of the DN30 PSP needs to be removed for loading or unloading the 30B-X cylinders into or from the DN30 PSPs.

For handling of the top half, there are two lifting lugs welded to each end of the outer shell of the DN30 PSP (see figure 1-9). These lifting lugs are designed for lifting the top half of the DN30 PSP only. During transport, they have to be rendered inoperable for lifting to prevent inadvertent use of these attachment points (e.g. for lifting the loaded package). Rendering the lifting lugs at the top half inoperable can be done e.g. by inserting bolts.

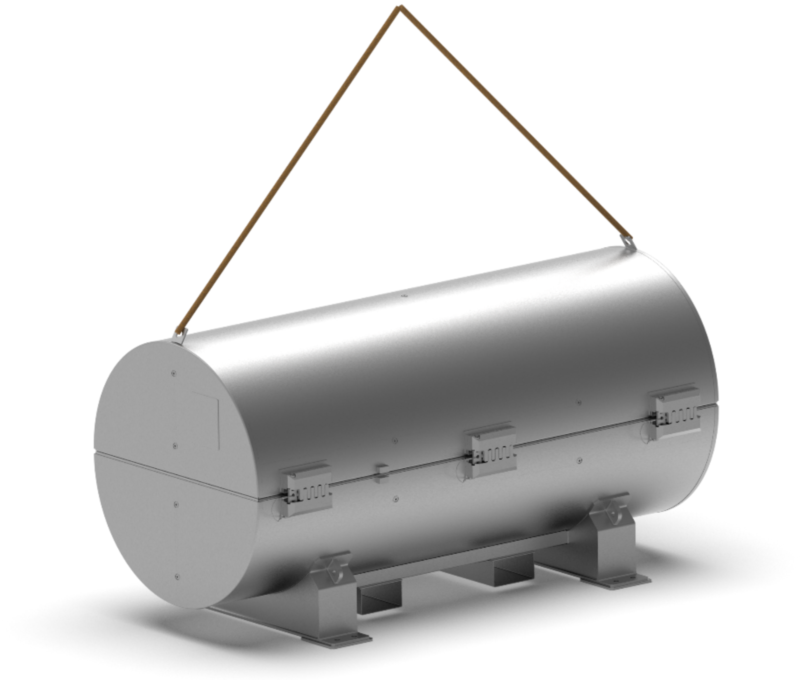

**Figure 1-9 Lifting of the top half of the DN30-X packaging**

### 1.4.2.5 Tie-Down Features of the DN30-X Packaging

For tie-down, the DN30 PSP is equipped with two feet. The base plates of the feet consist of 2 x 10 mm thick stainless-steel sheets which incorporate two holes at each end. The dimension and position of these holes are compatible with other PSP designs currently in use. During transport, the DN30 PSP is bolted to a dedicated flatrack (see figure 1-10).

According to international practice, tie-down of the DN30-X package on flatracks by bolts is performed taking into account accelerations of 2 g in axial, 2 g in lateral and 2 g in vertical direction of travel. However, the tie-down features of the DN30-X package are designed to withstand an acceleration of 10 g in axial, 5 g in lateral and 1 g ± 2 g in vertical direction of travel (see section 2.2.4). For application of such tie-down parameters, additional shocks or bumpers must be foreseen in the tie-down plan. However, this tie-down plan is not part of the application.

Only for the transport of DN30 PSP not loaded with a 30B-X cylinder and in case a dedicated flatrack cannot be made available, tie-down by using straps according to figure 1-11 is allowed. In that case, a tie-down plan has to be drawn up based on a tie-down calculation.

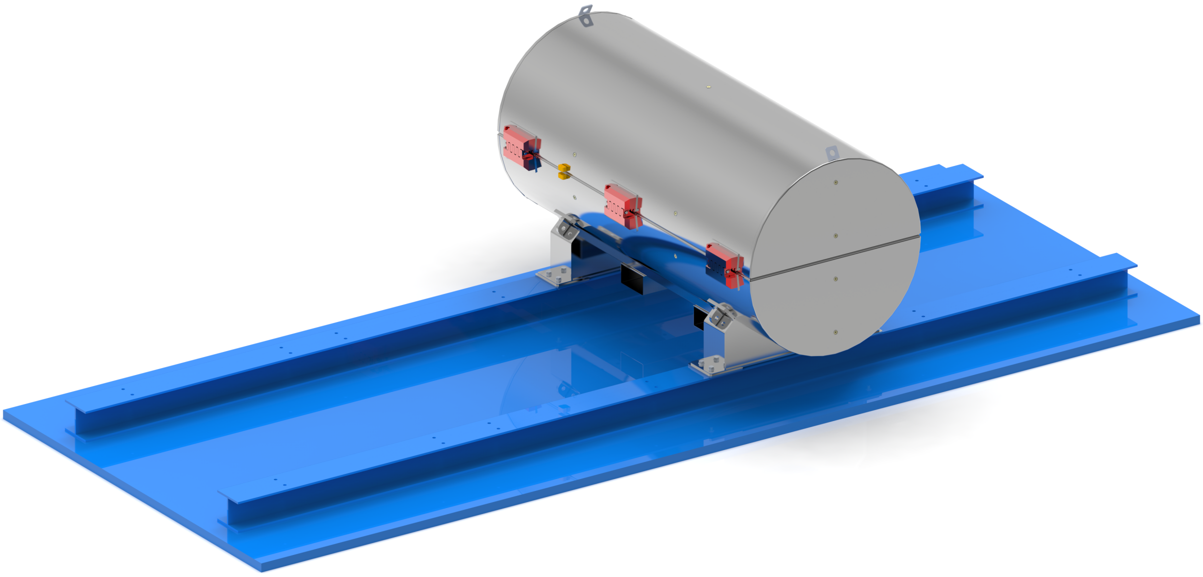

**Figure 1-10 General tie-down method for the DN30-X package / DN30 PSP**

**Figure 1-11 Tie-down of the empty DN30 PSP using straps**



### 1.4.3 Components of the Packaging Relevant for the Containment System

The containment system consists of:

- The 30B-X cylinder shell and heads together with the welding seams forming the pressure envelope
- The valve body and the stem including the threaded connection between the valve and the 30B-X cylinder body
- The plug including its threaded connection between the 30B-X cylinder body

### 1.4.4 Components of the Packaging Relevant for Shielding

The DN30-X packaging has no components primarily intended for shielding. However, some level of shielding is provided by the 30B-X cylinder shell as well as the inner and outer shells of the DN30 PSP.

### 1.4.5 Components of the Packaging Relevant for the Confinement System

The confinement system consists of:

- The components of the containment system (see section 1.4.3)
- The interior CCS of the 30B-X cylinder
- The inner and outer shells of the DN30 PSP

### 1.4.6 Components of the Packaging Relevant for Thermal Protection

The following components of the DN30 PSP are relevant for thermal protection:

- The inner and outer shells
- The RTS 120 and RTS 320 foam
- The microporous thermal insulation layer between the inner shell and RTS 120 foam
- The intumescent material attached to the inside of the inner shell

### 1.4.7 Components of the Packaging Relevant for Heat Dissipation

Because of the very low level of thermal power, there is no dedicated component for heat dissipation.

### 1.4.8 Protection against Corrosion

All outer and interior surfaces of the DN30 PSP are made of austenitic stainless steel and, thus, are resistant to corrosion. There is no corrosion due to the interaction of the intumescent material or its glue, since the material is certified halogen-free (see [DNT 2019]).

Like standard 30B cylinders, the 30B-X cylinder is coated with high quality paint that prevents excessive corrosion on all outer surfaces. Corrosion at the interior surfaces of the 30B-X cylinder is negligible, which is proven by the long term and world-wide experience with standard 30B cylinders. Within the 5-year recertification period or when these cylinders are appropriately stored while loaded with $UF_6$ or heels, there is no excessive corrosion, which could impair the safety functions of these cylinders. Since the same operation and maintenance procedures apply to the 30B-X cylinder, the corrosion behavior of standard 30B cylinders can be directly transferred to the 30B-X cylinder.

### 1.4.9 Protection Against Contamination

All outer and interior surfaces of the DN30 PSP are made of austenitic stainless steel and, thus, are easy to decontaminate. Furthermore, the intumescent material is protected by an easy to decontaminate coating.

The 30B-X cylinder is coated with paint that can be easily decontaminated. In transport configuration, the surface of the 30B-X cylinder is not accessible from the outside.

### 1.4.10 Shock Absorbing Components of the Packaging

The following components of the DN30 PSP are relevant for shock absorption:

- The inner and outer shells
- The RTS 120 and RTS 320 foam
- The valve protecting device

### 1.4.11 Evaluation of the Impact of Aging Mechanisms

To take into account ageing mechanisms in the design of the DN30-X package, care has been taken to use materials with a long usage history.

#### 1.4.11.1 DN30 PSP

The DN30 PSP consists of an inner and outer shell of austenitic stainless steel enclosing a shock absorbing structure made of a kind of polisocyanurate foam and a thermal protection made of inorganic materials.

- There is no tensile stress during routine conditions of transport (except during handling) in any of the metallic parts of the DN30 PSP, hence for the austenitic stainless steel aging is not a topic. Fatigue analysis of all parts used during handling and tie-down is described in section 2.2.1.2.3 of [DNT 2019].
- Interaction of the austenitic stainless steel with the shock absorbing material and the thermal protection materials has been thoroughly investigated. It was concluded that due to the properties of the shock absorbing material (closed cell structure, free of acids and halogens) and of the thermal protection materials (inorganic materials, free of acids and halogens) no negative effects are to be considered.
- Aging of the shock absorbing material is taken into account by the testing of samples as described in section 1.9.2.3 of [DNT 2019].
- The inorganic materials used as thermal protection do not show any deterioration of their thermal properties during long term use. Aging is for these materials not a topic.

#### 1.4.11.2 30B-X cylinder

The design of the 30B-X cylinder is based on the 30B cylinder as standardized in [ANSI N14.1], which has been in world-wide use for decades. The 30B-X cylinder (including the CCS except for the $B_4C$ filling of the CCRs) is made of the same materials as the 30B cylinder. Hence, it can be safely assumed that aging mechanisms will have no significant impact on the 30B-X cylinder.

Regarding the $B_4C$ filling of the CCRs, the material is extremely heat resistant, and since it is in powder form, it is not vulnerable to mechanical pressure. There is no concern of long-term loss of efficacy from neutron absorption due to the low neutron fluxes that the material is exposed to.

### 1.4.12 Transport Concept

Generally, the DN30-X package is transported on dedicated flatracks. A maximum of four DN30-X packages can be mounted onto a 20’ flatrack using the holes in the feet and suitable bolts.

- The components of the DN30-X packaging relevant for lifting the package or packaging are described in section 1.4.2.4.
- The components of the DN30-X packaging relevant for tie-down are described in section 1.4.2.5.

## 1.5 Package Performance Characteristics

### 1.5.1 Main Design Principles

The DN30-X packaging consists of the DN30 PSP that accommodates the 30B-X cylinder. Both, the DN30 PSP and the 30B-X cylinder are designed by ONCS, where the 30B-X cylinder is specifically designed in accordance with [ANSI N14.1], fulfilling the same requirements as a standard 30B cylinder.

The 30B-X cylinder is primarily designed to be used as a pressure vessel in enrichment and fuel manufacturing plants to accept $UF_6$ from the enrichment process and to feed enriched $UF_6$ into the process at the fuel manufacturer's site. Depending on the design, $UF_6$ with enrichments up to 10 or 20 wt.-% $^{235}U$ in uranium are permissible for the 30B-10 or 30B-20 cylinder, respectively. The 30B-X cylinder provides the containment and the confinement function of the DN30-X package.

For public transportation, the 30B-X cylinder is protected by the DN30 PSP against mechanical and thermal impacts as defined in [10 CFR Part 71] and [49 CFR Part 173] or [SSR-6 2018] so that the containment and confinement function of the 30B-X cylinder are maintained under RCT, NCT and HAC.

### 1.5.2 Performance Characteristics

#### 1.5.2.1 Performance Characteristics under RCT

Under RCT, the main performance characteristics are:

- Safe handling of the DN30-X package
- Safe tie-down of the DN30-X package
- Adequate design for accelerations and vibrations to be routinely expected
- Easy handling operations under the environmental conditions to be routinely expected
- Resistance against corrosion
- Long term usability by considering temperatures and ambient conditions to be routinely expected

#### 1.5.2.2 Performance Characteristics under NCT

Under NCT, the main performance characteristics are:

- Protection of the 30B-X cylinder against the mechanical loads to be expected under NCT
- Limitation of deformations to fulfill the requirement regarding dose rate increase

#### 1.5.2.3 Performance Characteristics under HAC

Under HAC, the main performance characteristics are:

- Protection of the 30B-X cylinder against mechanical loads to be expected under HAC
- Protection of the 30B-X cylinder against the thermal loads to be expected under HAC

### 1.5.3 Assumptions Used for the Safety Analysis

#### 1.5.3.1 Containment Function

The containment function is provided by the 30B-X cylinder and its installed valve and plug. It is assumed that the containment function is preserved if:

- Following the tests prescribed in [10 CFR Part 71] §59(a)(2) or [SSR-6 2018] para. 685(b), there is no physical contact between the valve or plug and any other component of the packaging other than their original points of attachment.
- Following the test prescribed in [10 CFR Part 71] §73(c)(4) or [SSR-6 2018] para. 728, the valve and the plug remain leak-tight.

#### 1.5.3.2 Dose Rates

The shielding function is provided by the shell of the 30B-X cylinder and the inner and outer shells of the DN30 PSP. For RCT and NCT, the foam between the inner and outer shell of the DN30 PSP is credited as well.

For the proof that the increase of the dose rate after the mechanical tests simulating NCT does not exceed the limits specified in the regulations, the reduction of the wall thickness of the DN30 PSP due to deformation is considered.

#### 1.5.3.3 Criticality Safety

The following assumptions are made for the proof of criticality safety:

- There are no requirements on the content, neither on its arrangement within the 30B-X cylinder nor regarding the distribution of impurities.
- Based on section 1.5.3.1, the containment function of the 30B-X cylinder is maintained. The maximal amount of water ingress under HAC is less than 3 g (see section 2.6.2.4).
- When taking impacts from HAC into account, the steel shells of the DN30 PSP will maintain a total thickness of at least 10 cm in radial direction (around the mantle) and at least 8 cm in axial direction (on the valve/plug ends).
- The closure system has to ensure that the top and bottom half of the DN30 PSP remain connected during RCT, NCT and HAC.

## 1.6 Compliance with Regulatory Requirements

### 1.6.1 Compliance with 10 CFR Part 71

In this section, the compliance of the Type AF package design DN30-X with the regulatory requirements [10 CFR Part 71] for the packaging and transportation of radioactive material is shown. The order of the paragraphs in column 1 of the tables follows [10 CFR Part 71]. Whenever possible, reference to the corresponding paragraphs from the IAEA regulations [SSR-6 2018] is provided in column 2 because a large portion of the safety analysis for the DN30-X package in Part 2 is based on the already licensed DN30 package, whose safety analysis in [DNT 2019] and supplemental documentation frequently refer to the IAEA regulations [SSR-6 2018].

#### 1.6.1.1 10 CFR Part 71 – Subpart A to D – General Provisions, Exemptions and Application for Package Approval

| 10 CFR §71 | IAEA SSR-6 | Remarks |
|---|---|---|
| 4 *(fissile)* | 222 | There is only the fissile nuclide $^{235}U$ present in the content (see section 1.3). |
| 4 *(Type A)* | 428 | The DN30-X package complies with the DOT regulations in [49 CFR Part 173] (see section 1.6.2). |
| 15 | 417 | There are no exceptions by one of the provisions specified in this paragraph (see specification of contents in section 1.3). |
| 31 | - | The application for approval under [10 CFR Part 71] includes the following information:<br>(a) A package description in section 1.4 as required.<br>(b) A package evaluation in part 2 as required.<br>(c) A reference to a previously approved quality assurance program (see section 1.9). |
| 33(a) | - | A detailed description of the DN30-X packaging is provided in section 1.4. |
| 33(b) | - | A detailed description of the contents of the DN30-X package is provided in section 1.3. |
| 35(a) | - | A demonstration that the DN30-X package satisfies the standards specified in subparts E and F of [10 CFR Part 71] is given in part 2 of this SAR. |
| 35(b) | - | The criticality safety index for the DN30-X package is defined in section 1.2.4. |
| 35(c) | - | Special controls and precautions for the DN30-X regarding transport, loading, unloading, and handling are specified in section 1.7. For the DN30-X, there are no special controls required in case of an accident or delay. |

| 10 CFR §71 | IAEA SSR-6 | Remarks |
|---|---|---|
| 37 | 306 | The management system of ONCS for the design, fabrication, assembly, testing, maintenance, repair, modification, and use of the DN30-X package is audited and certified by the German competent authority (see section 1.9). Appendix 1.9.3 (Quality Assurance Program) shows compliance of this system with the requirements of [10 CFR Part 71] – Subpart H and contains the corresponding NRC approval. |
| 41 | 701 | The effects on the DN30-X package of the tests specified in 10 CFR §71.71 and the tests specified in 10 CFR §71.73 are evaluated by<br>(a) subjecting specimens to a specific test (see [DNT 2019], Appendix 2.2.1.2 and 2.2.2.2) and<br>(b) analysis and calculations (see [DNT 2019] and part 2 of this SAR). |

### 1.6.1.2 10 CFR Part 71 – Subpart E – Package Approval Standards

| General standards for all packages | | |
|---|---|---|
| **10 CFR §71** | **IAEA SSR-6** | **Remarks** |
| 43(a) | 636 | The smallest overall dimension of the DN30-X package is not less than 10 cm (see section 1.4). |
| 43(b) | 637 | The outside of the DN30-X package incorporates a seal, that is not readily breakable and that, while intact, is evidence that the package has not been opened by unauthorized persons (see section 1.4.2.3.8). |
| 43(c) | 641 | The containment system of the DN30-X package is defined in section 1.4.3. The containment system cannot be opened unintentionally as it is enclosed by the DN30 PSP, which in turn is securely closed by a positive fastening device during transport (see section 1.4.2.3.4).<br>The containment system cannot be opened by a pressure that may arise within the package, as it withstands a hydraulic strength test at a pressure of 2.76 MPa, which is much higher than the internal pressure under RCT and NCT (see section 2.2.2.3). |
| 43(d) | 614 | The design of the 30B cylinder is standardized in [ANSI N14.1]. This design is world-wide in use since decades. The 30B-X cylinder is made of the same kind of materials as the 30B cylinder. Hence, it can be assumed that there will be no significant chemical, galvanic, or other reaction among the packaging components and the package contents. |
| 43(e) | 615, 646 | The 30B-X cylinder with its valve is enclosed by the DN30 PSP during transport and, thus, is also protected against unauthorized operation. |

| General standards for all packages | | |
|---|---|---|
| **10 CFR §71** | **IAEA SSR-6** | **Remarks** |
| 43(f) | 648 | The DN30-X package is designed, constructed, and prepared for shipment so that under the tests simulating NCT specified in 10 CFR §71.71 there is:<br>(a) No loss or dispersal of the radioactive $UF_6$ content (see section 2.4).<br>(b) No significant increase (not greater than 20 %) in external surface radiation levels (see section 2.5.8.4).<br>(c) No substantial reduction in the effectiveness of the packaging. |
| 43(g) | (654) | The DN30-X package is designed, constructed, and prepared for transport so that in still air at 38 °C and in the shade, no accessible surface of the package has a temperature exceeding 50 °C so that a nonexclusive use shipment is possible (see section 2.3 and [DNT 2019], Appendix 2.2.2.3). |
| 43(h) | - | The DN30-X package does not incorporate a feature intended to allow continuous venting during transport. |

| Lifting and tie-down standards for all packages | | |
|---|---|---|
| **10 CFR §71** | **IAEA SSR-6** | **Remarks** |
| 45(a) | 608, 609 | (a) The lifting attachments, that are a structural part of the DN30-X package, are designed with a minimum safety factor of 3 against yielding when used to lift the package in the intended manner (see section 2.2.3.3).<br>(b) They are designed so that failure of any lifting device under excessive load does not impair the ability of the DN30-X package to meet other requirements of [10 CFR Part 71].<br>(c) Any other structural part of the DN30-X package that could be used to lift the package is rendered inoperable for lifting the package during transport (see section 1.4.2.4.2). |
| 45(b)(1) | 613 | Each tie-down device that is a structural part of the DN30-X package withstands the acceleration forces required by 10 CFR §71.45(b) without generating stresses in any material of the package in excess of its yield strength (see section 2.2.4.1). |
| 45(b)(2) | - | There are no other structural parts of the DN30-X package that could be used for tie-down of the package. |
| 45(b)(3) | 638 | Each tie-down device that is a structural part of the DN30-X package is designed so that failure of this device under excessive load does not impair the ability of the package to meet other requirements of [10 CFR Part 71] (see section 2.2.4.1). |

| External radiation standards for all packages | | |
|---|---|---|
| **10 CFR §71** | **IAEA SSR-6** | **Remarks** |
| 47(a) | 526, 527 | For all permissible contents in section 1.3, the transport index (TI) of the DN30-X package is below 10 (see section 2.5.8.1). Furthermore, the radiation level at the surface of each DN30-X package does not exceed 2 mSv/h under conditions normally incident to transportation (see section 2.5.8.2). |
| 47(b) | 528, 573 | The DN30-X package does not exceed the radiation level limits specified in 10 CFR §71.47(a). Hence, the radiation level limits in this paragraph do not apply to the DN30-X package. |

| General requirements for fissile material packages | | |
|---|---|---|
| **10 CFR §71** | **IAEA SSR-6** | **Remarks** |
| 55(a) | 673 | The DN30-X package is designed and constructed in accordance with 10 CFR §71.41 through 71.47. As a Type AF package design, 10 CFR §71.51 does not apply. |
| 55(b) | 676, 677, 679-682 | The DN30-X package is so designed and constructed and its contents so limited that even if water were to leak into the containment system, it remains subcritical. Under the following conditions, maximum reactivity of the fissile material is attained:<br>(1) The chemical form of $UF_6$ is well known. For the isotopic compositions, maximal values of the fissile nuclide $^{235}U$ are assumed. Physical form, mass, concentration of impurities, moderation ratio or density and geometrical configuration are varied to determine the maximum neutron multiplication factor. The variation calculations are documented in section 2.6.5 and Appendix 2.2.5 (Criticality Safety Analysis).<br>(2) For the individual DN30-X package in isolation, it is assumed that water can leak into the containment system and optimal moderation is assumed (see section 2.6.2.2).<br>(3) The analysis for an individual package in isolation assumes a layer of 30 cm water surrounding the DN30-X package (see section 2.6.2.2). |
| 55(c) | - | Does not apply to the DN30-X package. |

| General requirements for fissile material packages | | |
|---|---|---|
| **10 CFR §71** | **IAEA SSR-6** | **Remarks** |
| 55(d) | 678 | The DN30-X package is so designed and constructed, and its contents so limited that after being subjected to the tests simulating NCT:<br>(1) The content is subcritical (see section 2.6.6).<br>(2) The geometric form of the package content is not substantially altered (see section 2.2.5).<br>(3) In the evaluation of the undamaged package, optimal moderation is assumed (see section 2.6.2.2).<br>(4) There is no substantial reduction in the effectiveness of the DN30-X packaging (see section 2.2.5), including:<br>i. No more than 5 % reduction in the total effective volume of the packaging on which nuclear safety is assessed.<br>ii. No more than 5 % reduction in the effective spacing between the fissile content and outer surface of the packaging.<br>iii. No occurrence of an aperture in the outer surface of the packaging large enough to permit the entry of a 10 cm cube. |
| 55(e) | 676, 677, 679-682 | The DN30-X package is so designed and constructed, and its contents so limited that after being subjected to the tests simulating HAC the package remains subcritical. For this determination, it is assumed in section 2.6 that:<br>(1) The fissile material is in the most reactive credible configuration consistent with the damaged condition of the package and the chemical and physical form of the content.<br>(2) Water moderation occurs to the most reactive credible extent consistent with the damaged condition of the package and the chemical and physical form of the content.<br>(3) There is full reflection by water on all sides, as close as is consistent with the damaged condition of the package. |
| 55(f) | 683 | The DN30-X package shall not be transported by air. |
| 55(g) | 680(b) | The exception for packages containing uranium hexafluoride with a maximum enrichment of 5 wt.-% $^{235}U$ in cannot be credited for the DN30-X package. |

| Standards for arrays of fissile material packages | | |
|---|---|---|
| **10 CFR §71** | **IAEA SSR-6** | **Remarks** |
| 59(a)(1) | 684 | The number N derived for the DN30-X package is infinite. The proof of subcriticality under NCT is provided in section 2.6.5.3. |
| 59(a)(2) | 685 | The number N derived for the DN30-X package is infinite. The proof of subcriticality under HAC is provided in section 2.6.5.3. |
| 59(b) | 686 | For the DN30-X package, the following applies: CSI = 0 (see section 1.2.4). |
| 59(c) | - | For the DN30-X package, the CSI = 0 so that package may be shipped by a carrier in a nonexclusive use conveyance. |

#### 1.6.1.3 10 CFR Part 71 – Subpart F – Package, Special Form, and LSA-III Tests

| **Normal Conditions of Transport** | | |
|---|---|---|
| **10 CFR §71** | **IAEA SSR-6** | **Remarks** |
| 71(a) | 719 | See remarks to 10 CFR §71.71(c)(7)-(10) below. |
| - | 720 | The time interval between the water spray test and the subsequent tests has no impact on the performance of the subsequent tests (see remark to 10 CFR §71.71(c)(6)). |
| 71(b) | - | During the mechanical tests with DN30 prototypes in [DNT 2019], Appendix 2.2.1.2, the ambient temperature was about 20 °C and there was no internal pressure within the containment (the 30B cylinder) as this is the more unfavorable condition. In the structural analysis of the DN30-X package, ambient temperatures between -40°C and +38°C including insolation are considered (see section 2.2 and [DNT 2019], Appendix 2.2.1.3). |
| 71(c)(1)-(2) | - | The design of the DN30-X package considers ambient temperatures ranging from -40 °C to +38 °C including insolation (see section 2.2 and [DNT 2019], Appendix 2.2.1.3). |
| 71(c)(3)-(4) | - | The internal pressure in the 30B-X cylinder during transport is below atmospheric. As the 30B-X cylinder withstands the hydraulic strength test at a test pressure of 2.76 MPa, the containment is not affected by a reduction of ambient pressure to 25 kPa (see section 2.2.5.5).<br>Furthermore, the 30B-X cylinder is designed for an external pressure of 172 kPa so that the containment is not affected by an increased external pressure of 140 kPa absolute (see section 2.2.5.5). |
| 71(c)(5) | - | The package is designed to withstand effects of any acceleration, vibration or vibration resonance that may arise under NCT (see section 2.2.4). |
| 71(c)(6) | 721 | The DN30 PSP is a fully closed and welded structure of stainless steel. Any influence of the water spray test on the properties of the DN30-X package can be excluded (see section 2.2.5.1). |
| 71(c)(7) | 722, 717 | The free drop test is analyzed in sections 2.2.5.2 and 2.2.6. It was also carried out with DN30 prototypes as documented in [DNT 2019], Appendix 2.2.1.2. The target for the experimental drop tests and the drop test analyses complies with the requirements of [SSG-26 2012] para. 717.2. |
| 71(c)(8) | - | The corner drop from a height of 0.3 m is not applicable as the mass of the DN30-X package exceeds 100 kg. |
| 71(c)(9) | 723 | The shape of the packaging effectively prevents stacking. Nevertheless, the DN30-X successfully passes the compression test as demonstrated in section 2.2.5.3. |
| 71(c)(10) | 724 | The DN30-X package is designed to withstand HAC. The puncture test specified in 10 CFR §71.73(c)(3) is much more severe than the penetration test specified in this paragraph (see also section 2.2.5.4). |

| Hypothetical Accident Conditions | | |
|---|---|---|
| **10 CFR §71** | **IAEA SSR-6** | **Remarks** |
| 73(a) | 726 | DN30 prototypes used for testing were subject to the cumulative effects of twice the mechanical tests specified in 10 CFR §71.71(c)(7), followed by twice the tests specified in 10 CFR §71.73(c)(1)-(3), and finally followed by the thermal test specified in 10 CFR §71.73(c)(4) (see [DNT 2019], Appendix 2.2.1.2 and Appendix 2.2.2.2). |
| 73(b) | - | During the mechanical tests with DN30 prototypes the ambient temperature was about 20 °C and there was no internal pressure within the containment (the 30B cylinder) as this is the more unfavorable condition (see [DNT 2019], Appendix 2.2.1.2). In the structural analysis of the DN30-X package in section 2.2, ambient temperatures between -40°C and +38°C including insolation are considered. |
| 73(c)(1) | 727(a), 717 | The performance of the DN30-X package subject to the free drop test from a height of 9 m is analyzed in section 2.2.6. It is based on the analyses for the DN30 package in [DNT 2019], Appendix 2.2.1.2 and 2.2.1.3 where several free drop tests with DN30 prototypes from a height of 9 m onto a flat, essentially unyielding, and horizontal surface were performed, striking the surface in different orientations for which maximum damage is expected. The target for drop tests complied with the requirements of [SSG-26 2012] para. 717.2. |
| 73(c)(2) | 727 (c) | The dynamic crush test is not applicable as the mass of the DN30-X package exceeds 500 kg. |
| 73(c)(3) | 727 (b) | The performance of the DN30-X package subject to the puncture test is analyzed in section 2.2.6. It is based on the analyses for the DN30 package in [DNT 2019], Appendix 2.2.1.2 and 2.2.1.3. The requirements for the bar and the drop target were fulfilled in these tests. |
| 73(c)(4) | 728 | The analysis of the DN30-X package subject to the thermal test is based on thermal tests that were carried out using DN30 prototypes that suffered the cumulative effects of twice the mechanical tests specified in 10 CFR §71.71(c)(7) followed by twice the tests specified in 10 CFR §71.73(c)(1)-(3). The test results are documented and analyzed in [DNT 2019], Appendix 2.2.2.2 and 2.2.2.3. |
| 73(c)(5) | 731-733 | The immersion test for fissile material is not applicable to the DN30-X package as optimal moderation and full flooding is assumed in the criticality safety analysis. Furthermore, the test conditions defined in 10 CFR §71.73(c)(6) are more demanding for the DN30-X package. |
| 73(c)(6) | 729 | The water immersion test is analyzed in section 2.2.6.3. Inleakage of water during this test is taken into account in the criticality safety analysis (see section 2.6 and Appendix 2.6 (Criticality Safety Analysis)). The test conditions before the water immersion test still comply with the test conditions required by 10 CFR §71.55. |

#### 1.6.1.4 10 CFR Part 71 – Subpart G – Operating Controls and Procedures

| 10 CFR §71 | IAEA SSR-6 | Remarks |
|---|---|---|
| 83 | - | The chemical form of $UF_6$ is well known. For the isotopic compositions, maximal values of the fissile nuclide $^{235}U$ are assumed. Physical form, mass, concentration of impurities, moderation ratio or density, and geometrical configuration are varied to determine the maximum neutron multiplication factor. |
| 85(a) | 501(b)-(c) | The manufacturing specifications 0045-SPZ-2021-01 in Appendix 1.9.2 (Manufacturing Specification 30B-X Cylinder) and 0023-SPZ-2016-001 (see [DNT 2019]) as well as the testing requirements and controls before first use in section 1.7.1 ensure that there are no cracks, pinholes, uncontrolled voids, or other defects that could significantly reduce the effectiveness of the DN30-X packaging:<br>(a) The effectiveness of the containment is within the limits specified for the DN30-X package as the 30B-X cylinder is manufactured and tested before its first use to prove its compliance with [ANSI N14.1].<br>(b) The effectiveness of the confinement is within the limits specified for the DN30-X package as the applied measures ensure that the CCS of the 30B-X cylinder is present and in proper condition.<br>(c) The effectiveness of the shielding, structural and thermal protection are within the limits specified for the package as the applied measures ensure that the 30B-X cylinder and the DN30 PSP are in proper condition. |
| 85(b) | 501(a) | The MNOP for the DN30-X package is defined in section 1.2.8 with 152 kPa. Consequently, the requirements of this paragraph are fulfilled, as a hydraulic strength test at a test pressure of 2.76 MPa is performed for the 30B-X cylinder, which is the containment system of the DN30-X package (see section 2.2.2.3). |
| 85(c) | 501, 533 | The DN30-X packaging is conspicuously and durably marked on the nameplate with its model number, serial number, gross weight, and the package identification number assigned by the NRC (see section 1.4).<br>Before the model number is applied to a DN30-X packaging, it is determined whether the packaging has been fabricated in accordance with the design approved by the Commission (see section 1.7.1). |
| 87(a) | 502 | The analyses in part 2 of this SAR prove that the DN30-X package is properly designed for the contents specified in section 1.3. Furthermore, administrative controls ensure that only the contents as specified in the certificate of package approval are loaded into the DN30 PSP (see section 1.7.2). |
| 87(b) | - | The testing requirements and controls before each transport in section 1.7.2 ensure that the DN30-X package is in unimpaired physical condition except for superficial defects such as marks or dents. |
| 87(c) | - | The testing requirements and controls before each transport in section 1.7.2 ensure that the closure devices of the DN30-X package (including any required gasket) are properly installed and secured and free of defects. |
| 87(d) | - | The testing requirements and controls before each transport in section 1.7.2 ensure that during transport the $UF_6$ is in solid form. However, to make provisions for filling effects, the 30B-X cylinder is always filled to less than 60 % taking care of the significant expansion of $UF_6$ during its solid to liquid phase change in case the $UF_6$ is liquefied during filling or emptying. |

| 10 CFR §71 | IAEA SSR-6 | Remarks |
|---|---|---|
| 87(e) | - | Does not apply to the DN30-X package as no specific pressure relief devices are present in the package design. |
| 87(f) | 503(c) | The handling instructions defined in section 1.7.4 ensure that the DN30-X package is loaded and closed in accordance with written procedures. |
| 87(g) | 501(c) | The manufacturing specifications in Appendix 1.9.2 (Manufacturing Specification 30B-X Cylinder) and the testing requirements and controls before first use in section 1.7.1 ensure that the CCS of the 30B-X cylinder is present and in proper condition. The handling instructions defined in sections 1.7.3 and 1.7.4, the testing requirements and controls before each transport in section 1.7.2 and the prescribed inspections in section 1.8 ensure that the proper condition of the CCS is maintained throughout the life-time of a 30B-X cylinder. |
| 87(h) | 503(a) | The handling instructions defined in sections 1.7.3 and 1.7.4 take into account the respective measures. |
| - | 507 | Other dangerous properties of $UF_6$ are taken into account (see section 1.7.6). |
| 87(i) | 508 | Contamination checks defined in section 1.7.2 take the specified limits specified in DOT regulations in 49 CFR §173.443 into account. |
| 87(j) | - | The external radiation levels around the DN30-X package and around the vehicle do not exceed the limits specified in 10 CFR §71.47 at any time during transportation (see section 1.6.1.2). |
| 87(k) | 503(b) | The accessible DN30-X package surface temperatures do not exceed the limits specified in 10 CFR §71.43(g) at any time during transportation (see section 1.6.1.2). |
| 89 | - | Special instructions needed to safely open the DN30-X package are documented in handling instruction 0045-HA-2021-001 (see Appendix 1.7.1 (Handling Instruction)). The handling instruction will be made available to all users of the DN30-X package (see section 1.9.3). |

### 1.6.1.5 10 CFR Part 71 – Subpart H – Quality Assurance

| 10 CFR §71 | IAEA SSR-6 | Remarks |
|---|---|---|
| Subpart H (101 – 137) | 306 | The management system of ONCS is audited and certified by the German competent authority (see section 1.9). Appendix 1.9.3 (Quality Assurance Program) shows compliance of this system with the requirements of this subpart and contains the corresponding NRC approval. |

### 1.6.2 Compliance with 49 CFR Part 173

In this section, the compliance of the Type AF package design DN30-X with the regulatory requirements [49 CFR Part 173] for the transport of radioactive material is shown. The order of the paragraphs in column 1 of the tables follows [49 CFR Part 173]. Whenever possible, reference to the corresponding paragraphs from the IAEA regulations [SSR-6 2018] is provided in column 2 because a large portion of the safety analysis for the DN30-X package in part 2 is based on the already licensed DN30 package, whose safety analysis in [DNT 2019] and supplemental documentation frequently refer to the IAEA regulations [SSR-6 2018].

#### 1.6.2.1 Definitions and General Design Requirements

| **General design requirements** | | |
|---|---|---|
| **49 CFR §173** | **IAEA SSR-6** | **Remarks** |
| 2(a) | 507, 618 | Other dangerous properties of $UF_6$ are taken into account (see section 1.7.6). |
| 403 (fissile) | 222 | There is only the fissile nuclide $^{235}U$ present in the content (see section 1.3). |
| 410(a) | 607 | The DN30-X package can be easily handled and properly secured during transport (see sections 1.4.2.4 and 1.4.2.5). |
| 410(b) | 608, 609 | (a) The lifting attachments, that are a structural part of the DN30-X package, are designed with a minimum safety factor of 3 against yielding when used to lift the package in the intended manner (see section 2.2.3.3).<br>(b) They are designed so that failure of any lifting device under excessive load does not impair the ability of the DN30-X package to meet other requirements of 49 CFR Subpart I.<br>(c) Any other structural part of the DN30-X package that could be used to lift the package is rendered inoperable for lifting the package during transport (see section 1.4.2.4.2). |
| 410(c) | 610 | The external surfaces of the DN30-X package, as far as practicable, are free from protruding features and consist of stainless steel. Therefore, they are easily decontaminated (see section 1.4.2). |
| 410(d) | 611 | The outer layer of the package prevents the collection and retention of water (see section 1.4.2). |
| 410(e) | 612 | There are no features added to the package at the time of transport that could reduce its safety (see section 1.4.2.5). |
| 410(f) | 613 | The DN30-X package is designed to withstand the effects of any acceleration, vibration or vibration resonance that may arise under RCT or NCT without any deterioration in the effectiveness of the closing devices on the various receptacles or in the integrity of the DN30-X package as a whole and without loosening or unintentionally releasing the nuts, bolts, or other securing devices even after repeated use (see section 2.2.4). |

| **General design requirements** | | |
|---|---|---|
| **49 CFR §173** | **IAEA SSR-6** | **Remarks** |
| 410(g) | 614 | The DN30-X packaging consists mainly of the materials stainless steel and foam. Those are physically and chemically compatible with each other. Any part in contact with the radioactive $UF_6$ content has been designed for this purpose (see section 1.4.2). |
| 410(h) | 615 | The valve and the plug of the 30B-X cylinder are protected by the DN30 PSP during transport and cannot be operated unauthorized (see section 1.4.2). |
| - | 616 | The DN30-X package is designed to comply with the requirements for fissile material packages. It takes into account ambient temperatures and pressures that are likely to be encountered under RCT. |
| - | 617 | The radiation level at the surface of the DN30-X package does not exceed 2 mSv/h under conditions normally incident to transportation (see section 2.5.8.2). |
| 410(i) | 619-621 | The DN30-X package shall not be transported by air. |

### 1.6.2.2 Additional Design Requirements for Type A Packages

| **Additional design requirements for Type A packages** | | |
|---|---|---|
| **49 CFR §173** | **IAEA SSR-6** | **Remarks** |
| 412 | 635 | The DN30-X package meets the general design requirements prescribed in 49 CFR §173.410 and is also designed to meet the requirements prescribed in 49 CFR §173.412(a)-(l). |
| 412(a) | 637 | The outside of the DN30-X package incorporates a seal, that is not readily breakable and that, while intact, is evidence that the package has not been opened by unauthorized persons (see section 1.4.2.3.8). |
| 412(b) | 636 | The smallest overall dimension of the DN30-X package is not less than 10 cm (see section 1.4). |
| 412(c) | 639 | The design of the DN30-X packaging takes into account temperatures ranging from -40 °C to +70 °C (see section 1.4.1). Special attention is given to the potential degradation of the packaging materials within the temperature range. |
| - | 640 | The design and manufacturing techniques for the 30B-X cylinder are in accordance with ASME and ANSI standards.<br>The design and manufacturing techniques for the DN30 PSP are in accordance with ISO and EN standards. |

| **Additional design requirements for Type A packages** | | |
|---|---|---|
| **49 CFR §173** | **IAEA SSR-6** | **Remarks** |
| 412(d) | 641, 642, 643 | The containment system of the DN30-X package is defined in section 1.4.3. The containment system cannot be opened unintentionally as it is enclosed in the DN30 PSP, which in turn is securely closed by a positive fastening device during transport (see section 1.4.2.3.4).<br>The containment system cannot be opened by a pressure that may arise within the package, as it withstands a hydraulic strength test at a pressure of 2.76 MPa, which is much higher than the internal pressure under RCT and NCT (see section 2.2.2.3). |
| 412(e) | 644 | The design of the 30B cylinder is standardized in [ANSI N14.1]. This design is world-wide in use since decades. The 30B-X cylinder is made of the same kind of materials as the 30B cylinder. Hence, it can be assumed that there will be no significant radiolytic decomposition of materials or generation of gas by chemical reaction and radiolysis. |
| 412(f) | 645 | The pressure in the 30B-X cylinder during transport is below atmospheric pressure. As the 30B-X cylinder withstands a test pressure of 2.76 MPa, the containment is not affected by a reduction of ambient pressure to 60 kPa. |
| 412(g) | 646 | The 30B-X cylinder with its valve is enclosed by the DN30 PSP during transport. |
| 412(h) | 647 | The 30B-X cylinder is enclosed in the DN30 PSP, which is securely closed by a positive fastening device (see section 1.4.2). |
| 412(i) | 638 | Each tie-down device that is a structural part of the DN30-X package is designed so that failure of this device under excessive load does not impair the ability of the package to meet other requirements of 49 CFR Subpart I (see section 2.2.4.1). |
| 412(j) | 648 | When evaluated against the performance requirements of this section and the tests specified in 49 CFR §173.465, the DN30-X packaging prevents:<br>(1) Loss or dispersal of the radioactive $UF_6$ contents (see section 2.4).<br>(2) A significant increase (more than 20 %) in the radiation levels recorded or calculated at the external surfaces for the condition before the test (see section 2.5.8.4). |
| 412(k)(1) | 649 | During transport the $UF_6$ is in solid form. However, to make provisions for filling effects, the 30B-X cylinder is always filled to less than 60 % taking care of the significant expansion of $UF_6$ during its solid to liquid phase change in case the $UF_6$ is liquefied during filling or emptying. |
| 412(k)(2) | 650 | Not applicable to the DN30-X package as during transport the $UF_6$ is in solid form. |
| 412(l) | 651 | Not applicable to the DN30-X package as during transport the $UF_6$ is in solid form. |

### 1.6.2.3 Authorized Type A and Fissile Material Packages

| 49 CFR §173 | IAEA SSR-6 | Remarks |
|---|---|---|
| 415 | - | The DN30-X is a Type AF packaging that meets the applicable standards for fissile materials in 10 CFR Part 71 and is used in accordance with 49 CFR §173.471. |
| 417 | - | The DN30-X is a Type AF packaging that meets the applicable standards for fissile material packages in 10 CFR Part 71. |

### 1.6.2.4 Uranium Hexafluoride

| 49 CFR §173 | IAEA SSR-6 | Remarks |
|---|---|---|
| - | 420 | The contents of the DN30-X package comply with the following requirements:<br>(a) The permissible mass of $UF_6$ is specified for the 30B-X cylinder in section 1.3.2.1.<br>(b) The permissible mass of $UF_6$ considers a minimal ullage of 5 % at the maximum temperature of the DN30-X package.<br>(c) When presented for transport, the $UF_6$ is in solid form and the internal pressure is below atmospheric pressure. |
| 420(a) | 420, 631, 632, 718 | (1) In addition to the other applicable requirements of 49 CFR Subpart I, the following is considered for the DN30-X package with regard to its $UF_6$ content:<br>(2) Before initial filling and during periodic inspection and test, the 30B-X cylinder is cleaned in accordance with [ANSI N14.1].<br>(3) The 30B-X cylinder is designed, fabricated, inspected, tested and marked in accordance with [ANSI N14.1] in effect at the time the 30B-X cylinder was manufactured.<br>(4) The DN30-X package is designed so that it will:<br>(i) Withstand a hydraulic strength test at an internal pressure of 2.76 MPa without leakage (see section 2.2.2.3).<br>(ii) Withstand the test specified in 49 CFR §173.465(c) without loss or dispersal of the $UF_6$ (see section 2.2.5).<br>(iii) Withstand the test specified in 10 CFR §71.73(c)(4) without rupture of the containment system (see section 2.2.6).<br>(5) The testing requirements and controls before each transport in section 1.7.2 ensure that during transport, the $UF_6$ is in solid form.<br>(6) The volume of the solid $UF_6$ content does not exceed 61 % of the certified volumetric capacity of the 30B-X cylinder at 20 °C to take care of the significant expansion of $UF_6$ during its solid to liquid phase change in case the $UF_6$ is liquefied during filling or emptying.<br>(7) The testing requirements and controls before each transport in section 1.7.2 ensure that during transport, the internal pressure in the 30B-X cylinder is below atmospheric pressure (less than 101.3 kPa at 20 °C). |
| - | 633 | The DN30-X package has no pressure relief valves. |

| 49 CFR §173 | IAEA SSR-6 | Remarks |
|---|---|---|
| - | 634 | Does not apply to the DN30-X package. |
| 420(b) | - | The inspections prescribed in section 1.8 ensure that the DN30-X package is periodically inspected, tested, marked and otherwise conform with [ANSI N14.1]. |
| 420(c) | - | Each repair to a 30B-X cylinder is performed in accordance with [ANSI N14.1] (see section 1.9.4). |
| 420(d)-(e) | 401, 419 | For the DN30-X package, the UN number UN 2977 shall be assigned. |

### 1.6.2.5 Activity Limits, Radiation Level and Thermal Limitations, Contamination Control and Transportation

| 49 CFR §173 | IAEA SSR-6 | Remarks |
|---|---|---|
| 431(a) | 429 | The activity in a DN30-X package licensed as Type AF package is limited to $1A_2$ (see section 1.3.2.5). |
| 433(d) | 430 | For mixtures of radionuclides, the respective formula is applied. |
| 441 | 527, 617 | For all permissible contents in section 1.3, the transport index (TI) of the DN30-X package is below 10 (see section 2.5.8.1). Furthermore, the radiation level at the surface of each DN30-X package does not exceed 2 mSv/h under conditions normally incident to transportation (see section 2.5.8.2). |
| 442 | (654), 679 | The DN30-X package is designed, constructed, and prepared for transport so that in still air at 38 °C and in the shade, no accessible surface of the package has a temperature exceeding 50 °C so that a nonexclusive use shipment is possible (see section 2.3 and [DNT 2019], Appendix 2.2.2.3). |
| 447 | 568 | For the DN30-X package, the CSI = 0 in all cases and, thus, also for groups of DN30-X packages the sum of the CSIs is 0. |
| - | 569 | Not applicable to the DN30-X package as the CSI = 0 in all cases. |
| - | 570 | Not applicable as the material defined in section 1.3 does not meet any of the provisions in 49 CFR §173.453. |
| 448(a) | 564 | The DN30-X package is transported by road, rail or sea on dedicated flat racks. The tie-down features of the package are designed such that shifting of the package during normal transportation conditions is prevented. |
| 448(b) | 565 | Not applicable to the DN30-X package. |
| 448(c) | 563 | Not applicable to the DN30-X package. |
| 448(d)-(g) | - | Not applicable to the DN30-X package. |
| - | 566(b) | The radiation level of a conveyance of several packages is below 2 mSv/h at any point of the external surface and below 0.1 mSv/h at 2 m distance from the external surface (see section 2.5.8.3). |

| 49 CFR §173 | IAEA SSR-6 | Remarks |
|---|---|---|
| 453 | 417 | There are no exceptions by one of the provisions specified in this paragraph (see specification of contents in section 1.3). |
| 457 | 525-528 | (a) A CSI and a TI in accordance with 49 CFR §173.403 will be assigned to the DN30-X package.<br>(b) The DN30-X package satisfies the radiation level restrictions of 49 CFR §173.441(a).<br>(c) For the DN30-X package, the CSI = 0 so that package may be shipped by a carrier in a nonexclusive use conveyance.<br>(d) For the DN30-X package, the CSI = 0 in all cases and, thus, also for groups of DN30-X packages the sum of the CSIs is 0.<br>(e) See (c).<br>(f) See (b).<br>(g) See 49 CFR §173.447.<br>(h) See section 1.6.2.7. |
| 459 | - | Not applicable to the DN30-X package. |

#### 1.6.2.6 Test Procedures

| General test procedures | | |
|---|---|---|
| **49 CFR §173** | **IAEA SSR-6** | **Remarks** |
| 461 | 701 | For the demonstration of compliance, the following methods are used:<br>(1) Performance of tests with DN30 prototypes (see [DNT 2019], Appendix 2.2.1.2 and 2.2.2.2).<br>(2) Analysis and calculations for the DN30-X package in part 2 of this SAR that refer to the analyses for the DN30 package in [DNT 2019]. |
| - | 702 | The DN30 prototypes used for the tests were assessed before and after the tests according to written procedures (see [DNT 2019], Appendix 2.2.1.2 and 2.2.2.2). |
| 462(a) | 713 | The DN30 prototypes used for the tests were inspected before each test according to a written procedure. The results of the inspection were documented. The inspection comprised at least:<br>(a) Divergence from the design<br>(b) Defects in manufacture<br>(c) Corrosion and deterioration<br>(d) Distortion of features<br>The inspection procedures are specified in [DNT 2019], Appendix 2.2.1.1 and 2.2.2.1. |

| **General test procedures** | | |
|---|---|---|
| **49 CFR §173** | **IAEA SSR-6** | **Remarks** |
| 462(b) | - | The deviations from the specified design for the DN30 PSP were taken into account in the subsequent evaluation of the DN30 package in [DNT 2019]. |
| 462(c) | 714 | The containment system of the DN30-X package is defined in section 1.4.3. |
| 462(d) | 715 | The DN30 prototypes used for the tests were marked with a serial No. and, therefore, could be easily referenced (see [DNT 2019], Appendix 2.2.1.1 and 2.2.2.1). |
| - | 716 | The results of the tests with DN30 prototypes were recorded, documented and assessed with respect to their influence on the integrity of the containment and confinement system (see [DNT 2019], Appendix 2.2.3.1 and 2.2.5). |

| **Type A packing tests and tests for demonstrating the ability of fissile materials packagings to withstand accident conditions in transportation** | | |
|---|---|---|
| **49 CFR §173** | **IAEA SSR-6** | **Remarks** |
| 465(a) | 719 | See 49 CFR §173.465(b)-(e). |
| 465(b) | 720,721 | The DN30 PSP is a fully closed and welded structure of stainless steel. Any influence of the water spray test on the properties of the DN30-X package can be excluded (see section 2.2.5.1). |
| 465(c) | 722 | The free drop test is analyzed in sections 2.2.5.2 and 2.2.6. It was also carried out with DN30 prototypes as documented in [DNT 2019], Appendix 2.2.1.2. The target for the experimental drop tests and the drop test analyses complies with the requirements of [SSG-26 2012] para. 717.2. |
| 465(c)(2) | - | The impact from preceding 0.3 m corner drops is estimated to be negligible for the DN30-X package (see section 2.2.5.2). |
| 465(c)(5) | 717 | The target for drop tests complies with the requirements of [SSG-26 2012] para. 718.2. |
| 465(d) | 723 | The shape of the packaging effectively prevents stacking. Nevertheless, the DN30-X successfully passes the compression test as demonstrated in section 2.2.5.3. |
| 465(e) | 724 | The DN30-X package is designed to withstand HAC. The puncture test (drop onto a bar) specified in 10 CFR §71.73(c)(3) is much more severe than the penetration test specified in this paragraph (see also section 2.2.5.4). |
| 466 | 725 | Not applicable as during transport, the $UF_6$ content is in solid form. |
| 467 | 726-733 | The DN30-X package meets the test requirements prescribed in 10 CFR Part 71 for the ability to withstand accident conditions in transportation (see section 1.6.1.3). |

| **Quality control for constructing of packaging and quality control requirements prior to each shipment** | | |
|---|---|---|
| **49 CFR §173** | **IAEA SSR-6** | **Remarks** |
| 474 | 501, 501(b) | The manufacturing specifications 0045-SPZ-2021-001 in Appendix 1.9.2 (Manufacturing Specification 30B-X Cylinder) and 0023-SPZ-2016-001 (see [DNT 2019]) as well as the testing requirements and controls before first use in section 1.7.1 ensure that:<br>(a) The DN30-X packaging meets the design and construction requirements as specified in 49 CFR Subpart I.<br>(b) The effectiveness of the shielding and containment are within the limits specified for the package. The DN30-X packaging has no dedicated component for heat dissipation because of the very low level of thermal power. |
| 475(a) | 502 | The administrative controls before shipment in section 1.7.2 ensure that only the contents as specified in the certificate of package approval are loaded into the DN30-X packaging. |
| 475(b) | - | The DN30-X packaging is in unimpaired physical condition, except for superficial marks. |
| 475(c) | - | Each closure device of the DN30-X packaging, including any required gasket, is properly installed, secured, and free of defects. |
| 475(d) | 501(c) | The manufacturing specification in Appendix 1.9.2 (Manufacturing Specification 30B-X Cylinder) and the testing requirements and controls before first use in section 1.7.1 ensure that the CCS of the 30B-X cylinder is present and in proper condition. The handling instructions defined in sections 1.7.3 and 1.7.4, the testing requirements and controls before each transport in section 1.7.2 and the prescribed inspections in section 1.8 ensure that the proper condition of the CCS is maintained throughout the life-time of a DN30-X package. |
| 475(e) | | Each special instruction for filling, closing, and preparation of the packaging for shipment has been followed. |
| 475(f) | 503(c) | Each closure, valve, or other opening of the containment system through which the radioactive content might escape is properly closed and sealed. |
| 475(g) | - | Not applicable to the DN30-X package. |
| 475(h) | - | The internal pressure of the containment system will not exceed the design pressure during transportation. |
| 475(i) | - | External radiation and contamination levels are within the allowable limits specified in 49 CFR Subpart I. |
| 476 | 803 | Not applicable to the DN30-X package. |

### 1.6.2.7 Additional Requirements Relating to Transport by Vessel

| 49 CFR §176 | IAEA SSR-6 | Remarks |
|---|---|---|
| 704(a) | 566 (b) | The radiation level of a conveyance of several packages is below 2 mSv/h at any point of the external surface and below 0.1 mSv/h at 2 m distance from the external surface (see section 2.5.8.3). |
| 704(b) | 575 | The radiation level at the surface of each package is below 2 mSv/h (see section 2.5.8.3). |

## 1.7 Operation

Operation is subdivided into four lifetime phases of the DN30-X packaging:

1. Testing and controls before its first use,
2. Regular usage and testing and controls before each transport,
3. Periodical inspection in defined intervals,
4. Repairs to return the DN30-X packaging to service.

All these phases are regulated in manufacturing specifications, handling and test instructions as specified below. At the time of application of these specifications and instructions, the user must make sure that valid revisions of these specifications and instructions are available.

### 1.7.1 Testing Requirements and Controls before first Use

The testing requirements and controls before the first use of the packaging are specified in:

- Specification 0045-SPZ-2021-001 for the 30B-X cylinder (see Appendix 1.9.2 (Manufacturing Specification 30B-X Cylinder))
- Specification 0023-SPZ-2016-001 for the DN30 PSP (see [DNT 2019])

### 1.7.2 Testing Requirements and Controls before each Transport

The testing requirements and controls before each transport are described in:

- Section 1.7.2.1 for the 30B-X cylinder
- Section 1.7.2.2 for the DN30 PSP
- For annual and 5-year inspection requirements as well as treatment of non-conformances and deviations see section 1.8.

#### 1.7.2.1 Inspection of the 30B-X Cylinder

Before filling the 30B-X cylinder, inspections in accordance with [ANSI N14.1] and at least as described in [USEC 651] (or in equivalent plant specific instructions) shall be carried out:

- The 30B-X cylinder shall be handled and filled in accordance with [ANSI N14.1] and at least as described in [USEC 651].
- The 30B-X cylinder has a valid maintenance certificate (valid date on the 30B-X cylinder's nameplate).
- 30B-X cylinders that have not been inspected and tested within the required 5-year period shall not be refilled until they are properly reinspected and retested. Prior to shipment, 30B-X cylinders that have not been recertified within the 5-year requirement shall be visually inspected for degradation of the cylinder wall. Any questionable conditions should be investigated. Details on the visual inspection are provided in 0045-PA-2021-001 (see Appendix 1.8 (Inspections of 30B-X Cylinders)).

- Any defective condition must be corrected before filling according to the requirements of [ANSI N14.1]:
  - The 30B-X cylinder shall be routinely examined as received and prior to sampling, withdrawal, filling, or shipping to ensure that it remains in a safe and usable condition.
  - Leakage, cracks, excessive distortion, bent or broken valves or plugs, broken or torn skirts, or other conditions that may affect the safe use of the cylinder shall warrant appropriate precautions, including removing the cylinder from service until the defective condition is satisfactorily corrected.
  - Questionable conditions should be referred to a qualified inspector for evaluation and for recommendations concerning use, repair, or condemnation of the cylinder in question.
  - Conditions of the 30B-X cylinder that might indicate excessive damage of the CCS, such as severe outer damages of the cylinder shell or skirts, should be referred to a qualified inspector. Reuse of such cylinders is only allowed after internal inspection of such cylinders and proof that the CCS is undamaged.
- Before filling, the cylinder is weighted to establish the net weight of the heels to ensure the fill limit will not be exceeded.
- To avoid overfilling, the 30B-X cylinder shall be weighted after being filled.

Before loading into the DN30 PSP, the inspection of the 30B-X cylinder should be carried out in accordance with [ANSI N14.1], and at least as described in [USEC 651] (or in equivalent plant specific instructions):

- The content of the 30B-X cylinder has to comply with the certificate of approval of the DN30-X package.
- Before shipping, the 30B-X cylinder shall be inspected for leak-tightness, damage, as well as other unacceptable conditions.
- $UF_6$ shall be shipped only in solid form and when the vapor pressure within the 30B-X cylinder is below atmospheric.
- The safe state of the 30B-X cylinder shall be recorded by the $UF_6$ supplier and the record shall be provided to the shipper.

Special care has to be taken to ensure that the filled cylinder fulfills the leak-tightness criteria of [ANSI N14.1] and the following requirements:

- The leak tightness of the valve seat of a filled cylinder shall be verified by leakage rate testing of the pigtail before disconnection and after closing the cylinder valve seat.
- As specified in section 1.2.9, a leakage rate larger than $L_{\mathrm{N}} = 1 \cdot 10^{-4}\ \mathrm{Pa \cdot m^3/s}$ shall not be permitted.
- The leakage test method shall comply to [ANSI N14.5] or [ISO 12807].
- If air is used for a pressure drop test, the air supply should be clean, dry and free from oil. If it is not, or if the quality of the air supply is uncertain, the test should be performed with nitrogen to ensure reliable results.

- Alternatively, a vacuum test may be performed by attaching a pigtail to the closed cylinder valve and drawing a vacuum.

  *Note: the cylinder's outer surface shall be approximately at ambient temperature and its vapor pressure below atmospheric pressure.*

#### 1.7.2.2 Inspection of the DN30 PSP

The inspection of the DN30 PSP is already described in the safety analysis of the licensed DN30 package. Therefore, the following is a replication of the prescribed inspections provided in [DNT 2019].

The DN30 PSP shall be inspected prior to loading according to handling instruction 0045-HA-2021-001 (see Appendix 1.7.1 (Handling Instruction)). The inspection comprises:

- A visual inspection
- A functional test of all movable parts

Following observations shall be cause for further investigation, replacement of parts or rejection of the DN30 PSP as specified in detail in test instruction 0023-PA-2015-016 (see [DNT 2019]):

- Structural changes of exterior or interior shells like excessive deformations, cracks, holes, etc.
- Excessive damage of flange areas
- Missing or damaged marking of the DN30 PSP
- Missing or damaged thermal plugs
- Missing or damaged gasket
- Damage of the mortise-and-tenon closure system
- Missing or damaged seals
- Damage of the valve protecting device as well as functional issues
- Damage of the rotation preventing device as well as functional issues
- Excessive wear and tear of the intumescent material
- Damage to any welding seams like cracks, holes, excessive corrosion
- Excessive damage of handling devices
- Excessive damage of the silicon pads

Test instruction 0023-PA-2015-016 contains in detail the criteria and measures in case of deviations during the visual inspections and functional tests. Measures could comprise cleaning, replacement of parts, minor repairs (on site) and major repairs (to be carried out by the license holder or an authorized repair shop qualified for such repair).

### 1.7.3 Handling and Tie-down Requirements

Handling of the DN30-X package, the DN30-X packaging and also its parts is described in section 1.4.2.4. For the handling operations, adequate means as described in the handling instruction 0045-HA-2021-001 (see Appendix 1.7.1 (Handling Instruction)) have to be used.

Tie-down of the DN30-X package and packaging is described in section 1.4.2.5. The procedures to be applied to ensure proper tie-down are specified in the handling instruction 0045-HA-2021-001 (see Appendix 1.7.1 (Handling Instruction)).

### 1.7.4 Loading Procedures for the 30B-X Cylinder and the DN30 PSP

Before each use, the 30B-X cylinder and the DN30 PSP shall be inspected as described in section 1.7.2.1 and section 1.7.2.2, respectively.

#### 1.7.4.1 Filling, Emptying and Washing of the 30B-X Cylinder

Filling with $UF_6$, and emptying and washing of 30B-X cylinders is described in site-specific operating handbooks that are not part of this SAR. Here, only those aspects are mentioned that are relevant regarding the transportation of 30B-X cylinders and what design features have been incorporated in the 30B-X cylinder to ensure that the presence of the interior CCS within the 30B-X cylinder does not adversely affect its operations.

##### 1.7.4.1.1 Transportation of Filled 30B-X Cylinders or 30B-X Cylinders Containing Heel Quantities

With regard to transportation of filled 30B-X cylinders or 30B-X cylinders containing heel quantities the following has to be taken into account:

- Before transport, it must be assured that the 30B-X cylinder was given ample time for cooling down such that the $UF_6$ is in solid form.
- The testing and controls described in section 1.7.2 shall be performed and documented prior to loading a 30B-X cylinder into the DN30 PSP.
- Any 30B-X cylinder filled with either $UF_6$ or heels from $UF_6$ shall comply with the transport regulatory requirements for $UF_6$.

##### 1.7.4.1.2 Filling of 30B-X Cylinders

With regard to the filling of 30B-X cylinders, the following has been considered in the design of the 30B-10 and 30B-20 cylinder:

- Today's standard filling procedures for already existing $UF_6$ cylinders use gaseous $UF_6$. Prior to filling, the pressure within a 30B-X cylinder is close to vacuum so that a stable gaseous flow of $UF_6$ is entering the cylinder through the valve. Distribution of the gaseous $UF_6$ within the 30B-X cylinder is hardly affected by the addition of the internal CCS as the minimal effective cross section of the cavity of the 30B-10 and 30B-20 cylinder still amounts to 48 % and 40 % of the standard 30B cylinder, respectively (see table 1-13).
- During filling, the outer surfaces of $UF_6$ cylinders are usually cooled. This causes the gaseous $UF_6$ to change to its solid form when it contacts the cylinder shell. With continued filling, more and more $UF_6$ is changing phase, building a layer of $UF_6$ at the cylinder shell. This subsequently increases the pressure in the cylinder, without affecting the stable flow of gaseous $UF_6$. Generally, the same applies to the 30B-X cylinder:
  - The distribution of the gaseous $UF_6$ within the 30B-X cylinder is not affected by the presence of the interior CCS.

  - The gaseous $UF_6$ entering the 30B-X will slowly heat up the interior CCS as there is no fixed connection between the pressure envelope of the 30B-X cylinder and the interior CCS that would enable sufficient cooling of the lattice holders or even the CCRs. Hence, a layer of $UF_6$ is primarily built at the 30B-X cylinder shell as well, and the filling process is expected to be identical to a standard 30B cylinder.
  - Nevertheless, to optimize the flow of gaseous $UF_6$ into the 30B-X cylinder, the two CCRs that are located in front of the valve and the plug have been shortened by 60 mm, respectively.
- Overfilling of 30B-X cylinders is avoided by measuring the 30B-X cylinder weight during filling, using a calibrated scale. As long as the gross weight is not exceeded, the 30B-X cylinder is compliant with its fill limits (see table 1-13). If a 30B-X cylinder has been found to be overfilled, the same procedures as for a standard 30B cylinder can be used to remove the excess in $UF_6$.

#### 1.7.4.1.3 Emptying of 30B-X Cylinders

With regard to the emptying of 30B-X cylinders, the following has been considered in the design of the 30B-10 and 30B-20 cylinder:

- Emptying of the 30B-X cylinder is generally identical to the standard 30B cylinder.
- For emptying, the 30B-X cylinder is heated so that the $UF_6$ within the cylinder changes to its gaseous form, and as all parts of the emptying system are insulated and heated, the $UF_6$ remains in the gas phase during emptying. Hence, the reduced effective cross sections of the 30B-10 and 30B-20 cylinder in comparison to a standard 30B cylinder hardly affect the emptying operation.
- However, the established site-specific emptying process has to ensure that the 30B-X cylinder is heated appropriately taking into account the increased heat sink due to the interior CCS within the 30B-X cylinder. The 30B-X cylinder valve shall not be opened when solid $UF_6$ is still present within the 30B-X cylinder to avoid that solid $UF_6$ could plug the cylinder valve.
- Furthermore, the established site-specific emptying process for the 30B-X cylinder may require lower evacuation speeds of the gaseous $UF_6$ in comparison to a standard 30B cylinder to avoid that the $UF_6$ changes to its solid form because of sudden pressure drops.
- As the minimum ullage at 121 °C is significantly larger for 30B-X cylinders in comparison to the standard 30B cylinder, the safety margins against hydraulic rupture of the pressure envelope during heating are increased compared to a standard 30B cylinder.
- Reducing cylinder heels may also be accomplished as for standard 30B cylinders (e.g. by using cold traps).

#### 1.7.4.1.4 Washing of 30B-X Cylinders

For washing of 30B-X cylinders, the same precautions apply as for standard 30B cylinders. Similar to the filling and emptying operations, these are described in site-specific operating handbooks that are not part of this SAR. Nevertheless, there are some additional aspects that need to be considered for washing of 30B-X cylinders:

- For the standard 30B cylinder, several washing procedures exist, but for the 30B-X cylinder only the tilt-roll method is suitable, which is due to the presence of the interior CCS within the 30B-X cylinder. Rolling the 30B-X cylinder constantly changes the contact points between the 30B-X cylinder shell and the interior CCS so that the wash solution reaches all interior surfaces.
- In contrast to the standard 30B cylinder, the amount of wash solution that can be used to clean a 30B-X cylinder is not limited by criticality safety aspects, as safe subcriticality is maintained even for optimal moderation with water. Accordingly, adding a boron solution into the 30B-X cylinder is not required to maintain safe subcriticality.
- The amount of wash solution that can be added into the 30B-X cylinder might be limited by other aspects than criticality safety (e.g. the heavy reaction of $UF_6$ with water). Therefore, the amount of solution that can be added into a 30B-X cylinder shall be specified in the site-specific operating handbook.
- Great care is required when syphoning the contaminated wash solution from the 30B-X cylinder into a container. Depending on the level of enrichment in $^{235}U$, the amount of solution that can be syphoned into a container might have to be reduced. The size of the container shall be specified in the site-specific operating handbook.
- Because of the presence of the interior CCS within the 30B-X cylinder, longer or more wash cycles might be required in comparison to the standard 30B cylinder to achieve the uranium concentration in samples specified in the site-specific operating handbook.
- The same applies to the removal of oil within the 30B-X cylinder.
- Finally, the interior inspection with a borescope might require more time.

Other than that, the washing procedure is similar to that for a standard 30B cylinder and, thus, consists of the following steps:

1. Check the weight of the 30B-X cylinder before the wash solution is added.
2. Transfer the 30B-X cylinder from the storage area to the tilt-roll stand.
3. Connect the 30B-X cylinder valve to a container, using appropriate hoses and fittings.
4. Add 20 liter of wash solution to the container.
5. Check the internal pressure by slightly opening the cylinder valve. If a positive pressure is experienced (appearance of bubbles in the hose), the cylinder valve must be closed, and the internal pressure must be reduced (e.g. by cooling the cylinder).
6. When no positive pressure is evident, the cylinder valve can be opened, allowing the wash solution to enter the 30B-X cylinder.
7. Close the cylinder valve and disconnect the hose.
8. Rotate and tilt the 30B-X cylinder for 10 minutes to hydrolyze the uranium compounds.
9. Remove the cylinder valve or plug.

10. Siphon the solution into a criticality safe container as specified by the site-specific operating handbook.
11. Repeat steps (4), (8), and (10) three times more and subsequently increase the amount of wash solution that is added into the 30B-X cylinder:
    - Add 50 liter of wash solution for the second wash cycle.
    - Add 100 liter of wash solution for the third wash cycle.
    - Add half the certified volume of the 30B-X cylinder plus 5 % $(1.05 \cdot V_{\text{certified}}/2)$ of wash solution for the fourth wash cycle.

    This procedure ensures that all CCRs are appropriately cleaned.
12. After the fourth wash cycle, sample the solution for total uranium concentration.
13. Repeat the water-solution wash, cylinder rotation, siphoning, and sampling until the uranium concentration is compliant with the site-specific operating handbook.
14. Using a borescope, visually inspect the interior of the 30B-X cylinder for any accumulations of uranium-bearing compounds.
15. Apply steam to the interior of the 30B-X cylinder for approximately 2 to 3 hours. Discard steam condensate solution. Provide local exhaust control to prevent atmospheric contamination.
16. Use the borescope to ascertain that the 30B-X cylinder has been completely cleaned.
17. Ensure that no hydrocarbons are present in the cylinder. If hydrocarbons are present in the cylinder remove those according to the site-specific operating handbook.
18. Steam the 30B-X cylinder for 10 to 20 minutes.
19. Rotate the 30B-X cylinder and siphon the condensate through the valve opening.
20. Dry the interior of the 30B-X cylinder with filtered dry air until the moisture content of the air in the 30B-X cylinder is less than -35 °C dew point.
21. Visually inspect the interior of the 30B-X cylinder with the borescope to ascertain that it is clean and dry.
22. Replace the valve, tag the 30B-X cylinder as being cleaned and washed, and transfer it to storage.



#### 1.7.4.2 Loading of the 30B-X Cylinder into the DN30 PSP

Loading of a 30B-X cylinder into the DN30 PSP is identical to loading a standard 30B cylinder into the DN30 PSP. Therefore, the following list of safety related loading steps is adopted from the description provided in [DNT 2019]:

1. The lever of the rotation preventing devices are in position “open”.
2. The valve protecting device and its housing are in position “open”.
3. Lower the 30B-X cylinder in horizontal orientation with the valve in 12°o’clock position into the bottom half of the DN30 PSP.

4. When the lower rim of the cylinder skirt has passed the valve protecting device, rotate the valve protecting device towards the cylinder head by about 90° until it gets in contact with the cylinder head. Then lower the cylinder until it rests on the inner shell of the bottom half of the DN30 PSP. Then push the housing in position “closed”.
5. Move the lever of the rotation preventing devices to position “closed”.
6. Lower the top half of the DN30 PSP onto the bottom half.
7. Insert the pins into the six mortise-and-tenon closure devices and fix the pins with the securing bolts.
8. Install the seals.

Details on each loading step are specified in handling instruction 0045-HA-2021-001 (see Appendix 1.7.1 (Handling Instruction))

#### 1.7.4.3 Unloading of the 30B-X Cylinder from the DN30 PSP

Unloading of a 30B-X cylinder from the DN30 PSP is identical to unloading a standard 30B cylinder from the DN30 PSP. Therefore, the following list unloading steps is adopted from the description provided in [DNT 2019]:

1. Check and remove the seals.
2. Loosen the securing bolts and remove the pins of the six mortise-and-tenon closure devices.
3. Lift off the top half of the DN30 PSP.
4. Move the lever of the rotation preventing devices to position “open”.
5. Pull the housing from the valve protecting device in position “open”.
6. Lift the 30B-X cylinder and rotate the valve protecting device by about 90° until it rests on the flange of the bottom half.
7. Lift the 30B-X cylinder out of the bottom half of the DN30 PSP.

Details on each unloading step are given in handling instruction 0045-HA-2021-001 (see Appendix 1.7.1 (Handling Instruction)).

### 1.7.5 Supplementary Equipment and Operational Controls

No supplementary equipment except means for tie-down are used during transport of the DN30-X package in any transport mode.

### 1.7.6 Precautions and Measures because of the other Dangerous Properties of the Content

No precautions and measures due to the other dangerous properties of the content are required except for the correct labeling according to the respective transport mode.

## 1.8 Inspection

### 1.8.1 Annual Inspection Requirements for the DN30 PSP

The annual inspections of the DN30 PSP were already established in the safety analysis of the DN30 package in [DNT 2019] and, therefore, are described in test instruction 0023-PA-2015-015 and test instruction 0023-PA-2015-016, in which the criteria for the checks are defined and measures in case of non-conformances or deviations are specified.

In the case that non-conformances or deviations might affect the safety of the DN30-X packaging the user of the packaging has to inform the owner of the certificate of package approval in writing about the non-conformance or deviation. It is then the decision of the owner of the certificate of package approval to undertake suitable measures to return the packaging to service in full compliance with the SAR and the certificate of package approval.

### 1.8.2 5-year Inspection Requirements for the 30B-X Cylinder and the DN30 PSP

The 5-year periodical inspections of the DN30-X packaging are subdivided into the periodical recertification of the 30B-X cylinder and the periodical inspection of the DN30 PSP.

The 5-year inspection of the 30B-X cylinder shall be performed in accordance with [ANSI N14.1] and at least as described in [USEC 651] (or in equivalent plant specific instructions). This inspection includes, but is not limited to, the following:

- 30B-X cylinders, except those already filled at the 5-year expiration date, are to be periodically inspected and tested throughout their service life.
- 30B-X cylinders that have not been inspected and tested within the required 5-year period shall not be refilled until they are properly reinspected and retested. Prior to shipment, 30B-X cylinders that have not been recertified within the 5-year requirement shall be visually inspected for degradation of the cylinder wall. Any questionable conditions should be investigated. Details on the visual inspection are provided in 0045-PA-2021-001 (see Appendix 1.8 (Inspections of 30B-X Cylinders)).
- The 5-year periodic inspections and tests consist of the following:
  - An internal and external examination of the 30B-X cylinder by a qualified inspector, including a visual inspection of the internal CCS as far as accessible.
  - A hydraulic strength test as described in [ANSI N14.1].
  - When a valve or plug change has occurred, a 100 psig pneumatic leak-test as described in [ANSI N14.1] is required.
- After a 30B-X cylinder is tested, its outer shell may be cleaned and repainted. At each 5-year periodic inspection, the cylinder shall have the tare weight re-established.
- A 30B-X cylinder shall be removed from service (for repair or replacement) when it is found to contain leaks, corrosion, cracks, bulges, dents, gouges, defective valves, damaged skirts, or other conditions that, in the opinion of a qualified inspector, render it unsafe or unserviceable in its existing condition.
- A 30B-X cylinder shall no longer be used in $UF_6$ service when the shell thickness has decreased below 11 mm.

The periodical inspections of the DN30 PSP were already established in the safety analysis of the DN30 package in [DNT 2019] and, therefore, are described in test instruction 0023-PA-2015-015 and test instruction 0023-PA-2015-016, in which the criteria for the checks are defined and measures in case of non-conformances or deviations are specified.

In case non-conformances or deviations might affect the safety of the DN30-X packaging, the user of the packaging has to inform the owner of the certificate of package approval in writing about the non-conformance or deviation. It is then the decision of the owner of the certificate of package approval to undertake suitable measures to return the packaging to service in full compliance with the SAR and the certificate of package approval.

## 1.9 Management System

The management system of company Orano NCS GmbH (ONCS) is laid down in the Integrated Management Handbook (see Appendix 1.9.1 (IMS)). The integrated management system (IMS) is certified according to:

- DIN EN ISO 9001
- DIN EN ISO 14001
- OSHAS 18001
- KTA 1401
- BAM GGR 011
- 10 CFR Part 71 – Subpart H

The IMS covers the design and development, manufacturing and operation of packagings for packages requiring approval by the competent authorities for the transport of radioactive material. Appendix 1.9.3 (Quality Assurance Program) provides a description of the ONCS quality assurance (QA) program that demonstrates compliance with the requirements of [10 CFR Part 71] – Subpart H. It also includes the NRC approval of this program.

### 1.9.1 Design, SAR, Documentation and Records

#### 1.9.1.1 General

ONCS is responsible for the design, development, safety analyses, manufacturer planning and surveillance, inspection, and controls before first use of DN30 PSPs and 30B-X cylinders. ONCS is also responsible for the operation of DN30 PSPs and 30B-X cylinders including maintenance and periodical recertification.

All documents like drawings, calculations, specifications etc. are written, checked and released in accordance with the IMS of ONCS. The author and the examiner must be experienced in the respective field of technology whereas the person releasing the document must be authorized according to the organizational structure of ONCS. For each field of technology, the different roles of the employees of ONCS are described in the IMS.

Any design modifications including any revisions of specifications, drawings and instructions are carried out according to the processes laid down in the IMS and documented accordingly. In case there are documents from suppliers, ONCS will check these documents according to the process laid down in the IMS.

#### 1.9.1.2 Design

ONCS is responsible for the whole design process from establishing the requirements based on the applicable regulations and standards up to the completion of the drawings, safety analyses, and the manufacturing specification. All individual steps necessary for the design process are stipulated in the IMS of ONCS.

Design modifications required due to the progress in carrying out the safety analyses or resulting from the outcome of physical tests with specimens or prototypes are introduced into the design process in compliance with the respective process described in the IMS of ONCS.

#### 1.9.1.3 Documents and Records

Traceability of each document and record relevant during the design process is assured by the requirements of the IMS of ONCS with respect to a unique numbering and filing system. During the design process the documents listed in Appendix 1.1 (List of Applicable Documents) are produced and filed.

For each document written and released by ONCS, the original workable document is stored together with the signed document as image. For documents and records of suppliers, only an image of the document might be made available and stored.

### 1.9.2 Manufacturing and Testing

#### 1.9.2.1 Manufacturing of 30B-X Cylinders

For the 30B-X cylinder, qualification and selection of the manufacturer as well as the requirements towards QA during material procurement, manufacturing and final inspection before first use are specified in manufacturing specification 0045-SPZ-2021-001 (see Appendix 1.9.2 (Manufacturing Specification 30B-X Cylinder)). This specification details among others the following requirements:

- Qualification of manufacturer
- Scope of services and responsibilities of manufacturer
- Responsibilities of ONCS
- Requirements for materials including certification
- Requirements concerning fabrication including welding
- Requirements concerning final acceptance test
- Treatment of non-conformances
- Manufacturing test sequence plan (MTSP)

#### 1.9.2.2 Manufacturing of Serial DN30 PSPs

The manufacturing of serial DN30 PSPs has already been established in [DNT 2019]. Therefore, qualification and selection of the manufacturer as well as the requirements towards QA during material procurement, manufacturing and final inspection before first use are specified in manufacturing specification 0023-SPZ-2016-001. This specification details the same requirements as listed for the 30B-X cylinder in section 1.9.2.1

### 1.9.3 Operation

The quality management requirements for operation are specified in handling instruction 0045-HA-2021-001 (see Appendix 1.7.1 (Handling Instruction)).

In case the DN30 PSP is leased to a customer for transports, the handling instruction is provided to this customer who has to confirm in writing that he will comply with the requirements stipulated there.

In case the DN30-X packaging is sold to a customer, the handling instruction and the test instruction regulating regular and periodical inspections are provided to this customer who has to confirm in writing that he will comply with the requirements stipulated there.

### 1.9.4 Maintenance and Repair

The quality management requirements for the recertification of 30B-X cylinders are described in test instruction 0045-PA-2021-001 (see Appendix 1.8 (Inspections of 30B-X Cylinders)) and a description of the non-conformances and deviations for which repair is required is included in this test instruction. Since, the same non-conformances and deviations apply to the visual inspection of the 30B-X cylinder, test instruction 0045-PA-2021-001 is also referenced in handling instruction 0045-HA-2021-001 (see Appendix 1.7.1 (Handling Instruction)). In addition, the following applies to repairs other than replacement of parts:

- For repair of 30B-X cylinders other than replacement of parts, the specification 0045-SPZ-2021-001 in Appendix 1.9.2 (Manufacturing Specification 30B-X Cylinder) must be complied with.

The quality management requirements for periodical inspections of DN30 PSPs were already established in the safety analysis of the DN30 package in [DNT 2019] and, therefore, are described in test instruction 0023-PA-2015-015 (see [DNT 2019]). The non-conformances and deviations for which repair of a DN30 PSP is required are described in test instruction 0023-PA-2015-016 (see [DNT 2019]). In addition, the following applies to repairs other than replacement of parts:

- For repair of DN30 PSPs other than replacement of parts, the specification 0023-SPZ-2016-001 (see [DNT 2019]) must be complied with.

In all cases in which repair of a 30B-X cylinder or a DN30 PSP is required, ONCS must be involved in the planning, authorization, and execution of the repair measures.

### 1.9.5 Compliance of any Activity with the SAR

Specifications 0045-SPZ-2021-001 in Appendix 1.9.2 (Manufacturing Specification 30B-X Cylinder) and 0023-SPZ-2016-001 (see [DNT 2019]) ensure that during manufacturing and final acceptance tests before first use, the requirements of this SAR towards the design of the 30B-X cylinder and the DN30 PSP are met. In detail the following requirements are considered:

- Specification of the material properties in material data sheets to comply with the properties used throughout this SAR
- Requirements for welders and welding to ensure the structural properties of the 30B-X cylinder and the DN30 PSP as defined in this SAR
- Specification of tests and documentation during manufacturing and before first use ensuring the design of the 30B-X cylinder and the DN30 PSP comply with the drawings

Handling instruction 0045-HA-2021-001 in Appendix 1.7.1 (Handling Instruction) and test instruction 0045-PA-2021-001 in Appendix 1.8 (Inspections of 30B-X Cylinders) ensure that during operation, the 30B-X cylinder is kept compliant with this SAR. For the DN30 PSP, this is ensured by the application of test instructions 0023-PA-2015-015 and 0023-PA-2015-016 (see [DNT 2019]).

### 1.9.6 Deviations

Deviations concerning the safety elements listed in table 1-15 and the corrective actions implemented are to be reported to the competent authority.

### 1.9.7 Safety Elements

The safety elements of the DN30-X package are summarized in table 1-15.

**Table 1-15 Safety elements**

| Element of the package | Safety function | Parameters |
|---|---|---|
| Closure system | Mechanical protection | • Welds<br>• Absence of structural defects<br>• Completeness |
| Outer shell | Mechanical protection | • Welds<br>• Absence of structural defects in the steel sheets |
| Foam | Mechanical protection | • Thickness<br>• Density |
| Microporous material | Thermal protection | • Thickness<br>• Thermal conductivity |
| Intumescent material | Thermal protection | • Thickness<br>• Completeness<br>• Thermal conductivity |
| Inner shell | Mechanical protection | • Welds<br>• Absence of structural defects in the steel sheets |
| Valve protecting device | Mechanical protection | • Welds<br>• Absence of structural defects in the steel sheets<br>• No unacceptable deformation of the housing<br>• Completeness |
| Plug protecting device | Mechanical protection | • Welds<br>• Absence of structural defects |
| Rotation preventing devices | Mechanical protection | • Welds<br>• Absence of structural defects of the bolts<br>• Completeness |
| 30B-X cylinder | Containment | • Welds<br>• Absence of structural defects<br>• Thickness |
| | Confinement | • Absence of structural defects<br>• Presence of neutron absorbing material |

## 1.10 Package Illustration

Figure 1-12 and figure 1-13 show illustrations of the DN30-X package. Detailed illustrations of the 30B-X cylinder are presented in section 1.4.2.1. Appendix 1.4.1A (Drawings 30B-X Cylinder) and Appendix 1.4.1B (Drawings DN30 PSP) contain the set of drawings for the DN30 PSP and the 30B-X cylinder, respectively.

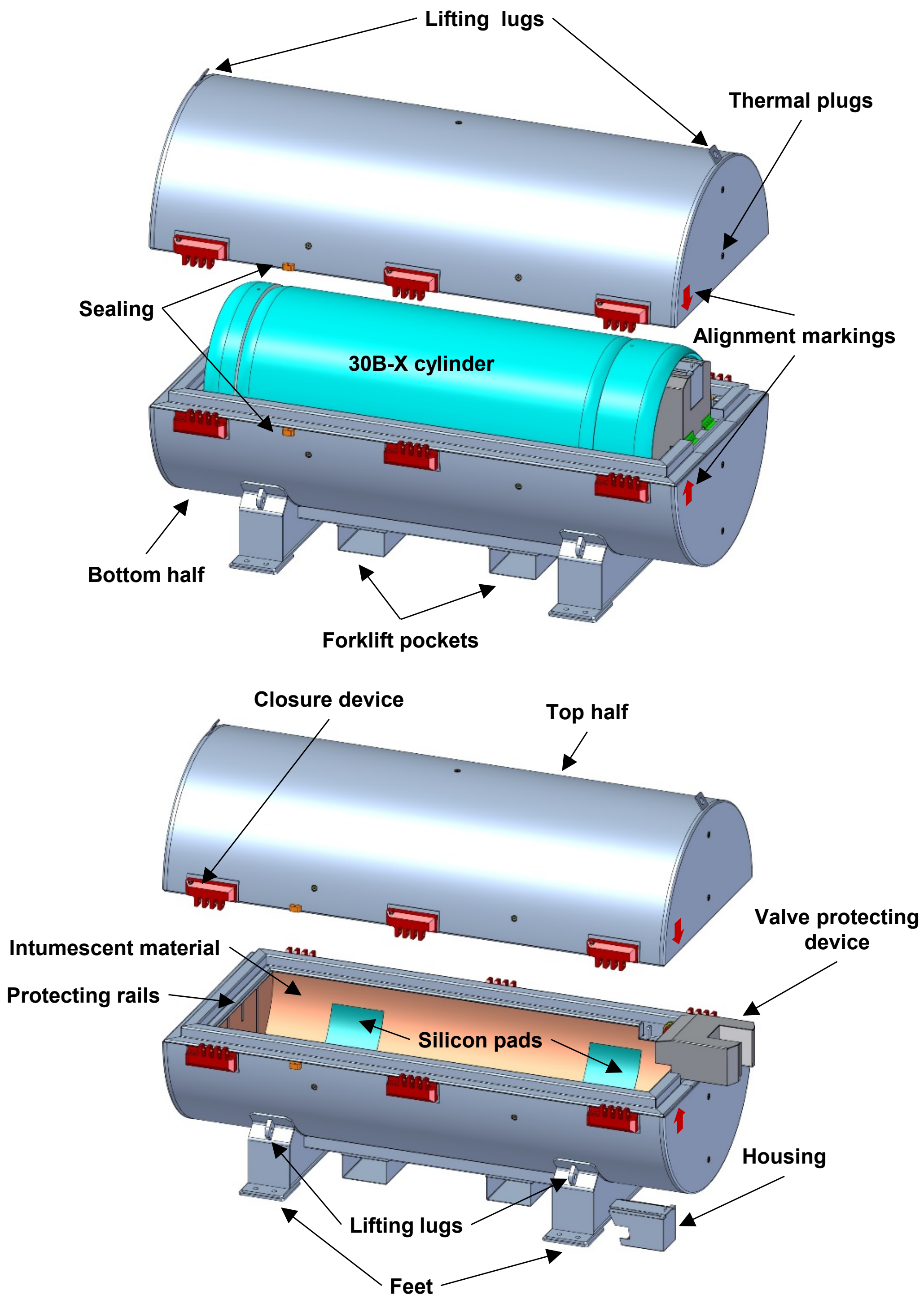


**Figure 1-12 DN30-X Package Overview**

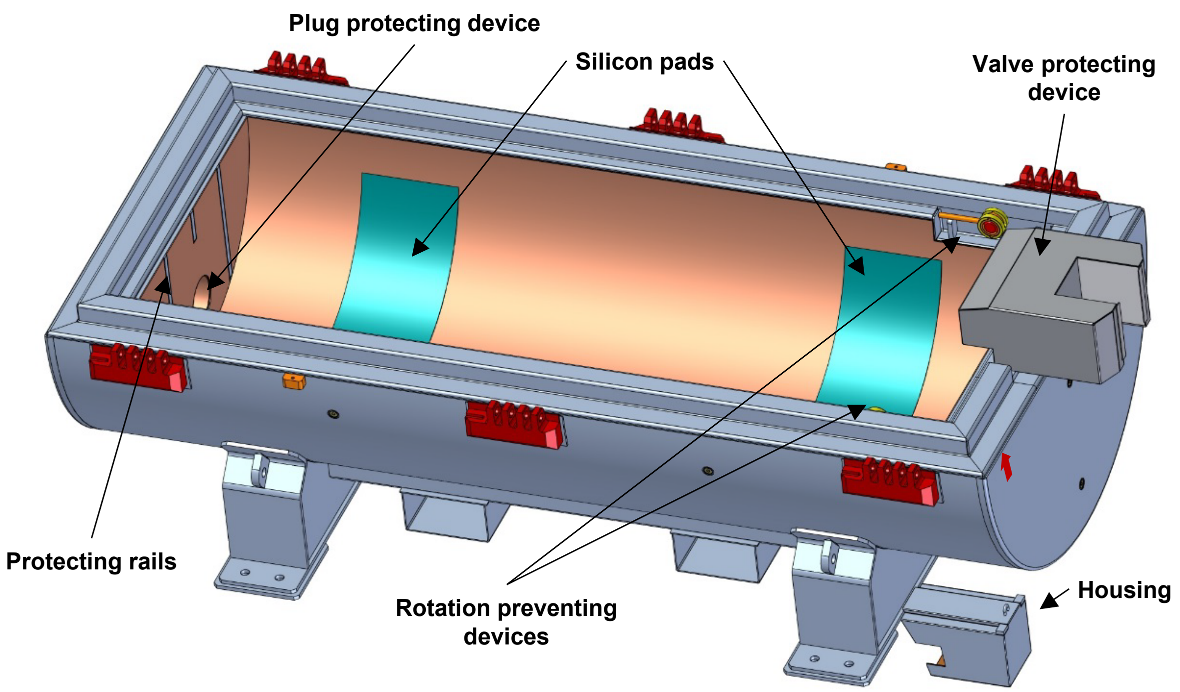


**Figure 1-13 DN30 PSP bottom half**

# PART 2
# TECHNICAL ANALYSES

## 2.1 Introduction

The technical analysis of the DN30-X package refers to a large extent to the technical analysis of the already licensed DN30 package [CoC 9362]. This is due to the strong similarity between the DN30 and the DN30-X package that allows to transfer or at least adapt a major part of the technical analyses of the DN30 to the DN30-X package. As demonstrated by argumentation in section 2.1.1, this is true for the thermal, the containment design and the external dose rates analysis. For the structural analysis, certain parts of the analysis for the DN30 package can also be transferred to the DN30-X package, but additions are required to prove compliance with [10 CFR Part 71] and [49 CFR Part 173] or [SSR-6 2018]. The criticality safety analysis of the DN30-X package is entirely new.

Section 2.1.1 provides a general guideline through the entire technical analysis of the DN30-X package. This includes the description and justification of the analysis methods for each part of the technical analysis and, for the thermal, the containment design and the external dose rates analysis, this also includes a detailed argumentation why the technical analyses of the DN30 package can be transferred to the DN30-X package. Because of the inclusion of parts of the technical analysis of the DN30 package, this SAR still references both the transport regulations [10 CFR Part 71] and [49 CFR Part 173] as well as the IAEA transport regulations [SSR-6 2018]. This allows to maintain compatibility with the supplemental documentation of the safety analysis of the DN30 package.

The guideline through the technical analysis is followed by the common provisions for all technical analyses in section 2.1.2. For each technical analysis, a summary of the package design forming the basis for the technical analyses and a description of the required content properties, fundamental properties of the specification of the 30B-X cylinder and the DN30 PSP as well as the material characteristics are provided in section 2.1.2.1. With this at hand, the acceptance criteria and design assumptions for the 30B-X cylinder and the DN30-X package are defined in section 2.1.2.2.

### 2.1.1 Guideline through Technical Analyses and Justification of Analysis Methods

#### 2.1.1.1 Structural Analysis

The structural analysis of the DN30-X package consists of two main parts:

1. The prove that the design requirements for normal operating conditions and recertification of the 30B-X cylinder are fulfilled.
2. The prove that the requirements of [10 CFR Part 71] and [49 CFR Part 173] or [SSR-6 2018] for Type AF packages for the transport of $UF_6$ are fulfilled.

The first part only pertains to the 30B-X cylinder. Further details on this part of the structural analysis are provided in section 2.1.1.1.1. The second part pertains to the entire DN30-X package and covers the structural analysis of the DN30-X for handling as well as under RCT, NCT and HAC. In these analyses, advantage is taken of the strong similarity between the DN30-X, consisting of the 30B-X cylinder and the DN30 PSP, and the already licensed DN30 package [CoC 9362], consisting of the standard 30B cylinder as specified in [ANSI N14.1] and the DN30 PSP.

As the 30B-X cylinder is also enclosed by the DN30 PSP and the maximum gross weight, outer dimensions as well as the valve and plug of the 30B-X cylinder are identical to the standard 30B cylinder, the analyses for handling and RCT performed in [DNT 2019] for the DN30 package remain valid as they solely consider the properties of the DN30 PSP and the total package mass. Further details on this part of the structural analysis are provided in section 2.1.1.1.2.

Only those aspects of the structural analysis that pertain to the interaction between the 30B-X cylinder and the DN30 PSP require further investigation. Namely, these are the structural analyses under NCT and HAC of the DN30-X package, which is discussed in section 2.1.1.1.3.

##### 2.1.1.1.1 Structural Analysis of the 30B-X Cylinder for Normal Operating Conditions

The structural analysis of the 30B-X cylinder for normal operating conditions performed in section 2.2.2 shows that the requirements towards design, fabrication, inspection and testing stipulated in the specification for the 30B-X cylinder in Appendix 1.9.2 (Manufacturing Specification 30B-X Cylinder) are fulfilled. The analysis for normal operating conditions comprises:

- The analysis of the 30B-X cylinder for an internal and external maximum allowable working pressure (MAWP) at the design temperature of 121 °C.
- The analysis of the 30B-X cylinder with regard to the minimum design metal temperature (MDMT) of -29 °C and the transport temperature of -40 °C.
- The analysis of the 30B-X cylinder for a hydraulic strength test at twice the MAWP.

Because the 30B-X cylinder features the same characteristics as the standard 30B cylinder, these analyses are carried out by argumentation and, as required, by additional hand calculations using well established formulas for stress and strain provided by the ASME boiler and pressure vessel code (BPVC) [ASME BPVC].

##### 2.1.1.1.2 Structural Analysis of the DN30-X for Handling and under RCT

The structural analysis of the DN30-X package for handling in section 2.2.3 and under RCT in section 2.2.4 comprises:

- Analysis of the lifting attachment points of the DN30 PSP.
- Analysis of the features of the DN30 PSP used for tie-down.

These analyses were carried out in [DNT 2019] for the DN30 package by hand calculations using well established formulas for stress and strain. They remain valid for the DN30-X package without limitation.

#### 2.1.1.1.3 Structural Analysis of the DN30-X under NCT and HAC

The structural analysis of the DN30-X under NCT in section 2.2.5 comprises the analysis of the following:

- Water spray test
- Free drop test
- Compression test
- Penetration test
- Reduced external pressure

Apart from the free drop test, these analyses are identical to the analyses for the DN30 package in [DNT 2019] because the corresponding proofs only credit the DN30 PSP. A more detailed argumentation is provided in the corresponding section of each test in section 2.2.5. Furthermore, as explained in section 2.2.5.2, the free drop test is analyzed in sequence with the drop tests under HAC.

The structural analysis of the DN30-X under NCT and HAC in section 2.2.6 comprises the analysis of the sequence of the following drop tests:

Test 1: 1.2 m free drop test

Test 2: 9 m free drop test

Test 3: Puncture test

The analysis of the drop tests under NCT and HAC takes advantage of the strong similarity between the DN30-X and the already licensed DN30 package [CoC 9362]. As demonstrated below, this allows the structural analysis of the DN30 package to serve as the basis for the analysis of the DN30-X package. To complete the analysis of the DN30-X package under NCT and HAC, only a few additional analyses are required accounting for the differences between the two packages.

The structural analysis of the DN30 package under NCT and HAC was carried out in [DNT 2019] in three major steps:

1. Pre-analysis of the behavior of the DN30 package by using proven simulation tools and selection of benchmarks for real drop tests with prototypes.
2. Real testing of prototypes of the DN30 package by applying the selected benchmark test sequences.
3. Refinement of the simulation model for the DN30 package based on the results of the test results and complete analysis of the behavior of the DN30 package under NCT and HAC for the operating temperature range of -40 °C to +60 °C.

Because of the high toxicity, radioactivity and heavy reaction with water of $UF_6$, the 30B cylinders loaded in the DN30 PSP prototypes were filled with a mixture of heavy concrete and steel shot as surrogate material of the $UF_6$ content. The structural analysis of the DN30 package in conjunction with the experimental drop tests proved that the following major requirements of [10 CFR Part 71] or [SSR-6 2018] are fulfilled:

- The DN30 package withstands the free drop test from a height of 1.2 m under NCT without loss or dispersal of the $UF_6$ content.
- The DN30 package withstands the free drop test from a height of 9 m and the puncture test under HAC without damage to the containment system.

The approach for the structural analysis of the DN30-X package under NCT and HAC is to assume that the impact the 30B-X cylinder has on the DN30 PSP is comparable to the impact the 30B cylinder has on the DN30 PSP. This approach is admissible because of the following:

1. The 30B-X cylinder has the same gross weight as the standard 30B cylinder while also having the same outer dimensions, shell thicknesses and material specifications of the pressure envelope and the cylinder skirts (see Appendix 1.9.2 (Manufacturing Specification 30B-X Cylinder) and table 1-13).
2. The 30B-X and the standard 30B cylinder are equipped with the same valve and plug.
3. The 30B-X and the standard 30B cylinder are both transported in the same DN30 PSP.

With regard to the structural analysis, the only difference between the DN30 and the DN30-X package is the slightly different distribution of the content mass within the 30B-X cylinder, which is due to the addition of the internal CCS. Furthermore, the combination of the CCS and the $UF_6$ content might interact slightly differently with the cylinder shells than the $UF_6$ content on its own. However, when the $UF_6$ is in solid form during transport, the CCS is essentially stuck in the content. The possibilities of CCS to move around within the 30B-X cylinder are therefore very limited. Consequently, the interaction of the content with the 30B cylinder and the interaction of the CCS stuck in the content with the 30B-X cylinder is comparable.

Based on this argumentation, the experimental drop tests performed for the DN30 package and the complete analysis of the behavior of the DN30 package under NCT and HAC for the operating temperature range of -40 °C to +60 °C are also covering for the DN30-X package. To complete the structural analysis of the DN30-X package under NCT and HAC, only a few additional analyses are required to account for the differences between the two packages. Consequently, the structural analysis of the DN30-X package under NCT and HAC consists of two fundamental parts:

1. The first part, described in detailed in section 2.1.1.1.3.1, aims at providing evidence that the interaction between the 30B-X cylinder and the DN30 PSP is comparable to the interaction between the 30B cylinder and the DN30 PSP. These analyses prove that the initially made assumptions are correct and sustain the analysis.
2. In the second part, described in detailed in section 2.1.1.1.3.2, analyses are performed that specifically consider the acceptance criteria established for the CCS of the 30B-X cylinder.

In the following, further details on each aspect of the structural analysis are given.

2.1.1.1.3.1 Comparison of Drop Test Analyses for the DN30-X and DN30 Package

For the structural analysis under NCT and HAC, the interaction between the DN30 PSP and the 30B-X cylinder must be considered to show that the 30B-X cylinder withstands these tests in a similar condition as the standard 30B cylinder. This is shown in section 2.2.6.2.5 by comparing the results in drop tests performed at room temperature for the DN30-X to the corresponding results for the DN30 package. Specifically, the deformations at the outer shells of the DN30 PSP as well as the plastic deformations and decelerations at the cylinders are compared. The results of the analyses together with the real drop tests performed with DN30 prototypes in [DNT 2019] prove that the requirements of [10 CFR Part 71] or [SSR-6 2018] are also fulfilled for the DN30-X package.

Because of the fissile properties of the $UF_6$ content, the structural analysis of the DN30-X must also demonstrate that the CCS retains its properties relevant to criticality control after the tests simulating NCT and HAC. This part of the structural analysis of the DN30-X represents the only major difference compared to the DN30 package. The criteria for the CCS of the 30B-X cylinder to ensure safe subcriticality after the tests simulating NCT and HAC are given in section 2.1.2.2.1.

2.1.1.1.3.2 Additional Analyses for the DN30-X Package

The acceptance criteria for the CCS of the 30B-X cylinder established in section 2.1.2.2.1 require the investigation of additional drop test scenarios for the DN30-X package that were not part of the structural analysis of the DN30 package in [DNT 2019]. These are included in section 2.2.6.2.6. To complete the structural analysis of the DN30-X package, this part also contains a discussion of the remaining drop test scenarios that were considered in the safety analysis of the DN30 package in [DNT 2019].

### 2.1.1.2 Thermal Analysis

The thermal analysis of the DN30-X package uses the results obtained through the thermal analysis of the already licensed DN30 package [CoC 9362]. The thermal behavior of the DN30 package has been analyzed in [DNT 2019] for RCT, NCT, and HAC. The analyses for the DN30 package under HAC are based on real-world thermal tests that were carried out with DN30 PSP prototypes and empty 30B cylinders complying with [ANSI N14.1]. Using empty cylinders minimizes the heat sink provided by the content and, thus, not only maximizes the thermal load acting on the cylinder shells and the valve/plug during the thermal test under HAC but also in the subsequent cooling phase. The thermal analysis in conjunction with the prototype tests proved that the requirements of [10 CFR Part 71] or [SSR-6 2018] with respect to the thermal behavior of the DN30 package are fulfilled, especially regarding containment and safety against rupture of the pressure envelope of the 30B cylinder.

For the reasons listed hereafter, the results obtained through the thermal analysis of the DN30 package are covering for the thermal behavior of the DN30-X package as well:

- The 30B-X cylinder has a larger nominal tare weight than the 30B cylinder while having the same outer dimensions, shell thicknesses, and material specifications of the pressure envelope and the cylinder skirts, respectively (see Appendix 1.9.2 (Manufacturing Specification 30B-X Cylinder) or table 1-13).
- The 30B-X cylinder is equipped with the same valve and plug.

- The assumed thermal load of 3 W for the $UF_6$ content is by far covering for all admissible enrichment levels for the DN30 and the DN30-X package (see section 1.3.2.7).
- The 30B and the 30B-X cylinder are both transported in the same DN30 PSP.

Because of the covering assumption for the thermal load of the content, the thermal behavior of the DN30 and the DN30-X package under RCT and NCT is unaffected by the type of cylinder being considered in the thermal analysis. The thermal behavior of both packages is solely determined by the DN30 PSP so that the analyses performed for the DN30 package under RCT and NCT are also valid for the DN30-X package.

The thermal analysis of the DN30 package in [DNT 2019] proves that the empty cylinder defines the worst-case scenario for the thermal test under HAC with regard to the temperatures at the cylinder. Considering the empty 30B-X cylinder has a larger heat sink than the 30B cylinder, this leads to the conclusion that the temperatures at the 30B-X cylinder are lower than the analyzed and measured temperatures at the 30B cylinder, as both cylinders are protected by the same DN30 PSP. Consequently, the thermal analysis of the DN30 package under HAC is generally also covering for the DN30-X package.

However, the case of a filled cylinder may not be covering for the DN30-X package because the 30B-X cylinder has lower fill limits than the 30B cylinder. This leads to a reduced heat sink of the filled 30B-X in comparison to the filled 30B cylinder. Therefore, additional thermal calculations under HAC are presented in section 2.3.2 that investigate the impact of the lower fill limits for the 30B-X cylinder on the temperatures at the cylinder.

In the following, further details on each aspect of the thermal analysis of the DN30-X package are given.

#### 2.1.1.2.1 Thermal Analysis under RCT and NCT

The thermal analysis under RCT and NCT comprises:

- Analysis of the DN30-X package at an ambient temperature of 38 °C without solar insolation.
- Analysis of the DN30-X package at an ambient temperature of 38 °C with constant solar insolation.

The analyses under RCT and NCT were carried out for the DN30 package in [DNT 2019]. They are also covering for the DN30-X package.

#### 2.1.1.2.2 Thermal Analysis under HAC

The thermal analysis under HAC comprises:

- Analysis of the DN30-X package subjected to the conditions of the thermal test with an ambient temperature of 800 °C and an exposure time of 30 min, followed by a subsequent cooling phase at an ambient temperature of 38 °C and 12 hours solar/ no solar insulation cycles.

The thermal analysis of the DN30 package under HAC in [DNT 2019] is generally also covering for the DN30-X package. Additional analyses are only required for the case of a filled cylinder, which is solely due to the differing fill limits of the 30B-X and the 30B cylinder. For these analyses, the same validated and calibrated calculation model of the DN30 PSP is used as in [DNT 2019].

Hence, the calculation models of the DN30-X and DN30 package differ only in the geometry of the 30B cylinder that is replaced by the 30B-X cylinder.

#### 2.1.1.3 Containment Design Analysis

The containment design analysis of the DN30-X package is carried out in the same manner as the containment design analysis for the already licensed DN30 package [CoC 9362]. The containment design of the DN30 package has been analyzed in [DNT 2019] for RCT, NCT and HAC. For RCT and NCT, the analysis was carried out according to [ISO 12807] and to prove that the standard helium leakage rate used in the containment analysis is not just applicable for RCT and NCT but also after HAC, the leakage rate of the 30B cylinders used for the DN30 prototypes was measured after the drop and thermal tests simulating HAC. This proved that the requirements of [10 CFR Part 71] or [SSR-6 2018] with respect to the containment function of the DN30 package are fulfilled.

For the following reasons, the containment design analysis of the DN30-X and the DN30 package can be carried out in the same manner:

- The pressure envelope of the 30B-X and the standard 30B cylinder including the valve and the plug is identical
- The DN30 and the DN30-X package are a Type AF package

Consequently, the required standard helium leakage rates for the DN30-X and the DN30 package solely differ from each other because of the differing content weight and certified minimum volume of the 30B-X and standard 30B cylinder (see table 1-13). All other aspects of the analysis like possible leakage paths etc. are identical.

As applicable to a Type AF package, RCT and NCT are considered in the containment design analysis of the DN30-X because there is no restriction on the radioactivity release under HAC, which is due to the limit of $1A_2$ for the radioactive content of Type A packages. For the containment design analysis, the allowable leakage rate of $L_\mathrm{N} = 1 \cdot 10^{-4}\ \mathrm{Pa} \cdot \mathrm{m}^3/s$ is applied for the 30B-X cylinder as specified in section 1.2.9.

#### 2.1.1.4 External Dose Rate Analysis

The external dose rates analysis for the DN30-X package is strongly based on the external dose rates analysis for the already licensed DN30 package [CoC 9362]. In [DNT 2019], a detailed analysis of the external dose rates at the DN30 package loaded with filled standard 30B cylinders as well as 30B cylinders containing heels under RCT and NCT has been performed. This analysis covers Commercial Grade and Reprocessed $UF_6$ with an enrichment up to 5 wt.-% $^{235}U$ in uranium.

The permissible mass of $UF_6$ for the 30B-10 and 30B-20 cylinder listed in Table 1-4 is generally smaller than for the standard 30B cylinder, whereas the shielding characteristics of the DN30 PSP are unchanged. However, the higher enrichments of up to 10 and 20 wt.-% $^{235}U$ in uranium for $UF_6$ grade HALEU 10 and HALEU 20 have an impact on the gamma source terms as the isotopic compositions differ from Commercial Grade and Reprocessed $UF_6$ (see table 1-2 and table 1-3).

Therefore, the external dose rates analysis of the DN30-X package is reperformed on the basis of the analysis for the DN30 package in [DNT 2019] considering the following:

- The internal CSS of the 30B-X cylinder is considered in the dose rates analysis.
- The analysis covers $UF_6$ grade HALEU 10 and HALEU 20.
- For the 30B-X cylinder, the minimal wall thickness of 1.1 cm as specified in table 1-13 is applied.

#### 2.1.1.4.1 External Dose Rate Analysis under RCT

The external dose rate analysis of the DN30-X package under RCT consists of:

- The analysis of the external dose rates at the surface of the DN30-X package and at a distance of 2 m from the external surface of the DN30-X package.
- The analysis of the external dose rates at a distance of 1 m from the external surface of the DN30-X package to provide an estimate for the TI to be expected. Nevertheless, the TI will always be determined by measurement before each transport.
- The analysis of the external dose rates at the surface of a standard vehicle routinely used for transportation of the DN30-X package and in a distance of 2 m from the external surface of the vehicle:
  - Therefore, it is assumed that four DN30-X packages are transported side-by-side on 20’ flatracks so that the dose rates at the surface of the vehicle are identical to the dose rates at the front surfaces of the DN30-X package.
  - For the analysis of the external dose rates in 2 m distance from the vehicle, the influence of all four DN30-X packages is taken into account.

#### 2.1.1.4.2 External Dose Rate Analysis under NCT

The external dose rates analysis under NCT consists of the comparison of the maximal dose rates for a non-damaged DN30-X package complying with the manufacturing drawings and for a damaged DN30-X package under NCT to prove that the increase in the maximal dose rates is not significant (not greater than 20 %).

### 2.1.1.5 Criticality Safety Analysis

The criticality safety analysis for the DN30-X package takes into account the maximal enrichments of 10 wt.-% $^{235}U$ for the DN30-10 and 20 wt.-% $^{235}U$ for the DN30-20. It is based on the following assumptions:

- For the single package in isolation, optimal water moderation of the $UF_6$ content is assumed.
- For the array of packages, flooding with water is excluded because of the results of analyses and drop tests described in the structural analysis in section.
- For all contents, the most reactive arrangement in the packaging is determined in all cases. Any credible rearrangement of contents in the package is taken into account in the analyses. Based on the results of analyses and drop tests described in the structural analysis, release of contents from the package does not need to be assumed.

- Water around the package is considered in different layer thicknesses in the analysis of the array of packages.
- Temperature changes are taken into account by assuming a conservatively high density for $UF_6$ and the theoretical maximal density of 1 g/cm³ for water. A decrease of water density caused by a temperature rise or freezing will lead to lower moderation that is less reactive.

### 2.1.2 Common Provisions for all Technical Analyses

#### 2.1.2.1 Package Design

Details of the DN30-X package design are described in section 1.3 for the content and in section 1.4 for the 30B-X cylinder and the DN30 PSP. In the following, the provisions for the content and the DN30-X packaging are given with respect to each part of the technical analysis. In addition, an overview of the materials used in the structural and thermal analysis is included. The material properties for all other technical analysis are given in the corresponding sections of those analyses.

##### 2.1.2.1.1 Content

As defined in section 1.3, the content is $UF_6$ for all technical analyses. However, referring to a specific analysis, only certain properties of the content may be relevant and, thus, are considered in the corresponding analysis. Further details on each of technical analysis are provided in table 2-1.

**Table 2-1 Provisions for the content of the DN30-X package used in the technical analyses**

| Technical analysis | Provisions made for the DN30-X |
|---|---|
| Structural | • The relevant physical property is the density.<br>• The content weight of the 30B-X cylinder is adopted such that the gross weight of standard 30B cylinder as specified in [ANSI N14.1] is obtained.<br>• Potential deformations of the content and, thus, energy absorption by the content are neglected in the analysis. |
| Thermal | • The relevant physical properties are the density, thermal conductivity, and specific heat capacity.<br>• Scenarios under HAC are investigated for empty, partially filled, and filled cylinders.<br>• For partially filled and filled cylinders, an evenly distributed air/$UF_6$-mixture is considered, which completely fills the cylinder cavity. |
| Containment design | • The relevant physical property is the viscosity of gaseous $UF_6$. For the containment analysis, the content configuration has no impact on results.<br>• The source terms and physical properties of the radioactive $UF_6$ contents are specified in section 1.3. |
| External dose rates | • The relevant physical properties are the density and the shielding properties of the $UF_6$ contents.<br>• Conservatively, a 100 % filled 30B-X cylinder is considered, which exceeds the permissible mass of $UF_6$ for the 30B-10 and 30B-20 cylinder listed in table 1-4. |

| Technical analysis | Provisions made for the DN30-X |
|---|---|
| | • For cylinders containing heels, a covering configuration with heels forming a puddle at the lower side of the 30B-X cylinder is investigated.<br>• The source terms and physical properties of the radioactive contents are specified in section 1.3. |
| Criticality safety | • The relevant physical properties are the density, the purity (hydrogen impurities) and the $^{235}U$ enrichment of the $UF_6$.<br>• Conservatively, a 100 % filled 30B-X cylinder is considered which exceeds the permissible mass of $UF_6$ for the 30B-10 and 30B-20 cylinder listed in table 1-4.<br>• For the single package in isolation, optimal moderation of the $UF_6$ contents with water is assumed. |

#### 2.1.2.1.2 30B-X Cylinder

The design of the 30B-X cylinder is defined in the drawings in Appendix 1.4.1A (Drawings 30B-X Cylinder). A detailed description of the 30B-X cylinder is provided in sections 1.4.1.1 and 1.4.2.1. Provisions made for each technical analysis with regard to the 30B-X cylinder are given in table 2-2.

**Table 2-2 Provisions for the 30B-X cylinder used in the technical analyses**

| Technical analysis | Provisions made for the 30B-X cylinder |
|---|---|
| Structural | • Nominal dimensions of the 30B-X cylinder are assumed.<br>• The influence of temperature on the mechanical behavior of the package is analyzed in variation calculations:<br>– The maximum package temperature is evaluated in the thermal analysis.<br>– The minimum temperature of -40 °C is required by the transport regulations. |
| Thermal | • Nominal dimensions of the 30B-X cylinder and standard physical properties of the materials of the 30B-X cylinder are assumed.<br>• The CCS is modeled in a simplified geometry for the 2D-environment. |
| Containment design | • Neither the dimensions nor the physical properties of the 30B-X cylinder are relevant.<br>• However, the free volume inside the 30B-X cylinder is part of the analysis and for the evaluation of this parameter the minimum volume of the 30B-X cylinder is assumed.<br>• Furthermore, the design of the valve, especially the connection to the cylinder shell and the seat of the valve are taken into account based on [ANSI N14.1]. |
| External dose rates | • A simplified 30B-X cylinder without skirts and with flat ends is assumed.<br>• The minimum wall thickness of the 30B-X cylinder is assumed to be 1.1 cm. |
| Criticality safety | • The skirts and domed heads of the cylinder are represented in the calculation model, while valve, plug and nameplate are neglected.<br>• For the CCS, only the CCRs are taken into account, the lattice holders and all other structural parts of the CCS are conservatively neglected.<br>• The geometry of the cylinder and CCS are varied to assess the most reactive values within the range of the manufacturing tolerances and HAC deformations. |

2.1.2.1.3 DN30 PSP

The design of the DN30 PSP is defined in the drawings in Appendix 1.4.1B (Drawings DN30 PSP). A detailed description of the DN30 PSP is provided in sections 1.4.1.2 and 0.. Provisions made for each technical analysis with regard to the DN30 PSP are given in table 2-3.

**Table 2-3 Provisions for the DN30 PSP used in the technical analyses**

| Technical analysis | Provisions |
|---|---|
| Structural | • Nominal dimensions of the DN30 PSP are assumed.<br>• The influence of temperature on the mechanical behavior of the package is analyzed in variation calculations:<br>– The maximum package temperature is evaluated in the thermal analysis.<br>– The minimum temperature of -40 °C is required by the transport regulations. |
| Thermal | • Under RCT and NCT, nominal dimensions of the DN30 PSP and nominal physical properties of the materials of the DN30 PSP are assumed.<br>• Under HAC, nominal dimensions and deteriorated physical properties of the materials of the DN30 PSP are assumed. Furthermore, a self-sustaining pyrolysis of the foam as experienced in the thermal test under HAC is considered. |
| Containment design | • The DN30 PSP is not part of the containment system and, thus, is not considered in the containment design analysis. |
| External dose rates | • Nominal dimensions of the DN30 PSP and standard physical properties of the materials of the DN30 PSP are assumed. |
| Criticality safety | • The foam material is neglected.<br>• The steel shells of the DN30 PSP are compacted around the 30B-X cylinder to a total thickness of 10 cm in radial direction and 8 cm in axial direction, thereby minimizing the distance between adjacent packages. |

### 2.1.2.2 Acceptance Criteria and Design Assumptions

2.1.2.2.1 Structural Design

The acceptance criteria and design assumptions for the structural design are:

- Lifting attachments that are a structural part of the DN30-X package are designed with a minimum safety factor of 3 against yielding when used to lift the package in the intended manner. Failure of any lifting device under excessive load does not impair the ability of the DN30-X package to meet other requirements of [10 CFR Part 71].
- Tie-down devices that are a structural part of the DN30-X package withstand, without generating stress in any material of the package in excess of its yield strength, a static force applied to the center of gravity of the package having a vertical component of 2 times the weight of the package with its contents, a horizontal component along the direction in which the vehicle travels of 10 times the weight of the package with its contents, and a horizontal component in the transverse direction of 5 times the weight of the package with its contents. Failure of the devices under excessive load does not impair the ability of the DN30-X package to meet other requirements of [10 CFR Part 71].
- No failure of the DN30 PSP closure system.

- No physical contact between the valve of the 30B-X cylinder and any other component of the packaging other than its original point of attachment.
- No physical contact between the plug of the 30B-X cylinder and any other component of the packaging other than its original point of attachment.
- No rupture of the 30B-X cylinder containment system.
- No failure of the 30B-X cylinder confinement system:
  - The relative dislocation of the CCRs must remain below 5 mm.
  - The increase in radial movability of the entire CCS out of the center of the 30B-X cylinder must remain below 3 mm.
  - The increase in axial movability of the entire CCS out of the center of the 30B-X cylinder must remain below 7 mm.
  - Failure of the lattice holders must not occur.
- Rupture of the CCRs must not occur.

The evaluation of these design criterions for the DN30-X package is possible without considering material damage or failure in the simulation model of the DN30-X package, even if local deformations of the DN30 PSP shells above the uniform elongation occur. However, the following must be considered in this case:

- The material models for the steel parts cover the inelastic range up to the uniform elongation. For plastic strains above the uniform elongation, the discrepancy compared to the real material behavior increases successively because of the negligence of a damage and failure model. Thus, failure analysis of certain parts of the DN30 PSP shall be based on the experimental drop tests only.
- Locations with plastic strains above the uniform elongation and close to or above the elongation at fracture can be compared with the corresponding areas of the prototypes used for the experimental drop tests. If those locations match and failure occurred in the experimental drop tests, the exact value of the plastic strain is of no importance for the safety of the DN30-X package because the thermal test under HAC was passed with fractures in the inner and outer shells of the DN30 PSP.
- An analysis with previously introduced cracks in the inner shell of the DN30 PSP simulation model, exceeding the cracks observed after the drop tests, proves that safety relevant simulation results are not sensitive to failure of the inner steel shells. The results of this sensitivity analysis are documented in [DNT 2019].

#### 2.1.2.2.2 Thermal Design

The acceptance criteria and design assumptions for the thermal design are:

- The temperatures at the 30B-X cylinder, including valve, plug and shell, should not exceed 131 °C during the thermal test simulating HAC for a package in the condition after the structural tests simulating NCT and HAC (see section 2.3.1.4). The leakage rate after the thermal test should be less than $1.0 \cdot 10^{-4}$ Pa·m³/s.
- Withstand, without rupture of the containment system (the 30B-X cylinder), the thermal test simulating HAC.

The thermal design considers different filling ratios from an empty cylinder up to a cylinder filled with the maximum admissible amount of $UF_6$.

#### 2.1.2.2.3 Containment System Design

The acceptance criteria and design assumptions for the containment system design are:

- Under NCT, the loss or dispersal of $UF_6$ must be prevented.
- The containment is the 30B-X cylinder with its valve and plug.
- The DN30 PSP has no containment function.

#### 2.1.2.2.4 External Dose Rate Assessment

The acceptance criteria and design assumptions for the external dose rate assessment are:

- The external dose rate limits for RCT, NCT, and HAC as defined in [49 CFR Part 173] or [SSR-6 2018] must not be exceeded.
- For the assessment of the dose rates, conservative assumptions with respect to the cylinder filling ratio and the shape of the 30B-X cylinder are used.
- For the assessment of the dose rate at the vehicle, two and four packages loaded side-by-side are considered, respectively.
- For the assessment of the dose rate increase after the tests simulating NCT, a permissible deformation is evaluated for filled cylinders (with respect to the limit of 20 % dose rate increase) and compared with the deformations calculated for NCT. Additionally, the dose rate increase is assessed for 30B-X cylinders containing heels of $UF_6$ by taking into account conservative assumptions.

#### 2.1.2.2.5 Criticality Safety Assessment

The acceptance criteria and design assumptions for the criticality safety assessment are:

- Criticality safety is ensured by the confinement system consisting of the 30B-X cylinder with the CCS and the steel shells of the DN30 PSP, which are compacted around the 30B-X cylinder to a total thickness of 10 cm in radial direction and 8 cm in axial direction, thereby minimizing the distance between adjacent packages.
- For RCT, NCT and HAC the criticality safety criterion is $k_{\text{eff}} + 3\sigma + \Delta k < 0.95$ (see section 2.6.1).

## 2.2 Structural Analysis

As described in the guideline through the technical analyses in section 2.1.1.1, the structural analysis of the DN30-X package, consisting of the 30B-X cylinder and the DN30 PSP, is based to a large extent on the already licensed DN30 package [CoC 9362], consisting of the 30B cylinder and the DN30 PSP. This is possible for the following reasons:

- The 30B-X cylinder has the same gross weight as the standard 30B cylinder while also having the same outer dimensions, shell thicknesses and material specifications of the pressure envelope and the cylinder skirts (see Appendix 1.9.2 (Manufacturing Specification 30B-X Cylinder) and table 1-13).
- The 30B-X and the standard 30B cylinder are equipped with the same valve and plug.
- The 30B-X and the standard 30B cylinder are both transported in the same DN30 PSP.

The only difference between the DN30 and the DN30-X package is the slightly different distribution of the content weight within the 30B-X cylinder, which is due to the addition of the internal CCS. Furthermore, the combination of CCS and $UF_6$ might interact differently with the cylinder shells than the $UF_6$ content on its own. However, since the $UF_6$ is in solid form during transport, the CCS is essentially stuck in the content and, thus, the possibilities of the CCS to move around within the 30B-X cylinder are very limited. Consequently, the interaction of the content with the 30B cylinder and the interaction of the CCS stuck in the content with the 30B-X cylinder is comparable.

Because of the above similarities between the two packages, the structural analysis of the DN30 package for handling and under RCT in [DNT 2019] is entirely valid for the DN30-X package. The corresponding calculations solely depend on the package weight and package dimensions, which are identical for the two packages. Hence, no calculations are required for the structural analysis of the DN30-X for handling and under RCT.

Using the same DN30 PSP for the DN30 and the DN30-X package also allows to transfer some of the analysis under NCT that only take into account the DN30 PSP and, thus, remain valid independent of the type of cylinder. Accordingly, no calculations are required for the water spray test, the compression test and the penetration test. The corresponding proves are also found in [DNT 2019].

Additional analyses are only required for the drop tests under NCT and HAC to account for the above-mentioned differences between the packages. However, it can safely be assumed that these differences are small so that the impact the 30B-X cylinder has on the DN30 PSP is comparable to the impact the 30B cylinder has on the DN30 PSP. Further details are provided in the introduction to the structural analysis of the DN30-X package under HAC in section 2.2.6.

Even though reference is made to [DNT 2019] for entire subparts of the structural analysis of the DN30-X package, a complete list of the basic assumptions for these calculations is provided in section 2.2.1. This includes the load assumptions for normal operating conditions of the 30B-X cylinder, handling of the DN30-X package, RCT, NCT and HAC as well as the material data used in these analyses. The corresponding analyses are included in sections 2.2.2 through 2.2.6. Here, reference is made to [DNT 2019] when appropriate and detailed analyses are provided otherwise.

### 2.2.1 Basic Assumptions for the Calculations

Basic assumptions for the calculations are listed in the following. They include load assumptions for different load cases, the definition of calculation methods and material parameters of the materials used for the proof.

#### 2.2.1.1 Load Assumptions

Individual load assumptions are made for normal operating conditions of the 30B-X cylinder as well as for handling, RCT, NCT and HAC for the DN30-X package. They are discussed in detail in the following sections.

##### 2.2.1.1.1 Normal Operating Conditions for the 30B-X Cylinder

With reference to [ANSI N14.1], Table 1, the load assumptions for normal operating conditions of the 30B-X cylinder are adapted as they stand for the standard 30B cylinder and include:

- The 30B-X cylinder is designed for an internal maximum allowable working pressure (MAWP) of 1.38 MPa gauge at a temperature of 121 °C.
- The 30B-X cylinder is designed for an external MAWP of 172 kPa gauge.
- The 30B-X cylinder is designed for a minimum design metal temperature (MDMT) of -29 °C at 1.38 MPa gauge.
- The 30B-X cylinder is designed for a transport temperature of -40 °C.
- The 30B-X cylinder withstands the hydraulic strength test at a test pressure of 2.76 MPa gauge (twice the MAWP) without generating unacceptable stress.

##### 2.2.1.1.2 Handling of the DN30-X Package

Load assumptions for handling include:

- Temperatures at the package corresponding to an ambient temperature of 38 °C and solar insolation (see section 2.3)
- Internal and external pressure
- Hoisting coefficients that are considered for handling operations

Load assumptions as basis for calculations for handling the package are listed in table 2-4.

**Table 2-4 Load assumptions for handling**

| Load assumption | Component | Value | Unit |
|---|---|---|---|
| Temperature | 30B-X cylinder | 64 | °C |
| | Lifting lugs at feet | 70 | °C |
| | Lifting lugs at top half | 100 | °C |
| | Feet | 70 | °C |
| Internal pressure | 30B-X cylinder | 152 | kPa |
| External pressure | | 100 | kPa |
| Hoisting coefficient | Lifting lugs | 2 | - |
| Load cycles for fatigue analysis | | 150000 | - |

#### 2.2.1.1.3 RCT for the DN30-X Package

Load assumptions for RCT include:

- Temperatures at the package corresponding to an ambient temperature of 38 °C and solar insolation (see section 2.3)
- Maximum transport accelerations according to [10 CFR Part 71] §45(b)(1)
- Vibrations during transport

Load assumptions as basis for calculations under RCT are listed in table 2-5.

**Table 2-5 Load assumptions for RCT**

| Load assumption | Component | Value | Unit |
|---|---|---|---|
| Temperature<br>(ambient temperature of 38 °C and solar insolation) | Outer shell, feet<br>30B-X cylinder | 70<br>64 | °C<br>°C |
| Temperature<br>(ambient temperature of -40 °C in the shade) | Complete packaging | -40 | °C |
| Accelerations | Complete packaging | | |
| axial | | 10.0 | g |
| lateral | | 5.0 | g |
| vertical | | -1.0 ± 2.0 | g |
| Vibrations | Complete packaging | 0.3 | g |

#### 2.2.1.1.4 NCT for the DN30-X Package

Load assumptions for NCT include:

- Temperatures at the package corresponding to an ambient temperature of 38 °C and solar insolation (see section 2.3)
- Tests for demonstrating the ability to withstand normal conditions of transport according to [10 CFR Part 71] §71(a) and [49 CFR Part 173] §465(a) or [SSR-6 2018] para. 719
- Reduction of ambient pressure

Load assumptions as basis for calculations under NCT are listed in table 2-6.

**Table 2-6 Load assumptions for NCT**

| Load assumption | Individual test | Component | Value |
|---|---|---|---|
| Temperature | Drop test, stacking test, penetration test | DN30 PSP | 60 °C |
| | | 30B-X cylinder | 64 °C |
| Tests according to [10 CFR Part 71] §71(a) and [49 CFR Part 173] §465 or [SSR-6 2018] para. 719 | Water spray | Packaging surface | [10 CFR Part 71] §71(c)(6) and [49 CFR Part 173] §465(b) or [SSR-6 2018] para. 721 |
| | Free drop | Complete package | [10 CFR Part 71] §71(c)(7) and [49 CFR Part 173] §465(c) or [SSR-6 2018] para. 722<br>Free drop height 1.2 m |
| | Compression | Complete package | [10 CFR Part 71] §71(c)(9) and [49 CFR Part 173] §465(d) or [SSR-6 2018] para. 723 |
| | Penetration | Packaging surface | [10 CFR Part 71] §71(c)(10) and [49 CFR Part 173] §465(e) or [SSR-6 2018] para. 724 |
| Ambient pressure | Reduced | 30B-X cylinder | [10 CFR Part 71] §71(c)(3) and [49 CFR Part 173] §412(f) or [SSR-6 2018] para. 645<br>25 kPa 1) |
| | Increased | 30B-X cylinder | [10 CFR Part 71] §71(c)(4)<br>140 kPa |

1) Only 60 kPa are required per [49 CFR Part 173] §412(f) or [SSR-6 2018] para. 645.

2.2.1.1.5 HAC for the DN30-X Package

Load assumptions for hypothetical accident conditions of transport include:

- Temperatures at the package corresponding to an ambient temperature of 38 °C and solar insolation (see section 2.3)
- Tests for demonstrating the ability to withstand accident conditions of transport according to [10 CFR Part 71] §73(a) or [SSR-6 2018] para. 726
- Internal and external pressure

Load assumptions for accident conditions of transport are listed in table 2-7.

**Table 2-7 Load assumptions for HAC**

| Load assumption | Individual test | Component | Value |
|---|---|---|---|
| Temperature | Free drop and puncture | Packaging main body outer shell | 60 °C |
| | | 30B-X cylinder | 64 °C |
| Tests according to [10 CFR Part 71] §73 or [SSR-6 2018] para. 726 | Free drop | Complete package | [10 CFR Part 71] §73(c)(1) or [SSR-6 2018] para. 727(a)<br>Free drop height 9 m |
| | Puncture | Complete package | [10 CFR Part 71] §73(c)(3) or [SSR-6 2018] para. 727 (b)<br>Free drop height 1 m |
| | Thermal | Complete package | [10 CFR Part 71] §73(c)(4) or [SSR-6 2018] para. 728 |
| | Immersion | 30B-X cylinder | [10 CFR Part 71] §73(c)(6) or [SSR-6 2018] para. 729<br>150 kPa for 8 h |
| Water pressure | Immersion (fissile material) | 30B-X cylinder | [10 CFR Part 71] §73(c)(5) or [SSR-6 2018] para. 731<br>9 kPa for 8 h |
| Pressure increase due to maximal temperatures during thermal test | Thermal | 30B-X cylinder | [10 CFR Part 71] §73(c)(4) or [SSR-6 2018] para. 728<br>106 kPa (see section 2.2.6.4.1) |

### 2.2.1.2 Material Data

#### 2.2.1.2.1 Material Data DN30 PSP

The materials of the DN30 PSP are specified in section 1.4.1.2. Since the same DN30 PSP is used for the DN30-X package as for the already licensed DN30 package [CoC 9362], the corresponding material data used in the safety analysis of the DN30-X package is already provided in [DNT 2019]. Among others, these include the minimally required yield stresses in the required temperature range according to the standards listed in section 1.4.1.2 as well as the materials strain hardening behavior and strain-rate sensitivity.

#### 2.2.1.2.2 Material Data 30B-X Cylinder

**Table 2-8 Material data for plates of material P355NL1 (grade 70)**

| Material property | Designation | Temperature | Value | EU standard | US standard |
|---|---|---|---|---|---|
| Density | $\varrho$ | 20 °C | 7.85 g/cm³ | DIN EN 10028-1 | ASTM A-516 |
| 0.2 % yield stress | $R_{p0.2}$ | 20 °C | 355 MPa | DIN EN 10028-3 | ASTM A-516 |
| | | 100 °C | 323 MPa | DIN EN 10028-3 | ASTM A-516 |
| | | 121 °C | 315 MPa | DIN EN 10028-3 | ASTM A-516 |
| Ultimate tensile strength | $R_m$ | 20 °C | 490-630 MPa | DIN EN 10028-3 | ASTM A-516 |
| Elastic modulus | $E$ | 20 °C | 2.12E5 MPa | DIN EN 10028-1 | ASTM A-516 |
| | | 100 °C | 2.07E5 MPa | DIN EN 10028-1 | ASTM A-516 |
| Poisson's ratio | $\nu$ | - | 0.3 | - | - |
| Elongation at fracture | $A$ | - | 22 % | DIN EN 10028-3 | ASTM A-516 |
| Linear thermal expansion coefficient | $\alpha$ | 20-100 °C | 12.5E-6 $K^{-1}$ | DIN EN 10028-1 | ASTM A-516 |

**Table 2-9 Material data for boron carbide**

| Material property | Designation | Temperature | Value | Standard |
|---|---|---|---|---|
| Density | $\varrho$ | 20 °C | 1.35 g/cm³ | Appendix 1.9.2 (Manufacturing Specification 30B-X Cylinder) |
| 0.2 % yield stress | $R_{p0.2}$ | 20 °C | 261 MPa | |
| Elastic modulus | $E$ | 20 °C | 3.62E5 MPa | |
| Poisson's ratio | $\nu$ | - | 0.18 | |
| Linear thermal expansion coefficient | $\alpha$ | 20-100 °C | 3.2-9.4E-6 $K^{-1}$ | |

### 2.2.2 Normal Operating Conditions for the 30B-X Cylinder

This part of the structural analysis covers the normal operating conditions for the 30B-X cylinder as defined in section 2.2.1.1.1. For these analyses, the 30B-X cylinder is assumed to comply with its specification provided in section 1.4.1.1.

#### 2.2.2.1 MDMT and Minimum Transport Temperature

Since the same material specifications according to table 1-9 (for the cylinder) and table 1-10 (for the valve and plug) apply to the standard 30B cylinder and to the 30B-X cylinder, the requirements in section 2.2.1.1.1 towards the MDMT of -29 °C at 1.38 MPa gauge and the minimum transport temperature of -40 °C are identically fulfilled for the 30B-X cylinder. Consequently, the requirements with regard to the materials ductility and resistance to brittle failure at low temperatures are also identically fulfilled for the 30B-X cylinder.

#### 2.2.2.2 MAWP

To prove the structural integrity of the 30B-X cylinder under the design conditions section 2.2.1.1.1, the whole design temperature range of -29 °C to 121 °C is considered:

1. The materials yield strength decreases with increasing temperature and vice versa.
2. Different thermal expansion coefficients of different materials or existing temperature gradients may cause thermally induced stresses.

##### 2.2.2.2.1 Variation of Material Strength within Design Temperature Range

The impact of a decrease in material strength is investigated by analyzing the developing stresses in the pressure envelope of the 30B-X cylinder at the maximum design temperature of 121 °C with the MAWP as internal pressure in comparison to the hydraulic strength test at room temperature and twice the MAWP. At the maximum design temperature of 121 °C, the design stress intensity of the standard 30B cylinder shell material decreases from 237 MPa to 209 MPa, while the internal pressure is only half as high as during the hydraulic strength test. Since the pressure envelope of the 30B-X cylinder is unaltered compared to a 30B cylinder and the material specifications for the 30B-X cylinder in table 1-9 and table 1-10 are identical to the standard 30B cylinder, both cylinders equally perform under the conditions of the hydraulic strength test at twice the MAWP. Following this argumentation, the impact of a decrease in material strength of the 30B-X cylinder at the maximum design temperature is always covered by the hydraulic strength test.



##### 2.2.2.2.2 Thermally Induced Stresses

Thermally induced stresses are effectively prevented by the design of the 30B-X cylinder. Different materials with different thermal expansion interact only in the CCRs due to their $B_4C$ filling. The linear thermal expansion coefficient of $B_4C$ is in the range of $3.2$ to $9.4 \cdot 10^{-6}\ \mathrm{K}^{-1}$ (see table 2-9), while the linear thermal expansion coefficient of the carbon steel of the 30B-X cylinder shell is about $12.5 \cdot 10^{-6}\ \mathrm{K}^{-1}$ (see table 2-8). Hence, only a decrease in temperature could theoretically cause thermally induced stresses in the CCRs due to faster shrinking of the steel pipes around the $B_4C$ filling. Given the $B_4C$ filling is either in powder form or provided as pellets with a smaller radius than the CCR pipes, this will have no practical consequences.

Furthermore, the entire CCS has no fixed connection to another component of the 30B-X cylinder. The positioning of the CCS within the cylinder is solely maintained by the CCS restraints that are welded to the inside of the cylinder shell. In the theoretical case of a sudden temperature drop, faster shrinking of the cylinder shells is admissible because of the 5 mm clearance between each CCS restraint and the two outer lattice holders of the CCS (see Appendix 1.4.1A (Drawings 30B-X Cylinder)). Consequently, the design imposes no restrictions on the longitudinal expansion of the 30B-X cylinder and, thus, avoids the development of thermally induced stresses due to temperature gradients between the exterior surfaces and interior components of the 30B-X cylinder. In the radial direction, the skirts of the 30B-X cylinder impose the same restrictions as for the standard 30B cylinder so that no further investigations are required in this regard.

#### 2.2.2.3 Hydraulic Strength Test

The pressure envelope of the 30B-X cylinder is unaltered compared to a standard 30B cylinder and the same material specifications apply that are in listed table 1-9 and table 1-10. The addition

of the internal CCS does not affect the stress distribution at the 30B-X cylinder shell because no fixed connection exists between these two components. If anything, the CCS restraint that is welded to the inside of the cylinder shell has a positive impact on the stress distribution as the fillet weld adds to the resilience of the cylinder shell in this area, slightly improving its pressure-loading capacity. Consequently, the 30B-X and the standard 30B cylinder equally perform under the conditions of the hydraulic strength test at twice the MAWP and the impact of the hydraulic strength test on the internal CCS of the 30B-X cylinder can be analyzed separately.

The CCS of the 30B-X cylinder consists of the CCRs, the three lattice holders and the longitudinal stiffeners between the lattice holders. Only the CCRs are affected by a hydrostatic load because all other components of the CCS are solid material, resulting in a hydrostatic stress in those components that corresponds to the test pressure. This level of stress is insignificant for the specified carbon steel for those components.

As specified in section 1.4.2.1, the CCRs have an outer diameter of 60.3 mm and a thickness of 5.54 mm. The $B_4C$ filling of the CCRs is neglected in the analysis of the hydraulic strength test, as the mass of the $B_4C$ does not affect the results. However, neglecting the $B_4C$ filling removes any internal support, increasing the risk of a plastic collapse of the CCR carbon steel pipes. To comply with the requirements stipulated in [ANSI N14.1], the analysis of the CCRs is performed on the basis of [ASME BPVC], Section VIII, Division 1. For tubes under external pressure, the following formula applies:

$$P_\mathrm{a} = \frac{4B}{3(D_\mathrm{o}/t)} = \frac{4 \cdot 121\ \mathrm{MPa}}{3(60.3\ \mathrm{mm}/5.54\ \mathrm{mm})} = 14.8\ \mathrm{MPa} \qquad (3)$$

The factor $B = 121\ \mathrm{MPa}$ in equation (3) is determined on the basis of [ASME BPVC], Section II, Part D, Subpart 3, Figure CS-2. The resulting admissible external pressure of $P_\mathrm{a} = 14.8\ \mathrm{MPa}$ is significantly higher than the test pressure of twice the MAWP during the hydraulic strength test. Hence, there is no risk of failure of the CCRs regarding the test conditions of the hydraulic strength test.

This and the argumentation in section 2.2.2.2 prove that the 30B-X cylinder is well designed to operate over the same design temperature range as a standard 30B cylinder.

### 2.2.3 Handling of the DN30-X Package

The DN30-X packaging is designed for the transport of $UF_6$. Specified contents are defined in section 1.3. Strains in the packaging result from the following loads:

- Internal and external pressure (see section 2.2.3.1)
- Assembling loads (see section 2.2.3.2)
- Handling loads (see section 2.2.3.3)
- Temperature gradients in the components (an analysis covering handling and RCT is provided in section 2.2.4.2)

The corresponding load assumptions are listed in table 2-4.

#### 2.2.3.1 Internal and External Pressure

During handling and transport, the $UF_6$ content of the 30B-X cylinder is in solid form. For the analysis of the DN30-X package, it is assumed that the $UF_6$ and the 30B-X cylinder both have a

temperature of 64 °C corresponding to the triple point of $UF_6$. In this condition, the gas pressure above the solid $UF_6$ is 152 kPa (see table 1-1). This value is used for the analytical proof of an internal pressure in the 30B-X cylinder. For the proof of an external pressure on the 30B-X cylinder, an increased external pressure of 140 kPa according to [10 CFR Part 71] §71(4) is assumed.

As shown in section 2.2.2.2, the 30B-X cylinder is designed for an external MAWP of 172 kPa and an internal MAWP of 1.38 MPa. Consequently, the requirements concerning the internal and external pressure for the 30B-X cylinder as well as for the DN30-X package are fulfilled.

#### 2.2.3.2 Assembling

During assembling, the components of the DN30-X packaging are inserted into each other without applying forces. Stresses in the components during assembling are negligible. For tightening the securing bolts of the closure system, tightening torques are defined in handling instruction 0045-HA-2021-001 (see Appendix 1.7.1 (Handling Instruction)).

#### 2.2.3.3 Handling Loads

The following handling processes are carried out with the DN30-X package:

- Handling of the loaded and empty package by using the lifting lugs at the feet (see figure 1-6)
- Handling of the loaded and empty package using a forklift (see figure 1-7)
- Handling of the empty package by using slings (see figure 1-8)
- Handling of the top half of the DN30 PSP by using the lifting lugs (see figure 1-9)

As described in the beginning of section 2.2, the structural analysis of these handling processes is identical to the calculations performed in [DNT 2019] for the already licensed DN30 package [CoC 9362]. The only influencing variables in these calculations are the DN30 package weight, the package dimensions, and the material properties of the DN30 PSP. Since the gross weight of the 30B-X cylinder is identical to the standard 30B cylinder and the same DN30 PSP is used for both packages, the same package weight, package dimensions and material properties of the DN30 PSP apply to the DN30-X package (see table 1-13 and table 1-14). Hence, the DN30-X package fulfills the following acceptance criteria defined in section 2.1.2.2.1 referring to [10 CFR Part 71] §45(a):

- All lifting attachments that are a structural part of the DN30-X package are designed with a minimum safety factor of 3 against yielding when used to lift the package in the intended manner.
- Failure of any lifting device under excessive load does not impair the ability of the DN30-X package to meet other requirements of [10 CFR Part 71].

The structural proof for handling the DN30-X package is completed by referencing the detailed analyses found in the SAR of the DN30 package in [DNT 2019].

### 2.2.4 Ability of the DN30-X Package to Withstand RCT

The DN30-X packaging is designed for the transport of $UF_6$. Specified contents are defined in section 1.3. Strains in the packaging result from the following loads under RCT:

- Maximum transport accelerations (see section 2.2.4.1)
- Vibrations during transport (see section 2.2.4.1)
- Temperature gradients in the components (see section 2.2.4.2)

The corresponding load assumptions are listed in table 2-5.

#### 2.2.4.1 Tie-down

The DN30-X package is transported by road, rail or sea. For the transport, common flat racks or dedicated transport means are used (see figure 1-10). The tie-down features are designed such that relative movement between the vehicle and the DN30-X package is excluded. Thus, only the maximum acceleration values defined in table 2-5 affect the package during transport.

As described in the beginning of section 2.2, the structural analysis of the DN30-X package under RCT is identical to the calculations performed in [DNT 2019] for the already licensed DN30 package [CoC 9362]. The same transport configurations apply to the DN30 package and the only influencing variables in these calculations are the package weight, the package dimensions and the material properties of the DN30 PSP. Since the gross weight of the 30B-X cylinder is identical to the standard 30B cylinder and the same DN30 PSP is used for both packages, the same package weight, package dimensions, and material properties of the DN30 PSP apply to the DN30-X package (see table 1-13 and table 1-14). Hence, the DN30-X package fulfills the following acceptance criteria defined in section 2.1.2.2.1 referring to [10 CFR Part 71] §45(b):

- All tie-down devices that are a structural part of the DN30-X package withstand, without generating stress in any material of the package in excess of its yield strength, a static force applied to the center of gravity of the package having a vertical component of 2 times the weight of the package with its contents, a horizontal component along the direction in which the vehicle travels of 10 times the weight of the package with its contents, and a horizontal component in the transverse direction of 5 times the weight of the package with its contents.
- Failure of the devices under excessive load does not impair the ability of the DN30-X package to meet other requirements of [10 CFR Part 71].

The structural proof for the tie-down devices of the DN30-X package is completed by referencing the detailed analyses found in the SAR of the DN30 package in [DNT 2019].

#### 2.2.4.2 Analysis of Stresses Caused by Temperature Influences

The analysis of stresses caused by temperature influences performed in [DNT 2019] for the DN30 package also applies to the DN30-X package. This is because the only influencing variables in these calculations are the dimensions and material properties of the DN30 PSP as well as the outer dimensions of the standard 30B cylinder including their manufacturing tolerances. Since these are identical to the 30B-X cylinder and the same DN30 PSP is used for both packages, the determined remaining clearance and thermally induced stresses are at least covering for the DN30-X package, especially considering the larger heat sink of the 30B-X cylinder results in lower temperatures (see section 2.3). Hence, the following applies to the DN30-X package with regard to stresses caused by temperature influences:

- The possibly different expansions of the top and bottom half of the DN30 PSP, caused by temperature differences that are due to differing insolating conditions on the top and bottom half, are small. The gaps between the flanges of the top and bottom half allow for sufficient relative movement to compensate for different expansions.
- There is sufficient clearance between the DN30 PSP and the 30B-X cylinder to compensate differing thermal expansions of the DN30 PSP and the 30B-X cylinder.

The analysis of thermally induced stresses for the DN30-X package under RCT is completed by referencing the detailed analyses found in the SAR of the DN30 package in [DNT 2019].

### 2.2.5 Ability of the DN30-X Package to Withstand NCT

#### 2.2.5.1 Water Spray Test

The water spray test as defined in [10 CFR Part 71] §71(c)(6) and [49 CFR Part 173] §465(b) or [SSR-6 2018] para. 721 requires the simulation of a heavy rainfall of approximately 5 cm for at least an hour.

Since the same DN30 PSP is used for the DN30-X package as for the already licensed DN30 package [CoC 9362], the argumentation regarding the water spray test provided in the safety analysis of the DN30 package in [DNT 2019] persists. Hence, there is no impact of this test on either the loss or dispersal of the radioactive contents or on the dose rate at any external surface of the DN30-X package with respect to the requirements in [10 CFR Part 71] §43(f) and [49 CFR Part 173] §412(j) or [SSR-6 2018] para. 648.

#### 2.2.5.2 Free Drop Test

The free drop test from a height of 1.2 m is analyzed in sequence with the tests simulating HAC (the 9 m free drop test and the puncture test). For better overview and comparison of the deformations after the 1.2 m free drop test and after the 9 m free drop test, the results of these sequences are both discussed in section 2.2.6. As the DN30-X package is designed to withstand HAC, the proof that the DN30-X package is also designed to withstand NCT is a direct consequence.

Preceding corner drops from a height of 0.3 m as required by [49 CFR Part 173] §465(c)(2) will not have any adverse effect on the DN30-X package. The free drop test from a height of 1.2 m was investigated for many drop angles in the safety analysis of the DN30 package in [DNT 2019]. Using the results of the comparing analyses between the DN30-X and the DN30 package in section 2.2.6.2.5, the results of the free drop tests with the DN30 package can be applied to the

DN30-X package. As the deformations of the steel parts of the DN30 PSP remained below 10 % after the free drop tests, the impact from preceding 0.3 m corner drops is estimated to be negligible and not investigated in detail for the DN30-X package.

In the following, the conditions for the proof of [10 CFR Part 71] §43(f) and [49 CFR Part 173] §412(j) or [SSR-6 2018] para. 648 are established.

##### 2.2.5.2.1 Conditions to Prevent Loss or Dispersal of the Radioactive Contents

In section 2.2.6, it is shown by analysis that even after a 10.2 m free drop test, there is no physical contact between the valve or the plug and any other component of the DN30-X packaging other than its original point of attachment. Hence, structural damaging of the valve or the plug of the 30B-X cylinder during the 1.2 m free drop test can be excluded.

Furthermore, it is shown in the safety analysis of the DN30 package in [DNT 2019] by real testing that the results of the drop test analysis for the DN30 package comply with the real tests. It is confirmed that there is no physical contact between the valve or the plug and any other component of the DN30 packaging other than its original point of attachment, even after the cumulative effects of the 1.2 m free drop test, the 9 m free drop test and the puncture test.

Furthermore, the leakage rate of the containment system (the 30B cylinder), was measured and documented after each test sequence. The measurements show that there is no increase of the leakage rate that could lead to a loss or dispersal of the radioactive content.

##### 2.2.5.2.2 Conditions to Prevent the Increase of the Maximum External Radiation Level

In section 2.5.6, it is shown that the maximum dose rate at the surface of the DN30-X package is to be expected in radial direction in the center of the side of the package. In section 2.2.6, the deformations to be expected after the 1.2 m free drop tests are analyzed. For the 1.2 m free drop onto the top of the package described in section 2.2.6.2.6.5, a reduction of the distance between the inner and outer shell of the DN30 PSP of 4 mm was determined. Conservatively, a distance reduction of 6 mm is assumed for the dose rate analysis.

#### 2.2.5.3 Compression Test

The outer shape of the DN30 PSP effectively prevents stacking. However, according to [10 CFR Part 71] §71(c)(9), a compression test must be performed for packages weighing up to 5000 kg. The package must be subjected, for a period of 24 hours, to a compressive load applied uniformly to the top and bottom of the package in the position, in which the package would normally be transported.

The compression test has already been analyzed in [DNT 2019] for the already licensed DN30 package [CoC 9362], consisting of the DN30 PSP and the standard 30B cylinder. Since the 30B cylinder has not been credited in any regard in this analysis and the same DN30 PSP is used for the DN30-X package, the simulation results provided in [DNT 2019] are also valid for the DN30-X package. Consequently, the DN30-X package fulfills the requirements of [10 CFR Part 71] §71(c)(9).

#### 2.2.5.4 Penetration Test

According to [10 CFR Part 71] §71(c)(10), the impact of the hemispherical end of a vertical steel cylinder of 3.2 cm diameter and 6 kg mass, dropped from a height of 1 m onto the exposed

surface of the DN30-X package has to be investigated that is expected to be most vulnerable to puncture. As demonstrated in section 2.2.6, the DN30-X package is designed to withstand the puncture test under HAC, which is much more severe for the DN30-X package weighing about 4100 kg than the penetration test. Hence, the test as defined in [10 CFR Part 71] §71(c)(10) and [49 CFR Part 173] §465(e) or [SSR-6 2018] para. 724 is covered by the test defined in [10 CFR Part 71] §73(c)(3) or [SSR-6 2018] para. 727(b).

There is no impact of this test on the loss or dispersal of the radioactive contents with respect to the requirement stipulated in [10 CFR Part 71] §43(f) and [49 CFR Part 173] §412(j) or [SSR-6 2018] para. 648(a).

In comparison to the free drop test from a height of 1.2 m, the impact of this test on the dose rate at any external surface of the DN30-X package with respect to the requirement stipulated in [10 CFR Part 71] §43(f) and [49 CFR Part 173] §412(j) or [SSR-6 2018] para. 648(b) is negligible.



#### 2.2.5.5 Reduced and Increased External Pressure

The 30B-X cylinder is designed for an external and internal MAWP of 172 kPa and 1.38 MPa, respectively. As defined in section 1.2.8, the MNOP of the DN30-X package during transport is 152 kPa. Hence, a reduction to 25 kPa or an increase to 140 kPa of the ambient pressure as specified in [10 CFR Part 71] §71(c)(3) and (4) will not affect the 30B-X cylinder (the containment system). This argumentation covers the reduction of the ambient pressure to 60 kPa as required by [49 CFR Part 173] §412(f) or [SSR-6 2018] para. 645.

### 2.2.6 Ability of the DN30-X Package to Withstand NCT and HAC

Based on the argumentation in the beginning of section 2.2, the experimental drop tests and the drop tests analysis under NCT and HAC performed for the DN30 package in [DNT 2019] in the operating temperature range of -40 °C to +60 °C are also covering the DN30-X package. To complete the structural analysis of the DN30-X package under NCT and HAC, only some additional analyses are required to account for the differences between the two packages. Therefore, section 2.2.6.1 contains a summary of the structural analysis of the DN30 package under NCT and HAC performed in [DNT 2019], but the actual structural analysis of the DN30-X package under NCT and HAC consists only of two fundamental parts:

1. The first part in section 2.2.6.2.5 provides evidence that the interaction between the 30B-X cylinder and the DN30 PSP is comparable to the interaction between the 30B cylinder and the DN30 PSP. These analyses prove that the initially made assumptions are admissible.
2. In the second part, analyses are performed that specifically consider the acceptance criteria established for the internal CCS of the 30B-X cylinder in section 2.2.6.2.6 and, therefore, also account for the differences between the DN30-X and the already licensed DN30 package. In addition, this part also contains a discussion of the remaining drop test scenarios that were considered in the safety analysis of the DN30 package in [DNT 2019].

Both the comparison between the two packages and the specific analyses for the DN30-X package consider a 30B-X cylinder design with 35 CCRs arranged in a 1 x 6 x 12 x 16 pattern, which deviates from the actual designs of the 30B-10 and 30B-20 cylinder having 33 and 43 CCRs, respectively. The impact of these deviations on the results of the structural analysis of the DN30-X package under NCT and HAC is discussed in section 2.2.6.5. The following sequential application of tests is considered in the analyses:

1. The free drop test under NCT as defined in [10 CFR Part 71] §71(c)(7) and [49 CFR Part 173] §465(c) or [SSR-6 2018] para. 722 (drop height 1.2 m)
2. The free drop test under HAC as defined in [10 CFR Part 71] §73(c)(1) or [SSR-6 2018] para. 727(a) (drop height 9 m)
3. The puncture test under HAC as defined in [10 CFR Part 71] §73(c)(3) or [SSR-6 2018] para. 727(b) (drop height 1 m)

Beside the two fundamental parts of the structural analysis of the DN30-X under NCT and HAC, the water immersion test for packages containing fissile material is discussed in section 2.2.6.3. Finally, the influence of the thermal test under HAC on the structural integrity of the DN30-X package is evaluated in section 2.2.6.4.



### 2.2.6.1 Summary of the Structural Analysis of the DN30 Package under NCT and HAC

In this section, a summary of the main points and results of the analyses and experimental drop tests performed for the already licensed DN30 package [CoC 9362] is provided. The structural analysis of the DN30 package under NCT and HAC is documented in [DNT 2019] and comprises the free drop test under NCT from a height of 1.2 m as well as the free drop test from a height of 9 m and the puncture test under HAC.

The analyses of these tests are valid for all filling ratios from standard 30B cylinders with heels up to standard 30B cylinders filled with the maximum amount of $UF_6$ of 2277 kg as defined in [ANSI N14.1]. They were carried out in three major steps:

1. Analysis of the deformation behavior of the DN30 package by using proven simulation tools. These pre-analysis resulted in the selection of certain drop test sequences that were used as benchmarks.
2. Real testing of DN30 PSP prototypes and standard 30B cylinders filled with heavy concrete as a surrogate material for the $UF_6$ content by applying the selected benchmark test sequences.
3. Validation of the simulation model of the DN30 package by comparison of the experimental drop test results with the calculation results. The structural analysis was then completed by performing analyses with the validated simulation model to cover the temperature range of -40 °C to +60 °C applicable to the DN30 package and other drop test scenarios.

The simulation model of the DN30 package was validated based on five drop test sequences that were performed for the experimental testing of the package. The results of these benchmark analyses are:

- Deformations of the DN30 PSP prototypes measured after the real drop tests are predicted with good accuracy by the calculation model with deviations remaining mostly below 10 % compared to the experiment. Thus, the deviations of the calculated deformations from the measured deformations are within the measurement error.

- Local effects like rupture of welding seams or puncture of the outer shell of the DN30 PSP can be predicted with sufficient accuracy by evaluating the strains and stresses in the respective parts of the DN30 PSP.
- Decelerations of the 30B cylinder are predicted with the calculation model with sufficient accuracy.
- In some cases, the non-deterministic behavior of the 30B cylinder with respect to the DN30 PSP due to an undefined position of the 30B cylinder at the time of impact leads to deceleration peaks, which cannot be predicted by the calculation model.
- The good agreement of the simulation and the experiment allows for the evaluation of the behavior of the DN30 package in the temperature range of -40 °C to +60 °C based on the drop test sequences 1 and 3.

In total, eight drop test sequences have been investigated taking into account the temperature range of -40 °C to +60 °C as well as a change in the order of the drop tests simulating HAC and different configurations of the content:

1. Inclined onto the valve side corner – Drop test sequence 1
2. Inclined onto the plug side corner – Drop test sequence 2
3. Flat onto the valve side – Drop test sequence 3
4. Flat onto the closure system – Drop test sequence 4
5. Inclined onto the feet (slap-down) – Drop test sequence 5
6. Flat onto the top side – Drop test sequence 8
7. Flat onto the plug side – Drop test sequence 9
8. Inclined onto the top (slap-down) – Drop test sequence 10

The results of the performed analyses show that the sequential application of the free drop test under HAC followed by the puncture test is much more demanding for the DN30 package than the reverse order. Furthermore, the results of the performed experimental drop tests in combination with the performed analyses prove that:

- The leakage rate after each of the drop test sequences is less than $1.0 \cdot 10^{-6}\ \mathrm{Pa \cdot m^3/s}$.
- All closure systems are intact after each drop test sequence.
- There is no contact between the valve and any other part of the DN30 PSP or the 30B cylinder except for its initial point of contact (the thread) in any drop test sequence.
- There is no contact between the plug and any other part of the DN30 PSP or the 30B cylinder except for its initial point of contact (the thread) in any drop test sequence.
- The valve protecting device fulfills its function during and after each drop test sequence.
- The plug protecting device fulfills its function during and after each drop test sequence.
- The rotation preventing device fulfills its function during and after each drop test sequence.
- The intumescent material as well as the housing are still present and undamaged after each drop test sequence.

Furthermore, the following applies for the analysis of drop test sequence 1 at -40 °C and +60 °C and drop test sequence 3 at -40 °C:

- The deformations for the free drop test under HAC at +60 °C increase by maximally 8 % compared to RT.
- The deformations for free drop test under HAC at -40 °C decrease by maximally 9 % compared to RT.
- The decelerations at -40 °C increase by less than 5 % for a cut-off frequency of 20 Hz compared to RT.
- There is neither at -40 °C nor at +60 °C a contact between the valve and any other part of the DN30 PSP or the 30B cylinder except for its initial point of contact (the thread).
- There is neither at -40 °C nor at +60 °C a contact between the plug and any other part of the DN30 PSP or the 30B cylinder except for its initial point of contact (the thread).
- The valve protecting device fulfills its function during and after each drop test sequence in the whole temperature range.
- The rotation preventing device fulfills its function during and after each drop test sequence in the whole temperature range.
- The plug protecting device fulfills its function during and after each drop test sequence in the whole temperature range.

Based on these results, the DN30 PSP is able to provide the required mechanical protection of the 30B cylinder under NCT and HAC for temperatures ranging from -40 °C to +60 °C.



#### 2.2.6.2 Structural Analysis of the DN30-X Package under NCT and HAC

As pointed out in the beginning of section 2.2.6, this part of the structural analysis of the DN30-X package provides evidence that the interaction between the 30B-X cylinder and the DN30 PSP is comparable to the interaction between the standard 30B cylinder and the DN30 PSP. This proves that the initially made assumptions are admissible and that the drop test analyses and experimental drop tests performed for the DN30 package in [DNT 2019] are also covering for the DN30-X package. The comparison of the drop test analyses for the DN30-X and the DN30 package is described in section 2.2.6.2.5.

With this at hand, additional analyses are performed in section 2.2.6.2.6 that specifically consider the acceptance criteria in section 2.1.2.2.1 that have been established for the internal CCS of the 30B-X cylinder and, therefore, also account for the minor differences between the DN30-X and the already licensed DN30 package. Furthermore, this part contains a discussion of the remaining drop test scenarios that were considered in the safety analysis of the DN30 package in [DNT 2019].

The analyses of the drop tests under NCT and HAC are valid for all filling ratios from 30B-X cylinders with heels up to 30B-X cylinders filled with the maximum amount of $UF_6$ as defined in table 1-4. Further details on the investigated analysis sequences and orientations are provided in section 2.2.6.2.1. Then, a brief introduction to the software being used to perform the simulations is provided in section 2.2.6.2.2.

The entire modelling procedure is described in section 2.2.6.2.3. Since the same simulation model is used for the DN30 PSP that has already been developed in [DNT 2019], this section focuses on the specific design for the 30B-X cylinder. Beside the deviations between the FEM

and the CAD models of the cylinders, the chosen element types, applied initial and boundary conditions as well as contact definitions and material models are described. The modelling of the DN30-X package is completed by a comprehensive description of the content modelling.

#### 2.2.6.2.1 Analysis Sequences and Orientations

The drop test analyses for the DN30-X package under NCT and HAC consider the following sequential application of tests:

1. The free drop test under NCT as defined in [10 CFR Part 71] §71(c)(7) and [49 CFR Part 173] §465(c) or [SSR-6 2018] para. 722 (drop height 1.2 m)
2. The free drop test under HAC as defined in [10 CFR Part 71] §73(c)(1) or [SSR-6 2018] para. 727(a) (drop height 9 m)
3. The puncture test under HAC as defined in [10 CFR Part 71] §73(c)(3) or [SSR-6 2018] para. 727(b) (drop height 1 m)

To improve the comparability of the simulation results for the DN30 and the DN30-X package, the free drop test from a height of 1.2 m and the free drop test from a height of 9 m are combined to a single 10.2 m drop test. The combination of those two drop tests proved to be more demanding than performing them in sequence[1] (see [DNT 2019]).

The simulation of entire drop test sequences is generally not required, as the results in [DNT 2019] prove that the performance of the DN30 package during the puncture test is mainly determined by the performance of the DN30 PSP. An increase in the deformations of the 30B cylinder during the puncture test only occurred in rare cases, without having any safety relevant impact. Hence, the impact of the puncture test on the DN30-X package is analyzed for each investigated drop test orientation by argumentation.

Detailed analyses are carried out for three drop test orientations of the DN30-X package:

1. Inclined onto the valve side so that the line between center of gravity and point of impact is perpendicular to the target surface
2. Flat onto the valve side
3. Flat onto the feet

The first two drop test orientations are investigated in section 2.2.6.2.5 and are used to provide evidence that the interaction between the 30B-X cylinder and the DN30 PSP is comparable to the interaction between the standard 30B cylinder and the DN30 PSP. The drop test flat onto the feet has not been investigated for the DN30 package, but this orientation is specifically relevant with regard to the acceptance criteria for the CCS inside the 30B-X cylinder defined in section 2.1.2.2.1. The flat drop test onto the feet is investigated in section 2.2.6.2.6.1.

The following drop test orientations, which have also been investigated for the DN30 package in [DNT 2019], are considered in the structural analysis of the DN30-X package as well:

- Flat onto the plug side
- Flat onto the closure system

---

[1] The reverse order of the tests under HAC has been considered in the safety analysis of the DN30 package, but it was shown in [DNT 2019] that the above order of the tests is the most demanding. The consideration of the order of the drop tests under HAC is only relevant with regard to the requirements in [SSR-6 2018].

- Flat onto the top side
- Inclined onto the plug side so that the line between center of gravity and point of impact is perpendicular to the target surface
- Inclined onto the closure system so that the line between center of gravity and point of impact is perpendicular to the target surface
- Inclined onto the feet (slap-down)
- Inclined onto the top side (slap-down)

However, the strong similarity between the DN30 and the DN30-X package allows to discuss the impact these drop test orientations have on the DN30-X package. Detailed drop test simulations are not required. The detailed discussion for each of the above drop test orientation is also provided in section 2.2.6.2.6.



#### 2.2.6.2.2 Description of the Calculation Codes

The results of the drop test simulations for the DN30-X package are obtained by the numerical solving of differential equations, which are based on finite element methods (FEM). Because of the highly dynamic nature of this kind of simulations, the FEM solver ANSYS LS-DYNA (MPP DP R11.2.0) [LS-Dyna 2018] is used. LS-DYNA is widely used for crash simulations by the automobile industry. Other applications include sheet metal forming and cutting in the manufacturing industry as well as bird strike, jet engine blade containment and structural failure in the aerospace industry.

A common aspect of the above-mentioned applications is a distinct nonlinear behavior. One key element of LS-DYNA, and why it is used in these cases, is the explicit time integration to solve the equations of motion. On the one hand, strong nonlinearities are handled effectively compared to implicit methods without running into stability problems. On the other hand, the explicit time integration is not unconditionally stable but has to satisfy the so-called Courant-Friedrichs-Lewy condition (CFL) at all time to remain stable. Through the materials velocity of sound, this condition leads to a relationship between the time step size and the mesh resolution, which implies a smaller time step size for a finer mesh. In other words, the solver LS-DYNA demands a regular mesh with similar element sizes to obtain accurate results in a reasonable computation time. This aspect is considered during the geometry discretization and mesh generation of the DN30-X package simulation model.

As a stand-alone FEM solver, LS-DYNA lacks any modelling features. Most of the modelling tasks are completed within ANSYS Workbench [ANSYS], providing several tools for geometry modifications and model assembly. The built-in software ANSYS SpaceClaim is used for the geometry modifications while the FEM model is built in ANSYS Mechanical. Then, an input file for the LS-DYNA solver is exported and last modelling details are finalized within the pre- and post-processor LS-PrePost (V4.8) [LS-PrePost]. The post-processing of the simulation results is performed in LS-PrePost as well.

#### 2.2.6.2.3 FEM Model

The FEM model of the DN30-X package is identical to that described in the SAR of the DN30 package in [DNT 2019], except for the model of the standard 30B cylinder and its content being replaced by the model of the 30B-X cylinder. Consequently, the same deviations and simplifications apply to the modelling of the DN30 PSP. Details on the meshing, the contact

definitions and the modelling of material behavior of the DN30 PSP are therefore provided in [DNT 2019]. Here, only those aspects of the FEM model of the DN30-X package are discussed that are relevant to the 30B-X cylinder.

As mentioned in the beginning of section 2.2.6, the model of the 30B-X cylinder used in the structural analysis of the DN30-X package considers 35 CCRs arranged in a 1 x 6 x 12 x 16 pattern. This number of CCRs lies between the actual designs of the 30B-10 and the 30B-20 cylinder having 33 and 43 CCRs. However, the way the content of the 30B-X cylinder is modelled always ensures that the maximal allowable gross weight of a standard 30B cylinder of 2912 kg is achieved for the 30B-X cylinder as well. Consequently, the differences in the number of CCRs in comparison to the actual 30B-10 and 30B-20 cylinder designs has no relevant impact on the simulation results. This aspect of the structural analysis of the DN30-X package is discussed in more detail in section 2.2.6.5

#### 2.2.6.2.3.1 Geometry

The calculation model of the 30B-X cylinder is based on the drawings in Appendix 1.4.1A (Drawings 30B-X Cylinder). The cylinder shells are identical to the standard 30B cylinder and are modelled according to their nominal values as specified in [ANSI N14.1]. Hence, the wall thicknesses of the cylinder shells and skirts are 13 mm (1/2 in) and 16 mm (10/16 in), respectively. The welding seams between the cylinder skirts and heads are not explicitly modelled but represented by tied contacts (see section 2.2.6.2.3.4). All other welding seams of the cylinder shell are represented as mesh connections.

As explained in the beginning of section 2.2.6, the internal CCS used in the structural analysis of the DN30-X package consists of 35 CCRs that are arranged in a 1 x 6 x 12 x 16 pattern. According to the specification of the 30B-X cylinder in section 1.4.1.1, the carbon steel pipes of the CCRs have an outer diameter of 60.3 mm and a wall thickness of 5.54 mm. In the FEM model, a radial gap of 0.6 mm exists between the pipes and the $B_4C$ filling. This is mainly to avoid the presence of initial penetrations in the FEM model, but it also allows the CCRs to be radially compressed and, thus, accounts for some densification of the $B_4C$ filling.

The lattice holders of the internal CCS are modelled in full detail, except for the small rounds of 4 mm that are removed in the calculation model. This simplification has no significant impact on the structural stiffness of the lattice holders, but it avoids small elements in these areas keeping the simulation runtime reasonable.

Only the two backing bars of the CCS restraints are included in the calculation model of the 30B-X cylinder while the rotation preventing devices of the CCS restraints are neglected. This part of each CCS restraint solely avoids the rotation of the entire CCS inside the 30B-X cylinder. As the investigated drop test scenarios all represent a symmetric loading of the DN30-X package, the internal CCS does not rotate. Consequently, the rotation preventing devices of the CCS restraints experience no load. Finally, the fillet weld between the CCS restraint and the 30B-X cylinder shell is replaced by a tied contact in the calculation model. A detailed calculation model of the fillet weld is analyzed in section 2.2.6.2.7.

#### 2.2.6.2.3.2 Mesh

The geometry of the 30B-X cylinder FEM model is discretized with shell and solid elements. Solid elements are used for the valve, plug and their half couplings as well as the CCS restraints, the lattice holders and the neutron absorbing material within the CCRs. The cylinder shells, skirts and

the pipes of the CCRs are modeled using shell elements. The settings for the chosen element types available for the LS-DYNA solver are listed in table 2-10.

**Table 2-10 DN30-X FEM model – Settings for element formulations**

| Element type | Material | Element parameters | | | | Hourglass control | |
|---|---|---|---|---|---|---|---|
| | | ELFORM[1] | SHRF[2] | NIP[3] | QR[4] | IHQ[5] | QM[5] |
| Shell | Steel | 2 | 5/6 | 5 | 0 | 4 | 0.1 |
| Solid | Steel | 1 | - | - | - | 6 | 0.01 |
| | Boron Carbide | 1 | - | - | - | 6 | 0.01 |

1) ELFORM: Parameter defining the element formulation in LS-DYNA
1) SHRF: Shear correction compensating for violation of zero-traction on top and bottom shell surfaces
2) NIP: Number of integration points across the shell thickness
3) QR: Quadrature rule used for integration, with “0” corresponding to the Gauss quadrature rule
4) IHQ/QM: Type of Hourglass control and Hourglass coefficient (see [LS-Dyna 2018] for details)

For solid elements, the default element formulation ELFORM=1 is used in nearly all cases. This is an eight-node solid hexahedron element with one-point integration and constant stress within each element. Advantages and disadvantages in the use of this element formulation have already been discussed in [DNT 2019]. The valve is discretized using the standard tetrahedral element formulation with one-point-integration. Since the valve is solely modelled to detect a contact, it is represented as a rigid body in the FEM model. In this case, the element formulation has no impact on the simulation results, but using tetrahedral elements simplifies the meshing of the complex geometry of the valve body.

Without exception, the default shell element formulation ELFORM=2 is used. It is based on the Reissner-Mindlin theory of plates and, thus, can be used for thick shells if the reduction of the shell thickness does not play a major role (the cross-section of the shell remains flat and unstretched). It is an extremely effective 4-node element that uses one-point integration and can describe small deformations with large rotations due to an updated co-rotational Lagrangean formulation. Advantages and disadvantages in the use of this element formulation have also been discussed in [DNT 2019].

The shell formulation ELFORM=2 is based on a first order shear deformation theory that yields constant transverse shear strains. This violates the condition of zero traction on the top and bottom surfaces of the shell, which is attempted to be compensated by the shear correction factor (SHRF). The LS-DYNA Keyword Manual [LS-Dyna 2018] suggests a value of 5/6 for isotropic materials that are applied in the 30B-X cylinder FEM model.

The number of integration points (NIP) defines how many quadrature points are distributed over the shell thickness. For complex plastic deformations, five integration points are sufficient.

As reduced integration is applied for all element formulations, the so-called zero energy modes (Hourglass modes) need to be controlled since the corresponding deformations usually represent unphysical behavior. The type of Hourglassing control is defined through the keyword *HOURGLASS.

The mesh statistics for the 30B-X cylinder FEM model are listed in table 2-11. They do not include the DN30 PSP, whose mesh statistics are provided in the SAR of the DN30 package in [DNT 2019].

**Table 2-11 DN30-X FEM model – Mesh statistics for 30B-X cylinder**

| Parameter | Solid elements | | Shell elements | |
|---|---|---|---|---|
| | min | max | min | max |
| Characteristic length in mm | 3.28 | 8.52 | 3.23 | 18.7 |
| Aspect ratio | 1.02 | 3.33 | 1.0 | 2.76 |
| Min. angle in ° | 36.0 | 89.9 | 40.4 | 90.0 |
| Max. angle in ° | 90.1 | 145 | 90.0 | 144 |
| Minimum time step in s | $2.37 \cdot 10^{-7}$ | | $5.34 \cdot 10^{-7}$ | |
| Number of elements | 266220 | | 189834 | |
| Total number of elements | 456054 | | | |



The following figures figure 2-1 to figure 2-3 show the meshing of the 30B-X cylinder. The meshing of the pressure-containment and the CCS restraint is shown in figure 2-1. A section of the cylinder shells has been cut to enable the view on the backing bar of the CCS restraint. The meshing of the CCS is shown in figure 2-2. Further details on the meshing of the lattice holders and the CCRs are provided in figure 2-3.

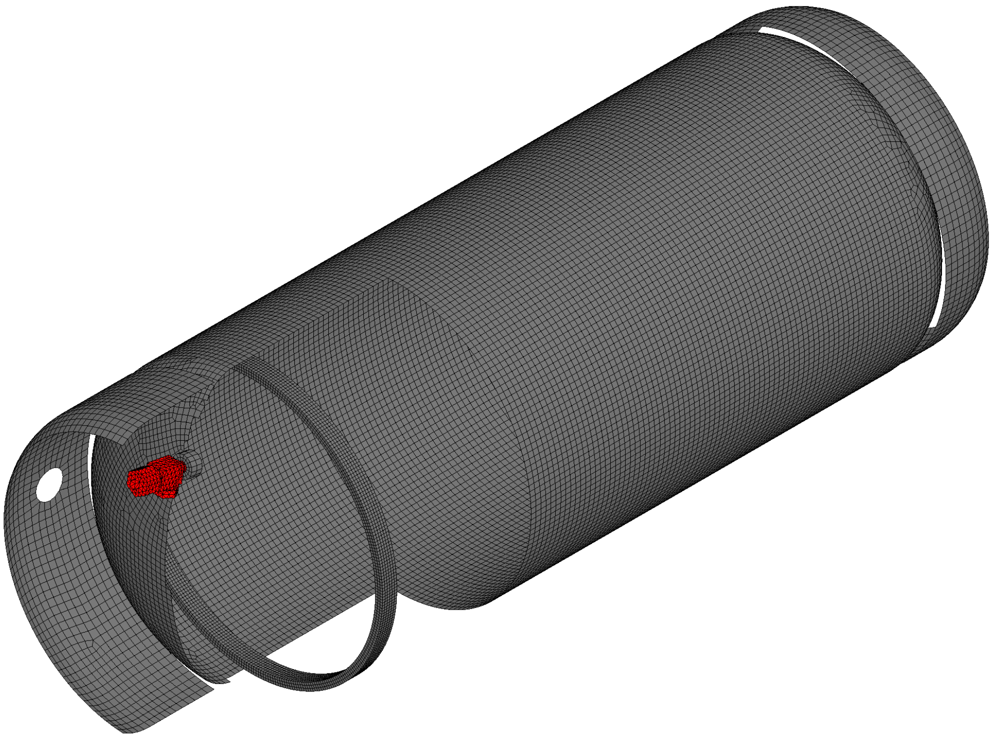

**Figure 2-1 DN30-X FEM model – Mesh of the 30B-X cylinder shells**

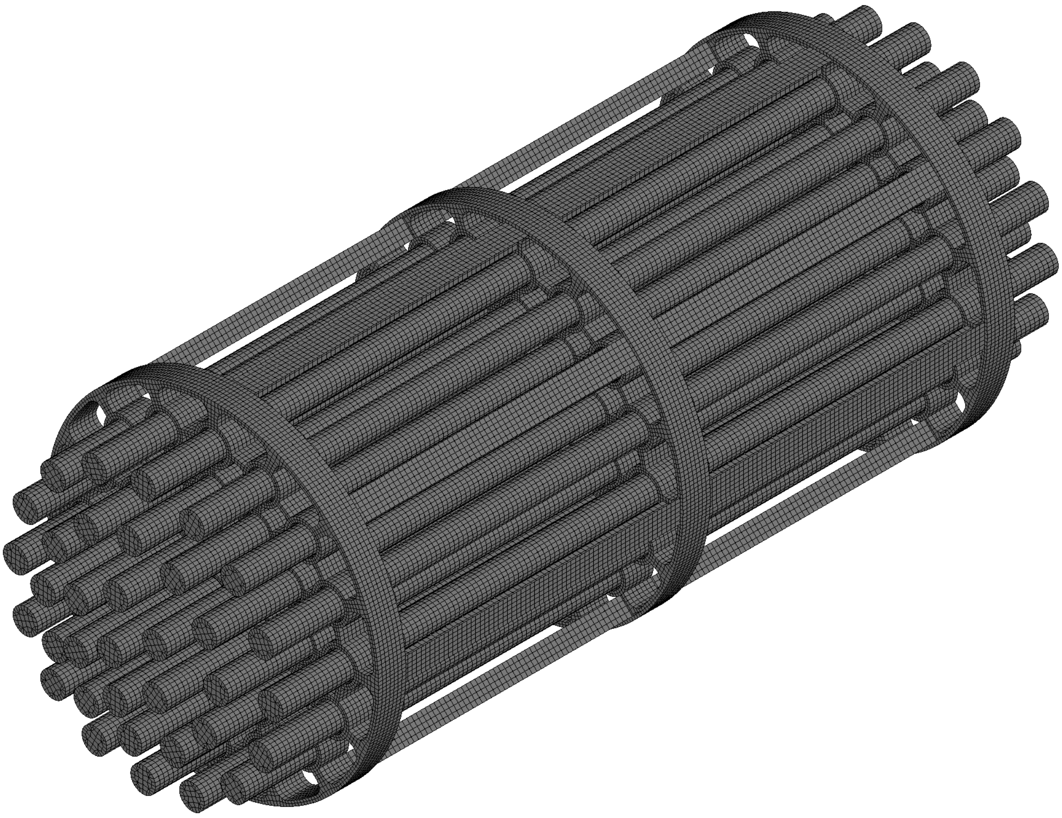

**Figure 2-2 DN30-X FEM model – Mesh of the CCS of the 30B-X cylinder**

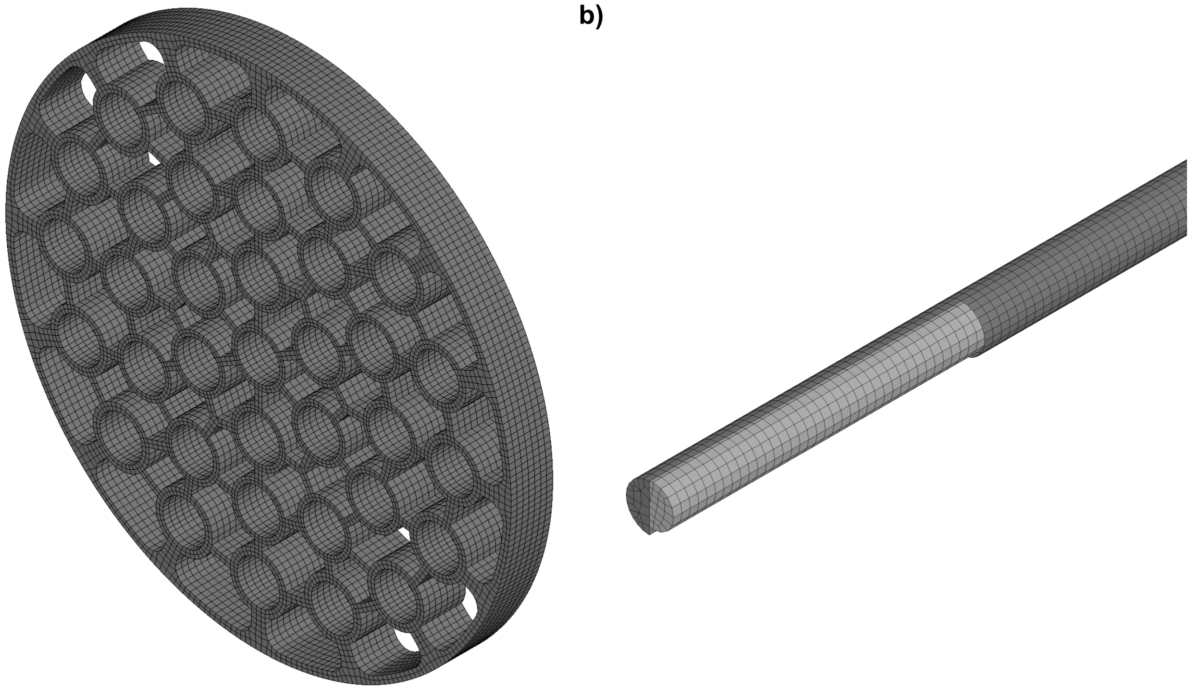

a) b)

**Figure 2-3 DN30-X FEM model – Mesh of: a) lattice holders and b) CRR pipes with neutron absorbing material**

#### 2.2.6.2.3.3 Boundary Conditions

As described in section 2.2.6.2.1, the free drop test from a height of 1.2 m and the free drop test from a height of 9 m are combined to a single 10.2 m drop test to improve the comparability of the simulation results for the DN30 and the DN30-X package. The combination of those two drop tests proved to be more demanding than performing them in sequence (see [DNT 2019]). To simulate the drop height of 10.2 m, the DN30-X package has an initial speed of 14.1 m/s. The velocity vector is orientated vertically downwards to the target (a flat rigid surface), which is fixed in all degrees of freedom. Beside the calculation of the initial speed, gravity is not considered because of its expected negligible influence on the deformations of the package.

If required, entire drop test sequences may be simulated for the safety analysis of the DN30-X package consisting of the sequential application of the 1.2 m free drop test, the 9 m free drop test and the puncture test. Depending on the simulated drop test, the DN30-X package has an initial speed of 4.85 m/s (1.2 m free drop test), 13.3 m/s (9.0 m drop free drop test) and 4.43 m/s (puncture test).

#### 2.2.6.2.3.4 Contacts

As for the DN30 PSP, most welded joints of the 30B-X cylinder like the circumferential head weld and longitudinal seam are realized by mesh connections in the FEM model. This reduces the amount of contact definitions and represents a suitable modelling approach for through-welded but joints. In situations where different element types need to be connected or the definition of a shared topology for parts that shall be connected to each other cannot be realized, tied contacts are used to join parts.

In the FEM model of the 30B-X cylinder, five different types of tied contacts are used that primarily differ in the degrees of freedom being transmitted. They are represented by the following keywords:

1. *CONTACT_TIED_NODES_TO_SURFACE_OFFSET
2. *CONTACT_TIED_NODES_TO_SURFACE_CONSTRAINED_OFFSET
3. *CONTACT_TIED_SHELL_EDGE_TO_SOLID
4. *CONTACT_TIED_SHELL_EDGE_TO_SURFACE
5. *CONTACT_TIED_SHELL_EDGE_TO_SURFACE_BEAM_OFFSET

Table 2-12 lists all tied contacts in the FEM model of the 30B-X cylinder and the involved parts of the slave and master sides of each contact definition.

The penalty-based nodes-to-surface contact with the offset option is used to tie the rigid body representations of the valve and the plug to their corresponding half coupling. The constrained version of this contact keyword is used to connect the solid elements of the CCS restraint to the mid surfaces of cylinder shell. The nodes of the 4-noded solid elements of the CCS restraint lack rotational degrees of freedom. Hence, this contact can only transmit rotations when multiple nodes of a certain element are connected to multiple nodes of another element. As this is the case, all degrees of freedom are accurately transmitted between the CCS restraint and the cylinder shell.

This is not the case for edges of shell elements connected to surfaces. Therefore, the shell-edge-to-solid, shell-edge-to-surface and shell-edge-to-beam-offset contacts are used, with the former two being s constraint-based and the latter being s penalty-based contact.

Including the _OFFSET option in the keyword leaves the geometry unaltered. Without the _OFFSET option, the nodes of the slave side are moved onto the master surface during initialization of the simulation. Considering numerical stability, the latter approach represents the more reliable way to join parts. However, it is not always admissible to alter the geometry, which leads to the chosen contact types listed in table 2-12.

Most settings for the tied contacts are left at the default values, the only exceptions being the viscous damping coefficient VDC, which is set to 20 %, and the values for SST and MST that are changed if not all the desired nodes are successfully tied to the master surface. In this regard, the MPP parameter PARMAX is also altered within 1.0 and 1.15 to ensure all nodes are tied appropriately.

**Table 2-12 DN30-X FEM model – Tied contact definitions for the 30B-X cylinder**

| LS-DYNA Keyword | Slave | Master |
|---|---|---|
| *CONTACT_TIED_NODES_TO | | |
| _SURFACE_OFFSET | Valve | Valve half coupling |
| | Plug | Plug half coupling |
| _SURFACE_CONSTRAINED_OFFSET | CCS Restraint | Cylinder shell |
| *CONTACT_TIED_SHELL_EDGE_TO | | |
| _SOLID | Head (valve side) | Valve half coupling |
| | Head (plug side) | Plug half coupling |
| _SURFACE | Longitudinal stiffeners | Lattice holders |
| _SURFACE_BEAM_OFFSET | Skirt (valve side) | Head (valve side) |
| | Skirt (plug side) | Head (plug side) |
| | Lattice holder clamps | CCRs |

#### 2.2.6.2.3.5 Steel

The 30B-X cylinder shells, skirts and the entire CCS mostly consist of the same type of steel, the only exceptions being the valve and plug material as well as the neutron absorber material withing the CCRs. The material behavior of these steel components is modelled using the same elastic-plastic material model with isotropic piecewise linear hardening that was used for the standard 30B cylinder in the structural analysis of the DN30 package in [DNT 2019]. The LS-DYNA keyword *MAT_PIECEWISE_LINEAR_PLASTICITY is used to model this type of the material behavior. The true stress-strain curves at -40 °C, 20 °C and 60 °C that are applied to this keyword are shown figure 2-4. They are taken from [DNT 2019] as well and only shown for the sake of completeness.

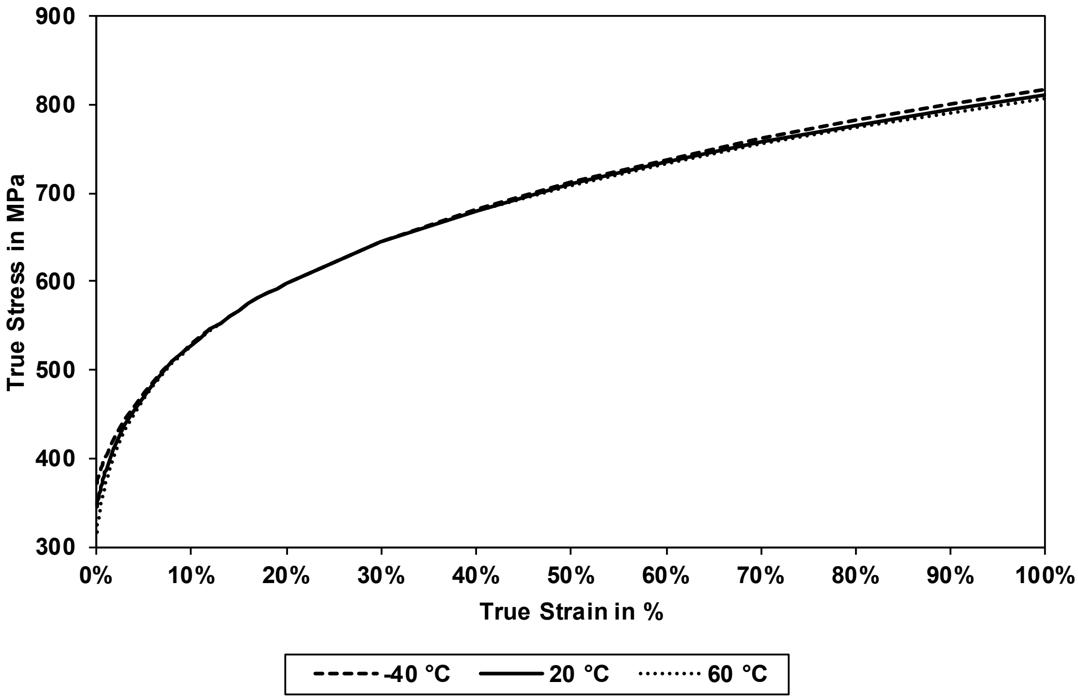


**Figure 2-4 DN30-X FEM model – True stress-strain curve for material P355NL1 (grade 70)**

The true stress-strain curves for material P355NL1 (grade 70) presented in figure 2-4 are based on the so-called Swift approximation [Swift 1952]. The parameters $a$, $\varphi_0$ and $n$ of the Swift approximation are determined by optimization, employing a least-square fit for the minimally required values for the yield strength $R_\mathrm{p}$ and the tensile strength $R_\mathrm{m}$. The optimization is constrained by the instability criterion $\varphi_0 + \varphi_\mathrm{gl} = n$ for the flow curve, where $\varphi_\mathrm{gl}$ is the uniform elongation. Details on this optimization procedure are provided in the structural analysis of the DN30 package in [DNT 2019].

Data for the yield strength $R_\mathrm{p}$ and the tensile strength $R_\mathrm{m}$ are taken from [DIN EN 10028-3] and listed in table 2-8. The uniform elongation is not available from standards and a second pair of stress and strain is also not available. Therefore, accepting some error, the value for the elongation at fracture is taken as the corresponding strain to $R_\mathrm{m}$. The influence of this error on the simulation results is judged to be negligible as deformations of the 30B-X cylinder close to the elongation at fracture are inadmissible anyway. Because of this requirement, a failure criterion is also not required for the materials of the 30B-X cylinder.

Since the yield and tensile strength provided in [DIN EN 10028-3] are determined in quasi static conditions, the resulting flow curves are multiplied with a factor of 1.3 to simulate the observed dynamic strain hardening of the steel. This factor was also applied in the simulations of the DN30 package in [DNT 2019].

2.2.6.2.3.6 Boron Carbide

The neutron absorbing material within the CCRs is considered in the FEM model of the 30B-X cylinder solely because of its mass. Accordingly, a simple approach is used to model the material behavior of the $B_4C$ filling. With the material properties in table 2-9 a perfectly plastic material model is set up using the keyword *MAT_PIECEWISE_LINEAR_PLASTICITY. However, plasticity is only considered for numerical reasons.

2.2.6.2.3.7 Content of the 30B-X Cylinder

In the FEM simulations of the DN30 package in [DNT 2019], the content of the standard 30B cylinder was simulated by a clumped mass of heavy concrete having a density of 5.1 g/cm³ and a simulated mass of 2277 kg. In theory, the same approach can be applied to model the content of the 30B-X cylinder in the DN30-X FEM model, by introducing cutouts in the content geometry to avoid intersections with the internal CCS. The major downside on this approach is that the geometry of the content block becomes very complicated because of the many cutouts required to incorporate the CCS. This drastically increases the number of elements in the model and, thus, the computational effort. More importantly, the material behavior of the content significantly affects the deformation of the internal CCS as the content provides a substantial amount of support to the CCS. There is simply not enough information available about the material behavior of $UF_6$ that would allow for such an approach. Therefore, a different modelling approach is used for the $UF_6$ content of the 30B-X cylinder.

In the FEM model of the DN30-X package, the $UF_6$ content (the net weight $m_{\mathrm{net}}$ of the 30B-X cylinder) is taken into account by increasing the nodal mass of each mesh node of the outer CCR surfaces. This is realized by the introduction of so-called mass elements that are part of the LS-DYNA implementation (see [LS-Dyna 2018]). The net weight of the $UF_6$ content is calculated by subtracting the tare mass $m_{\mathrm{tare}}$ of the 30B-X cylinder FEM model from its gross weight $m_{\mathrm{gross}}$ defined in table 1-13. The determination of $m_{\mathrm{net}}$ is based on the FEM model of the 30B-X cylinder and not taken from table 1-13 to compensate for the simplifications of the 30B-X cylinder geometry introduced in the FEM model (see section 2.2.6.2.3.1). The resulting tare and net weights of the 30B-10 and the 30B-20 cylinder in comparison to the FEM model of the 30B-X cylinder are listed in table 2-13.

**Table 2-13 DN30-X FEM model – Comparison of simulated content masses**

| Weight in kg | 30B-10 cylinder | | | 30B-20 cylinder | | |
|---|---|---|---|---|---|---|
| | Table 1-13 | FEM Model | Difference | Table 1-13 | FEM Model | Difference |
| Tare | 1452 | 1464 | 12 | 1641 | 1464 | -177 |
| Gross | 2912 | 2912 | 0 | 2912 | 2912 | 0 |
| Net | 1460 | 1448 | -12 | 1271 | 1448 | 177 |

In the FEM model, the mass elements show up as colored dots at each node location, which is shown in figure 2-5. The added mass elements simply increase the corresponding nodal masses of the outer CCR surfaces so that the $UF_6$ content is simulated as an additional mass per area (area density) on each CCR that is permanently affixed to the outer CCR surfaces. Based on the specification of the 30B-X cylinder in section 1.4, the outer CCR diameter is $d_{\mathrm{o,CCR}} = 60.3\ \mathrm{mm}$. The total lengths of the CCRs add up to $l_{\mathrm{CCR}} = 51.9\ \mathrm{m}$, $67.4\ \mathrm{m}$ and $54.9\ \mathrm{m}$ for the 30B-10 cylinder, the 30B-20 cylinder and the 30B-X cylinder FEM model, respectively. Then, with the net weights given in table 2-13, the area density of $UF_6$ on each CCR is calculated by:

$$\varrho_{\mathrm{A,UF_6}} = \frac{m_{\mathrm{net,FEM}}}{l_{\mathrm{CCR}} \cdot \pi \cdot d_{\mathrm{o,CCR}}} \qquad (4)$$

Using equation (4) results in an area density of $\varrho_{\mathrm{A,UF_6}} = 14.85\ \mathrm{g/cm^2}$, $9.96\ \mathrm{g/cm^2}$ and $14.1\ \mathrm{g/cm^2}$ for the 30B-10 cylinder, the 30B-20 cylinder and the 30B-X cylinder FEM model, respectively.

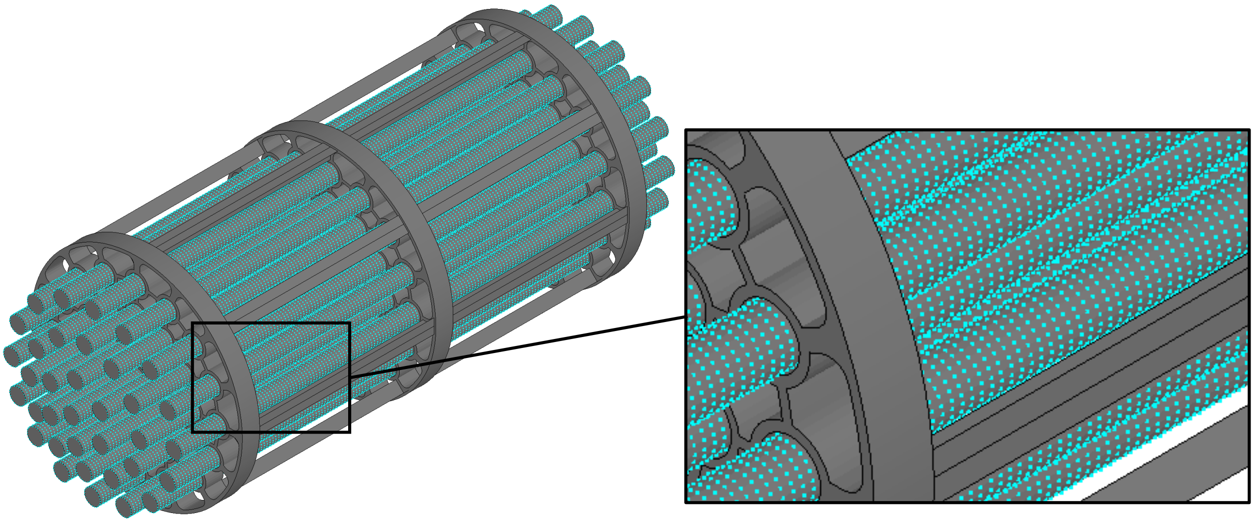


**Figure 2-5 DN30-X FEM model – Distribution of mass elements on outer CCR surfaces**

Modelling the content by increasing the area density of the outer CCR surfaces leads to a very conservative and covering structural analysis of the DN30-X package. This is especially true with regard to the acceptance criteria for the integrity of the pressure-containment and the integrity of the CCS of the 30B-X cylinder established in section 2.1.2.2.1.

The following applies to the pressure-containment of the 30B-X cylinder:

- The fact that the content does not provide any support during an impact not only imposes the highest demands on the CRRs but also on the cylinder shells. Neglecting any support of the content increases the risk of a plastic collapse of the containment parts of the 30B-X cylinder, especially in case of the vertical drop test onto the valve side as a significant portion of the load is transmitted through the valve protecting device of the DN30 PSP onto the 30B-X cylinder head.
- The limited space between the CCRs and the lattice holders does not allow for free movement of large solid $UF_6$ chunks. Consequently, assuming the $UF_6$ permanently adheres to the CCRs during and after the drop tests simulating NCT and HAC, is more challenging for the cylinder shells in every situation.

The following applies to the CCS of the 30B-X cylinder:

- In a vertical drop scenario, the load upon the CCS restraint of the 30B-X cylinder and the lattice holders is maximized. At the time of impact, the whole inertial mass of the CCS as well as the $UF_6$ content are acting on the CCS restraint and the lattice holders. This scenario is very pessimistic, since in reality at least some of the $UF_6$ will detach from the CCRs decreasing the load on the CCS restraint and the lattice holders.
- In a horizontal drop scenario, the load upon the structural integrity of the CCRs due to the large inertial forces resulting from the increased weight of the CCRs is maximized. As mentioned above, the $UF_6$ can be expected to support the CCRs to a certain degree in reality.

#### 2.2.6.2.4 Modeling of the Drop Test Sequences

As described in section 2.2.6.2.1, the 1.2 m and 9.0 m free drop test are combined to a single 10.2 m free drop test in the comparison simulations between the DN30-X and DN30 package in section 2.2.6.2.5. Therefore, the initial speed of 14.1 m/s is applied immediately at the beginning of the simulation.

When entire drop test sequences are simulated, the same procedure as for the DN30 package in [DNT 2019] is applied. First the 1.2 m drop is calculated using the generated LS-DYNA input file for a specific drop test sequence. After that, an LS-DYNA simple restart calculation is performed where the velocity of the entire DN30-X package model is set to zero and the target is moved and rotated in the correct position as required for the next drop test. This intermediate step is necessary because the DN30-X package model may rotate during the previous drop test. In the simple restart analysis, all information about internal stresses and strains are retained in the model.

The short time without loads being applied to the DN30-X package model is also required for relaxation, which reduces internal oscillations in the model. After that, a simple restart calculation of the 9.0 m drop test is carried out prescribing the corresponding initial velocity. The 9 m free drop test is again followed by another relaxation period, where the bar for the puncture test is repositioned. Finally, the puncture test is carried out in the same manner.

In summary, the sequence of the free drop test from a height of 1.2 m, the free drop test from a height of 9 m and the puncture test requires a normal simulation followed by four simple restart simulations:

1. Simulation of the free drop test with the initial drop orientation modified in LS-PrePost.
   - Measurement of relative angles and displacements between the drop target and an undeformed part of the DN30 PSP in LS-PrePost.
   - Simple restart simulation where the velocity of the package is set to zero and the drop target is rotated and repositioned to obtain the desired relative orientation and position of the DN30-X package to the drop target.
2. Simple restart simulation with an adjusted velocity vector that corresponds to a drop height of 9m and that is perpendicular to the drop target.
   - Measurement of relative angles and displacements between the bar and an undeformed part of the DN30 PSP.
   - Simple restart simulation where the velocity of the DN30-X package is set to zero and the bar is rotated and repositioned to obtain the desired relative orientation and position of the DN30 PSP to the bar.
3. Simple restart simulation with an adjusted velocity vector that corresponds to a drop height of 1m (puncture test) and that is perpendicular to the bar.

##### 2.2.6.2.4.1 Evaluation of Deformations

After each simulated drop test, deformations are measured at the DN30 PSP using the measurements tool of LS-PrePost [LS-PrePost]. The measurements work on the basis of distances between mesh nodes.

2.2.6.2.4.2 Evaluation of Decelerations

For the evaluation of decelerations, the built-in SAE low-pass filter of LS-PrePost is used. In the comparison of decelerations, the same cut-off frequencies of 20 Hz, 100 Hz, 200 Hz and 584 Hz as in [DNT 2019] are chosen for this low-pass filter, where the cut-off frequency of 584 Hz is determined based on the recommendations in [SSG-26 2012], para. 701.9.

The decelerations are determined using the *ELEMENT_SEATBELT_ACCELEROMETER keyword in LS-DYNA. These elements require a rigid body, whose nodes define the coordinate system of the accelerometer. In the FEM model of the 30B-X cylinder, a simple cube is used to represent the rigid body, which is tied to the 30B-X cylinder skirts with a tied contact based on a penalty formulation. The positions of the accelerometers in the valve and the plug area of the 30B-X cylinder are identical to those used for the standard 30B cylinder in [DNT 2019]. For the sake of completeness, they are shown in figure 2-6 and figure 2-7.

As in [DNT 2019], only the resultant decelerations $a_{\text{res}}$ are used in the comparison of the DN30-X and DN30 simulation results. To obtain the resultant low-pass filtered decelerations, each of the three acceleration components $a_{\text{x}}$, $a_{\text{y}}$ and $a_{\text{z}}$ is filtered separately. Afterwards, the resultant acceleration is calculated based on the filtered acceleration components. This filtering method avoids that high frequency fluctuations in each component are randomly superimposed in the resultant acceleration and, thus, leads to more reliable results. However, filtering the measured decelerations leads to non-zero decelerations at the beginning of each drop test simulation. This effect refers to the impulse response of the filter and, thus, cannot be avoided.

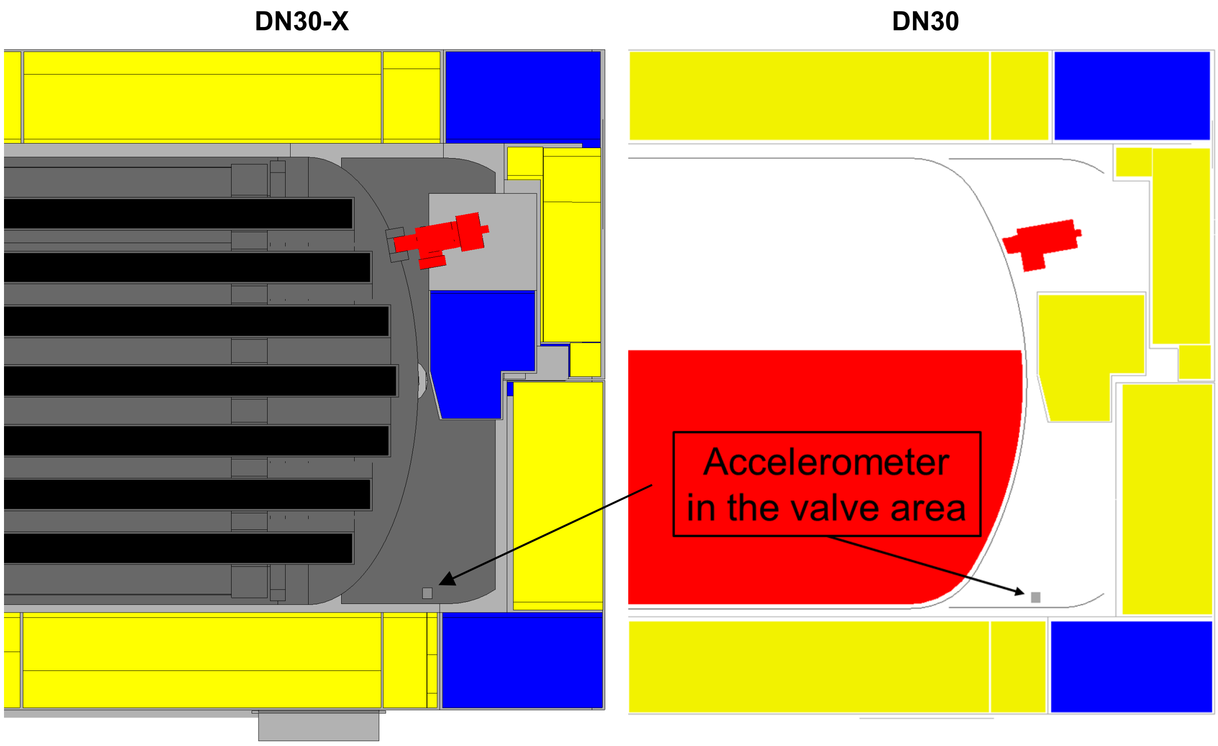


**Figure 2-6 DN30-X FEM model – Instrumentation with acceleration sensors in the valve area**

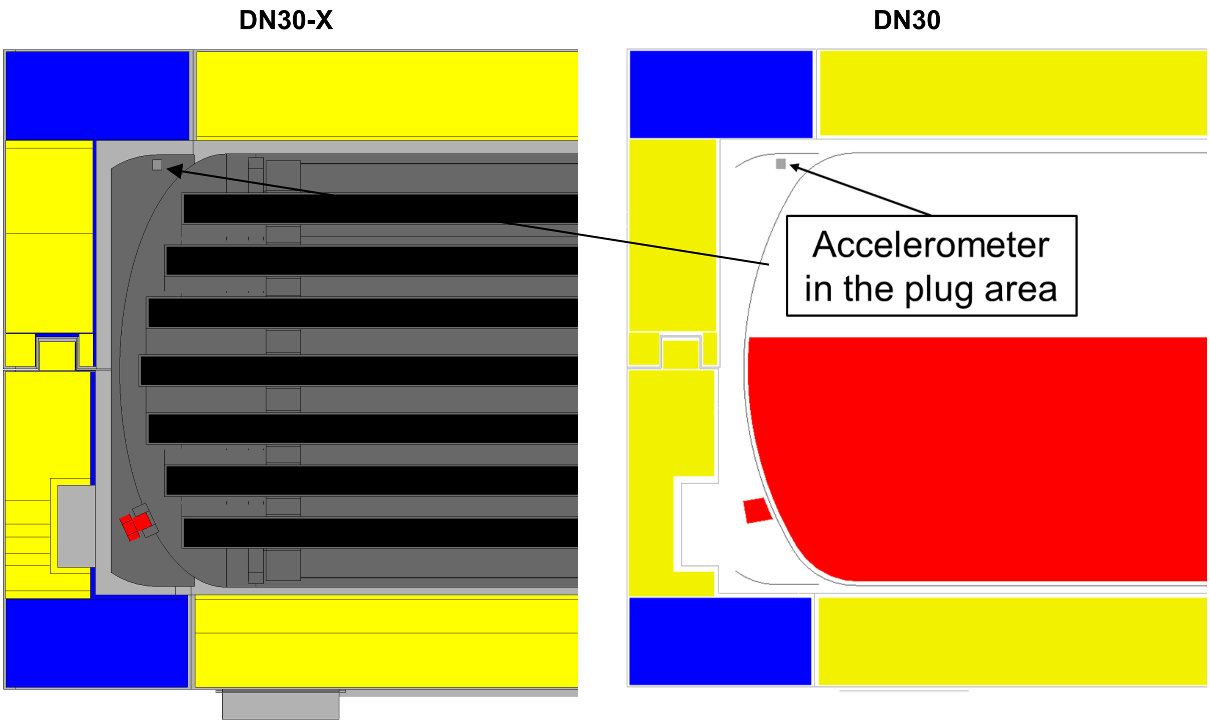


**Figure 2-7 DN30-X FEM model – Instrumentation with acceleration sensors in the plug area**

#### 2.2.6.2.5 Comparison of Drop Test Analyses for the DN30-X and DN30 Package

##### 2.2.6.2.5.1 Corner Drop onto the Valve Side – Drop Test Sequence 1

The structural analysis of the DN30 package in [DNT 2019] showed that the corner drop onto the valve side, that is part of drop test sequence 1 for the DN30 package, is one of the most critical drop test orientations regarding the amount of deformations of the DN30 PSP in the valve area. As the valve is the most vulnerable part of the containment system, this drop test orientation is used in the comparison analysis between the DN30-X and DN30 package.

From the mechanical point of view, the DN30-X package design has to ensure that after the flat drop test onto the valve side simulating HAC, all acceptance criteria as defined in section 2.1.2.2.1 are met:

- No failure of the DN30 PSP closure system.
- No physical contact between the valve of the 30B-X cylinder and any other component of the packaging other than its original point of attachment.
- No physical contact between the plug of the 30B-X cylinder and any other component of the packaging other than its original point of attachment.
- No rupture of the 30B-X cylinder containment system.
- No failure of the 30B-X cylinder confinement system:
  - The relative dislocation of the CCRs must remain below 5 mm.
  - The increase in radial movability of the entire CCS out of the center of the 30B-X cylinder must remain below 3 mm.

- The increase in axial movability of the entire CCS out of the center of the 30B-X cylinder must remain below 7 mm.
- Failure of the lattice holders must not occur.
- Rupture of the CCRs must not occur.

For the corner drop onto the valve side, the angle between the longitudinal axis of the DN30 PSP and the normal of the drop target has been varied in [DNT 2019]. The maximal deformation of the DN30 PSP and, thus, minimal volume of the foam in the valve area where obtained for an angle of 22°. The corresponding initial state of the DN30-X and DN30 package is shown in figure 2-8.

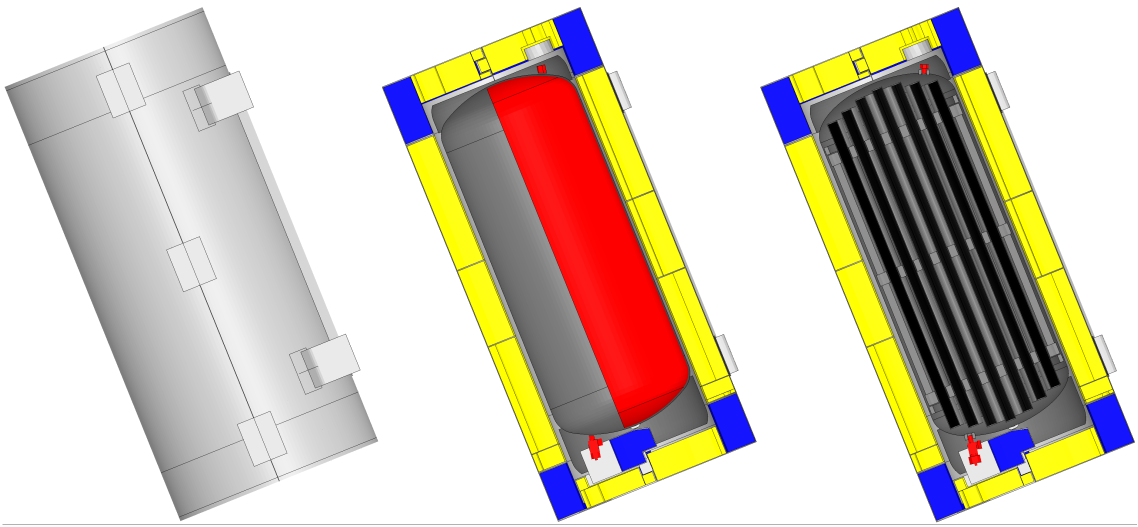

**Figure 2-8 Corner drop onto the valve side from a height of 10.2 m – Undeformed initial state of the DN30-X and the DN30 package**

2.2.6.2.5.1.1 General Results

The analysis of the 10.2 m free drop test takes a total duration time of 0.05 s. As proven by the data in figure 2-9, this duration times suffices to capture all relevant aspects of the drop test because both the kinetic and the internal energy reach a constant level.

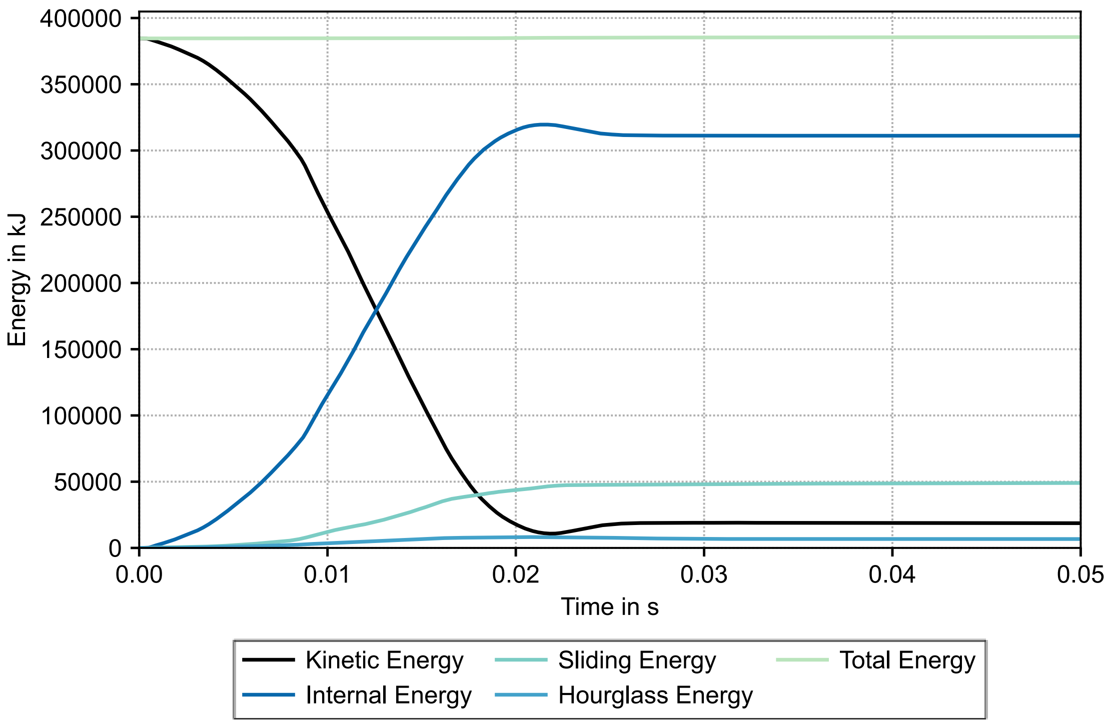


**Figure 2-9 Corner drop onto the valve side from a height of 10.2 m – Energy distribution**

At the impact around 1 ms, the kinetic energy starts to decrease and is continuously transformed into internal energy. The maximum internal and minimum kinetic energy refer to the state of maximal deformation. After this state, the internal energy begins to decrease due to the relieve of elastic strains. In addition, as can be concluded from the increase in the kinetic energy, this relieve causes a rebound of the package off the drop target. Due to the absence of gravitation in the FEM model, the package receives no further acceleration so that the kinetic energy reaches a constant level as soon as the package has lost contact to the drop target. After the relieve of elastic strains has completed, the internal energy reaches a constant level as well. Other energies like the hourglass and sliding energy are small in comparison to the internal energy ensuring that the deformations of the DN30-X package are not underestimated. The resulting energy ratio for this drop test simulation ranges from 0.999748 to 1.00263, indicating very good energy conservation.

Figure 2-10 shows the contact energy of the automatic single surface contact. The contact energy remains positive and drops below the frictional energy only in the second half of the simulation. In addition, the dissipation of frictional energy only increases or remains constant, but never decreases. The contact energy distribution may be improved by reducing the contact stiffness. However, this leads to an increase in the contact energy and, thus, a decrease in the internal energy, potentially resulting in smaller deformations. Hence, the contact stiffness is a reasonable choice to achieve a stable simulation and to obtain reliable deformation results.

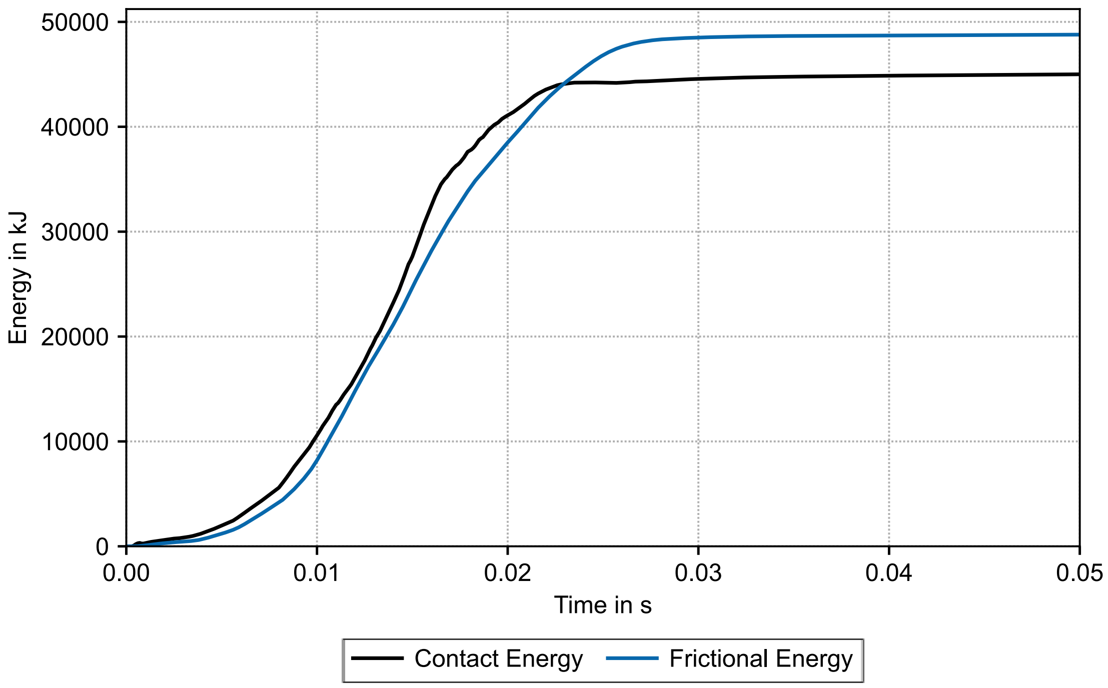


**Figure 2-10 Corner drop onto the valve side from a height of 10.2 m – Contact energy of the automatic single surface contact**

Figure 2-11 compares the hourglass energy to the internal energy during the free drop test from a height of 10.2 m. The hourglass energy remains well below the upper limit of 10 % of the internal energy without any sudden increases.

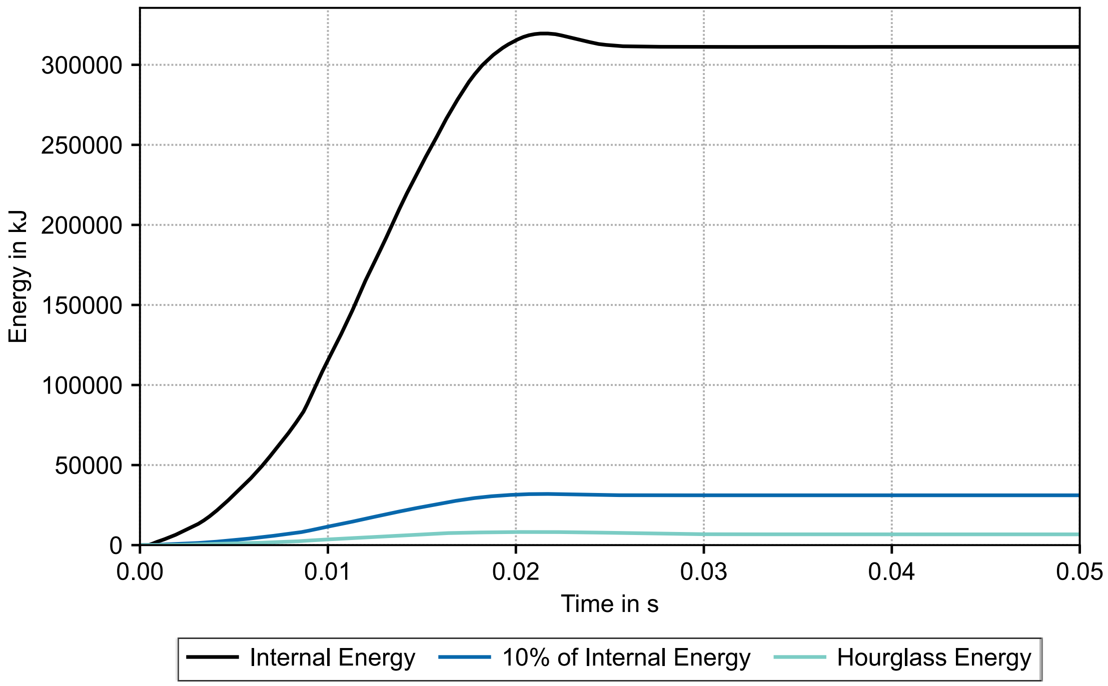


**Figure 2-11 Corner drop onto the valve side from a height of 10.2 m – Hourglass energy**

2.2.6.2.5.1.2 Deformations

2.2.6.2.5.1.2.1 DN30 PSP and Cylinder Pressure Envelope

The state of maximal deformation for the DN30-X to the DN30 package during the corner drop test onto the valve side is compared in figure 2-12. For both packages, the compression of the foam in the valve area and the deformations of the inner and outer DN30 PSP shell are nearly identical. This is also reflected in very small differences in plastic strain at the outer shell that reach 38.3 % and 38.5 % in case of the DN30-X and DN30 package, respectively. Minor differences in the deformations are only visible regarding the buckling of the inner shell. Most likely, this can result from the different approaches to model the content of the DN30-X and DN30 package. The stronger coupling of the content to the 30B-X cylinder shell causes an increase in friction between the inner DN30 PSP shell and the 30B-X cylinder resulting in more pronounced folds in this area.

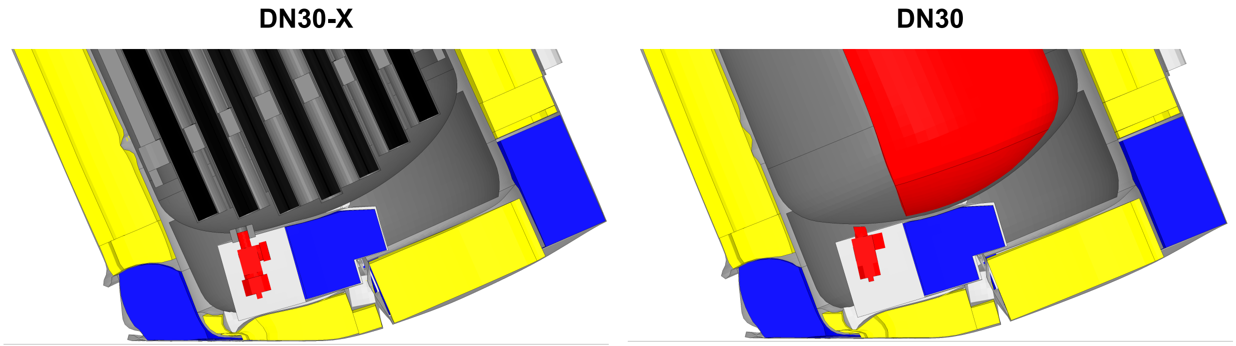


**Figure 2-12 Corner drop onto the valve side from a height of 10.2 m – State with the maximal deformation of the DN30-X and DN30 package**

The maximum plastic strain at the inner shell of the DN30 PSP reaches 41 % in the simulation of the 10.2 m free drop test with the DN30 package. In case of the DN30-X package, 46 % are reached showing that the amount of deformation is comparable. As for the DN30, no physical contact at the valve is detected for the DN30-X other than its initial point of attachment.

At the end of the simution, the deformations of the DN30 PSP are determined using two measurement locations at the impact zone (see figure 2-13). In addition, the Euclidian norm of the measured distances at the first measurement location is calculated, as this provides further information on the extent of the impacted area. The same measurement locations were used in [DNT 2019] to validate the FEM model of the DN30 package against the experimental drop tests performed with DN30 PSP prototypes. Table 2-14 lists the resulting values and provides a comparison to the corresponding results for the DN30 package.

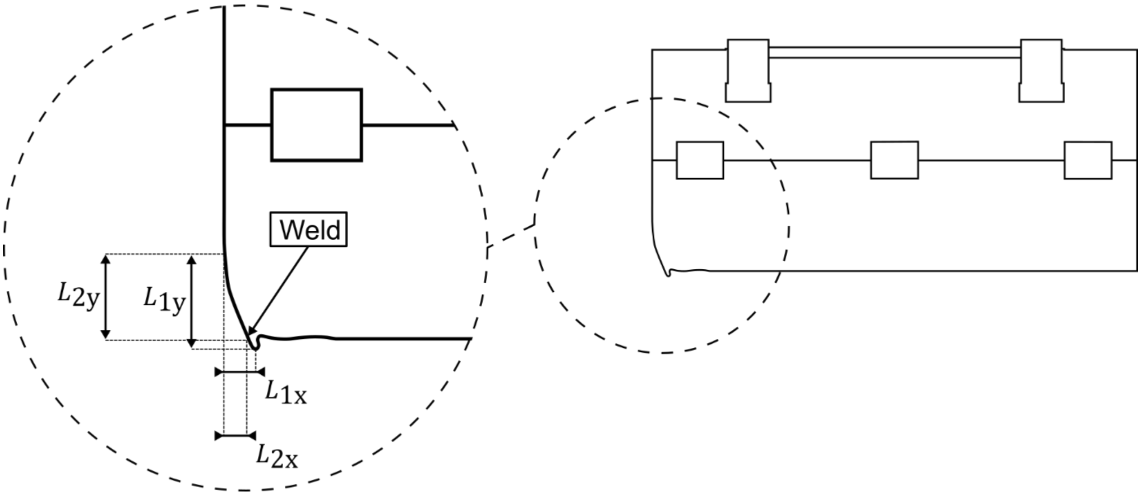


**Figure 2-13 Measured distances for the corner drop onto the valve side**

**Table 2-14 Corner drop onto the valve side from a height of 10.2 m – Measured distances at the impact zone after the drop test**

| Measurement point | Parameter | Deformation in mm | | Change in % |
|---|---|---|---|---|
| | | DN30-X | DN30 | |
| Largest Fold | $L_{1x}$ | 175 | 167 | 5.0 |
| | $L_{1y}$ | 392 | 396 | -0.9 |
| | $L_1 = \sqrt{L_{1x}^2 + L_{1y}^2}$ | 430 | 429 | ≈ 0 |
| Weld between head and outer shell | $L_{2x}$ | 163 | 156 | 4.8 |
| | $L_{2y}$ | 368 | 372 | -0.8 |

The obtained results for the measured distances in table 2-14 correspond well to the very similar deformations visible in figure 2-12. The changes in $L_{1x}$ and $L_{2x}$ are increased by about 5 %, while the changes in $L_{1y}$ and $L_{2y}$ are slightly smaller. Most likely this can be attributed to the different approach in modelling the content of the DN30-X in comparison to the DN30 package. As already mentioned above, the implicit modelling of the content using mass elements causes a strong connection between the movement of the content and the 30B-X cylinder while the content in the standard 30B cylinder is allowed to move freely to a certain extent. In case of an inclined drop test orientation, like the corner drop onto the valve side, the strong connection increases the moment of inertia, resulting in a larger rotation of the entire DN30-X package towards the drop target. The angle between the drop target and the axis of the DN30 PSP is about 67° in case of the DN30 package and only 61° in case of the DN30-X package. This explains the differences in the measured distances listed in table 2-14. However, the extent of the impacted area measured by the Euclidian norm $L_1$ is nearly identical for both packages, proving that the deformations are comparable.

As a more global comparison between the deformations of the DN30-X and the DN30 package, the energy absorption behavior during the corner drop test onto the valve side is investigated. Figure 2-14 shows the distribution of the kinetic energy, the totally absorbed energy as well as the energy absorbed by the DN30 PSP for both the DN30-X and the DN30 package.

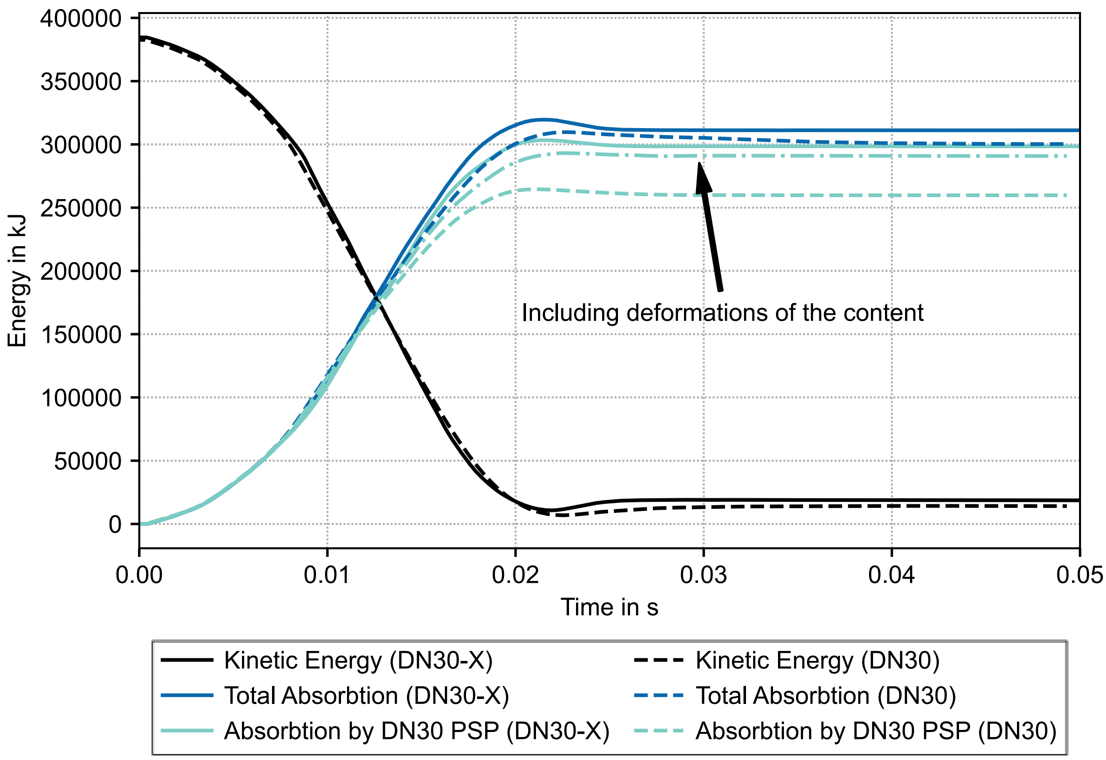


**Figure 2-14 Corner drop onto the valve side from a height of 10.2 m – Comparison of energy absorption of the DN30 PSP in case of the DN30-X and the DN30 package**

Based on this comparison, it is seen that the kinetic energy and the totally absorbed energy are nearly identical for both packages. The only noticeable difference occurs for the energy absorbed by the DN30 PSP, which is due to the different approaches used to model the content of the DN30-X and the DN30 package. In case of the corner drop onto the valve side, the content block of the DN30 package also absorbs some of the kinetic energy, which is indicated in figure 2-14 by a dash-dotted line. However, since the content is incorporated in the FEM model of the DN30-X by using mass elements, it cannot contribute to the energy absorption. Therefore, the DN30 PSP and the 30B-X cylinder are absorbing a larger fraction of energy. Increased deformations of the DN30 PSP and the 30B-X cylinder are to be expected, further emphasizing the conservatism of the approach to model the content of the DN30-X package.

As a final comparison of the deformations of the DN30-X and DN30 package after the corner drop test onto the valve side, explicit values of the maximal equivalent plastic strains are evaluated. The results are listed in table 2-15 for the foam and selected steel parts of the DN30 PSP as well as the 30B-X and standard 30B cylinder pressure envelope. Table 2-15 also includes the corresponding values of the densification strains and elongations at fracture that are taken from [DNT 2019] for the DN30 PSP (foam RTS 120 / RTS 320 and stainless steel 1.4301) and listed in table 2-8 for the 30B-X and 30B cylinder pressure envelope.

**Table 2-15 Corner drop onto the valve side from a height of 10.2 m – Plastic deformations of foam and selected steel parts of the DN30 PSP and the cylinder pressure envelope**

| Part | EPS[1)] in % | | Absolut change in % | DS / EF[2)] in % |
|---|---|---|---|---|
| | DN30-X | DN30 | | |
| DN30 PSP | | | | |
| RTS 120 | 89.3 | 89.9 | -0.4 | 89 |
| RTS 320 | 54.8 | 52.4 | 2.4 | 82 |
| Valve protecting device | 1.8 | 1.1 | 0.7 | 45 |
| Plug protecting device | 0.0 | 0.0 | 0.0 | 45 |
| Inner front plate (top half) | 40 | 36.7 | 3.3 | 45 |
| Inner front plate (bottom half) | 9.2 | 10.2 | -1.0 | 45 |
| Inner back plate (top half) | 0.0 | 0.0 | 0.0 | 45 |
| Inner back plate (bottom half) | 0.4 | 0.1 | 0.3 | 45 |
| 30B-X cylinder / standard 30B cylinder | | | | |
| Pressure envelope | 4.0 | 1.1 | 2.9 | 22 |

1) Equivalent plastic strain
2) Densification strain / elongation at fracture

The maximal equivalent plastic strains of parts of the DN30 PSP are generally very similar for the DN30-X and the DN30 package. A distinct difference in case of a relevant deformation occurs only in case of the inner front plate at the top half. Most likely this can be referred to the missing capability of the content of the DN30-X package to absorb some of the kinetic energy. However, an increase of 3.3 % is still acceptable for the stainless steel, especially as the plastic deformations remain below the elongation at fracture. In all other cases with larger differences between the DN30-X and DN30 simulation results, the absolute values of the plastic strain are so small that the increase is irrelevant.

Figure 2-15 shows the distribution of the equivalent plastic strain at the inner front plate of the DN30 PSP for the DN30-X and DN30 package. Even though small differences between the maximal plastic strains exist, this comparison shows that the distribution of the deformations is nearly identical for the DN30-X and DN30 package.

**DN30-X**

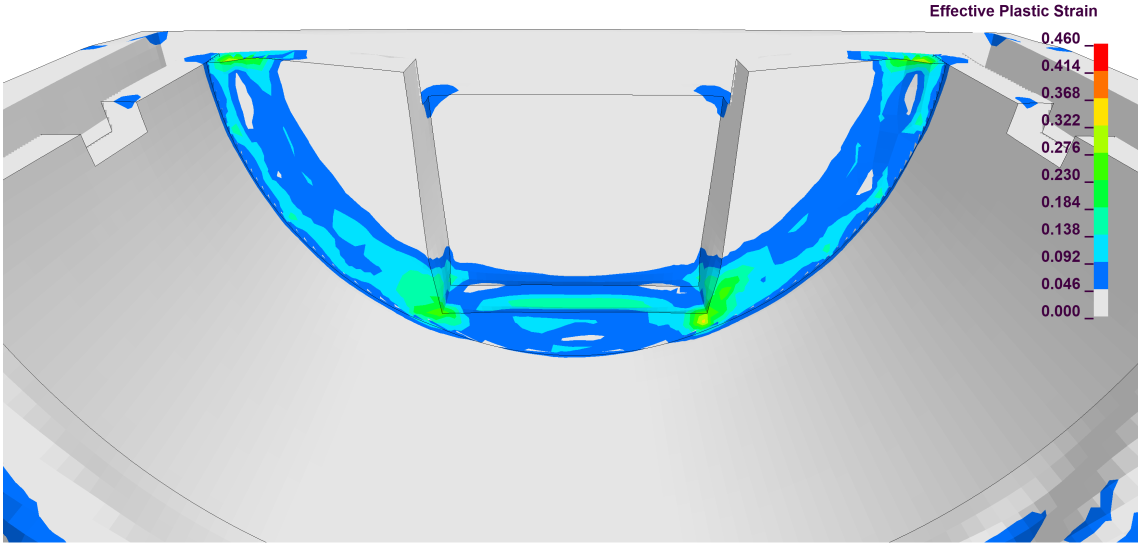


**DN30**

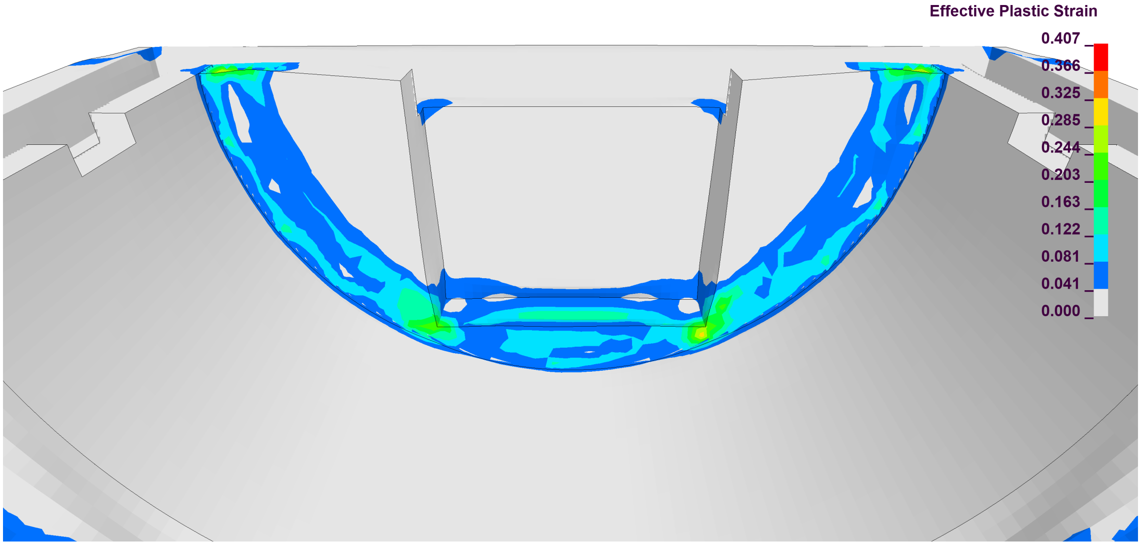


**Figure 2-15 Corner drop onto the valve side from a height of 10.2 m – Comparison of equivalent plastic strain at the inner shell**

In case of the cylinder pressure envelope, the determined increase in plastic strain from 1.1 % for the standard 30B to 4.0 % for the 30B-X cylinder was to be expected because the content is only implicitly incorporated in the FEM model of the DN30-X. Without any internal support for the cylinder shell provided by the content, the cylinder head is much more prone to a plastic collapse. As can be seen in figure 2-16, this leads to increased deformations at the 30B-X cylinder head on the valve side. The regions of plastic strains that are visible on the side of the standard 30B cylinder do not occur for the 30B-X cylinder as these are deformations that result from the content block that impacts the cylinder shell on the inside. Despite those differences that solely refer to the content modelling, 4.0 % maximal plastic strain are significantly below the elongation at fracture of the cylinder shell material so that rupture of the containment system can safely be excluded.

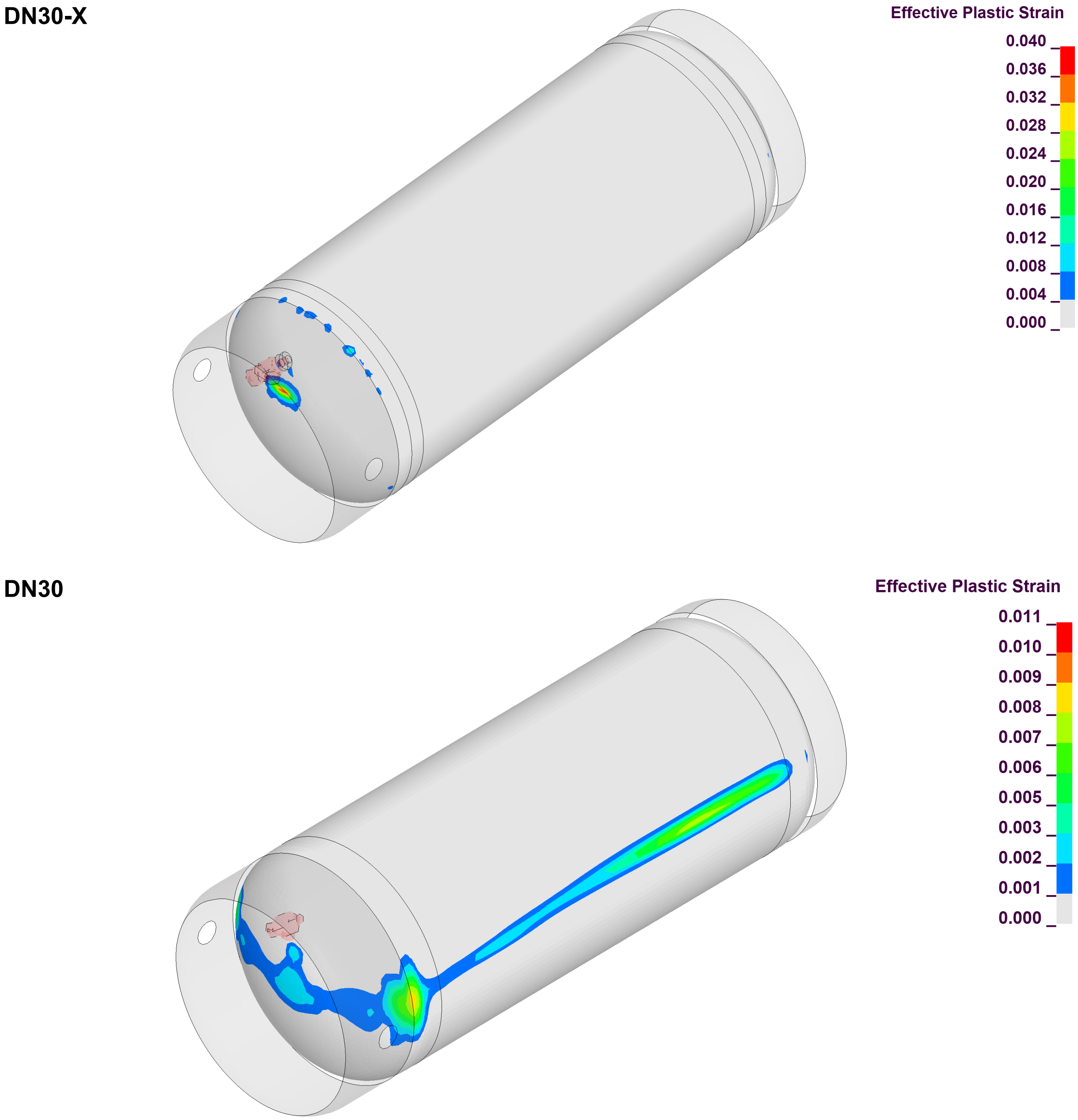


**Figure 2-16 Corner drop onto the valve side from a height of 10.2 m – Comparison of equivalent plastic strain at the cylinder pressure envelope**

2.2.6.2.5.1.2.2 Criticality Control System of the 30B-X Cylinder

In this section, the deformations of parts that are specific to the 30B-X cylinder design are investigated. These are the deformations of the CCS restraint, the lattice holders including the longitudinal stiffeners and the CCRs. The relative dislocation between the CCRs and the movability of the entire CCS within the cylinder are not investigated here as other drop test orientations like the flat drop onto the valve side and the flat drop onto the feet analyzed in section 2.2.6.2.5.2 and 2.2.6.2.6.1, respectively, are much more severe in this regard.

The deformations of the CCS restraints and the lattice holders are shown in figure 2-17. There are only local regions with very low plastic deformations at the CCS restrains where some of the spokes of the lattice holders get in contact with the CCS restraint on the valve side. Noticeable plastic strains occur only in the lower half of the lattice holder on the valve side and near the

connection between the lattice holders and the longitudinal stiffeners. The maximal plastic strain in these areas reach 2.1 % and 1.6 %, respectively. This level of plastic strain is acceptable for the lattice holders and the longitudinal stiffeners, especially considering those parts have no containment function. Safety relevant is only the relative dislocation between the CCRs, which can be expected to be very small as the pipe clamps of the lattice holders hardly experience any plastic deformations.

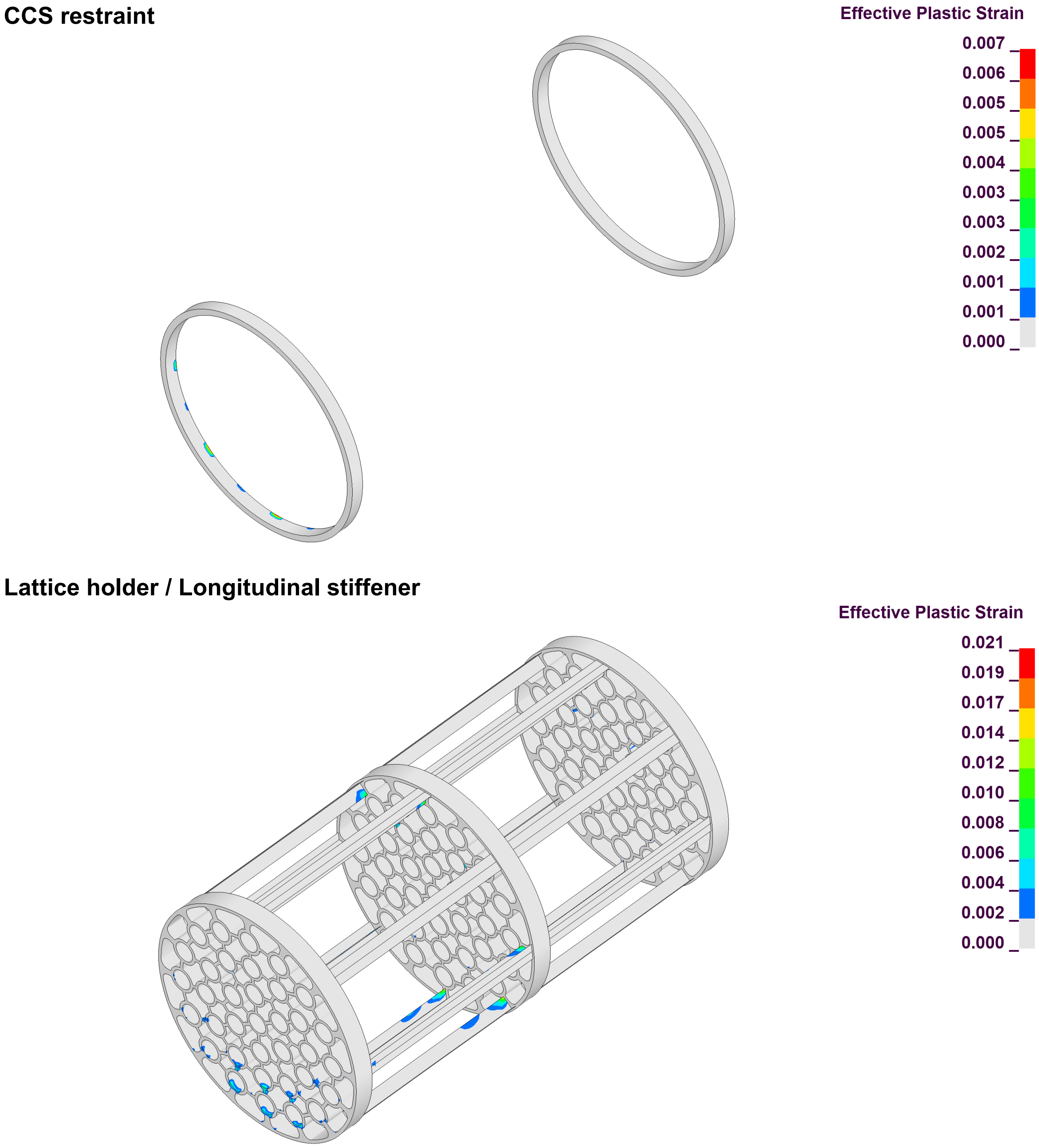


**Figure 2-17 Corner drop onto the valve side from a height of 10.2 m – Equivalent plastic strain at the CCS restraint and the lattice holders of the CCS**

The plastic strains at the CCRs are shown in figure 2-18. Even though the CCRs have no containment function and failure of a CCR would only lead to a contamination of the content with neutron absorbing material, the same acceptance criteria as for the pressure envelope of the 30B-X cylinder defined in section 2.1.2.2.1 is applied to the CCRs. With maximally 1.0 %, there is still a very large safety margin to the elongation at fracture of the carbon steel listed in table 2-8.

Moreover, only the CCRs in the lower half of the outer ring are affected, which is due to the deformations of the lattice holder on the valve side. For the CCRs of the middle and inner ring pattern, only negligible plastic deformations occur.

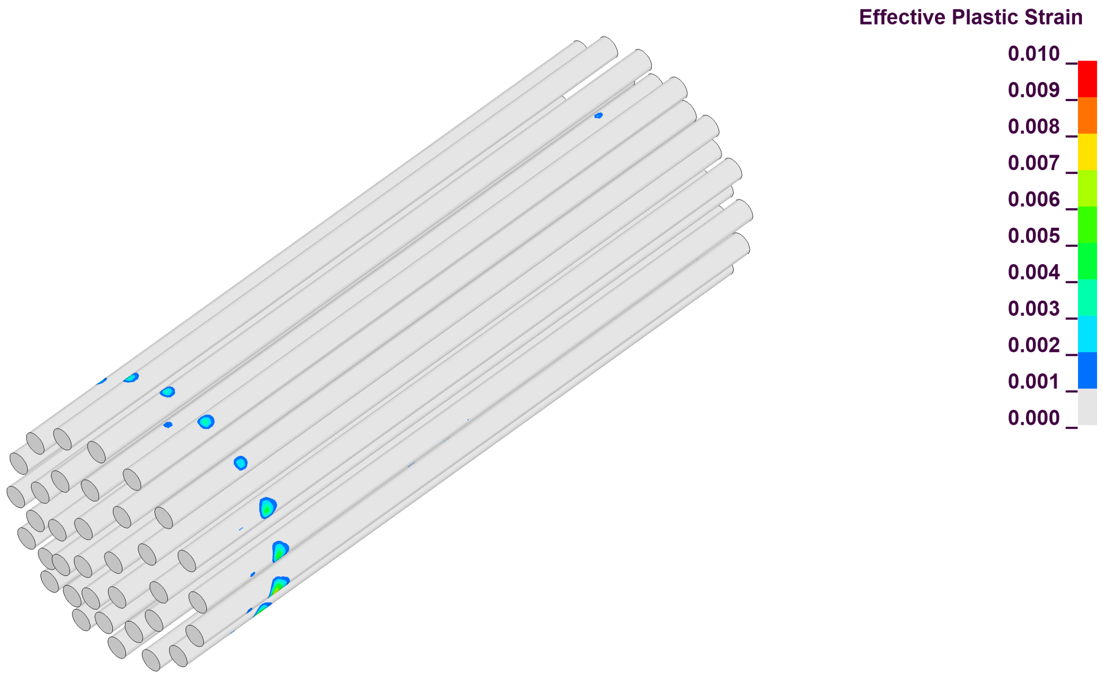


**Figure 2-18 Corner drop onto the valve side from a height of 10.2 m – Equivalent plastic strain at the CCRs of the CCS**

2.2.6.2.5.1.3 Decelerations

Figure 2-19 to figure 2-22 show the comparison of the low-pass filtered decelerations measured at the 30B-X and standard 30B cylinder for the corner drop onto the valve side. The determined decelerations are based on the data recorded by the accelerometer mounted in the valve area of the corresponding cylinder to comply with the evaluation in [DNT 2019]. As described in section 2.2.6.2.4.2, the deceleration curves are obtained by filtering the data with a low-pass SAE filter with cut-off frequencies of 20 Hz, 100 Hz, 200 Hz and 584 Hz.

The decelerations measured at the 30B-X cylinder are generally more irregular than those measured at the standard 30B cylinder, showing additional peaks and dips throughout the simulation. This behavior is to be expected because the explicitly modelled content of the 30B cylinder provides a significant amount of damping. In contrast to that, the cylinder shells of the 30B-X cylinder model hardly experience any damping and thus, more high-frequency oscillations are excited.

Furthermore, the decelerations at the 30B-X cylinder are higher on average than those measured at the standard 30B cylinder. At a cut-off frequency of 20 Hz shown in figure 2-19, this becomes quite evident. As already mentioned above, this can probably be attributed to the different approaches to model the content. In case of the 30B-X cylinder, the content remains attached to the outer surfaces of the CCRs, while the content block can move freely inside the standard 30B cylinder to a certain degree. Hence, the content of the 30B cylinder contributes less kinetic energy to the initial impact, leading to a generally lower level of decelerations. Furthermore, the very stiff contact between the lattice holders and the CCS restraint of the 30B-X cylinder can be expected to result in a higher deceleration peak as well. This peak can be seen in figure 2-20 at

around 0.012 s, which is missing entirely in case of the DN30 package. With increasing cut-off frequency, these characteristics of the deceleration behavior of the 30B-X cylinder become more and more apparent (see figure 2-21 and figure 2-22). Therefore, the comparison of the deceleration curves is generally not meaningful in case of the corner drop onto the valve side.

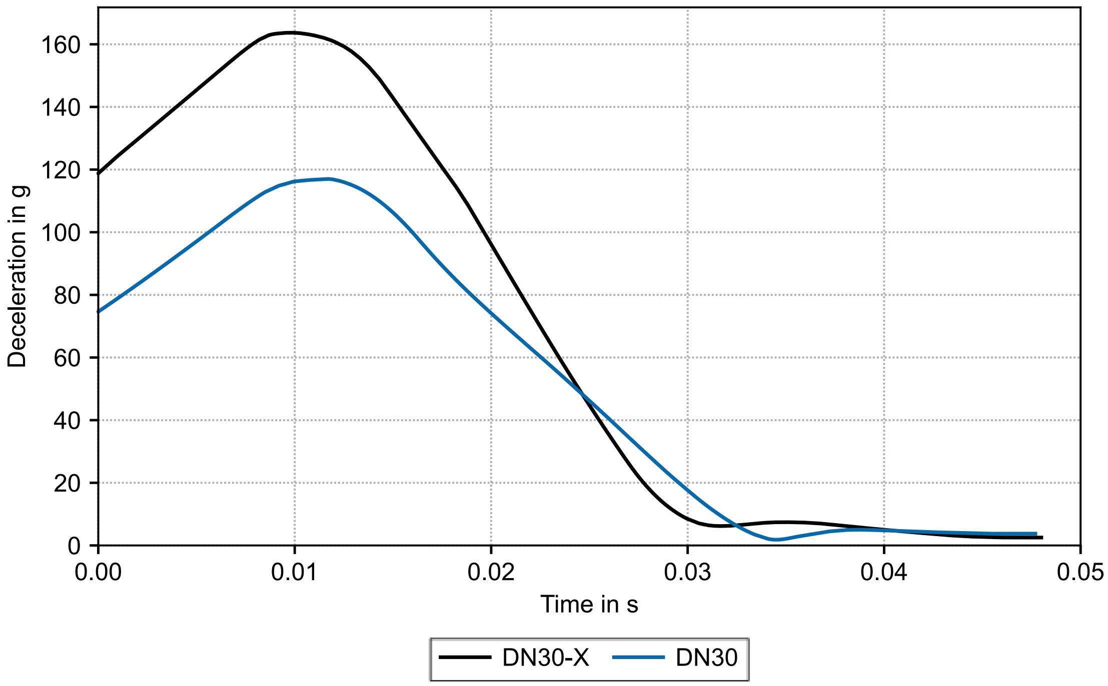


**Figure 2-19 Corner drop onto the valve side from a height of 10.2 m – Deceleration in the plug area – Low-pass filtered (SAE, 20 Hz cut-off)**

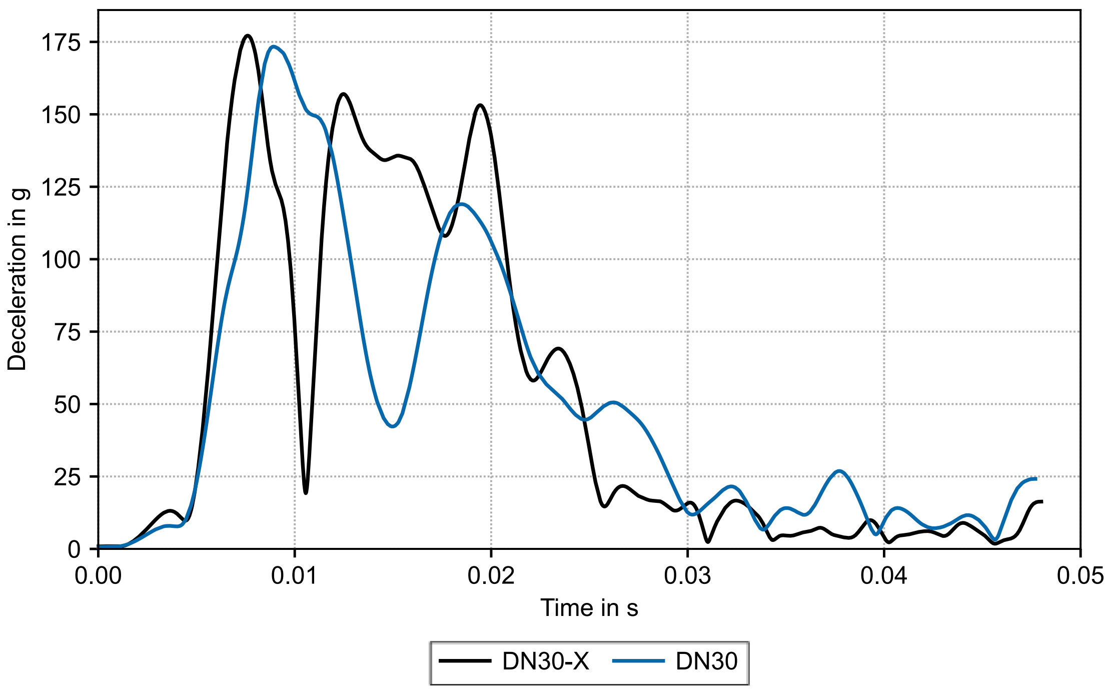


**Figure 2-20 Corner drop onto the valve side from a height of 10.2 m – Deceleration in the plug area – Low-pass filtered (SAE, 100 Hz cut-off)**

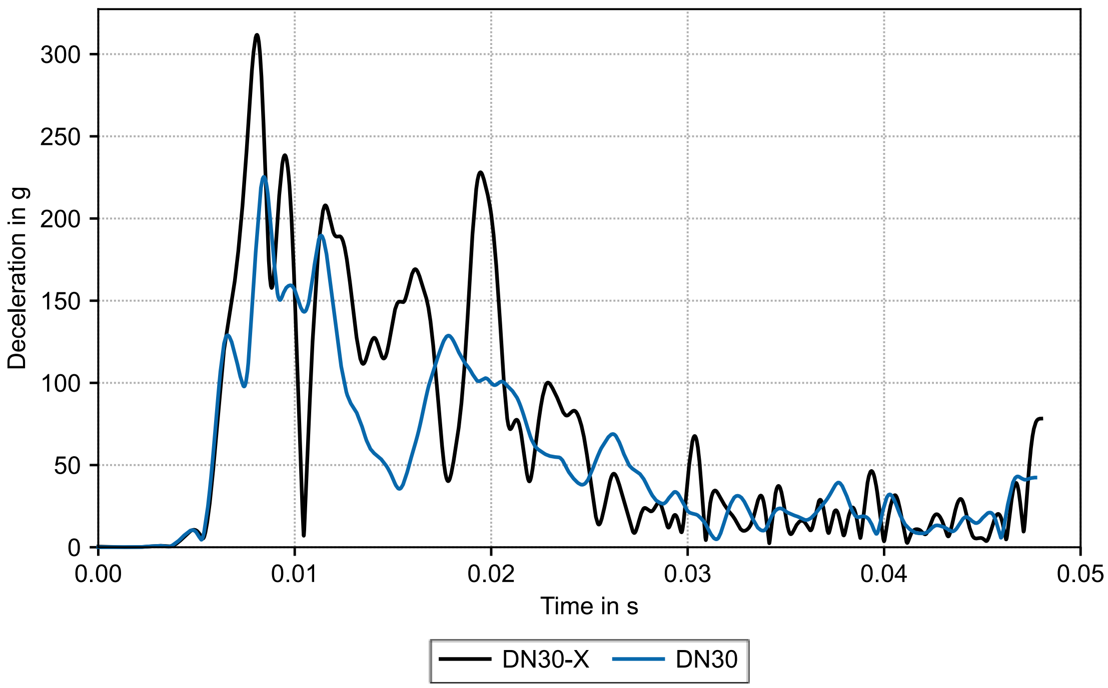


**Figure 2-21 Corner drop onto the valve side from a height of 10.2 m – Deceleration in the plug area – Low-pass filtered (SAE, 200 Hz cut-off)**

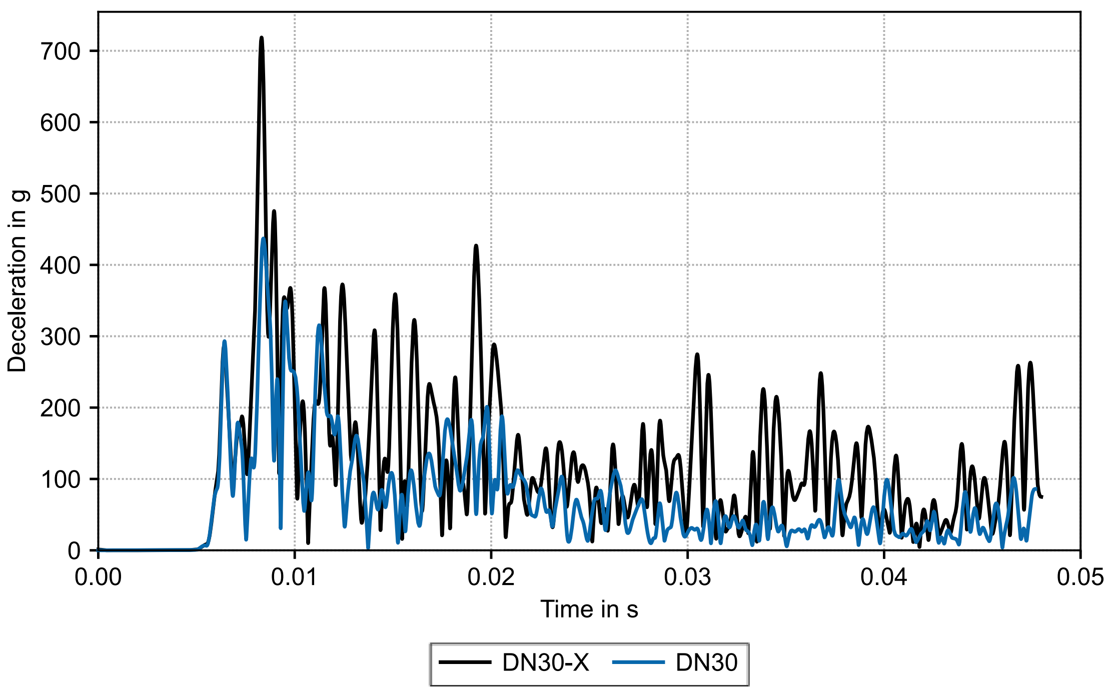


**Figure 2-22 Corner drop onto the valve side from a height of 10.2 m – Deceleration in the plug area – Low-pass filtered (SAE, 584 Hz cut-off)**

2.2.6.2.5.1.4 Summary

The DN30-X package design ensures that after the corner drop test onto the valve side simulating HAC, all acceptance criteria as defined in section 2.1.2.2.1 are met:

- There is no failure of the DN30 PSP closure system.

- There is no physical contact between the valve of the 30B-X cylinder and any other component of the packaging other than its original point of attachment.
- There is no physical contact between the plug of the 30B-X cylinder and any other component of the packaging other than its original point of attachment.
- There is no rupture of the 30B-X cylinder containment system.
- There is no failure of the 30B-X cylinder confinement system:
  - The relative dislocation of the CCRs remains below 5 mm.
  - The increase in radial movability of the entire CCS out of the center of the 30B-X cylinder remains below 3 mm.
  - The increase in axial movability of the entire CCS out of the center of the 30B-X cylinder remains below 7 mm.
  - There is no failure of the lattice holders.
  - There is no rupture of the CCRs.

2.2.6.2.5.2 Flat Drop onto the Valve Side – Drop Test Sequence 3

With the corner drop onto the valve side, as described in section 2.2.6.2.5.1, maximal deformations are reached in the valve area. In contrast to that, maximal acceleration and, therefore, maximal forces at the valve are expected for the flat drop onto the valve side. This drop test orientation was part of drop test sequence 3 in the safety analysis of the DN30 package in [DNT 2019].

As the valve is the most vulnerable part of the containment system, the flat drop onto the valve side is used in the comparison analysis between the DN30-X and DN30 package. Furthermore, this drop test orientation puts the highest demands on the lattice holders and the CCS restraints of the 30B-X cylinder and, therefore, provides additional information on the structural integrity of the interior CCS of the 30B-X cylinder.

From the mechanical point of view, the DN30-X package design has to ensure that after the flat drop test onto the valve side simulating HAC, all acceptance criteria as defined in section 2.1.2.2.1 are met:

- No failure of the DN30 PSP closure system.
- No physical contact between the valve of the 30B-X cylinder and any other component of the packaging other than its original point of attachment.
- No physical contact between the plug of the 30B-X cylinder and any other component of the packaging other than its original point of attachment.
- No rupture of the 30B-X cylinder containment system.
- No failure of the 30B-X cylinder confinement system:
  - The relative dislocation of the CCRs must remain below 5 mm.
  - The increase in radial movability of the entire CCS out of the center of the 30B-X cylinder must remain below 3 mm.
  - The increase in axial movability of the entire CCS out of the center of the 30B-X cylinder must remain below 7 mm.
  - Failure of the lattice holders must not occur.
  - Rupture of the CCRs must not occur.

The initial states for the flat drop test onto the valve side of the DN30-X and DN30 package are shown in figure 2-23.

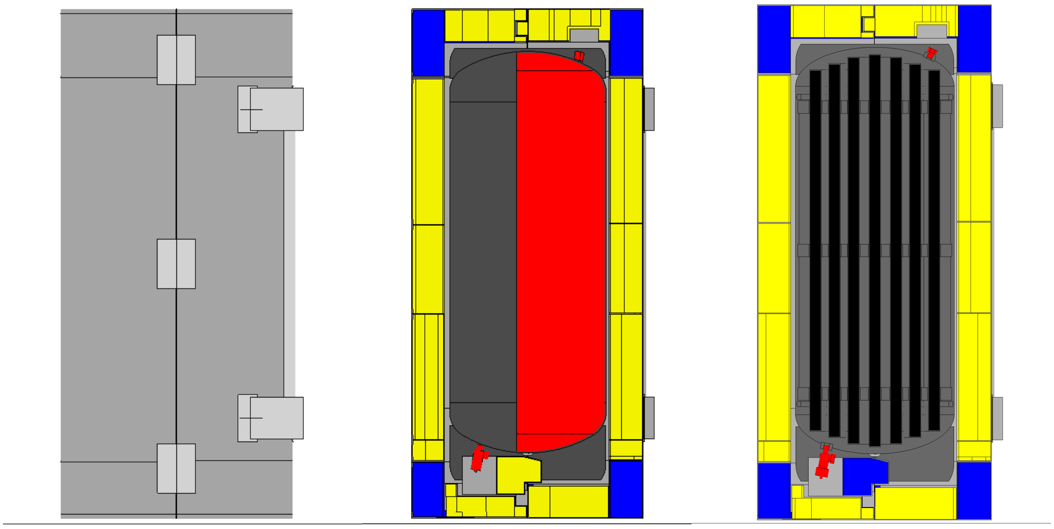

**Figure 2-23 Flat drop onto the valve side from a height of 10.2 m – Undeformed initial state of the DN30-X and the DN30 package**

2.2.6.2.5.2.1 General Results

A real time of 0.03 s suffices to capture all relevant aspects of the flat drop test onto the valve side. As can be seen in figure 2-24, the kinetic and the internal energy both reach a constant level towards the end of the simulation, indicating that all deformation processes have been completed and that only rigid body motions are left.

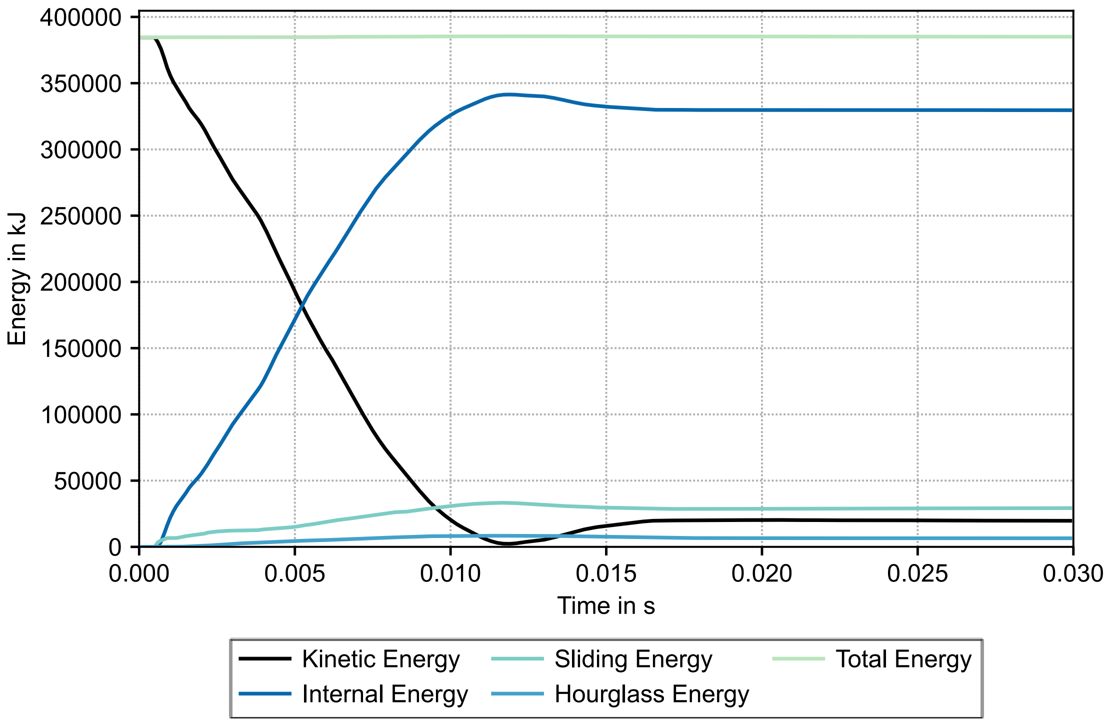


**Figure 2-24 Flat drop onto the valve side from a height of 10.2 m – Energy distribution**

The distribution of energies in figure 2-24 that contribute to the total energy show the same characteristics as for the corner drop onto the valve side in section 2.2.6.2.5.1. As no gravitation is considered in the FEM model, the kinetic energy does not drop to zero but reaches a constant

level after the package has lost contact to the drop target. Again, the hourglass and sliding energy are small in comparison to the internal energy ensuring that the deformations of the DN30-X package are not underestimated. The resulting energy ratio for this drop test simulation ranges from 0.999649 to 1.00204, indicating very good energy conservation.

Figure 2-25 shows the contact energy of the automatic single surface contact. The contact energy remains positive throughout the simulation, but drops below the frictional energy in the second half of the simulation. This behavior could be improved by reducing the contact stiffness, which would increase the energy fraction that is stored in the contact. Consequently, there is less energy available that needs to be absorbed by the DN30-X package potentially resulting in smaller deformations. The chosen contact stiffness therefore provides a good balance between a stable simulation and reliable deformation results.

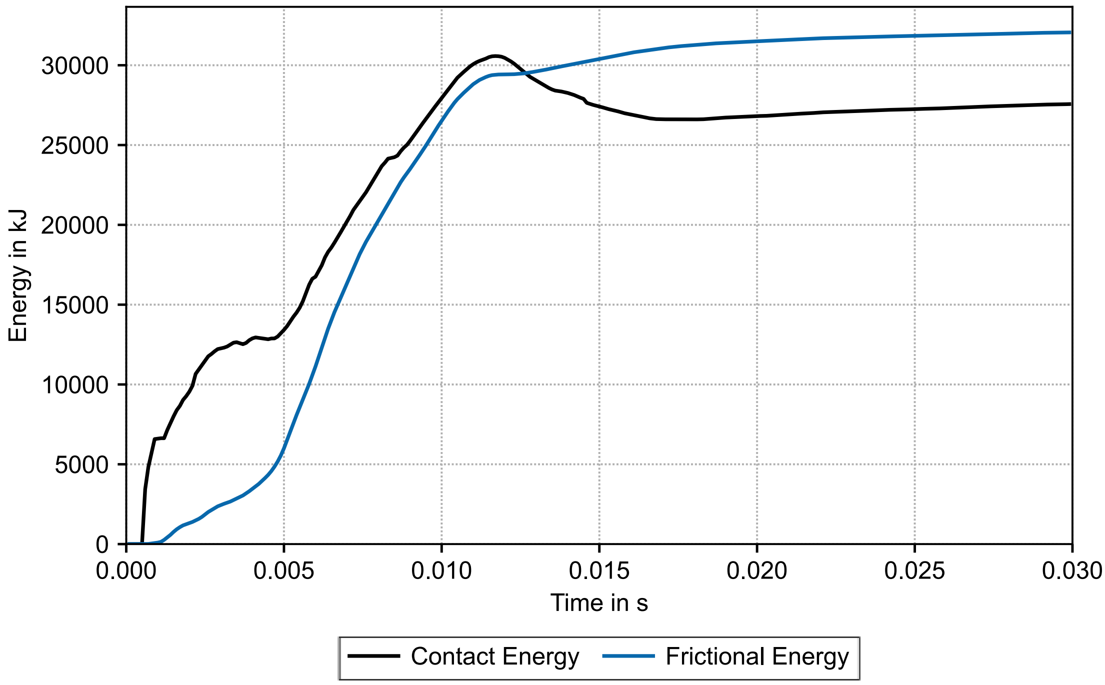


**Figure 2-25 Flat drop onto the valve side from a height of 10.2 m – Contact energy of the automatic single surface contact**

The hourglass energy in comparison to the internal energy is shown in figure 2-26. This comparison proves that the upper limit of 10 % of the internal energy is complied with and that there are no sudden increases in the hourglass energy.

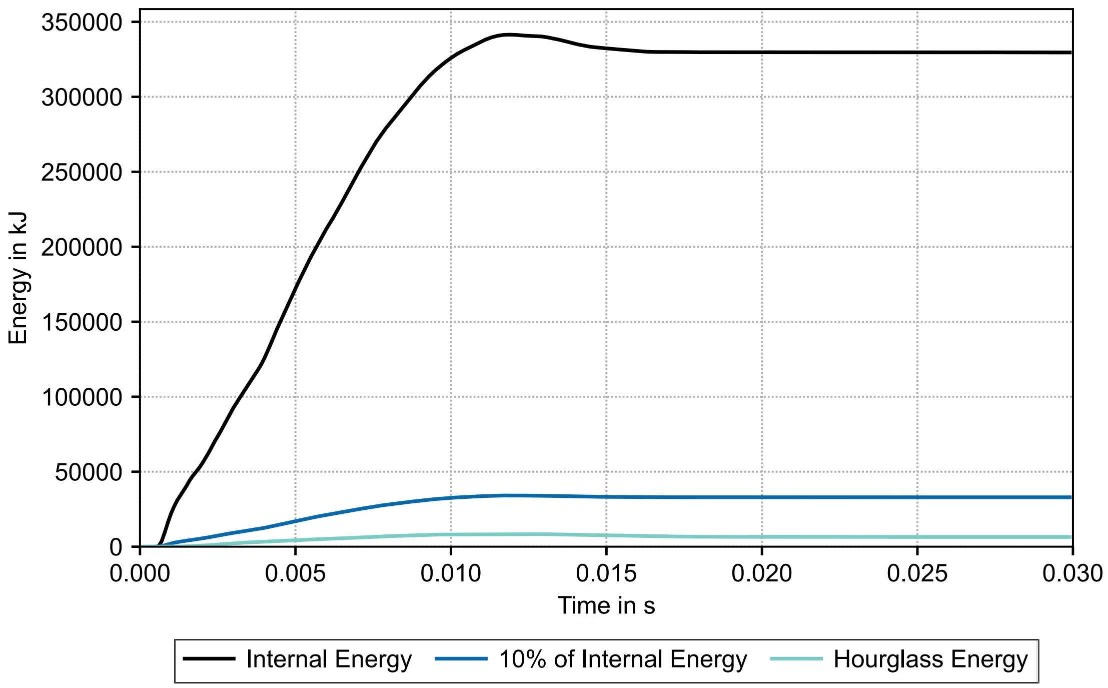


**Figure 2-26 Flat drop onto the valve side from a height of 10.2 m – Hourglass energy**

2.2.6.2.5.2.2 Deformations

2.2.6.2.5.2.2.1 DN30 PSP and Cylinder Pressure Envelope

The state of maximal deformation for the DN30-X to the DN30 package during the flat drop test onto the valve side is compared in figure 2-27. For both packages, the compression of the foam in the valve area and the deformations of the inner and outer DN30 PSP shell are nearly identical. This is also reflected in very small differences in plastic strain at the outer shell that reach 38 % and 37 % in case of the DN30-X and DN30 package, respectively.

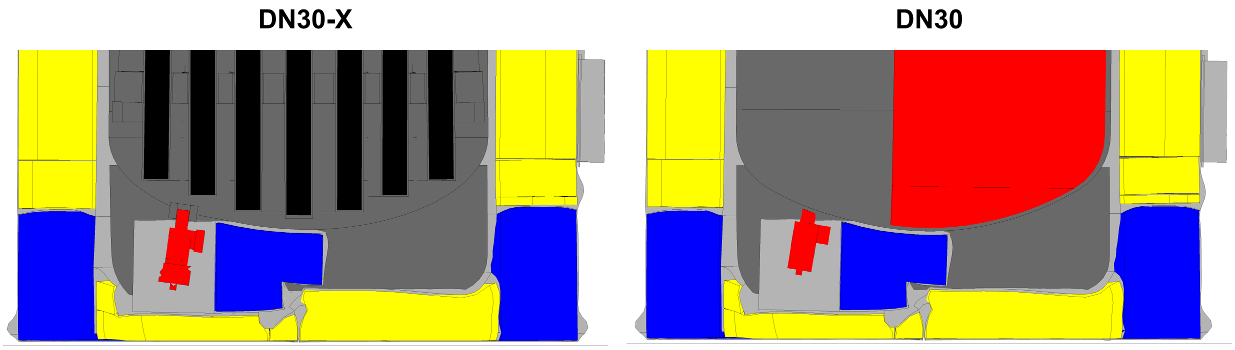


**Figure 2-27 Flat drop onto the valve side from a height of 10.2 m – State with the maximal deformation of the DN30-X and DN30 package**

As for the DN30 package, no physical contact at the valve is detected for the DN30-X other than its initial point of attachment. The maximum plastic strain at the inner shell of the DN30 PSP reaches 52 % in the simulation of the 10.2 m free drop test with the DN30 package. In case of the DN30-X package, 51 % are reached showing that the amount of deformation is comparable.

At the end of the simution, three distances are measured at the DN30 PSP to determine the amount of deformation at the impact zone (see figure 2-28). The same distances were used in [DNT 2019] to validate the FEM model of the DN30 package against the experimental drop tests performed with DN30 PSP prototypes. Table 2-16 lists the resulting values and provides a comparison to the corresponding results for the DN30 package.

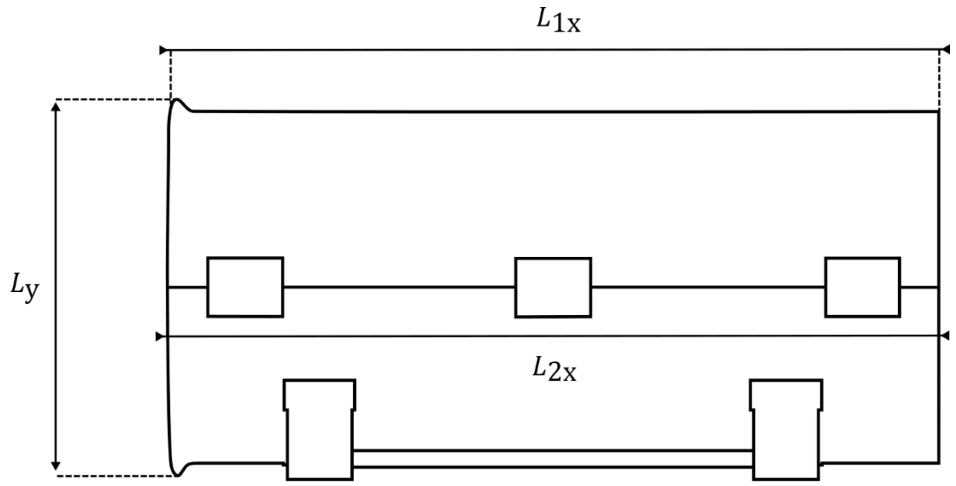


**Figure 2-28 Measured distances for the flat drop onto the valve side**

**Table 2-16 Flat drop onto the valve side from a height of 10.2 m – Measured distances at the impact zone after the drop test**

| Measurement point | Parameter | Deformation in mm | | Change in % |
|---|---|---|---|---|
| | | DN30-X | DN30 | |
| Fold | $L_{1x}$ | 2419 | 2419 | ≈0 |
| | $L_y$ | 1142 | 1149 | -0.6 |
| Gap between top and bottom half | $L_{2x}$ | 2417 | 2418 | ≈0 |

The obtained results for the measured distances in table 2-16 correspond well to the deformations visible in figure 2-27. The changes in $L_{1x}$ and $L_{2x}$ are negligible and the extent $L_y$ of the fold at the impact zone is only slightly smaller in case of the DN30-X. However, buckling is an instability phenomenon so that the extent of the fold at the impact zone can be affected by small differences between the two calculation models of the DN30-X and the DN30 package like the different approaches to model the content of the two packages.

Beside the distances in table 2-16, the permanent axial reduction in the wall thickness of the DN30 PSP is evaluated in the valve area, which is required as input for the criticality safety analysis in section 2.6. As can be seen in figure 2-27, the flat drop test onto the valve side provides a good estimate of the closest axial approach of two neighboring DN30-X packages. The minimal wall thickness is determined by measuring the distance between the inner and outer head shell of the DN30 PSP. Including their sheet thicknesses, a minimal permanent wall thickness of the DN30 PSP of 103 mm is obtained.

As a more global comparison between the deformations of the DN30-X and the DN30 package, the energy absorption behavior during the flat drop test onto the valve side is investigated.

Figure 2-29 shows the distribution of the kinetic energy, the totally absorbed energy as well as the energy absorbed by the DN30 PSP for both the DN30-X and the DN30 package.

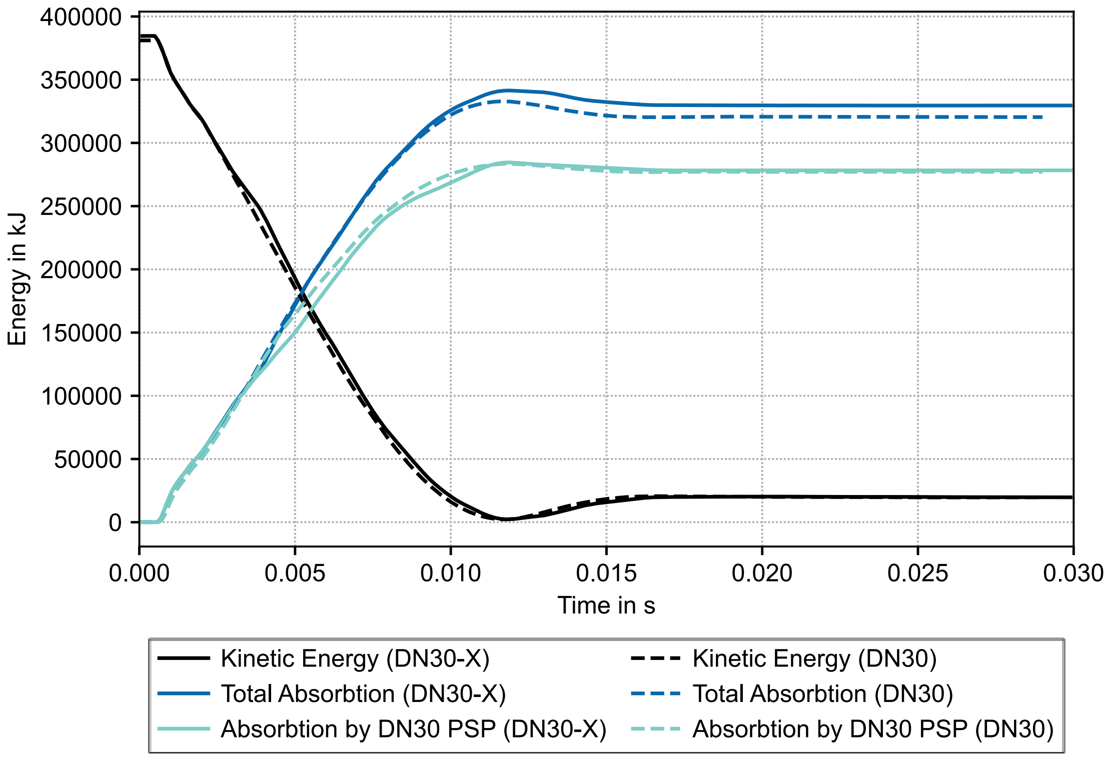


**Figure 2-29 Flat drop onto the valve side from a height of 10.2 m – Comparison of energy absorption of the DN30 PSP in case of the DN30-X and the DN30 package**

Based on this comparison, it is clearly seen that the kinetic energy and the energy absorbed by the DN30 PSP are nearly identical for both packages, showing the strong similarity between the two packages. The only noticeable difference occurs for the totally absorbed energy, which is due to the different approaches used to model the content of the DN30-X and the DN30 as well as the internal CCS of the 30B-X cylinder. Since the content is only implicitly incorporated in the FEM model of the DN30-X by using mass elements, there is no internal support provided by the content. This leads to slightly increased deformations of the 30B-X cylinder so that a larger fraction of kinetic energy is absorbed by the cylinder shells and the CCS. This further emphasizes the conservatism of the approach to model the content of the DN30-X package.

As a final comparison of the deformations of the DN30-X and DN30 package after the flat drop test onto the valve side, explicit values of the maximal equivalent plastic strains are evaluated. The results are listed in table 2-17 for the foam and selected steel parts of the DN30 PSP as well as the 30B-X and standard 30B cylinder pressure envelope. Table 2-17 also includes the corresponding values of the densification strains and elongations at fracture, which are taken from [DNT 2019] for the DN30 PSP (foam RTS 120 / RTS 320 and stainless steel 1.4301) and listed in table 2-8 for the 30B-X and standard 30B cylinder pressure envelope.

**Table 2-17 Flat drop onto the valve side from a height of 10.2 m – Plastic deformations of foam and selected steel parts of the DN30 PSP and the cylinder pressure envelope**

| Part | EPS[1)] in % | | Absolut change in % | DS / EF[2)] in % |
|---|---|---|---|---|
| | DN30-X | DN30 | | |
| DN30 PSP | | | | |
| RTS 120 | 78.2 | 76.6 | 1.6 | 89 |
| RTS 320 | 35.5 | 33.8 | 1.7 | 82 |
| Valve protecting device | 18.5 | 18.7 | -0.2 | 45 |
| Plug protecting device | 0.0 | 0.0 | 0.0 | 45 |
| Inner front plate (top half) | 51.1 | 52 | -0.9 | 45 |
| Inner front plate (bottom half) | 16.7 | 16.5 | 0.2 | 45 |
| Inner back plate (top half) | 0.3 | 0.2 | 0.1 | 45 |
| Inner back plate (bottom half) | 4.5 | 4.5 | 0.0 | 45 |
| 30B-X cylinder / standard 30B cylinder | | | | |
| Pressure envelope | 4.0 | 1.8 | 2.2 | 22 |

1) Equivalent plastic strain
2) Densification strain / elongation at fracture

The maximal equivalent plastic strains of parts of the DN30 PSP are generally very similar for the DN30-X and the DN30 package. A difference in case of a relevant deformation occurs only for the RTS 120 and RTS 320 foam. However, increases below 2.0 % are acceptable for the foam, especially as the foam compression remains far below their corresponding densification strain. In all other cases with large differences between the DN30-X and DN30 simulation results, the absolute values of the plastic strain are so small that the increase is irrelevant.

At the inner front plate of the top half of the DN30 PSP, the equivalent plastic strains are above the elongation at fracture of stainless steel 1.4301. Hence, cracks are very likely to occur, which was also observed after the experimental drop tests of Sequence 3 (see [DNT 2019]). However, as demonstrated in [DNT 2019], cracks in this area do not compromise the safety functions of the DN30 PSP. Figure 2-30 shows the distribution of the equivalent plastic strain at the inner front plate of the DN30 PSP for the DN30-X and DN30 package. This comparison proves that not only the maximal deformation is comparable for the DN30-X and DN30 but also the distribution of those deformations.

**DN30-X**

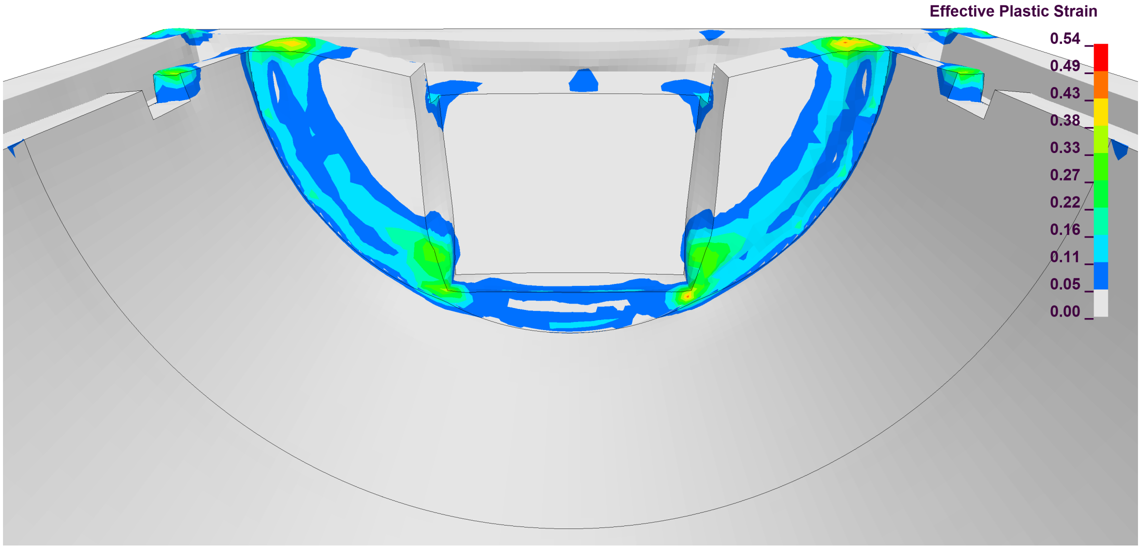


**DN30**

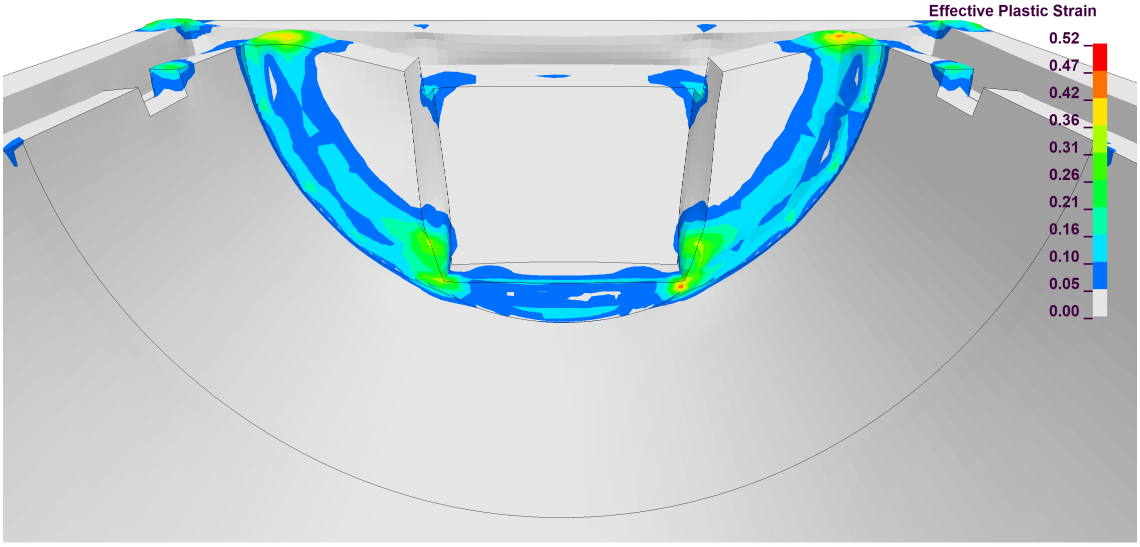


**Figure 2-30 Flat drop onto the valve side from a height of 10.2 m – Comparison of equivalent plastic strain at the inner shell**

In case of the cylinder pressure envelope, the determined increase in plastic strain from 1.8 % for the standard 30B to 4.0 % for the 30B-X cylinder was to be expected because the content is only implicitly incorporated in the FEM model of the DN30-X. Without any internal support for the cylinder shell provided by the content, the cylinder head is much more prone to a plastic collapse. As can be seen in figure 2-31, this leads to increased deformations at the 30B-X cylinder head on the valve side as well as to an extended contact area between the valve protecting device of the DN30 PSP and the cylinder head. Nevertheless, the regions where plastic strains occur are identical for both cylinders. Furthermore, 4.0 % maximal plastic strain are significantly below the elongation at fracture of the cylinder shell material so that rupture of the containment system can safely be excluded.

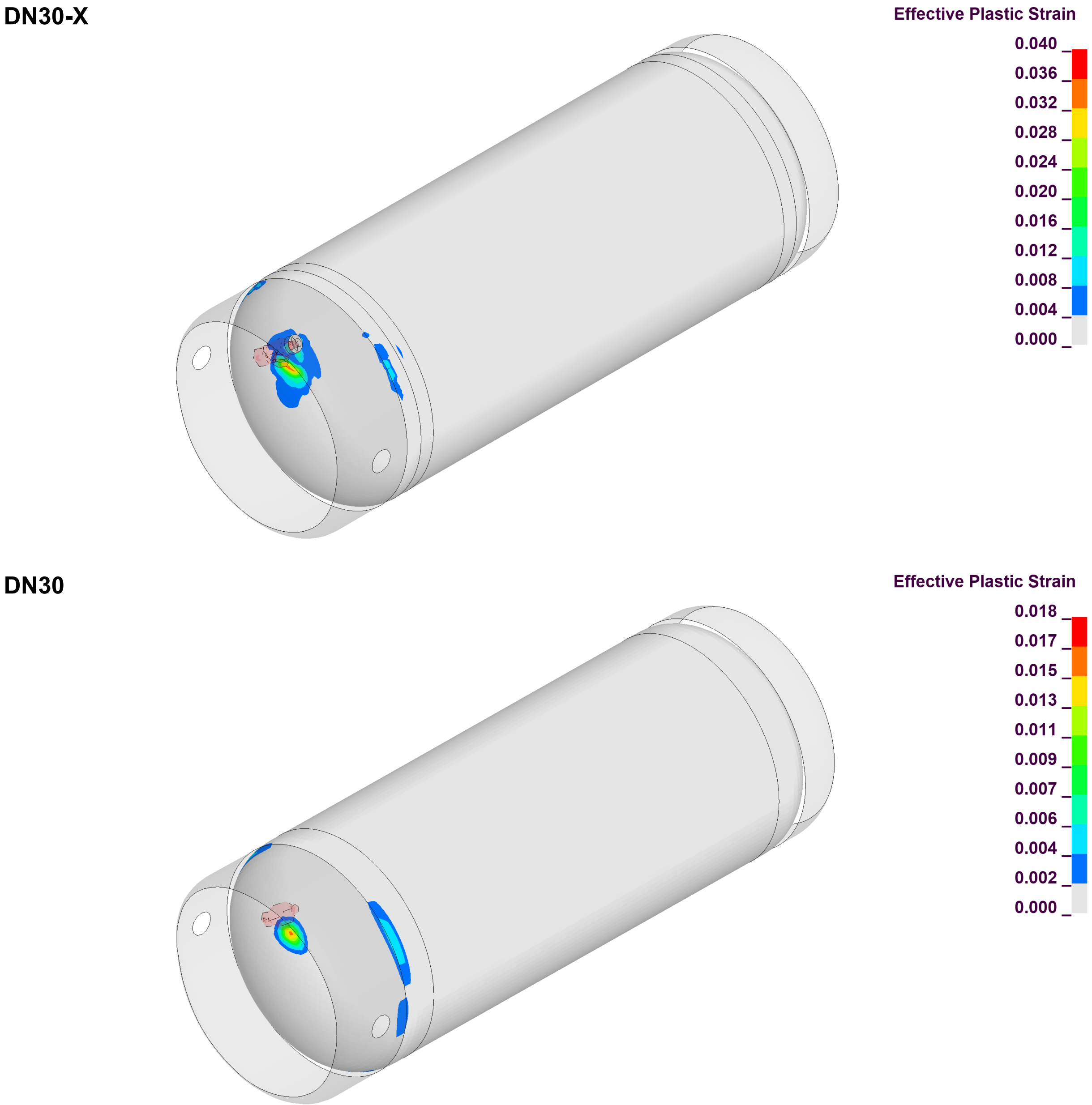


**Figure 2-31 Flat drop onto the valve side from a height of 10.2 m – Comparison of equivalent plastic strain at the cylinder pressure envelope**

2.2.6.2.5.2.2.2 Criticality Control System of the 30B-X Cylinder

In this section, the deformations of parts that are specific to the 30B-X cylinder design are investigated. These are the deformations of the CCS restraint, the lattice holders including the longitudinal stiffeners and the CCRs. Furthermore, the relative dislocation between the CCRs and the movability of the entire CCS within the cylinder are investigated.

The deformations of the CCS restraint and the lattice holders are shown in figure 2-32. Noticeable plastic strains occur only at the most outer spokes of the lattice holders and near the connection between the lattice holders and the longitudinal stiffeners. The maximal plastic strain in these areas reach 2.6 % and 2.1 %, respectively. This level of plastic strain is acceptable for the lattice holders and the longitudinal stiffeners, especially considering those parts have no containment function. Safety relevant is only the relative dislocation between the CCRs, which can be expected

to be small as the pipe clamps of the lattice holders hardly experience any plastic deformations. A detailed analysis of the relative dislocation between the CCRs is provided at the end of this section.

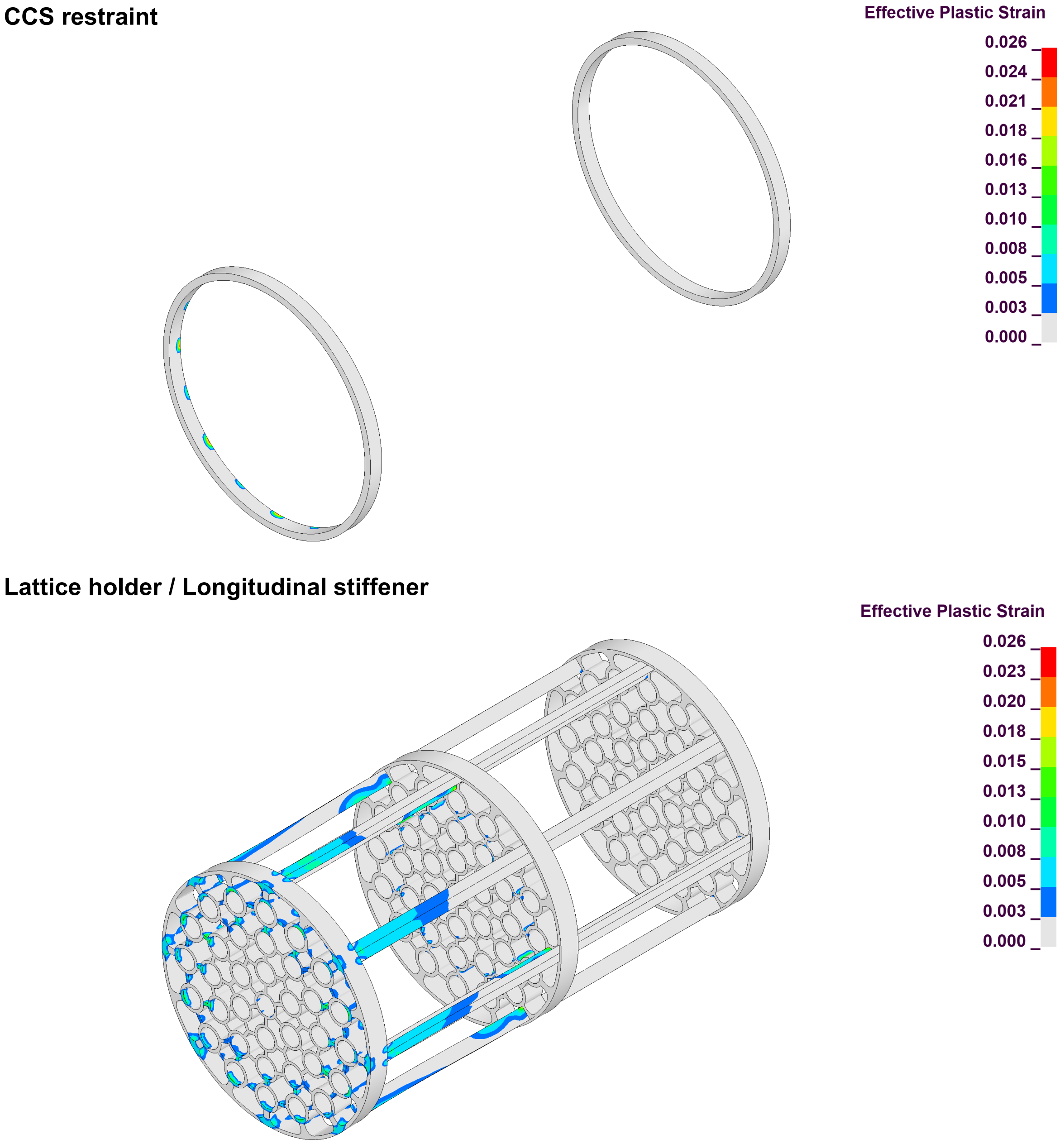


**Figure 2-32 Flat drop onto the valve side from a height of 10.2 m – Equivalent plastic strain at the CCS restraint and the lattice holders of the CCS**

The plastic strains at the CCRs are shown in figure 2-33. Even though the CCRs have no containment function and failure of a CCR would only lead to a contamination of the content with neutron absorbing material, the same acceptance criteria as for the pressure envelope of the 30B-X cylinder defined in section 2.1.2.2.1 is applied to the CCRs. With maximally 3.4 %, there is still a large safety margin to the elongation at fracture of the carbon steel listed in table 2-8. Moreover, only the CCRs in the outer ring are affected, which is due to the deformations of the lattice holder spokes in this area. For the CCRs of the middle and inner ring pattern, only negligible plastic deformations below 1 % occur.

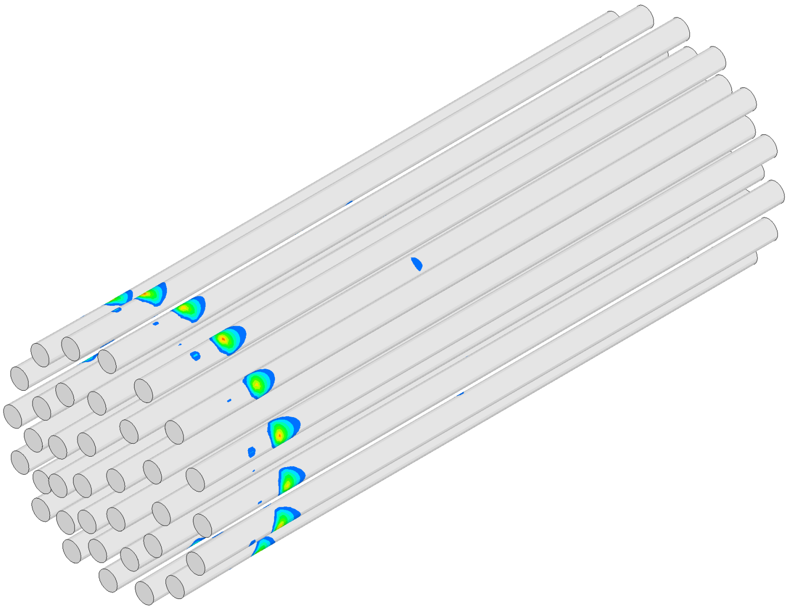


**Figure 2-33 Flat drop onto the valve side from a height of 10.2 m – Equivalent plastic strain at the CCRs of the CCS**

Regarding the acceptance criteria for the CCS defined in section 2.1.2.2.1, the relative dislocations between the CCRs and also the movement of the entire CCS relative to the 30B-X cylinder shell have to be evaluated. Considering the plastic deformations at the lattice holders are limited to their outermost spokes, there are no permanent relative dislocations between the CCRs and the relative dislocations between the CCRs are reduced to momentary oscillations during the drop test that are solely due to elastic deformations of the pipes.

For the flat drop onto the valve side, there are only negligible deformations that would increase the radial movability of the entire CCS within the 30B-X cylinder. Hence, the maximal radial movability of the entire CCS is still determined by the initial gap that exists between the lattice holders and the 30B-X cylinder shell.

The axial movability of the entire CCS within the cylinder is evaluated by measuring the change in distance between the cylinder head on the valve and on the plug side to the corresponding nearest lid of the central CCR. As shown in figure 2-34, the distance on the plug side increases by maximally 11.7 mm, while the distance on the valve side is reduced by maximally 14.9 mm. This difference is due to the deformations of the cylinder head on the valve side, while the cylinder head on the plug side experiences no deformations. Towards the end of the drop test simulation, the CCS returns to its initial position, but the permanent deformations of the lattice holders and the cylinder shell now allow for an increased axial movability of the CCS within the 30B-X cylinder in comparison to the undeformed initial state. The amount of additional movability of the CCS is estimated by the change in distance between the cylinder head on the plug side and the lid of the central CCR in the moment of contact release between the lattice holder and the CCS restraint of the 30B-X cylinder. At the time of contact release, most of the elastic strains have relaxed, which provides a more accurate estimate of the permanent deformations that affect the movability of the CCS within the 30B-X cylinder. The time of contact release is determined by evaluating the contact force between the CCS restraint and the lattice holder on the valve side and is indicated in figure 2-34. The corresponding value of the change in distance at that time is 6.3 mm. Taking into account the initially existing gap between the lattice holders and the CCS restraint of 5 mm, the axial movability of the entire CCS has increased by approximately 2 mm.

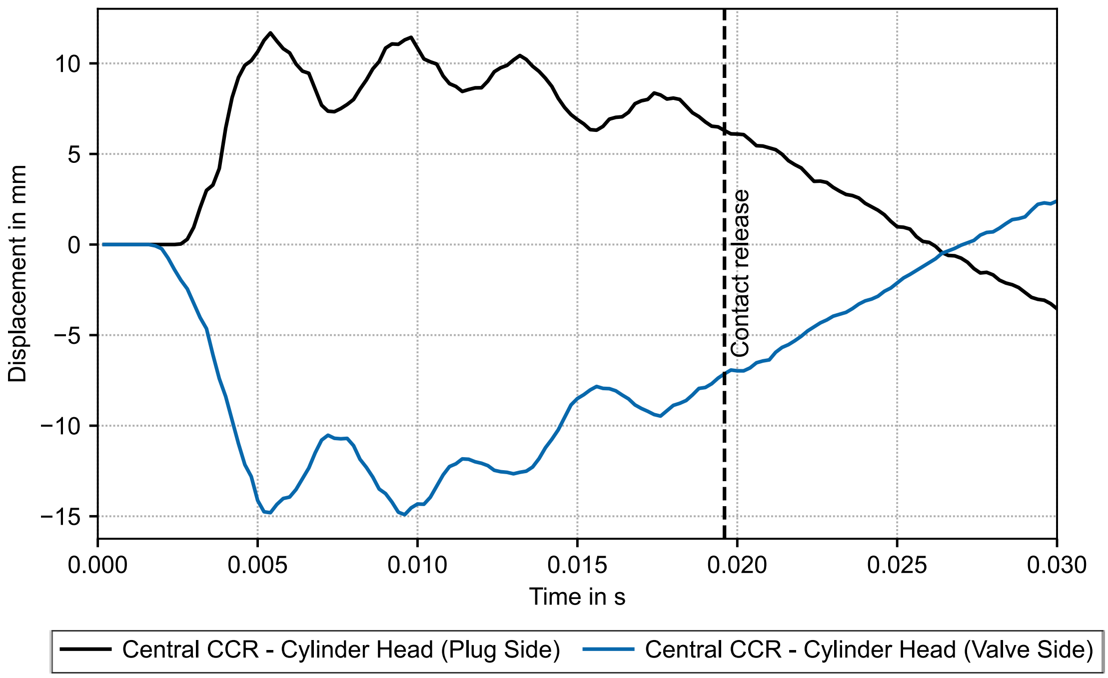


**Figure 2-34 Flat drop onto the valve side from a height of 10.2 m – Axial displacement of CCS within the 30B-X cylinder**

2.2.6.2.5.2.3 Decelerations

Figure 2-35 to figure 2-38 show the comparison of the resulting low-pass filtered decelerations for the flat drop onto the valve side. The decelerations are evaluated on the basis of the accelerometer located in the plug area to comply with the evaluations in [DNT 2019]. As described in section 2.2.6.2.4.2, the curves are obtained by filtering the data with a low-pass SAE filter with cut-off frequencies of 20 Hz, 100 Hz, 200 Hz and 584 Hz.

Overall, the deceleration curves measured for the 30B-X cylinder are more irregular than those for the standard 30B cylinder. Such a result was to be expected, as the explicitly modelled content of the 30B cylinder provides a substantial amount of damping, while the cylinder shells of the 30B-X cylinder model hardly experience any damping.

For the cut-off frequency of 20 Hz in figure 2-35, the deceleration curves measured at the 30B-X and the standard 30B cylinder are nearly identical. However, when the cut-off frequency is increased, the initial deceleration peak is much higher in case of the 30B-X cylinder and, generally, more peaks occur (see figure 2-36 to figure 2-38). These higher and additional deceleration peaks are mainly caused by the internal CCS that impacts the CCS restraint of the 30B-X cylinder. Since such an event does not occur in case of the standard 30B cylinder, the comparison of the deceleration curves at higher cut-off frequencies is not meaningful. Furthermore, such high deceleration peaks are not expected to occur under real conditions when the content significantly impedes the free motion of the internal CCS.

A comparison is therefore only feasible for the cut-off frequency of 20 Hz because the higher frequency components that are excited by the impact of the CCS on the CCS restraint of the 30B-X cylinder are no longer present. The deceleration curves in figure 2-35 represent the general deceleration behavior of the 30B-X and the standard 30B cylinder, which is primarily determined by the DN30 PSP. This comparison provides further evidence that the impact the 30B-X cylinder

has on the DN30 PSP is comparable to the impact the standard 30B cylinder has on the DN30 PSP.

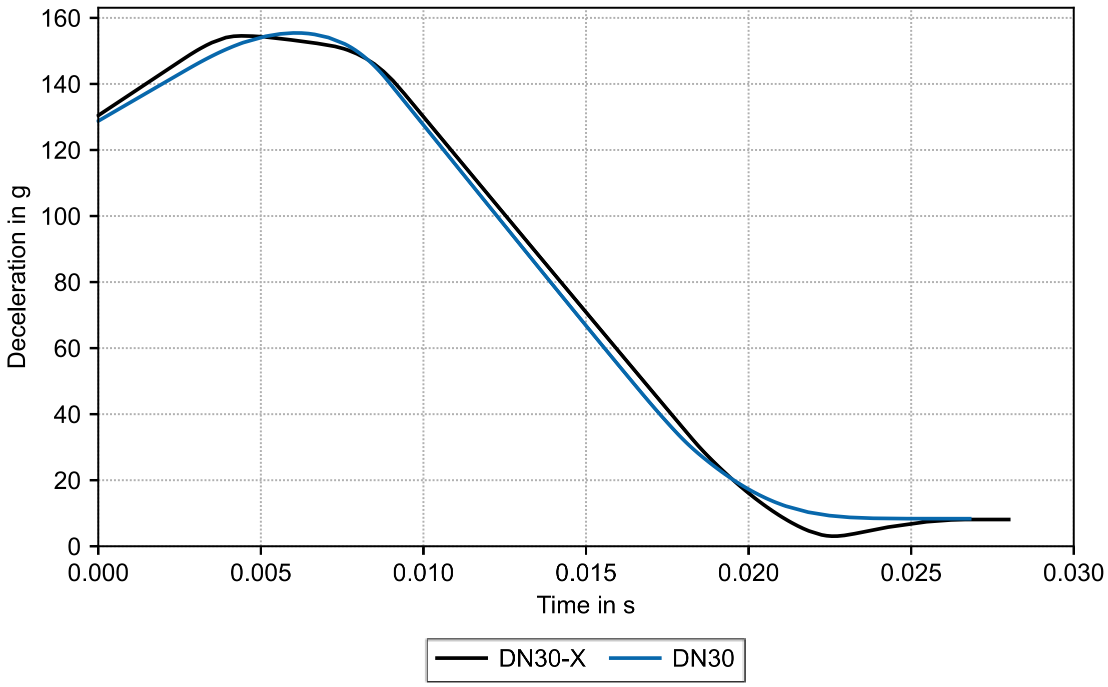


**Figure 2-35 Flat drop onto the valve side from a height of 10.2 m – Deceleration in the plug area – Low-pass filtered (SAE, 20 Hz cut-off)**

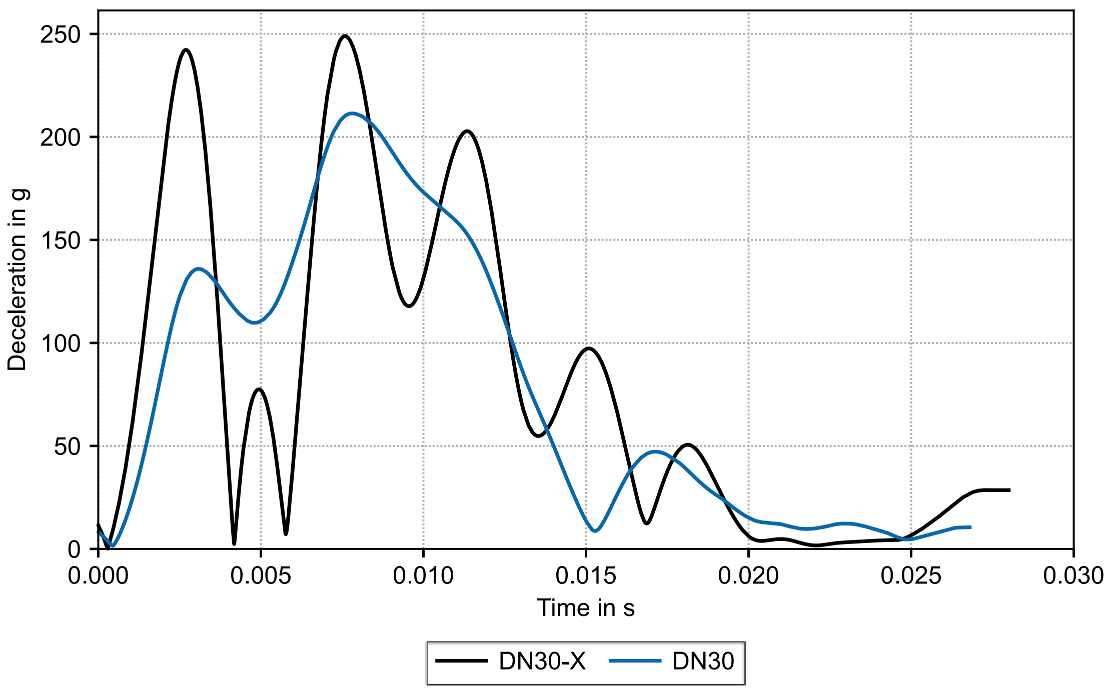


**Figure 2-36 Flat drop onto the valve side from a height of 10.2 m – Deceleration in the plug area – Low-pass filtered (SAE, 100 Hz cut-off)**

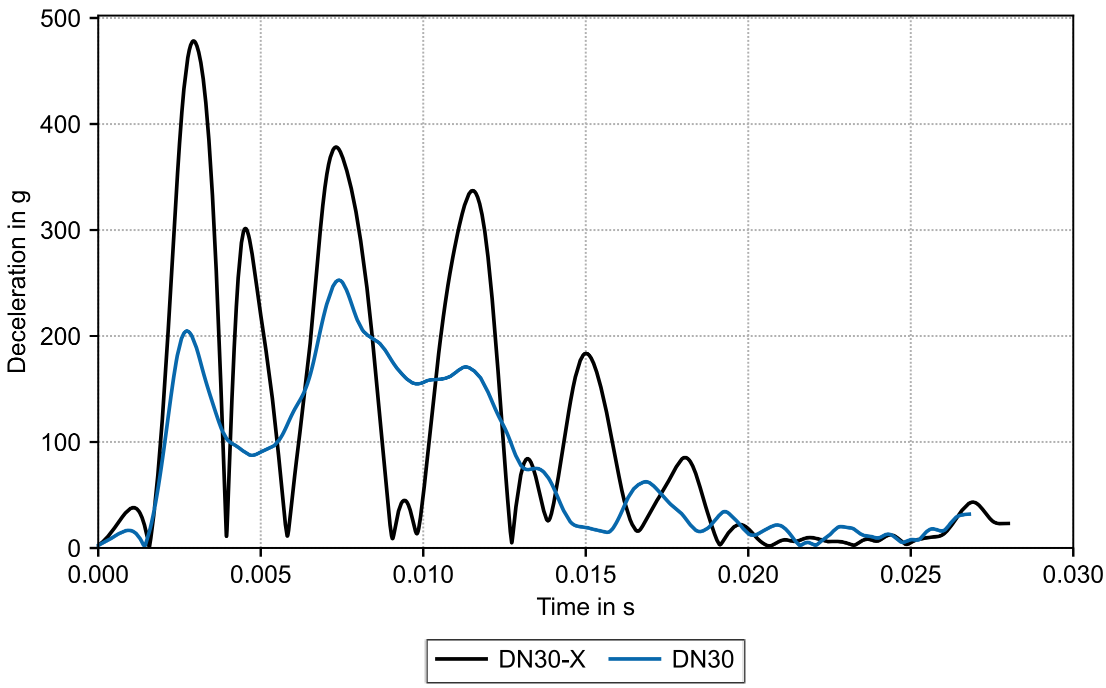


**Figure 2-37 Flat drop onto the valve side from a height of 10.2 m – Deceleration in the plug area – Low-pass filtered (SAE, 200 Hz cut-off)**

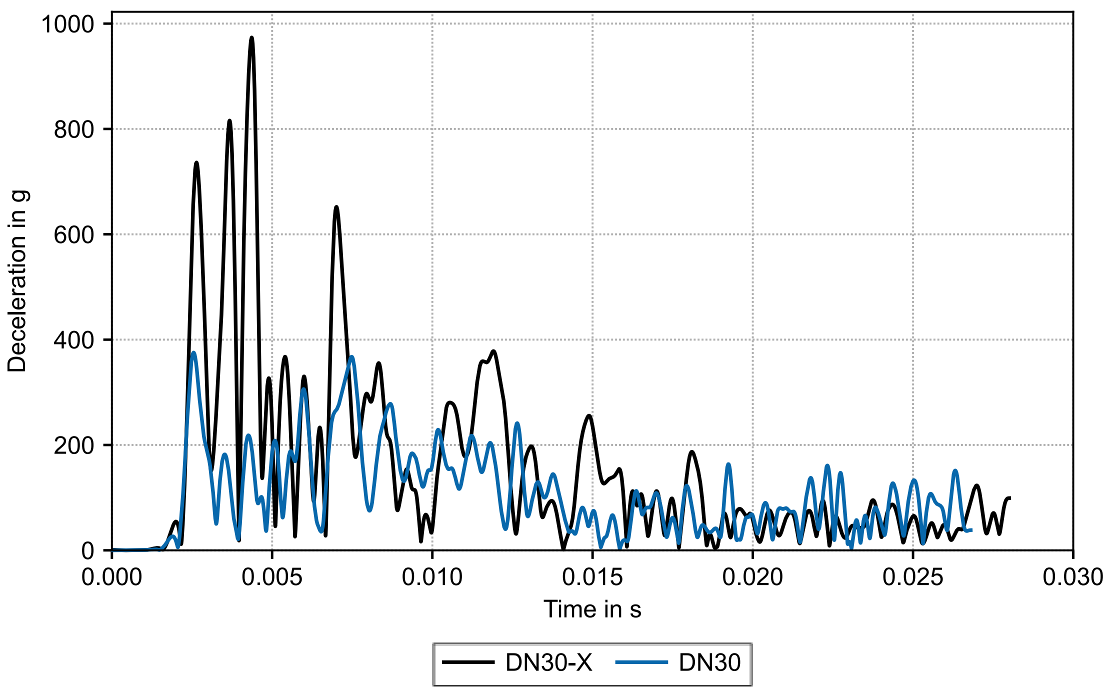


**Figure 2-38 Flat drop onto the valve side from a height of 10.2 m – Deceleration in the plug area – Low-pass filtered (SAE, 584 Hz cut-off)**

2.2.6.2.5.2.4 Sensitivity Analysis for the Content Weight Being Attached to the CCRs

The drop test simulation of the flat drop onto the valve side considers several conservative assumptions among which the implicit modelling of the content weight is expected to result in much higher stresses than in a real drop test scenario. The reasons for this have already been

discussed in section 2.2.6.2.3.7. In the following, a sensitivity analysis is performed, where the content weight is gradually shifted from the outer CCR surfaces to the 30B-X cylinder shell. Starting with the base model, 50 % of the content weight is shifted from the outer CCR surfaces to the cylinder shell. In a second step, the remaining content weight that is still attached to the outer CCR surfaces is also shifted to cylinder shell. This procedure is explained in figure 2-39.

**0 % of content weight on cylinder shell and 100 % on outer CCRs surfaces**

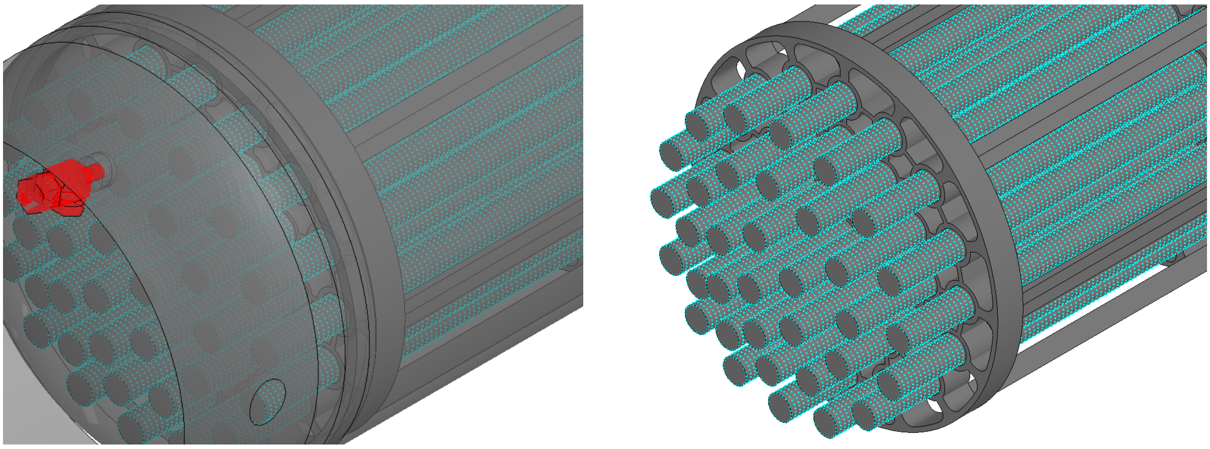

**50 % of content weight on cylinder shell and 50 % on outer CCRs surfaces**

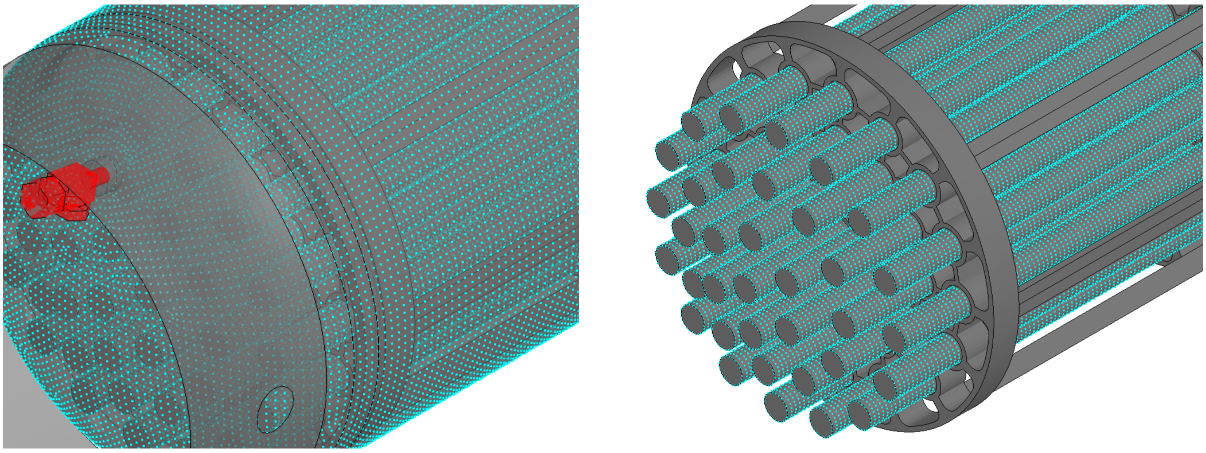

**100 % of content weight on cylinder shell and 0 % on outer CCRs surfaces**

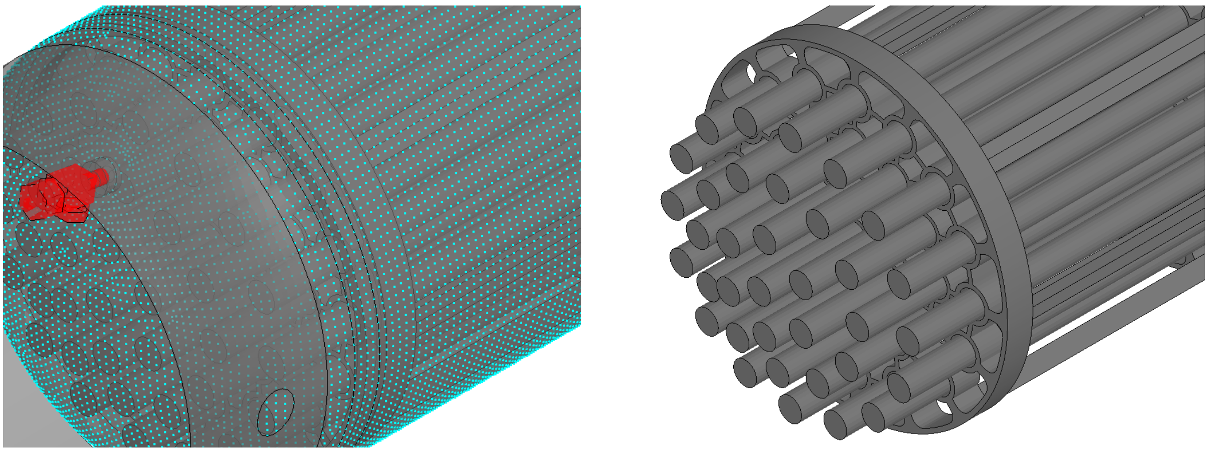

**Figure 2-39 Flat drop onto the valve side from a height of 10.2 m – Sensitivity analysis for content distribution – Distribution of mass elements**

Shifting the content weight from the CCRs to the cylinder shell can be expected to have a negligible impact on the deformations of the DN30 PSP. The gross weight of the 30B-X cylinder is kept constant in this sensitivity analysis, and it was already shown that replacing the standard 30B cylinder by the 30B-X cylinder only has a very subtle impact on the DN30 PSP. Therefore, the impact of the amount of content that sticks to the outer CCR surfaces is solely evaluated by the maximal equivalent plastic strain at the lattice holders of the CCS and the cylinder shell.

The results for the cylinder pressure envelope are shown in figure 2-40. Since the gross weight of the 30B-X cylinder is kept constant, there is almost no impact on the equivalent plastic strain at the cylinder shell, which is varying between 4 % and 4.4 % without a firm tendency. In contrast to the cylinder shell, the equivalent plastic strain at the lattice holders of the CCS continuously decreases with the content mass being shifted towards the cylinder shell. As shown in figure 2-41, the remaining plastic deformations of the lattice holders are negligible when the entire content weight is shifted towards the cylinder shell.

Nevertheless, even when the entire content weight is shifted towards the cylinder shell, the situation can still be expected to be conservative as the implicitly modelled content does not provide any support for the cylinder shell and the CCS. Consequently, the CCS is still impacting the CCS restraint of the 30B-X cylinder without being slowed-down by the content that actually would surround the CCS. The conservatism of the implicit modelling of the content becomes more apparent by evaluating the contact force between the CCS restraint on the valve side and the corresponding lattice holder, which is shown in figure 2-42.

Reducing the content weight that is attached to the CCRs by half, reduces the combined weight of the CCS and the content by 32 %. However, the peak contact force between the CCS restraint and the lattice holder only reduced by 5.5 %. A noticeable decrease of 24 % of the contact force only occurs, when the entire content weight is shifted towards the cylinder shell (reduces the combined weight of the CCS and content by 64 %). Nevertheless, the reduction of the contact force between the CCS restraint and the lattice holders is highly disproportionate to the reduction of the impacting mass. This is mainly due to the high stiffness of the interacting parts that are both made of carbon steel. Assuming that the CCS is actually surrounded by the $UF_6$ content, would not only close the initially existing gap between the CCS restraints and the lattice holders but would also reduce the stiffness between those two parts, as the $UF_6$ can be expected to have a much softer deformations behavior than carbon steel. Given that the contact stiffness in LS-DYNA linearly depends on the materials bulk modulus, the resulting contact force between the CCS restraint and the lattice holders approximately reduces in the same way (see [LS-Dyna 2018]).

The above discussion shows how conservative the analysis of the flat drop test onto the valve side is for the DN30-X package. Nevertheless, the analysis of the welding seam between the CCS restraint and the cylinder shell in section 2.2.6.2.7 is performed on the basis of the maximal contact force in figure 2-42, which is achieved when the entire content weight is attached to the CCRs.

**0 % of content weight on cylinder shell and 100 % on outer CCRs surfaces**

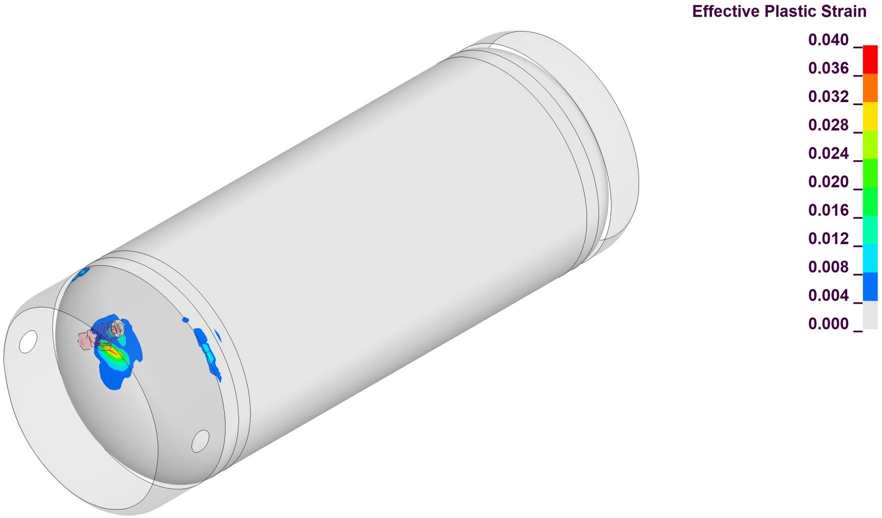


**50 % of content weight on cylinder shell and 50 % on outer CCRs surfaces**

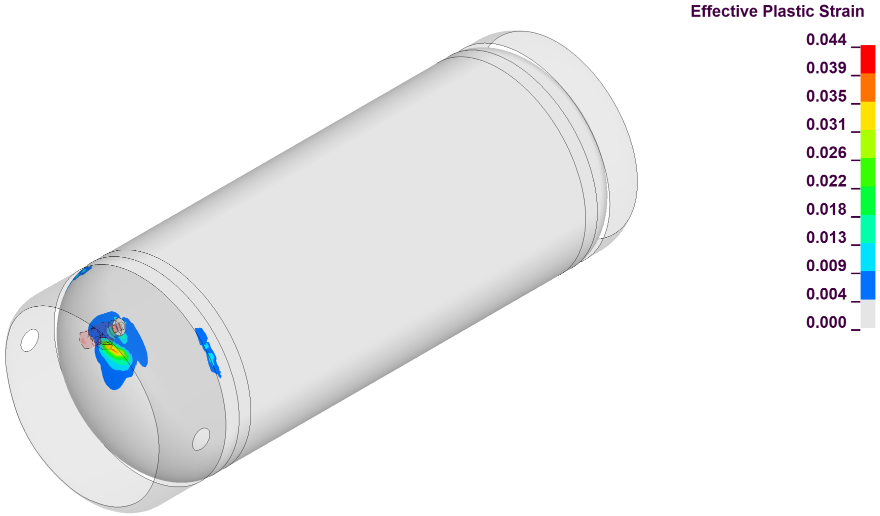


**100 % of content weight on cylinder shell and 0 % on outer CCRs surfaces**

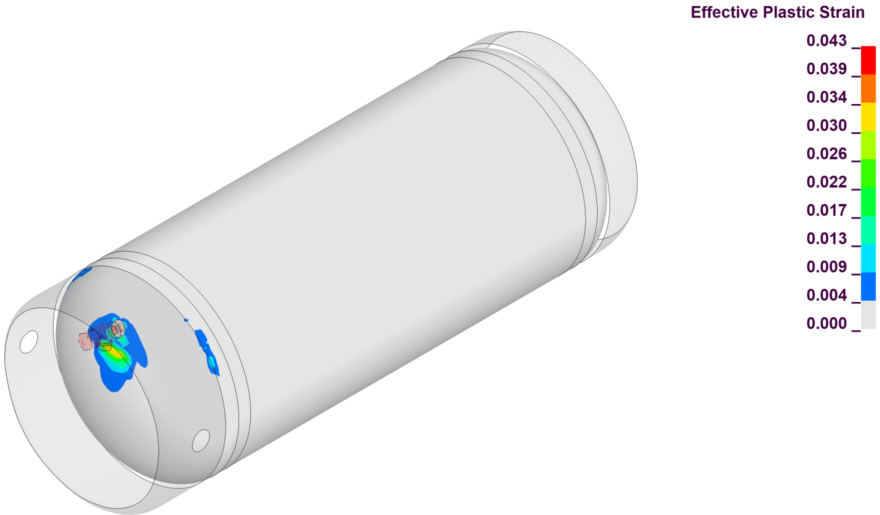


**Figure 2-40 Flat drop onto the valve side from a height of 10.2 m – Sensitivity analysis for content distribution – Comparison of equivalent plastic strain at the cylinder pressure envelope**

**0 % of content weight on cylinder shell and 100 % on outer CCRs surfaces**

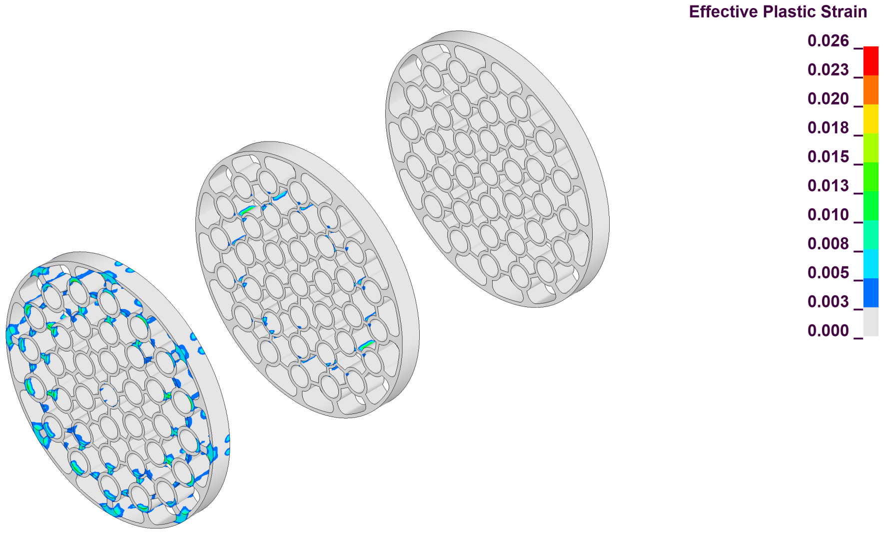


**50 % of content weight on cylinder shell and 50 % on outer CCRs surfaces**

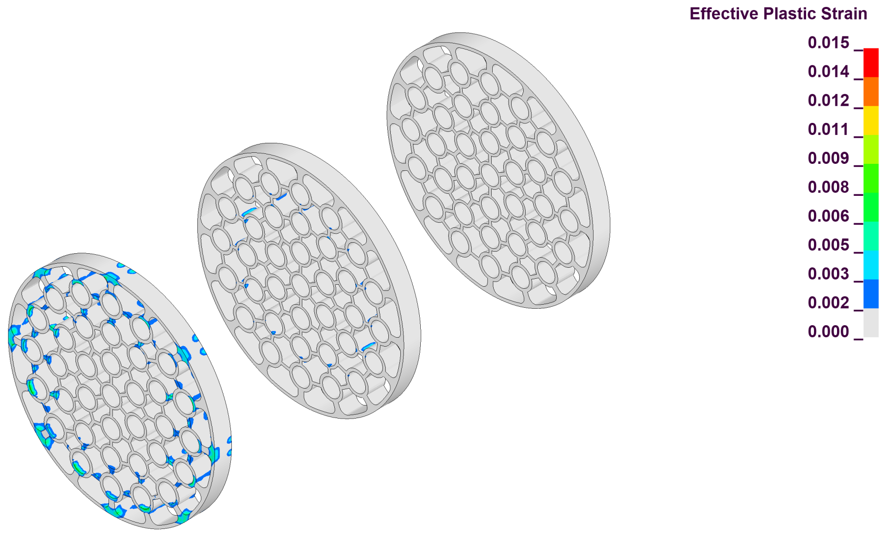


**100 % of content weight on cylinder shell and 0 % on outer CCRs surfaces**

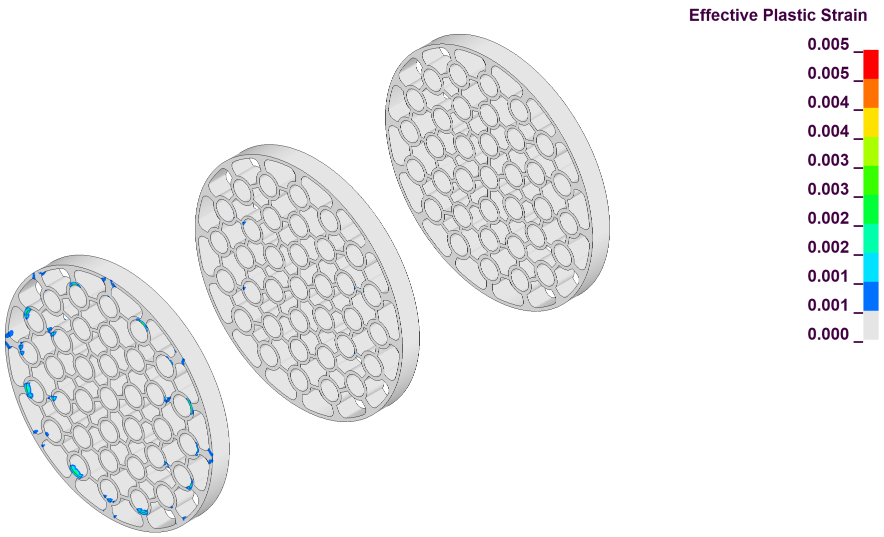


**Figure 2-41 Flat drop onto the valve side from a height of 10.2 m – Sensitivity analysis for content distribution – Comparison of equivalent plastic strain at the lattice holders**

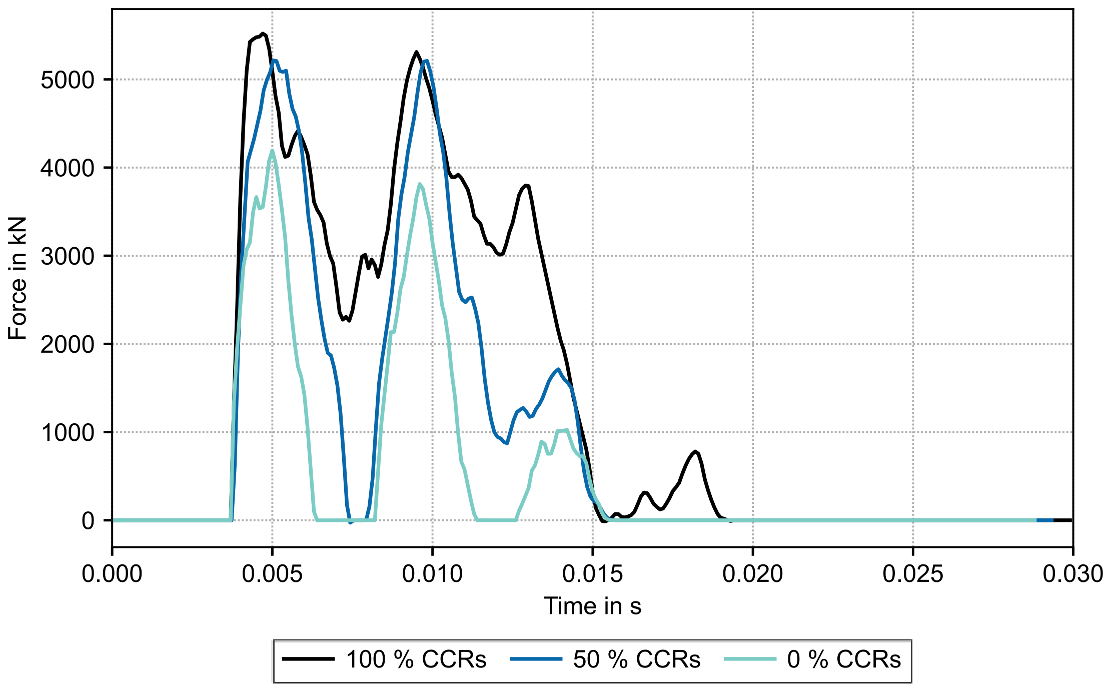


**Figure 2-42 Flat drop onto the valve side from a height of 10.2 m – Sensitivity analysis for content distribution – Comparison of contact force between the CCS restraint and the lattice holders**

2.2.6.2.5.2.5 Summary

The DN30-X package design ensures that after the flat drop test onto the valve side simulating HAC, all acceptance criteria as defined in section 2.1.2.2.1 are met:

- There is no failure of the DN30 PSP closure system.
- There is no physical contact between the valve of the 30B-X cylinder and any other component of the packaging other than its original point of attachment.
- There is no physical contact between the plug of the 30B-X cylinder and any other component of the packaging other than its original point of attachment.
- There is no rupture of the 30B-X cylinder containment system.
- There is no failure of the 30B-X cylinder confinement system:
  - The relative dislocation of the CCRs remains below 5 mm.
  - The increase in radial movability of the entire CCS out of the center of the 30B-X cylinder remains below 3 mm.
  - The increase in axial movability of the entire CCS out of the center of the 30B-X cylinder remains below 7 mm.
  - There is no failure of the lattice holders.
  - There is no rupture of the CCRs.

### 2.2.6.2.6 Additional Drop Test Analyses for the DN30-X Package

#### 2.2.6.2.6.1 Flat Drop onto the Feet – Drop Test Sequence 9

With the corner drop and the flat drop onto the valve side as described in section 2.2.6.2.5.1 and 2.2.6.2.5.2, two drop test orientations have been investigated for the DN30-X that have also been used to validate the DN30 package FEM model against experimental drop test results in [DNT 2019]. These two drop test scenarios put high stress on the DN30 PSP, but in case of the flat drop onto the valve side, the internal CCS of the 30B-X cylinder also experiences high loads, especially the lattice holders and the CCS restraints. In contrast to this, the investigation of the flat drop onto the feet aims at generating maximal accelerations at the CCRs perpendicular to their axis resulting in maximal bending stresses and, thus, the highest risk of kinking of the CCRs. As this drop test orientation is only relevant for the internal CCS of the 30B-X cylinder and was not part of the safety analysis of the DN30 package in [DNT 2019], the evaluation of the simulation results focuses on the deformations of the 30B-X cylinder.

From the mechanical point of view, the DN30-X package design has to ensure that after the flat drop onto the feet simulating HAC, all acceptance criteria as defined in section 2.1.2.2.1 are met:

- No failure of the DN30 PSP closure system.
- No physical contact between the valve of the 30B-X cylinder and any other component of the packaging other than its original point of attachment.
- No physical contact between the plug of the 30B-X cylinder and any other component of the packaging other than its original point of attachment.
- No rupture of the 30B-X cylinder containment system.
- No failure of the 30B-X cylinder confinement system:
  - The relative dislocation of the CCRs must remain below 5 mm.
  - The increase in radial movability of the entire CCS out of the center of the 30B-X cylinder must remain below 3 mm.
  - The increase in axial movability of the entire CCS out of the center of the 30B-X cylinder must remain below 7 mm.
  - Failure of the lattice holders must not occur.
  - Rupture of the CCRs must not occur.

The initial state of the DN30-X package for the flat drop test onto the feet is shown in figure 2-43.

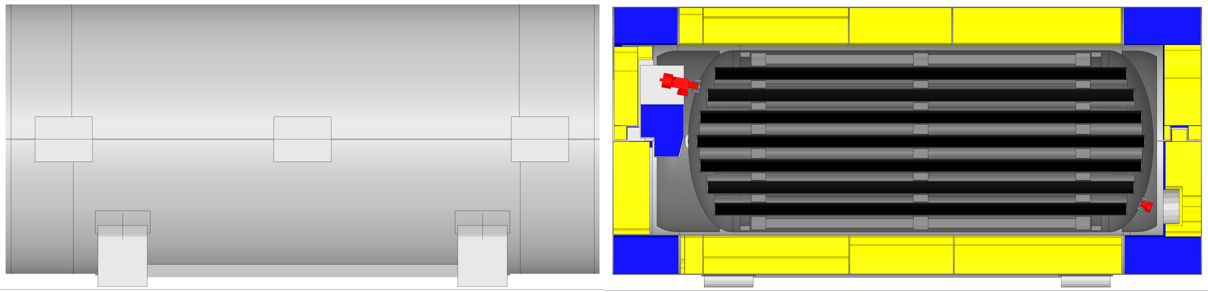

**Figure 2-43 Flat drop onto the feet from a height of 10.2 m – Undeformed initial state of the DN30-X package**

2.2.6.2.6.1.1 General Results

The simulation of the 10.2 m free drop test corresponds to a real time of 0.03 s, which suffices to capture all relevant aspects of the drop test. As shown in figure 2-44, the kinetic and the internal energy both remain constant indicating that the elastic relaxation phase has finished.

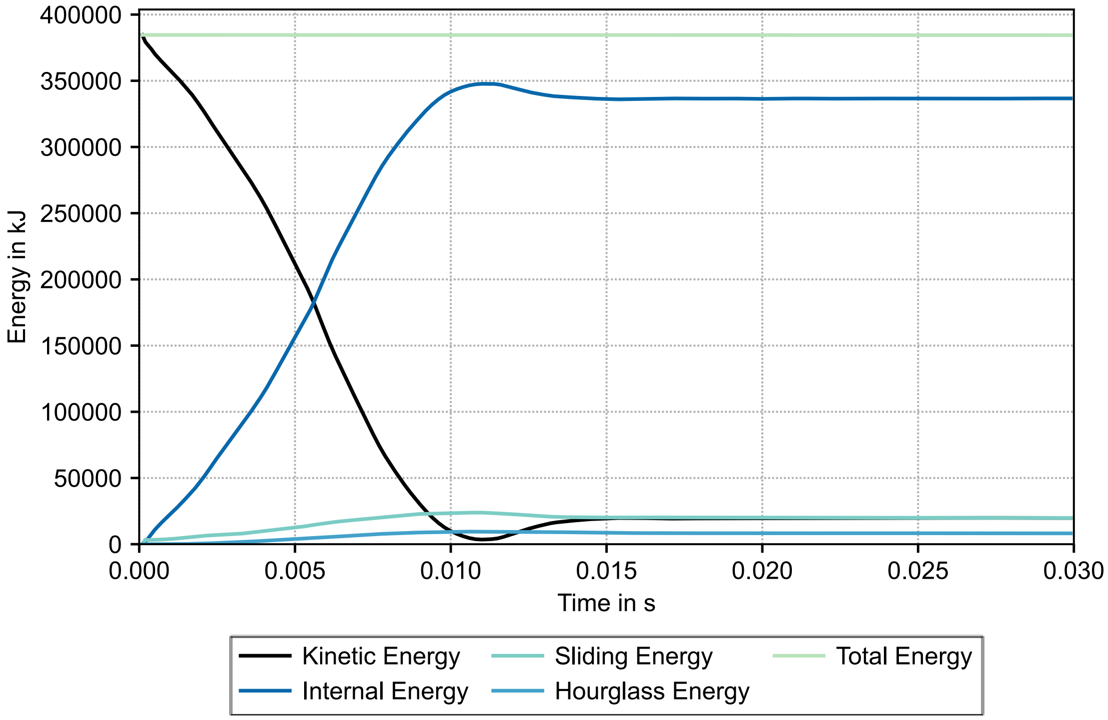


**Figure 2-44 Flat drop onto the feet from a height of 10.2 m – Energy distribution**

The DN30-X package does not come to rest after the impact because of the absence of gravitation in the FEM model. Hence, the package receives no further acceleration so that the kinetic energy reaches a constant level as soon as the package has lost contact to the drop target. Other energies like the hourglass and sliding energy (contact energy) are small in comparison to the internal energy ensuring that the deformations of the DN30-X package are not underestimated. The resulting energy ratio for this drop test simulation ranges from 0.999639 to 1.0, indicating very good energy conservation.

A more detailed plot of the contact energy of the automatic single surface contact in the FEM model is shown figure 2-45. Throughout the simulation, the contact energy remains below the frictional energy. In addition, the dissipation of frictional energy only increases or remains constant, but never decreases. Hence, the chosen contact stiffness results in a physically correct simulation and reliable deformation results.

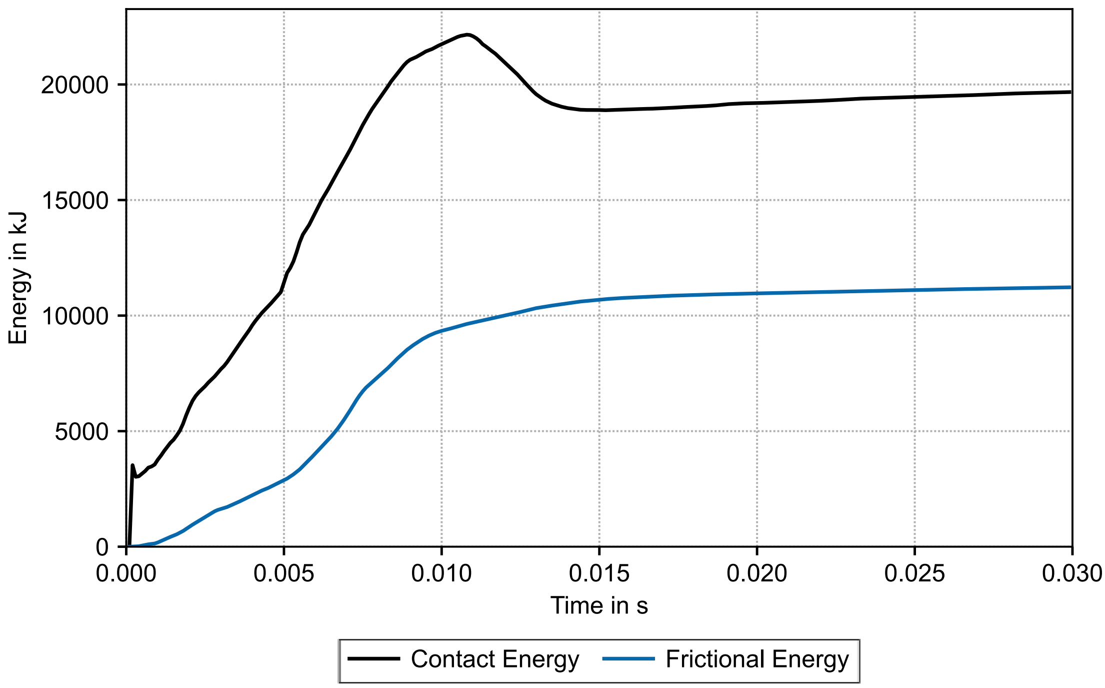


**Figure 2-45 Flat drop onto the feet from a height of 10.2 m – Contact energy of the automatic single surface contact**

Figure 2-46 compares the hourglass energy to the internal energy. The hourglass energy remains well below the upper limit of 10 % of the internal energy without any sudden increases.

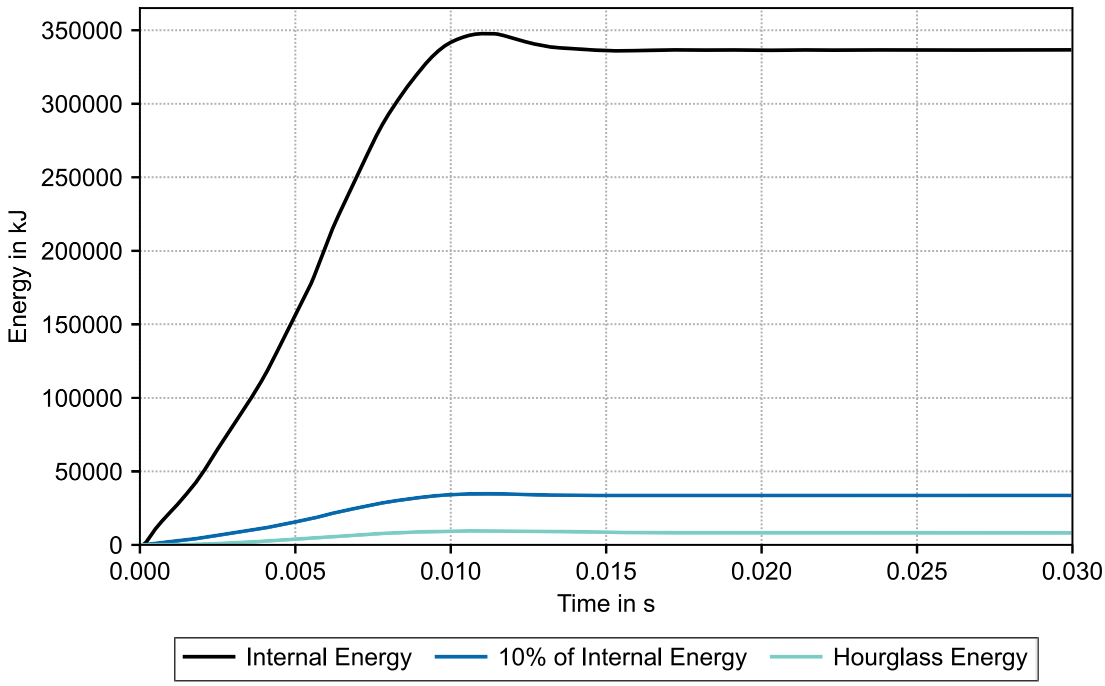


**Figure 2-46 Flat drop onto the feet from a height of 10.2 m – Hourglass energy**

2.2.6.2.6.1.2 Deformations

2.2.6.2.6.1.2.1 DN30 PSP and Cylinder Pressure Envelope

Figure 2-47 shows the state of maximal deformation for the DN30-X package during the flat drop test onto the feet. The feet undergo severe buckling and are pushed into the outer shell of the DN30 PSP. The largest equivalent plastic strain in the outer shell is 29 % and occurs in the area where the feet are pushed into the outer shell. At the feet, the plastic deformations are far above the elongation at fracture of material 1.4301 of 45 % and, thus, cracks at the feet are to be expected. Nevertheless, the occurring plastic deformations of the inner steel parts remain below 10 %. Furthermore, the rotation preventing, valve and plug protecting device are nearly undamaged after the flat drop test onto the feet and no contact at the valve is detected, except for its initial point of attachment.

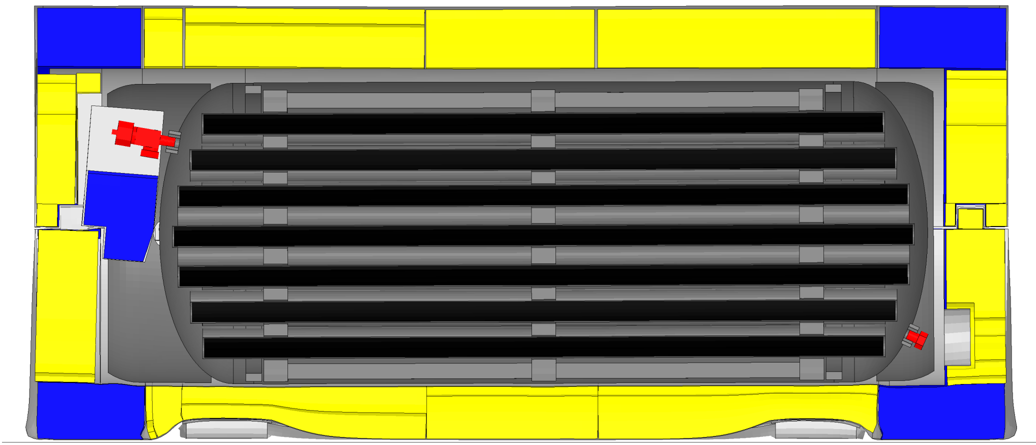

**Figure 2-47 Flat drop onto the feet from a height of 10.2 m – State with the maximal deformation of the DN30-X and DN30 package**

The flat drop test onto the feet is used to determine the permanent radial reduction in the wall thickness of the DN30 PSP, which is required as input for the criticality safety analysis in section 2.6. The remaining wall thickness of the DN30 PSP is evaluated by measuring the distance between the inner and outer shell of the DN30 PSP in the center between the two feet. As can be seen in figure 2-47, this provides a good estimate of the closest radial approach of two neighboring DN30-X packages. Including the sheet thicknesses of the inner and outer shell, a minimal permanent wall thickness of the DN30 PSP of 134 mm is obtained.

To show the effectiveness of the DN30 PSP in preventing damage to the 30B-X cylinder, the energy absorption behavior during the flat drop test onto the feet is investigated. Figure 2-48 shows the distribution of the kinetic energy, the totally absorbed energy as well as the energy absorbed by the DN30 PSP for the DN30-X package.

This comparison proves that the DN30 PSP absorbs about 97 % of the kinetic energy during the flat drop test onto the feet. Hence only a small energy fraction needs to be absorbed by the 30B-X cylinder. In reality, this energy fraction is even smaller because of the $UF_6$ content surrounding the internal CCS of the 30B-X cylinder. The energy absorption capabilities of the content are not considered in the simulation as the content is only implicitly incorporated in the FEM model of the DN30-X by using mass elements.

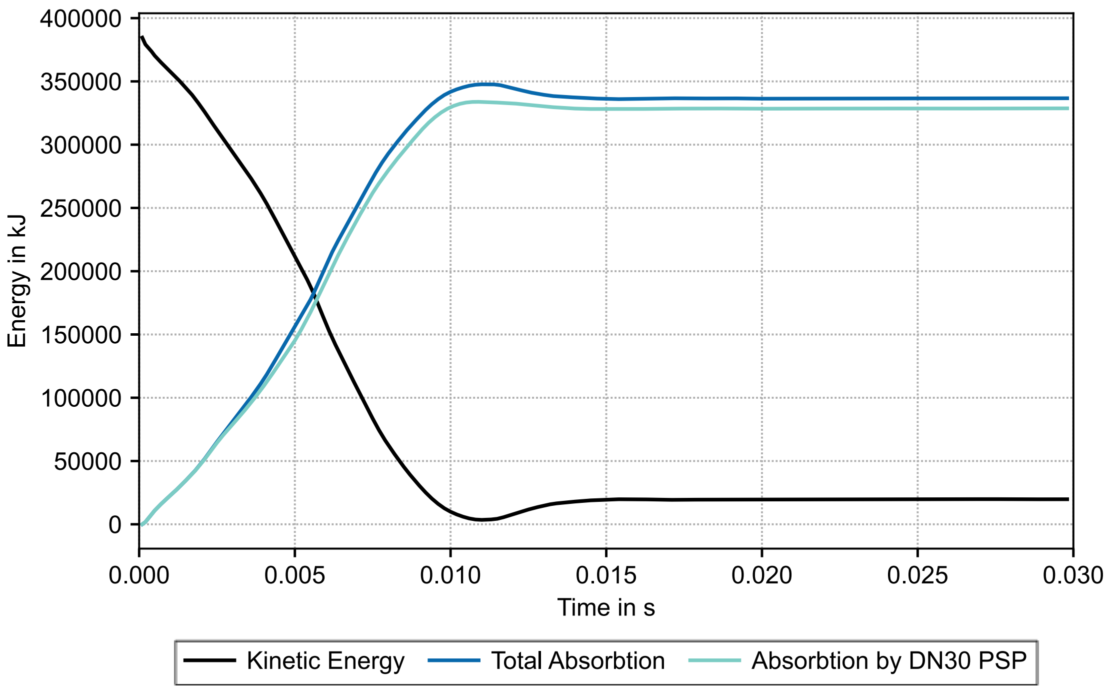


**Figure 2-48 Flat drop onto the feet from a height of 10.2 m – Comparison of energy absorption of the DN30 PSP in case of the DN30-X and the DN30 package**

Finally, explicit values of the maximal equivalent plastic strains are evaluated for the foam and selected steel parts of the DN30 PSP as well as the 30B-X cylinder pressure envelope. The results are listed in table 2-18. Table 2-18 also includes the corresponding values of the densification strains and elongations at fracture, which are taken from [DNT 2019] for the DN30 PSP (foam RTS 120 / RTS 320 and stainless steel 1.4301) and listed in table 2-8 for the 30B-X and standard 30B cylinder pressure envelope.

**Table 2-18 Flat drop onto the feet from a height of 10.2 m – Plastic deformations of foam and selected steel parts of the DN30 PSP and the cylinder pressure envelope**

| Part | EPS1) | DS / EF2) in % |
|---|---|---|
| DN30 PSP | | |
| RTS 120 | 62.8 | 89 |
| RTS 320 | 47.6 | 82 |
| Valve protecting device | 1.8 | 45 |
| Plug protecting device | 0 | 45 |
| Inner front plate (top half) | 0.2 | 45 |
| Inner front plate (bottom half) | 0 | 45 |
| Inner back plate (top half) | 0 | 45 |
| Inner back plate (bottom half) | 0.2 | 45 |
| 30B-X cylinder | | |
| Pressure envelope | 2.4 | 22 |

1) Equivalent plastic strain
2) Densification strain / elongation at fracture

The maximal equivalent plastic strains of relevant parts of the DN30 PSP are generally non-critical and far below their allowable values. As shown in figure 2-49, the inner shells of the DN30 PSP are only very locally deformed while most of the inner shells hardly experience any deformations.

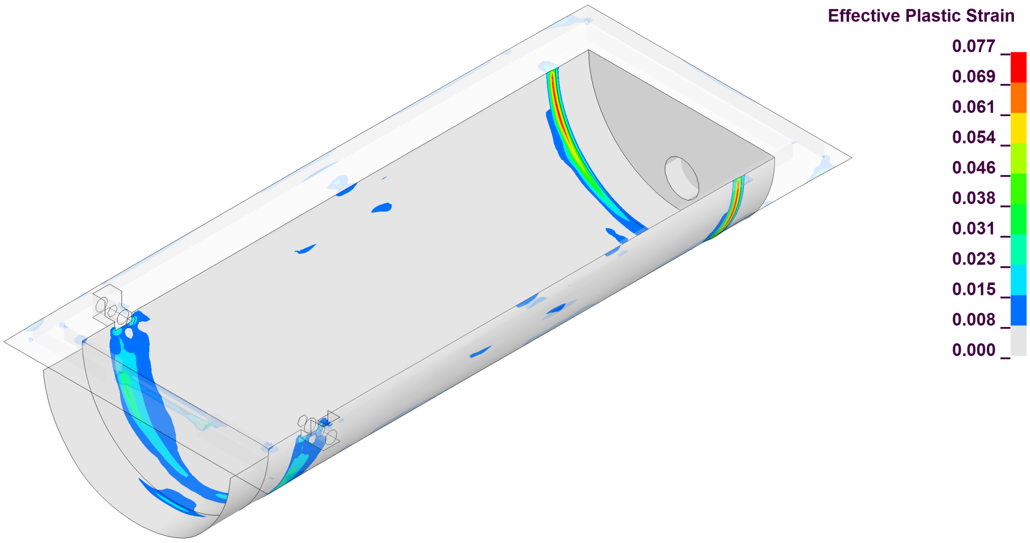


**Figure 2-49 Flat drop onto the feet from a height of 10.2 m – Equivalent plastic strain at the inner shell**

In case of the cylinder pressure envelope, the maximal equivalent plastic strain of 2.4 % is reached at the bottom of the cylinder, where the three lattice holders impact the cylinder shell (see figure 2-50). This was to be expected as the content is only implicitly incorporated in the FEM model of the DN30-X, which results in an undamped and very local load introduction through the lattice holders. In reality, the lattice holders would be slowed-down while moving through the $UF_6$ content, and the weight of the CCS would be distributed across a larger area of the cylinder shell. Nevertheless, a maximal plastic strain of 2.4 % is significantly below the elongation at fracture of the cylinder shell material so that rupture of the containment system can safely be excluded.

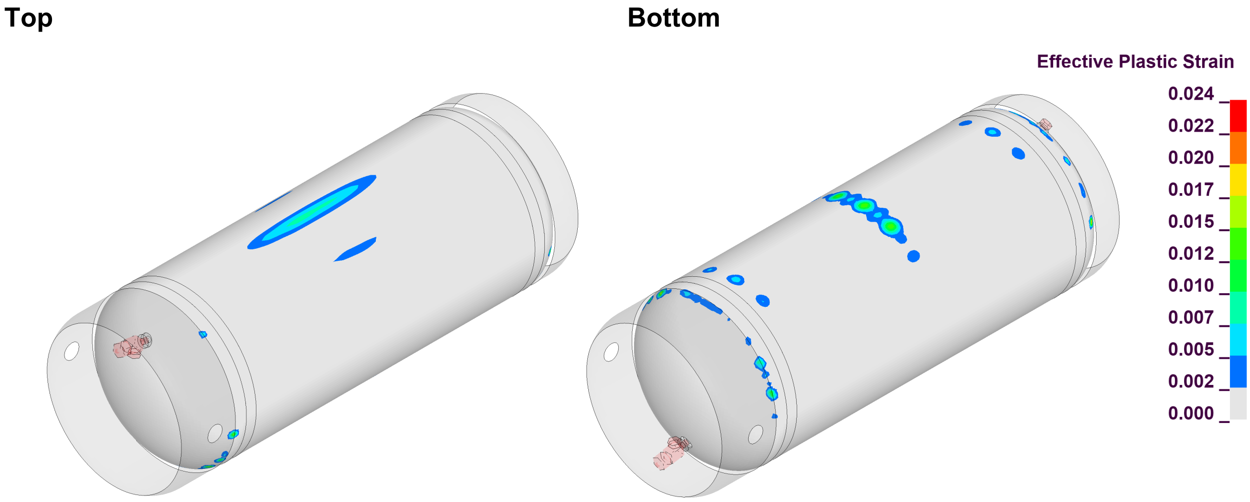


**Figure 2-50 Flat drop onto the feet from a height of 10.2 m – Equivalent plastic strain at the cylinder pressure envelope**

2.2.6.2.6.1.2.2 Criticality Control System of the 30B-X Cylinder

The deformations of the CCS restraint and the lattice holders are shown in figure 2-51. In this horizontal drop test scenario, there is no direct load acting on the CCS restraint. The CCS restraint mainly avoids the ovalization of the 30B-X cylinder by providing some radial support. However, this does not result in permanent deformations of the CCS restraint. Similarly, the longitudinal stiffeners experience no direct load resulting in only small plastic deformations up to 1 %. Noticeable plastic deformations up to 3.1 % only occur at the lower half of the lattice holders. With such small deformations, the relative dislocations between the CCRs can still be expected to be small as most of the pipe clamps of the lattice holders hardly experience any plastic deformations. This will be investigated in more detail at the end of this section.

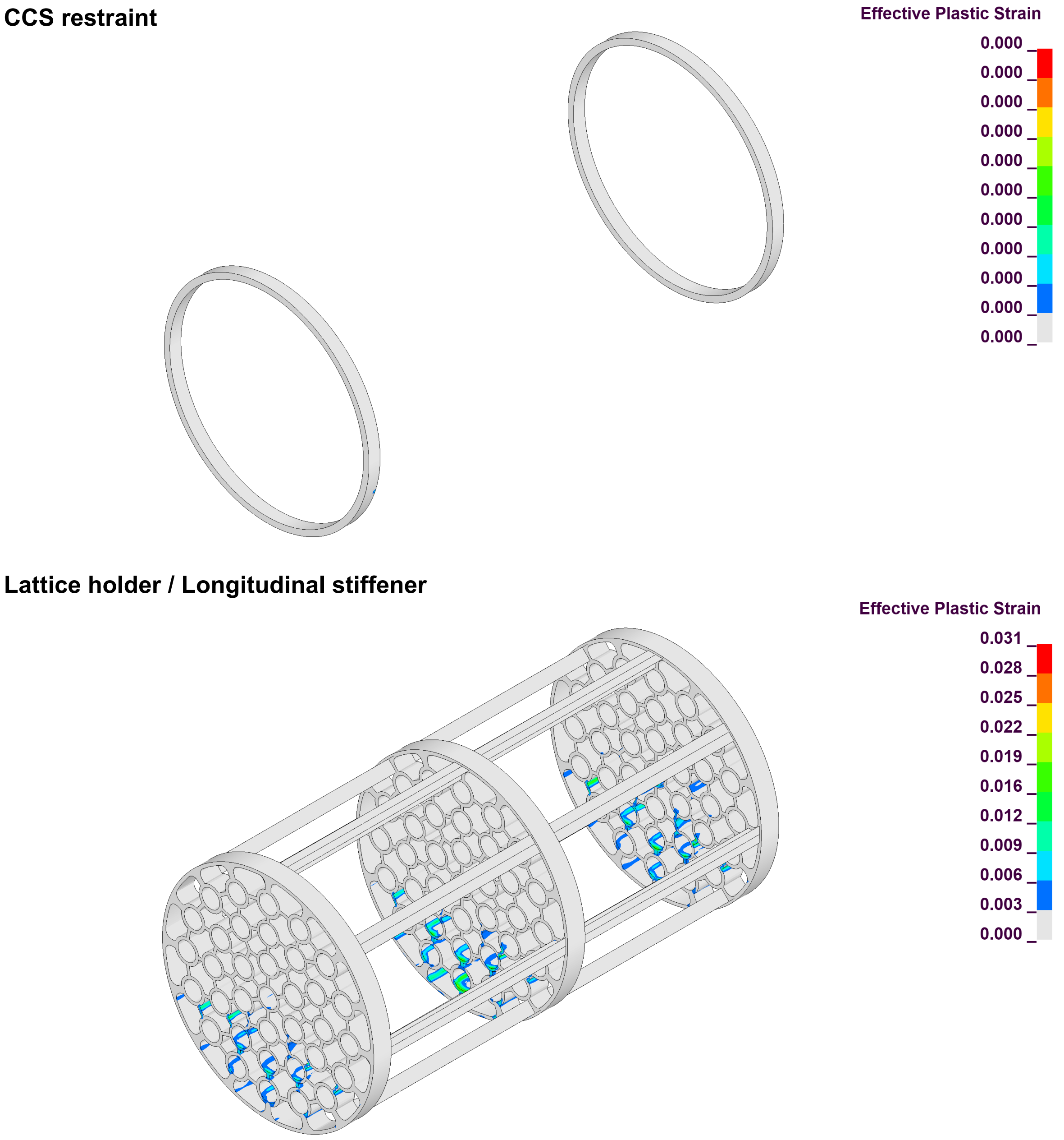


**Figure 2-51 Flat drop onto the feet from a height of 10.2 m – Equivalent plastic strain at the CCS restraint and the lattice holders of the CCS**

Figure 2-52 shows a bottom view of the CCRs and the corresponding distribution of plastic strains. Even though the CCRs have no containment function and failure of a CCR would only lead to a contamination of the content with neutron absorbing material, the same acceptance criteria as for the pressure envelope of the 30B-X cylinder defined in section 2.1.2.2.1 is applied to the CCRs. However, the plastic deformations with maximally 1.4 % are irrelevant in this regard. Moreover, only the lowest CCR in the outer and middle ring experience noticeable deformations, which is due to the deformations of the central lattice holder in these areas. For all other CCRs, only negligible plastic deformations below 0.1 % occur.

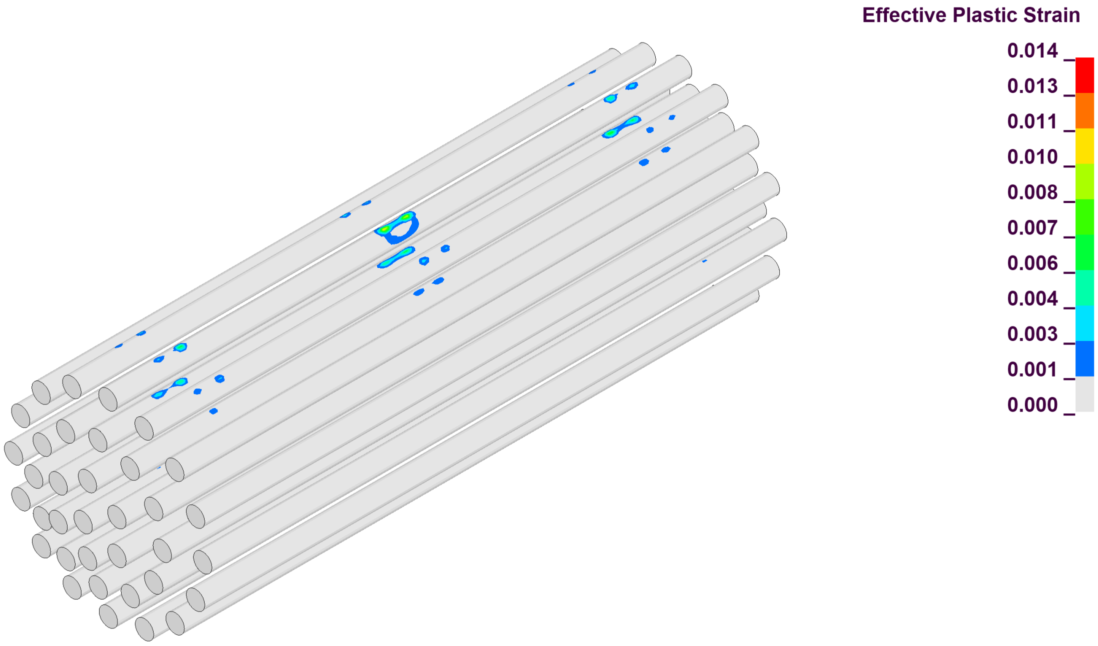


**Figure 2-52 Flat drop onto the feet from a height of 10.2 m – Equivalent plastic strain at the CCRs of the CCS**

Regarding the acceptance criteria for the CCS defined in section 2.1.2.2.1, the relative dislocations between the CCRs and also the movement of the entire CCS relative to the 30B-X cylinder shell have to be evaluated. Considering the plastic deformations at the lattice holders are limited to their lower half and only the two lowest CCRs of the outer and middle ring experience noticeable plastic deformations, the investigation of permanent relative dislocations between the CCRs can be limited to those two CCRs. All other relative dislocations between the CCRs are momentary oscillations during the drop test that are solely due to elastic deformations of the pipes.

The relative dislocations are determined by measuring the distance between the inner and middle CCR as well as the middle and outer CCR at four different points, respectively. The chosen measurement points are shown in figure 2-53. The measurement points have been chosen such that the distances to the neighboring lattice holders are maximal, potentially resulting in the largest relative dislocations.

During the drop test simulation, the CCRs oscillate making it difficult to determine the permanent relative dislocation between the CCRs. Therefore, the measured distances are filtered by an SAE low-pass filter using a cut-off frequency of 60 Hz. As can be seen in figure 2-54, using this cut-off frequency still maintains the fundamental movement of the CCRs without leaving to many oscillations in the data. In the second half of the simulation, the distance change between the inner and middle CCR reaches a relatively constant value. The permanent relative dislocation is then determined by calculating the average distance change in that time interval. The

corresponding average values at each measurement point are shown by dashed lines of the same color in figure 2-54. Hence, the maximal permanent relative dislocation between the inner and middle ring is -0.31 mm.

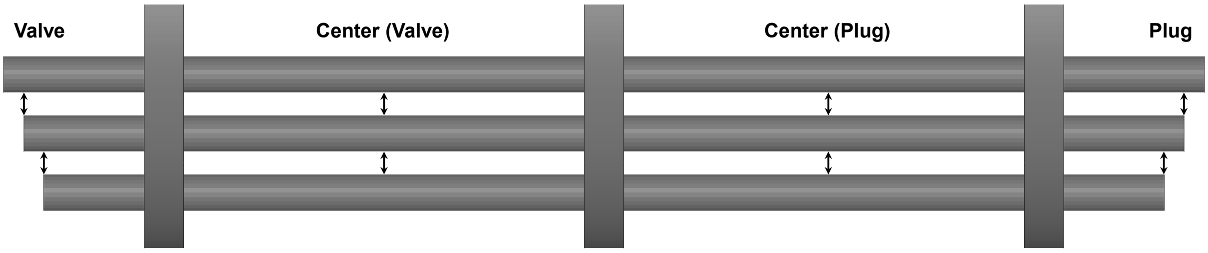


**Figure 2-53 Flat drop onto the feet from a height of 10.2 m – Measurement points for the evaluation of relative dislocations of CCRs**

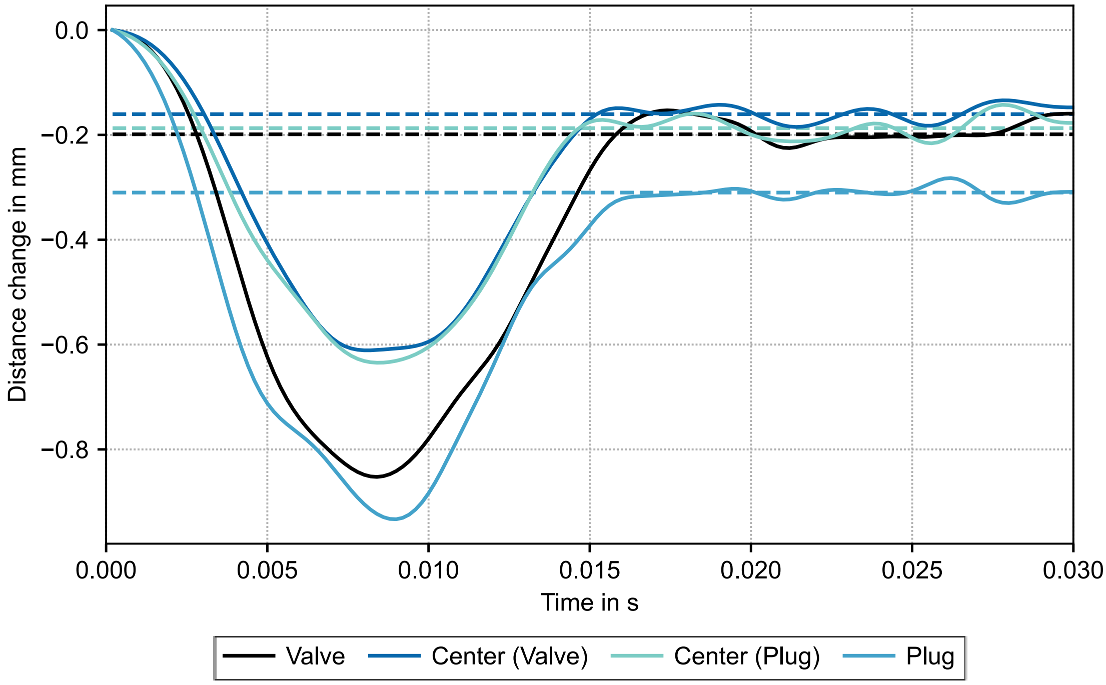


**Figure 2-54 Flat drop onto the feet from a height of 10.2 m – Relative dislocation between the inner and middle ring of the CCS**

Applying the same procedure to the middle and outer ring results in a maximal permanent relative dislocation of -0.75 mm (see figure 2-55). In summary, the determined permanent relative dislocations allow for the following conclusion:

- The permanent relative dislocations of the CCRs after the flat drop test onto the feet simulating HAC are all negative, meaning the CCRs are moved closer together.
- Hence, the permanent relative dislocations are mainly determined by the deformations of the lattice holders.
- Even though the horizontal drop test orientation potentially puts the highest stresses on the CCRs with regard to bending, there are no permanent relative dislocations of the CCRs that refer to such deformations of the CCRs.

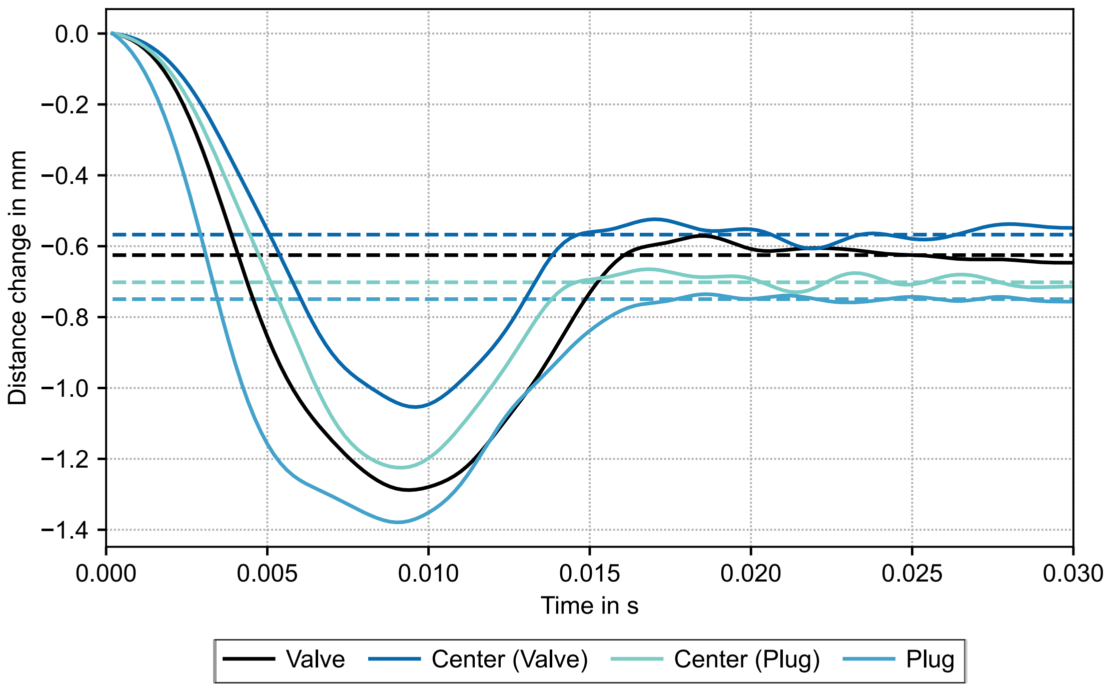


**Figure 2-55 Flat drop onto the feet from a height of 10.2 m – Relative dislocation between the middle and outer ring of the CCS**

For the flat drop onto the feet, there are only negligible deformations that would increase the axial movability of the entire CCS within the 30B-X cylinder. Hence, the axial movability of the entire CCS is still determined by the initial gap of 5 mm that exists between the lattice holders and the CCS restraints of the 30B-X cylinder.

The radial movability of the entire CCS within the cylinder is evaluated by measuring the radial gap between the central lattice holder and the cylinder shell as the maximal plastic deformations of the lattice holders and the cylinder shell occur in this area. The radial gap is measured at the top and bottom of the central lattice holder. Similar to the procedure for the relative dislocations of the CCRs, an SAE low-pass filter with a cut-off frequency of 60 Hz is applied to the measured gaps to compensate for the oscillations of the cylinder shell during the drop test simulation. The filtered measurements at the top and bottom of the central lattice holder are shown in figure 2-56.

At the bottom, the initial gap is closed during the simulation, which increases the radial gap at the top by maximally 12 mm. However, this is mainly due to the elastic ovalization of the cylinder shell and, thus, does not represent a permanent state. Towards the end of the drop test simulation, the CCS is almost back in its initial position, but the permanent deformations of the lattice holders and the cylinder shell now allow for an increased radial movability of the CCS within the 30B-X cylinder in comparison to the undeformed initial state. The point in time, when the increase in the radial gap is equal for the top and bottom measurement point, is used to estimate the increase in radial movability of the CCS from the center of the 30B-X cylinder. This point is annotated in figure 2-56 and the corresponding value is 2.1 mm.

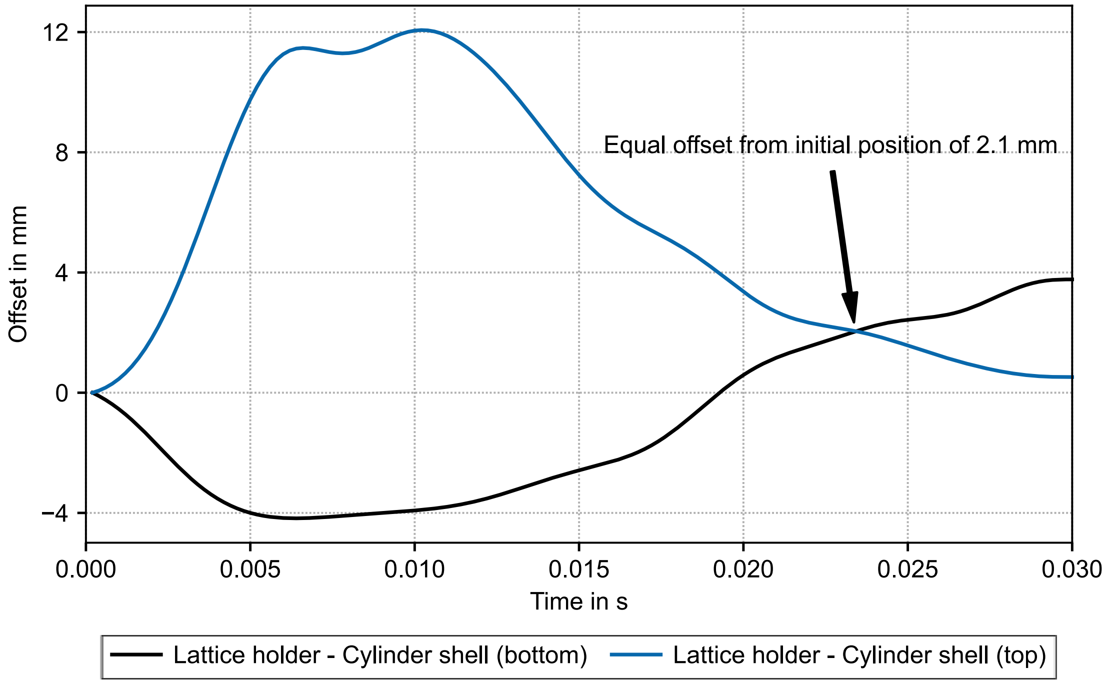


**Figure 2-56 Flat drop onto the feet from a height of 10.2 m – Radial offset of CCS within the 30B-X cylinder**

2.2.6.2.6.1.3 Decelerations

Figure 2-57 and figure 2-58 show the low-pass filtered decelerations for the flat drop test onto the feet in the valve area. Since there is no data for comparison available, results for only two cut off frequencies of 20 Hz and 584 Hz are shown.

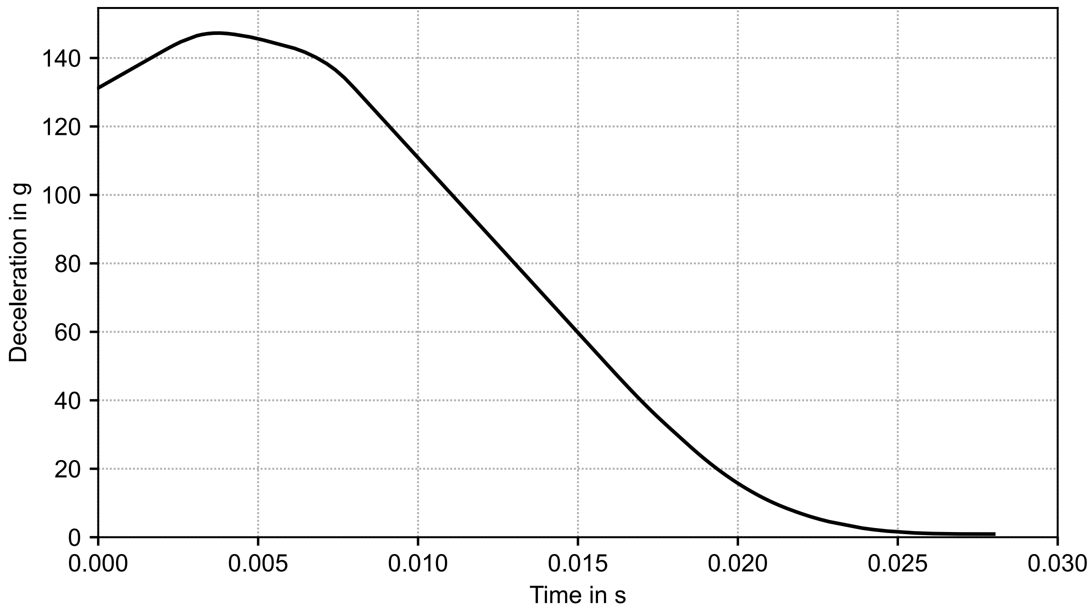


**Figure 2-57 Flat drop onto the feet from a height of 10.2 m – Deceleration in the plug area – Low-pass filtered (SAE, 20 Hz cut-off)**

At a cut-off frequency of 20 Hz, the deceleration is on the same level when compared to the deceleration for the DN30 package during the flat drop test onto the valve side (see figure 2-35). Therefore, the level of deceleration for this drop test is judged to be admissible.

At a cut-off frequency of 584 Hz, high deceleration peaks up to 590 g occur. Similar to the flat drop test onto the valve side, these peaks result from the interaction between the CCS and the 30B-X cylinder. However, since the cylinder shell and not the CCS restraint is involved this time, the contact is not as stiff as in case of the flat drop test onto the valve side, which results in peaks that are not that high. Nevertheless, such high deceleration peaks are not expected to occur under real conditions when the content significantly impedes the free motion of the internal CCS.

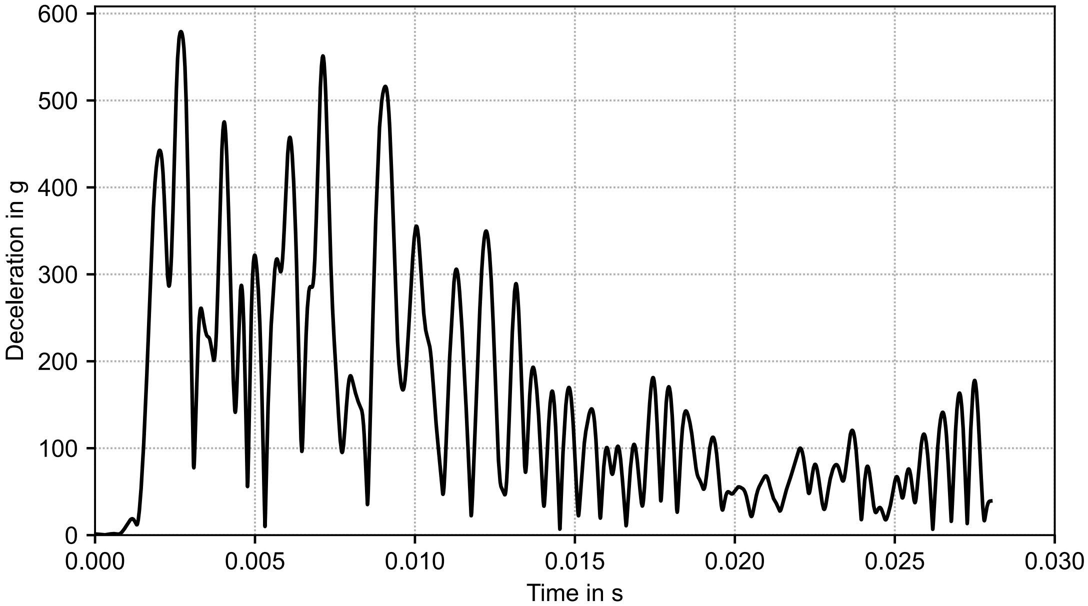


**Figure 2-58 Flat drop onto the feet from a height of 10.2 m – Deceleration in the plug area – Low-pass filtered (SAE, 584 Hz cut-off)**

2.2.6.2.6.1.4 Summary

The DN30-X package design ensures that after the flat drop test onto the feet simulating HAC, all acceptance criteria as defined in section 2.1.2.2.1 are met:

- There is no failure of the DN30 PSP closure system.
- There is no physical contact between the valve of the 30B-X cylinder and any other component of the packaging other than its original point of attachment.
- There is no physical contact between the plug of the 30B-X cylinder and any other component of the packaging other than its original point of attachment.
- There is no rupture of the 30B-X cylinder containment system.
- There is no failure of the 30B-X cylinder confinement system:
  - The relative dislocation of the CCRs remains below 5 mm.
  - The increase in radial movability of the entire CCS out of the center of the 30B-X cylinder remains below 3 mm.
  - The increase in axial movability of the entire CCS out of the center of the 30B-X cylinder remains below 7 mm.
  - There is no failure of the lattice holders.
  - There is no rupture of the CCRs.

#### 2.2.6.2.6.2 Corner Drop onto the Plug Side – Drop Test Sequence 2

The in-depth comparison of the deformations of the DN30-X and the DN30 package for the corner drop onto the valve side proves that the impact the 30B-X cylinder has on the DN30 PSP is comparable to the impact the 30B cylinder has on the DN30 PSP. Considering the following similarities between the design of the DN30-X and the DN30 package, this finding can be transferred to the corner drop onto the plug side:

- The shell thickness on the valve and the plug side of the outer and the inner shell of the DN30 PSP is identical, respectively.
- A similar amount of foam of the same type fills the space between the outer and the inner shell of the DN30 PSP.
- The gross weight, outer dimensions and materials of the 30B-X are identical to the standard 30B cylinder.
- The valve and the plug of the 30B-X are identical to the standard 30B cylinder.

These similarities of the DN30-X and the DN30 package cover the relevant aspects that contribute to the structural response of the packages and, accordingly, there is no reason to expect deformations of the DN30-X that differ from the deformations of the DN30 package by more than 5 %. Performing an in-depth analysis of the corner drop onto the plug side therefore does not provide any gain in safety for the DN30-X package design.

#### 2.2.6.2.6.3 Flat Drop onto the Plug Side

In the analysis of the DN30 package in [DNT 2019], it was already pointed out that the response during the flat drop onto the valve side and the flat drop onto the plug side is very similar. This is solely attributed to the similar design of the valve and plug side of the DN30 PSP and, therefore, is independent of the type of cylinder being transported in the DN30 PSP. Consequently, an in-depth analysis of the flat drop onto the plug side with the DN30-X package is not required.

#### 2.2.6.2.6.4 Flat drop onto the Closure System – Drop Test Sequence 4

The flat drop onto the closure system was performed in the safety analysis for the DN30 package in [DNT 2019] to test the performance of the DN30 PSPs closure system and rotation preventing device:

- During the 9 m free drop test, the closure system on both sides of the DN30 PSP experiences tensile loads. The deceleration of the loaded 30B cylinder results into forces acting on the inside of the top and bottom half of the DN30 PSP that are comparable to an inner pressure.
- During the puncture test with the impact of the bar on the central closing device, there are high transversal loads on the closure system of the DN30 PSP.
- Maximal loads are expected on the rotation preventing device, because in this drop test scenario, the moment caused by the eccentric loading of the 30B cylinder is maximal.

The performance of the DN30 PSP with regard to these aspects mostly depends on the gross weight of the 30B cylinder and the stiffness of its shells and skirts. Since both are identical for the standard 30B and the 30B-X cylinder, the resulting deformations of the DN30 PSP can be expected to be almost identical for the flat drop onto the closure system with either cylinder. Hence, without a detailed analysis of the drop test flat onto the closure system for the DN30-X package, its design ensures that after the tests simulating HAC:

- There is no failure of the DN30 PSP closure system.
- There is no physical contact between the valve of the 30B-X cylinder and any other component of the packaging other than its original point of attachment.
- There is no physical contact between the plug of the 30B-X cylinder and any other component of the packaging other than its original point of attachment.
- There is no rupture of the 30B-X cylinder containment system.
- There is no failure of the 30B-X cylinder confinement system:
  - The relative dislocation of the CCRs remains below 5 mm.
  - The increase in radial movability of the entire CCS out of the center of the 30B-X cylinder remains below 3 mm.
  - The increase in axial movability of the entire CCS out of the center of the 30B-X cylinder remains below 7 mm.
  - There is no failure of the lattice holders.
  - There is no rupture of the CCRs.
- The extent of the rotation of the 30B-X cylinder relative to the DN30 PSP does not affect the function of the valve protecting device or the plug protecting device.
- The leakage rate of the containment does not exceed the limit specified in section 2.4.

2.2.6.2.6.5 Flat Drop onto the Top Half – Drop Test Sequence 8

The drop test sequence flat onto the top of the DN30 PSP was performed in the safety analysis for the DN30 package in [DNT 2019] because of its relevance with regard to the determination of the increase in the maximal dose rate after the tests simulating NCT. Furthermore, the simulation provided information about the extent of the reduction of the thickness of the DN30 PSP for the thermal analysis of the DN30 package.

For the drop test flat onto the top of the DN30 PSP, the following applies with regard to the deformations of the 30B-X cylinder pressure envelope and the CCS:

- The top of the DN30 PSP consists of thin stainless-steel shells and soft foam that easily deform and, thus, absorb a significant amount of kinetic energy during a drop test flat onto the top. This reduces the impact on the 30B-X cylinder shells and the CCS in comparison to the drop test onto the closure system in Sequence 4 or a drop test flat onto the feet in where either the closure system or the feet increases the stiffness in the impacted area of the DN30 PSP.
- The deformations of the 30B-X cylinder can be expected to be very similar to the standard 30B cylinder, even though very different approaches have been used to model the content:

- As the content of the 30B cylinder was still located in the lower half of the cylinder for this drop test sequence, the 30B cylinder shells were not supported by the weight of the content near the area of impact (see [DNT 2019]).
- This situation is very similar to the FEM model of the 30B-X cylinder, where the content is only implicitly incorporated by increasing the weight of the CCR surfaces. If anything, the lattice holders of the CCS improve the structural integrity of the 30B-X cylinder shells providing additional margins of safety.

Hence, the drop test of the DN30-X package onto the top of the DN30 PSP is covered by the analysis for the DN30 package in [DNT 2019] and the design of DN30-X package ensures that after the tests simulating HAC:

- There is no failure of the DN30 PSP closure system.
- There is no physical contact between the valve of the 30B-X cylinder and any other component of the packaging other than its original point of attachment.
- There is no physical contact between the plug of the 30B-X cylinder and any other component of the packaging other than its original point of attachment.
- There is no rupture of the 30B-X cylinder containment system.
- There is no failure of the 30B-X cylinder confinement system:
  - The relative dislocation of the CCRs remains below 5 mm.
  - The increase in radial movability of the entire CCS out of the center of the 30B-X cylinder remains below 3 mm.
  - The increase in axial movability of the entire CCS out of the center of the 30B-X cylinder remains below 7 mm.
  - There is no failure of the lattice holders.
  - There is no rupture of the CCRs.
- The extent of the reduction of the wall thickness of the DN30 PSP after NCT amounts to maximally 4 mm and, thus, is such that the increase of the dose rate does not exceed the limit specified in section 2.5.1.
- The extent of the reduction of the thickness of the DN30 PSP after HAC is such that the thermal protection properties of the DN30 PSP are still sufficient to limit the temperature increase in the thermal tests to the limits specified in section 2.3.1.



#### 2.2.6.2.6.6 Slap-down Drop onto the Feet – Drop Test Sequence 5

The slap-down drop onto the feet of the DN30 PSP was performed in the safety analysis for the DN30 package in [DNT 2019] because this is the only drop test sequence that causes a significant load for the pins of the closure devices and, therefore, was used as the basis for the detailed stress analysis of the closure devices. Two subsequent impacts are part of this drop test:

- The primary impact onto the plug side of the DN30 PSP causes less deformation at the plug side compared to a drop test onto the corner on the plug side of the DN30 PSP because only a fraction of the drop test energy is absorbed during this impact.
- However, a heavy secondary impact onto the feet on the valve side of the DN30 PSP occurs because the impact velocity at that point is higher than in a flat drop.

- The impact point for the puncture test is at the center of the outer shell of the top half of the DN30 PSP because there are no structural supports like the feet of the DN30 PSP. An angle of 25° between the axis of the bar and the normal of the outer DN30 PSP shell has been chosen because this angle is the most critical one with respect to a penetration of the outer shell.

The performance of the DN30 PSP with regard to these aspects mostly depends on the gross weight of the 30B cylinder and the stiffness of its shells and skirts. Since both are identical for the standard 30B and the 30B-X cylinder, the resulting deformations of the DN30 PSP can be expected to be almost identical for the slap-down drop onto the feet with either cylinder. Furthermore, the flat drop test onto the feet of the DN30 PSP is more severe for the internal CCS of the 30B-X cylinder. During the slap-down drop onto the feet, the gap between the cylinder shell and the lattice holders gets closed after the primary impact onto the corner on the plug side of the DN30 PSP. This significantly reduces the peak load for the lattice holders in comparison to the flat drop test onto the feet and increases the energy dissipation because of friction between the lattice holders and the cylinder shell.

Hence, the analysis of the slap-down drop onto the feet of the DN30 PSP for the DN30-X package is covered by the analysis for the DN30 package in [DNT 2019] and the design of DN30-X package ensures that after this test simulating HAC:

- There is no failure of the DN30 PSP closure system.
- There is no physical contact between the valve of the 30B-X cylinder and any other component of the packaging other than its original point of attachment.
- There is no physical contact between the plug of the 30B-X cylinder and any other component of the packaging other than its original point of attachment.
- There is no rupture of the 30B-X cylinder containment system.
- There is no failure of the 30B-X cylinder confinement system:
  - The relative dislocation of the CCRs remains below 5 mm.
  - The increase in radial movability of the entire CCS out of the center of the 30B-X cylinder remains below 3 mm.
  - The increase in axial movability of the entire CCS out of the center of the 30B-X cylinder remains below 7 mm.
  - There is no failure of the lattice holders.
  - There is no rupture of the CCRs.

#### 2.2.6.2.7 Static Structural Analysis of the Fillet Weld between the CCS Restraint and the 30B-X Cylinder Shell

In this section, it is proven that the fillet weld between the CCS restraints and the cylinder shell of the 30B-X cylinder is dimensioned appropriately for the maximal loads to be expected. These maximal loads occur during the flat drop test onto the valve side, which has been investigated in section 2.2.6.2.5.2. In this drop test orientation, the CCS restraint has to withstand the highest inertial forces resulting from the combined weight of the CCS and the content. As soon as an inclined or even horizontal drop test orientation would be considered, this inertial force would reduce with increasing drop angle towards the vertical.

According to the drawings in Appendix 1.4.1A (Drawings 30B-X Cylinder), the fillet weld has an effective thickness of 10 mm. As shown in figure 2-59, the root and toes of the fillet weld are rounded by a 1 mm radius. Between the backing bar and the 30B-X cylinder shell there is a 0.1 mm gap, which is based on the fact that the backing bar is fitted to the cylinder shell.

Because of the rotational symmetry of loading during the flat drop test into the valve side, the analysis is based on a 10°-section of the 30B-X cylinder. The dimensioning of the fillet weld is then evaluated based on notch stresses that are determined using the guideline [FKM 2012]. Therefore, a linear-elastic static structural analysis is performed using [ANSYS] Workbench. Performing a static analysis on the basis of the maximally occurring load, heavily overestimates the energy that is applied to the fillet weld, as this is actually a highly dynamic short-term load. Hence, the chosen approach to prove the appropriate dimensioning of the fillet weld is very conservative.

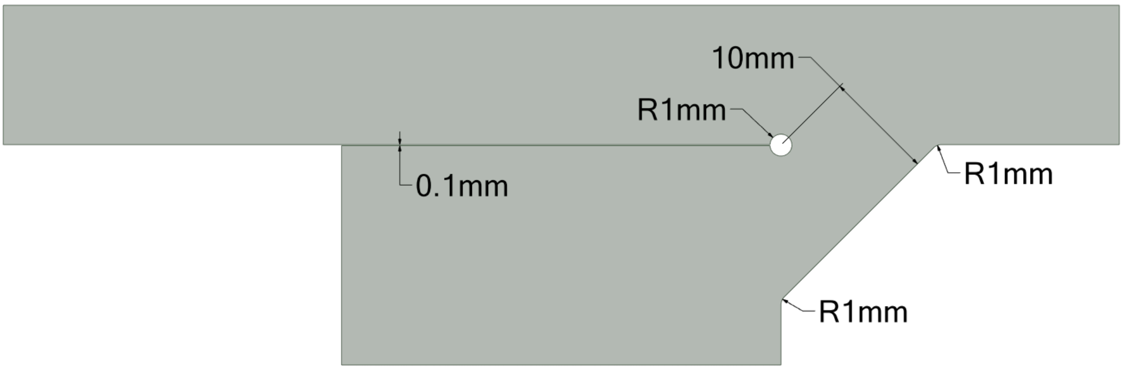


**Figure 2-59 Analysis of CCS restraint fillet weld – Cross section of the fillet weld geometry**

### 2.2.6.2.7.1 Mesh generation

The mesh of the 10 °-sector of the 30B-X cylinder is shown in figure 2-60. For the discretization of the geometry, tetrahedral elements with quadratic shape functions are applied. In these areas, the mesh size is set to 0.1 mm to achieve the required mesh resolution for the evaluation of notch stresses. Some quality statistics about the generated mesh are provided in table 2-19.

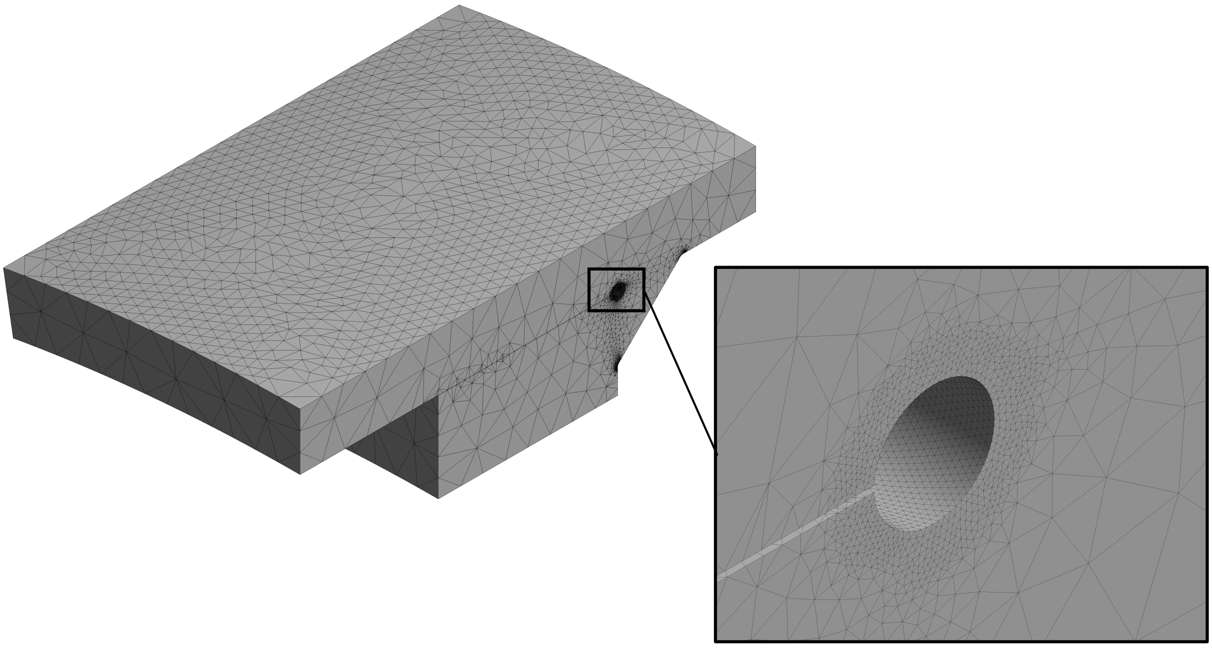

**Figure 2-60 Analysis of CCS restraint fillet weld – Generated mesh**

**Table 2-19 Analysis of CCS restraint fillet weld – Mesh statistics**

| Parameter | Minimum | Maximum | Average | Standard deviation |
|---|---|---|---|---|
| Quality | 0.117 | 1.0 | 0.71 | 0.139 |
| Aspect ratio | 1.16 | 13.5 | 2.32 | 0.714 |
| Jacobian ratio | 1.00 | 1.41 | 1.01 | 0.03 |
| Maximal corner angle in ° | 70.8 | 162.4 | 104.8 | 14.51 |
| Number of Elements | | | 110226 | |

2.2.6.2.7.2 Boundary conditions

The boundary conditions that are applied to the 10°-sector of the 30B-X cylinder consist of prescribed forces at the cross sections of the 30B-X cylinder shell and the CCS restraint as well as fixed displacements and rotations. A graphical presentation of the applied boundary conditions is shown in figure 2-61 and the corresponding values are listed in table 2-20.

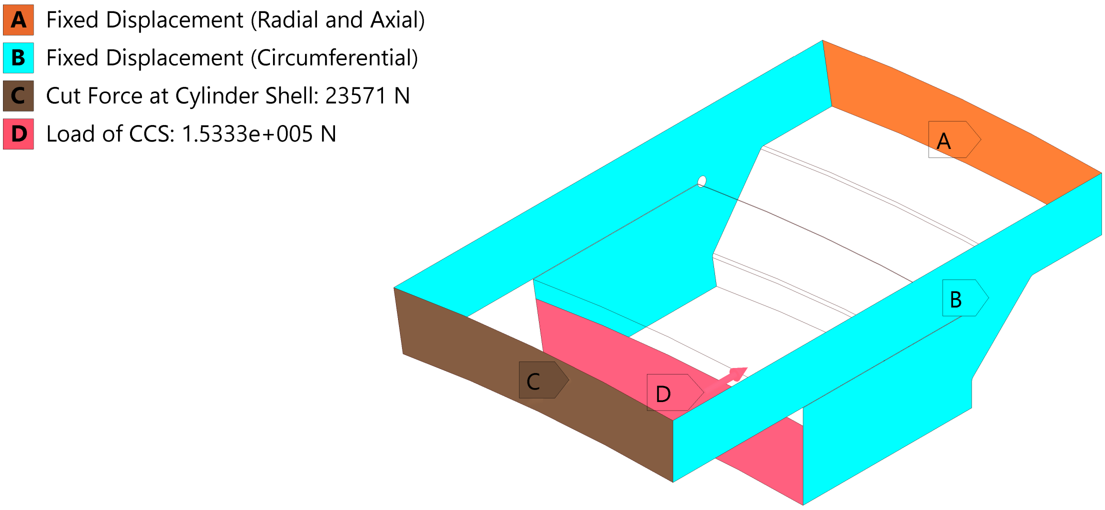


**Figure 2-61 Analysis of CCS restraint fillet weld – Boundary conditions**

**Table 2-20 Analysis of CCS restraint fillet weld – Boundary conditions**

| Surface | Displacements in mm | | | Rotations in ° | | | $F_z$ in kN |
|---|---|---|---|---|---|---|---|
| | $u_r$ | $u_\varphi$ | $u_z$ | $R_r$ | $R_\varphi$ | $R_z$ | |
| A | 0.0 | - | 0.0 | 0.0 | 0.0 | - | - |
| B | - | 0.0 | - | 0.0 | - | 0.0 | - |
| C | - | - | - | - | - | - | -23.571 |
| D | - | - | - | - | - | - | 153.33 |

The prescribed displacements and rotations at cross section A in figure 2-61 represent the interaction with the DN30 PSP. The skirts of the 30B-X cylinder impact the inner front plate of the DN30 PSP and, hence, suppress further axial displacements $u_z$ of the 30B-X cylinder. For the same reason, the radial displacements $u_r$ and rotations $R_r$ and $R_\varphi$ are fixed at cross section A. The prescribed displacements and rotations at cross section B are used to force axial symmetry of the calculation model.

The values of the applied forces are obtained by determining the maximal contact force between the lattice holder and CCS restraint on the valve side during the vertical drop test onto the valve side analyzed in section 2.2.6.2.5.2. The evaluation of the contact force for the entire CCS restraint on the valve side is shown in figure 2-42 and gives a maximum of $F_z = 5520\ \mathrm{kN}$. The projection onto the modelled 10°-sector of the 30B-X cylinder leads to the value listed in table 2-20. Afterwards, the section force at cross section C is evaluated at the same time step and is also projected onto the 10°-sector.

### 2.2.6.2.7.3 Material Models and Parameters

The analysis of the fillet weld between the CCS restraint and the 30B-X cylinder shell in accordance with [FKM 2012] requires two different material models. The evaluation of notch stresses is based on a basic linear elastic material model that requires the density, the elastic modulus and the Poisson's ratio. The values for the carbon steel of the 30B-X cylinder shell and the CCS restraint used in this analysis are listed in table 2-8. In addition to the linear elastic material model, a perfectly plastic material model is required to determine the stress concentration

factor that is required to calculate the allowable stress according to [FKM 2012]. For this material model, the additionally required yield stress of the carbon steel is listed in table 2-8 as well.

2.2.6.2.7.4 Analysis settings

The analysis settings in [ANSYS] Workbench are mostly left at their default values, with the only exceptions being the solver type that is set to “direct” and “large deflections” turned on. Furthermore, “auto time stepping” is activated in the simulation that is used to determine the stress concentration factor. Two instants of time are relevant in this regard:

1. The last time step at which only elastic deformations are present in the model.
2. The time step representing the maximal possible loading so that an increase in the load would result in a fully plasticized cross section. After this time step, the simulation would no longer converge because of the applied perfectly plastic material model.

Therefore, a high number of initial and maximum substeps is used to capture these instants in time. The chosen time step settings are listed in table 2-21.

**Table 2-21 Analysis of CCS restraint fillet weld – Analysis settings**

| Parameter | Value |
|---|---|
| Initial substeps | 50 |
| Minimum substeps | 10 |
| Maximum substeps | 100 |

2.2.6.2.7.5 Simulation results

An overview of the resulting equivalent von Mises stress at the fillet weld between the CCS restraint and the 30B-X cylinder shell is provided in figure 2-62. As those results are obtained by using a linear elastic material model, high stresses up to 1176 MPa are visible at the root of the fillet weld. However, these high stresses are only a very local occurrence. A few millimeters away from the root, they are already below 300 MPa and, thus, below the yield strength of the carbon steel. Nevertheless, local plastic deformations are to be expected in this area causing a redistribution of those high stresses. Allowing some plastic deformations at the root of the fillet weld, significantly increases its load capacity. If a complete failure of the fillet weld can be excluded, this is acceptable as the high loads considered in this analysis represent HAC and, therefore, only occur once in the lifetime of a 30B-X cylinder.

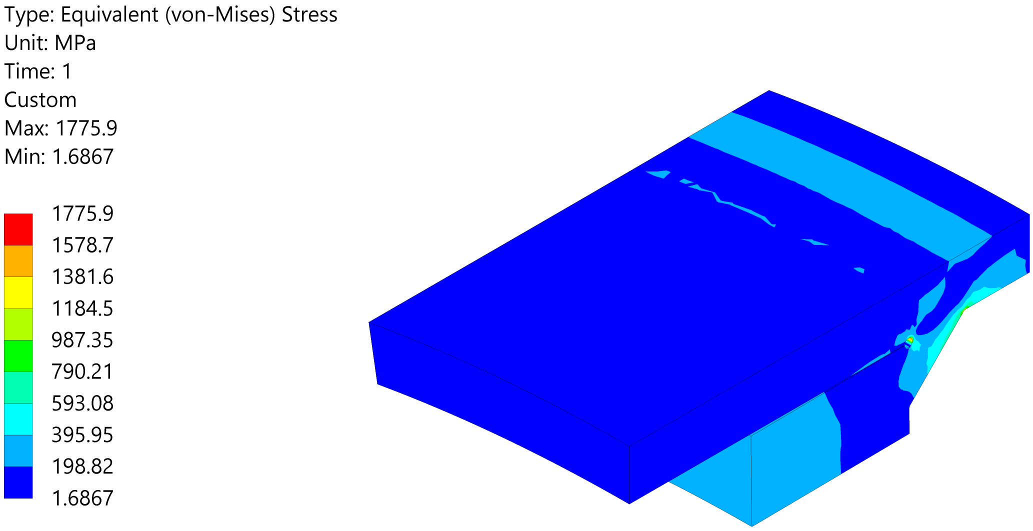


**Figure 2-62 Analysis of CCS restraint fillet weld – Distribution of equivalent von Mises stress**

The assessment of the additional load capacity of the fillet weld is performed in accordance with [FKM 2012]. Therefore, the distribution of the equivalent von Mises stress at the root and toes of the fillet weld is required assuming a plane state of stress:

$$\sigma_{\mathrm{v,wK}} = \sqrt{\sigma_{1,\mathrm{wK}}^2 - \sigma_{1,\mathrm{wK}} \cdot \sigma_{2,\mathrm{wK}} + \sigma_{2,\mathrm{wK}}^2} \qquad (5)$$

In equation (5), $\sigma_{1,\mathrm{wK}}$ and $\sigma_{2,\mathrm{wK}}$ are the principle stresses at the surface of the root and toes of the fillet weld. Similarly, the hydrostatic stress $\sigma_{\mathrm{H,wK}}$ and the triaxiality of the stress state $h_{\mathrm{wK}}$ are calculated in these areas, as they are also required for the assessment of the fillet weld per [FKM 2012]:

$$\sigma_{\mathrm{H,wK}} = \frac{1}{3}\left(\sigma_{1,\mathrm{wK}} + \sigma_{2,\mathrm{wK}}\right) \qquad (6)$$

$$h_{\mathrm{wK}} = \frac{\sigma_{\mathrm{H,wK}}}{\sigma_{\mathrm{v,wK}}} \qquad (7)$$

The corresponding distributions of the equivalent von Mises stress $\sigma_{\mathrm{v,wK}}$, hydrostatic stress $\sigma_{\mathrm{H,wK}}$ and triaxiality of the stress state $h_{\mathrm{wK}}$ are shown in figure 2-63.

a)
b)
c)

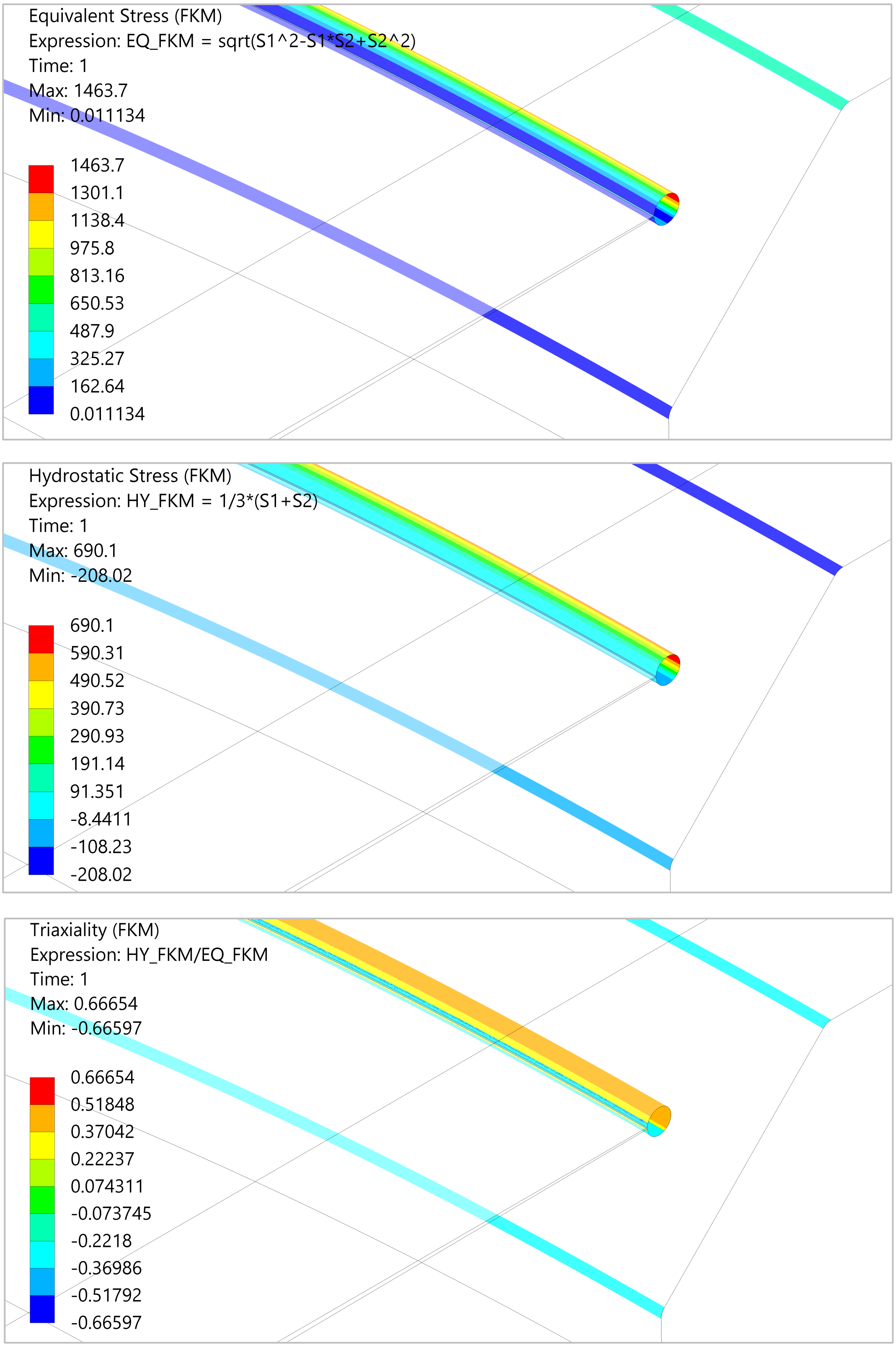


**Figure 2-63 Analysis of CCS restraint fillet weld – Results at fillet weld root: a) Equivalent von Mises stress b) Hydrostatic stress c) Triaxiality of stress state**

It has to be proven that the maximum stress $\sigma_{v,wK}$ remains below the admissible stress $\sigma_{SK,w}$. According to [FKM 2012], this is ensured by the following criterion:

$$a_{\mathrm{SK,wK}} = \frac{\sigma_{\mathrm{v,wK}}}{\sigma_{\mathrm{SK,wK}}/j_{\mathrm{ges}}} \leq 1 \tag{8}$$

The safety factor in equation (8) is set to $j_{\mathrm{ges}} = 1.35$ and the admissible stress $\sigma_{\mathrm{SK,wK}}$ is determined based on the yield stress $R_{\mathrm{p}}$ of the carbon steel listed in table 2-8 by:

$$\sigma_{\mathrm{SK,wK}} = R_{\mathrm{p}} \cdot n_{\mathrm{pl,wK}} \tag{9}$$

The parameter $n_{\mathrm{pl,wK}}$ is the plastic support number, which characterizes the increased load capacity of a component because of its capability to redistribute high stresses through plastic deformations. The plastic support number depends on the material, the load as well as the design of a component. It is calculated as follows:

$$n_{\mathrm{pl,wK}} = \min\left(\sqrt{\frac{E \cdot \varepsilon_{\mathrm{ertr,wK}}}{R_{\mathrm{p}}}}, K_{\mathrm{p}}\right) \quad \text{where} \quad \varepsilon_{\mathrm{ertr,wK}} = \varepsilon_{\mathrm{ref,wK}} \quad \text{if} \quad h_{\mathrm{wK}} \leq \frac{1}{3} \tag{10}$$

For yield stresses lower than 460 MPa, [FKM 2012] defines $\varepsilon_{\mathrm{ref,wK}} = 0.17$. What remains is the determination of the plastic stress concentration factor $K_{\mathrm{p}}$, which is determined according to [FKM 2012] by:

$$K_{\mathrm{p}} = \frac{\text{Plastic limit load}}{\text{Elastic limit load}} \tag{11}$$

As already mentioned above, both loads are determined by performing a simulation with a perfectly plastic material model, where the load is linearly increased up to $F_{\mathrm{z}} = 200\ \mathrm{kN}$. This way, some of the additional load capacity of the fillet weld is utilized, but a sufficient margin of safety is maintained because neither the strain nor the strain rate hardening is considered in the perfectly plastic material model. The development of the equivalent plastic strain in the course of the simulation is listed in table 2-22.

Based on these results, it can be seen that no plastic strains are present in the model up to 0.115 s. Consequently, the elastic limit load is:

$$F_{\mathrm{el,limit}} = \frac{0.115\ \mathrm{s}}{1\ \mathrm{s}} \cdot 200\ \mathrm{kN} = 23\ \mathrm{kN}$$

Similarly, the plastic limit load is determined by the last converged time step listed in table 2-22:

$$F_{\mathrm{pl,limit}} = \frac{0.7925\ \mathrm{s}}{1\ \mathrm{s}} \cdot 200\ \mathrm{kN} = 158.5\ \mathrm{kN}$$

Then, the calculation of the plastic stress concentration factor as defined in equation (11) yields:

$$K_{\mathrm{p}} = \frac{F_{\mathrm{pl,limit}}}{F_{\mathrm{el,limit}}} = 6.9$$

**Table 2-22 Analysis of CCS restraint fillet weld – Determination of elastic and plastic limit load – Results of equivalent plastic strain**

| Time step in s | Equivalent plastic strain in % | Limit load analysis |
|---|---|---|
| 0.02 | 0.00 | - |
| 0.04 | 0.00 | - |
| 0.07 | 0.00 | - |
| 0.115 | 0.00 | Elastic limit load |
| 0.1825 | 0.01 | - |
| 0.2825 | 0.13 | - |
| 0.3825 | 0.36 | - |
| 0.4825 | 0.65 | - |
| 0.5825 | 1.09 | - |
| 0.6825 | 2.23 | - |
| 0.7825 | 10.8 | - |
| 0.7925 | 15.8 | Plastic limit load |

As shown in figure 2-63 c), the criterion for the triaxiality in equation (10) is fulfilled in the area where the maximum notch stress $\sigma_{\mathrm{v,wK}}$ occurs. Consequently, the plastic support number reduces to:

$$n_{\mathrm{pl,wK}} = \min(10.1, 6.9) = 6.9$$

Finally, the allowable stress criterion in equation (8) can be evaluated:

$$a_{\mathrm{SK,wK}} = \frac{\sigma_{\mathrm{v,wK}}}{\sigma_{\mathrm{SK,wK}}/j_{\mathrm{ges}}} = \frac{1464\ \mathrm{MPa}}{355\ \mathrm{MPa} \cdot 6.9/1.3} = 0.78 \leq 1$$

Consequently, the allowable stress criterion is fulfilled. Moreover, the safety margin can be expected to be much higher in reality as multiple conservative assumptions have been made to calculate the above utilization factor:

- The content does not slow-down the CCS as it is only implicitly incorporated in the global FEM model of the 30B-X cylinder that is used to determine the load acting on the CCS restraint.
- The determination of the load acting on the CCS restraint is based on the assumption that the entire content remains attached to the CCRs so that the combined weight of the content and the CCS impacts the CCS restraint.
- The determination of the load acting on the CCS restraint is based on a 10.2 m drop test instead of the sequential application of a 1.2 m and 9 m drop test.
- Neither the strain nor the strain-rate hardening of the carbon steel is considered in the assessment of the fillet weld according to [FKM 2012].

Considering the small differences in the stress-strain curves of the carbon steel in the temperature range between -40 °C and 60 °C (see figure 2-4) as well as the highly conservative approach to

calculate the utilization factor for the fillet weld between the CCS restraint and the 30B-X cylinder shell, specific analyses at -40 °C and 60 °C are not required. As discussed in section 2.2.6.2.5.2.4, the determination of the load acting on the CCS restraint is mostly affected by the contact stiffness between the CCS restraint and the lattice holder on the valve side. With increasing temperature, the contact stiffness reduces, which also reduces the load on the CCS while the material strength almost remains the same. At -40 °C, it is exactly the other way around. Consequently, a failure of the fillet weld between the CCS restraint and the 30B-X cylinder shell can safely be excluded throughout the entire temperature range that is relevant for transportation of the DN30-X package.

### 2.2.6.3 Water Immersion Test for all Packages

The containment (the 30B-X cylinder) is designed in accordance with [ANSI N14.1] for an external MAWP of 172 kPa. The water immersion test for all packages defined in [10 CFR Part 71] §73(c)(6) or [SSR-6 2018] para. 729 requires the immersion of the specimen under a head of water of at least 15 m for a period of not less than 8 hours. This is equal to an external gauge pressure of 150 kPa, which is below the external MAWP. Hence, the DN30-X package is designed to withstand the water immersion test.

### 2.2.6.4 Influence of the Thermal Test under HAC on the Structural Integrity of the DN30-X Package

#### 2.2.6.4.1 Internal Pressure

The pressure build-up during the thermal test is investigated in the thermal analysis in sections 2.3.1.4 referring to the already licensed DN30 package [CoC 9362]. As discussed in section 2.1.1.2, the thermal analysis of the DN30 package and, thus, also the analysis of the pressure build-up during the thermal test, is covering for the DN30-X package. Consequently, the maximum pressure in the 30B-X cylinder during the thermal test caused by elevated temperatures and by melted $UF_6$ contents is also below the admissible pressure. Damage of the 30B-X cylinder, valve or plug and, thus, an influence of the thermal test on the containment system of the DN30-X package can be excluded.

#### 2.2.6.4.2 Pressure Development because of Expansion of Intumescent Material

In case of a fire accident, the expansion of the intumescent material is triggered when its expansion temperature is reached. This may cause the development of a pressure that is acting on the 30B-X cylinder. In case of a standard 30B cylinder, this scenario has already been investigated in SAR of the DN30 package in [DNT 2019]. The only influencing variables in this analysis are the gross weight of the cylinder and its outer dimensions. Since these are identical for the 30B-X and the 30B cylinder, the analysis in [DNT 2019] is also valid for the DN30-X package. The results are as follows:

- The maximal pressure load on the cylinder shells caused by the expanding intumescent material was found to be 27 kPa, which is well below the external MAWP of 172 kPa for the 30B-X cylinder.

- The gaps between the housing of the valve protecting device and the valve itself are more than 20 mm in each direction. The maximal pressure development because of the expansion of the intumescent material for such a gap was found to be 2.3 kPa. However, after 60 min at 300 °C there was no pressure remaining so that any damage to the valve can be excluded.
- The distance between the plug and the inner shell is limited by the skirt of the 30B-X cylinder on the plug side so that the distance is always greater than 13 mm (see Appendix 1.4.1A (Drawings 30B-X Cylinder). For this gap, the pressure caused by the expanding intumescent material is far too small to cause any damage to a solid structure like the plug.

Consequently, neither the 30B-X cylinder shells nor the valve or the plug will be damaged by the expansion of the intumescent material.



#### 2.2.6.4.3 Stresses Caused by Temperatures Reached during HAC

As described in the guideline through the technical analyses in section 2.1.1.2, the thermal analysis of the DN30-X package, consisting of the DN30 PSP and the 30B-X cylinder, is covered by the thermal analysis of the already licensed DN30 package [CoC 9362], consisting of the DN30 PSP and the 30B cylinder. Following the same argumentation as in [DNT 2019], the clearance between the steel shells of the DN30 PSP and the foam parts increases during the first stages of the thermal test under HAC, as the steel shells heat up faster than the foam. Then, the foam partly loses its structural integrity and is reduced in volume, which is due to the observed incineration of the foam during the thermal test under HAC. Hence, no stresses can occur in the DN30 PSP shells during or after the thermal test.

### 2.2.6.5 Impact of Deviations between the Calculation Model of the 30B-X Cylinder and the Designs of the 30B-10 and 30B-20 Cylinder on the Results of the Structural Analysis for the DN30-X Package

The entire structural analysis of the DN30-X package is performed using a 30B-X cylinder design with 35 CCRs arranged in a 1 x 6 x 12 x 16 pattern. Hence, some design differences exist in comparison to the actual designs of the 30B-10 cylinder with 33 CCRs and the 30B-20 cylinder with 43 CCRs. In the following, it is laid down by argumentation that the existing differences between the cylinder designs can only have a negligible impact on the results of the structural analysis.

This is mainly because the weight of the content of the 30B-X cylinder calculation model and the two actual cylinder designs is adopted such that the gross weight complies with that of a standard 30B cylinder. Hence, the differences between the designs and the calculation model are narrowed down to the number of CCRs and the design of the lattice holders, while the gross weight of the cylinder being loaded into the DN30 PSP stays the same. Because of this, there can only be very small differences in the results that refer to the differences in the distribution of the weight within each cylinder and the structural strength of the lattice holders.

The former can only have a minor impact on the results of the structural analysis of the DN30-X package. The comparison analysis between the DN30-X and the DN30 package in section 2.2.6.2.5 already proves that even the major differences in the weight distribution within the 30B-X and the standard 30B cylinder hardly have an impact on the deformations of the DN30 PSP. Consequently, the even smaller differences resulting from the different CCR patterns

for the 30B-10 and 30B-20 cylinder are judged to be irrelevant for the structural analysis of the DN30-X package.

To evaluate the impact of the differences in the structural strength of the lattice holders, the specific designs have to be considered. In case of the 30B-10 cylinder, the pattern is identical to the calculation model of the 30B-X cylinder, except for the number of CCRs in the outer ring that is reduced from 16 to 14. As a consequence, the number of the outer spokes of the lattice holders are also reduced from 16 to 14. However, considering the generally very low deformations of the lattice holders in this area throughout all the investigated drop test scenarios, this reduction can only lead to small increases in the deformations of the lattice holders that have no impact on the safety of the 30B-10 cylinder. In case of the 30B-20 cylinder, the higher number of CCRs in each ring requires a higher amount of cross links between the CCRs. This increases the structural strength of the lattice holders, while the content weight is reduced. Hence, the deformations of the lattice holders of the 30B-20 cylinder are expected to be even smaller than those determined by the calculation model of the 30B-X cylinder.

The argumentation above proves that the differences between the calculation model for the 30B-X cylinder and the actual designs of the 30B-10 and 30B-20 cylinder can only have a negligible impact on the deformations of the DN30 PSP. Furthermore, the level of structural safety of the 30B-10 and 30B-20 cylinder shells is identical to the calculation model, and the structural integrity of their internal CCS is either not affected or improved compared to the calculation model. Hence, the obtained results of the structural analysis for the DN30-X package are also valid for the actual designs of the DN30-10 and DN30-20 package.

#### 2.2.6.6 Conclusion

The structural analysis of the DN30-X package, consisting of the 30B-X cylinder and the DN30 PSP, is based to a large extent on the already licensed DN30 package [CoC 9362], consisting of the 30B cylinder and the DN30 PSP. Taking this approach was possible because of the following reasons:

- The 30B-X cylinder has the same gross weight as the standard 30B cylinder while also having the same outer dimensions, shell thicknesses and material specifications of the pressure envelope and the cylinder skirts.
- The 30B-X and the standard 30B cylinder are equipped with the same valve and plug.
- The 30B-X and the standard 30B cylinder are both transported in the same DN30 PSP.

Since the $UF_6$ content is in solid form during transport, the internal criticality control system (CCS) of the 30B-X cylinder is essentially stuck in it. Hence, the possibilities of the CCS to move around within the 30B-X cylinder cavity are very limited, which lead to the conclusion that the interaction of the content with the 30B cylinder and the interaction of the CCS stuck in the content with the 30B-X cylinder has to be comparable.

Because of the similarities between the DN30 and the DN30-X package, the structural analysis for handling and under RCT performed in [DNT 2019] for the DN30 package remained entirely valid for the DN30-X package. Using the same DN30 PSP for both packages also allows to transfer the results for the water spray test, the compression test, and the penetration test under NCT because the corresponding proves only credit the DN30 PSP and, thus, remain valid independent of the type of cylinder. Additional analyses were only required for the drop tests under NCT and HAC to account for the subtle differences between the packages.

In line with this approach, the structural analysis of the DN30-X package for the drop tests under NCT and HAC was split into two fundamental parts:

1. The first part in section 2.2.6.2.5 provided evidence that the interaction between the 30B-X cylinder and the DN30 PSP is indeed comparable to the interaction between the 30B cylinder and the DN30 PSP.
2. The second part in section 2.2.6.2.6 contains analyses that specifically consider the acceptance criteria for the internal CCS of the 30B-X cylinder and, therefore, also account for the subtle differences between the DN30-X and the DN30 package. Furthermore, the impact of the drop test scenarios that were considered in the safety analysis of the DN30 package in [DNT 2019], but not analyzed in detail for the DN30-X package, were also discussed in this part.

The comparison between the DN30 and the DN30-X package proved that the deformations of the DN30 PSP is indeed very similar for both packages, as the differences in the deformations were mostly below 1 %. In cases where slightly larger differences up to 5 % were found, this could be referred to the differing approaches to model the content of the 30B-X and 30B cylinder (see section 2.2.6.2.3.7). This conclusion is supported by the energy absorption behavior of the DN30 PSP that was nearly identical for both packages in the corresponding drop test analyses.

Hence, the analysis of the drop test sequences and the experimental drop tests for the DN30 package performed in [DNT 2019] in conjunction with the comparing analyses between the DN30-X and the DN30 package in section 2.2.6.2.5 show that:

- The leakage rate after each drop test sequence is less than $1.0 \cdot 10^{-6}\ \mathrm{Pa} \cdot \mathrm{m}^3/s$ (based on the findings in [DNT 2019]).
- There is no failure of the DN30 PSP closure system in any drop test sequence.
- There is no physical contact between the valve of the 30B-X cylinder and any other component of the packaging other than its original point of attachment in any drop test sequence.
- There is no physical contact between the plug of the 30B-X cylinder and any other component of the packaging other than its original point of attachment in any drop test sequence.
- The valve protecting device of the DN30 PSP fulfills its function after each drop test sequence.
- The rotation preventing device of the DN30 PSP fulfills its function after each drop test sequence.
- The plug protecting device of the DN30 PSP fulfills its function after each drop test sequence.
- The intumescent material as well as the housing are still present and undamaged after each of the drop test sequences.
- There is no rupture of the 30B-X cylinder containment system in any drop test sequence.

Furthermore, the following conclusions for the DN30-X package are drawn from the analysis of sequence 1 at -40 °C and +60 °C and sequence 3 at -40 °C that were performed for the DN30 package in [DNT 2019]:

- The deformations of the DN30-X package at +60 °C have to be very similar to the deformations of the DN30 package at 60 °C.
- The deformations of the DN30-X package at -40 °C have to be very similar to the deformations of the DN30 package at -40 °C.
- Neither at -40 °C nor at +60 °C a physical contact between the valve of the 30B-X cylinder and any other component of the packaging other than its original point of attachment is detected.
- Neither at -40 °C nor at +60 °C a physical contact between the plug of the 30B-X cylinder and any other component of the packaging other than its original point of attachment is detected.
- The valve protecting device of the DN30 PSP fulfills its function after each drop test sequence in the whole temperature range.
- The rotation preventing device of the DN30 PSP fulfills its function after each drop test sequence in the whole temperature range.
- The plug protecting device of the DN30 PSP fulfills its function after each drop test sequence in the whole temperature range.

Finally, the additional analyses in section 2.2.6.2.6 performed specifically with regard to the acceptance criteria for the internal CCS of the 30B-X cylinder prove that the deformations of the 30B-X cylinder and its internal CCS are such that there is no failure of the confinement system of the DN30-X package:

- The relative dislocation of the criticality control rods (CCRs) remains below 5 mm.
- The increase in radial movability of the entire CCS out of the center of the 30B-X cylinder remains below 3 mm.
- The increase in axial movability of the entire CCS out of the center of the 30B-X cylinder remains below 7 mm.
- There is no failure of the lattice holders.
- There is no rupture of the CCRs.

Consequently, it can be concluded that the DN30 PSP provides the required mechanical protection of the 30B-X cylinder for the temperature range of -40 °C to +60 °C under RCT, NCT, and HAC.

## 2.3 Thermal Analysis

As described in the guideline through the technical analyses in section 2.1.1.2, the thermal analysis of the DN30-X package, consisting of the DN30 PSP and the 30B-X cylinder, is based on the thermal analysis of the already licensed DN30 package [CoC 9362], consisting of the DN30 PSP and the 30B cylinder. This is possible because of the following reasons:

- The standard 30B and 30B-X cylinders are transported in the same DN30 PSP.
- The assumed thermal load of 3 W for the $UF_6$ content is by far covering for all admissible enrichment levels for the DN30-X package (see section 1.3.2.7).
- Because of the internal CCS, the 30B-X cylinder has a larger nominal tare weight than the standard 30B cylinder, while the outer dimensions and shell thicknesses of the pressure envelope and the cylinder skirts remain the same (see table 1-13). As the maximal temperatures of the envelope of the standard 30B cylinder were calculated for an empty cylinder in [DNT 2019], a higher tare weight of the 30B-X cylinder is equivalent to an increased heat sink that results in lower maximal temperatures for the empty 30B-X cylinder.
- The possible pressure build-up of melted $UF_6$ contents for temperatures above the triple point of $UF_6$ (64 °C/147.3 °F) is lower because of the increased ullage of the 30B-X cylinder (see table 1-13).

Therefore, the temperatures at the DN30 package under RCT and NCT determined in the thermal analysis of the DN30 package in [DNT 2019] also apply to or at least cover the DN30-X package. Generally, the same proof applies to the thermal analysis under HAC. However, because of the lower net weight of the 30B-X cylinder in comparison to the standard 30B cylinder, it is expected that its heat sink is lower as well in case of a filled cylinder. Therefore, additional calculations are conducted for the DN30-X package under HAC in section 2.3.2 considering a filled 30B-X cylinder.

### 2.3.1 Objective of Verification

#### 2.3.1.1 Verification for all Types of Packages

It is verified that the design of the DN30-X package takes into account ambient temperatures and pressures that are likely to be encountered under RCT. Even though such a requirement is neither stipulated in [10 CFR Part 71] nor in [49 CFR Part 173], it is required to fulfill [SSR-6 2018] para. 616.

#### 2.3.1.2 Verification for Packages Containing Uranium Hexafluoride

It is verified that the DN30-X package withstands the thermal test specified in [10 CFR Part 71] §73(c)(4) or [SSR-6 2018] para. 728 without rupture of the containment system.

#### 2.3.1.3 Verification for Packages Containing Fissile Material

The consequences of the thermal test specified in [10 CFR Part 71] §73(c)(4) or [SSR-6 2018] para. 728 on the DN30-X package subjected to the mechanical tests specified in [10 CFR Part 71] §73(a), §73(c)(1), §73(c)(3) and §73(c)(6) or [SSR-6 2018] paras. 726, 727(a), 727(b) and 729 are analyzed to verify the requirements of [10 CFR Part 71] §55(d), §55(e) and

§59(a)(2) or [SSR-6 2018] para. 682 and 685. The verification is provided in the criticality safety analysis in section 2.6.

#### 2.3.1.4 Admissible Component Temperatures of the DN30-X Package

The containment system of the DN30-X package consists of the 30B-X cylinder shells with installed valve and plug. The admissible temperature for these components is defined as 131 °C (267.8 °F). This admissible temperature has been determined in the safety analysis of the DN30 package in [DNT 2019] for the standard 30B cylinder and is applied to the 30B-X cylinder as well.

The limiting factor in the determination of this admissible temperature was the pressure build-up caused by melted $UF_6$ contents, which is significantly lower for the 30B-X cylinder than for the standard 30B cylinder because of its increased minimum ullage specified in table 1-13. Nevertheless, the application of this admissible temperate to the 30B-X cylinder is justified by investigating the pressure build-up in the 30B-X cylinder caused by melted $UF_6$ contents for temperatures above the triple point of $UF_6$ (64 °C/147.3 °C). In this investigation the increased minimum ullage of the 30B-10 and 30B-20 cylinder in comparison to the standard 30B cylinder is considered. Furthermore, the following conservative assumptions are used:

- The admissible temperature of 131 °C calculated in [DNT 2019] for a standard 30B cylinder is assumed to be the average temperature of all $UF_6$ contents in the 30B-X cylinder. Calculations in section 2.3.2.4 show, that only the outmost region of the $UF_6$ in contact with the 30B-X cylinder shell will reach the maximum temperature while the core of the $UF_6$ is well below that temperature.
- For the calculation of the pressure build-up, the pressure in the empty 30B-X cylinder is assumed to be 5 psi instead of 3 psi (compare [USEC 651], sections 5.3.5 and 8.3).
- The calculations for the pressure build-up are performed with the maximum net weight and minimum volume of the 30B-X cylinder listed in table 1-13. Using this approach, the increased ullages of the 30B-10 and 30B-20 cylinder in comparison to the required minimum ullage of 5 % as specified in [ANSI N14.1] for the standard 30B cylinder are appropriately considered in the analysis.
- The admissible pressure under HAC is based on the hydraulic test pressure of twice the MAWP as specified in [ANSI N14.1]. To consider the elevated temperature of 131 °C/267.8 °F, which is above the design limit of 121 °C/250 °F according to the [ASME BPVC], this test pressure is modified. The corresponding calculation for the 30B-X cylinder is identical to the 30B cylinder, which is detailed in [DNT 2019]. Therefore, the admissible pressure under HAC is set to 2.74 MPa/397.36 psig for the 30B-X cylinder including its valve and plug.

Hereafter, the pressure build-up is investigated for filling ratios of 50 % and 100 % for the admissible temperature of 131 °C/267.8 °F. The vapor pressure data of $UF_6$ required for these calculations is extracted from [DeWitt 1960] and listed in table 2-23.

**Table 2-23 Vapor pressure of $UF_6$**

| Temperature in °C | Vapor pressure[1)] in MPa |
|---|---|
| 63.88 | 0.1506 |
| 64.20 | 0.1527 |
| 91.88 | 0.3395 |
| 99.94 | 0.4174 |
| 108.07 | 0.5091 |
| 116.03 | 0.6129 |
| 124.17 | 0.7349 |
| 133.19 | 0.8892 |
| 141.44 | 1.0517 |
| 149.50 | 1.2300 |
| 180.57 | 2.1313 |
| 207.32 | 3.2436 |
| 230.20 | 4.6103 |

1) The data for the vapor pressure is extracted from [DeWitt 1960]. The pressure for 63.88 °C is the vapor pressure of the solid, while the pressure for all other temperatures is the vapor pressure of the liquid.

The calculation of the total pressure is based on [USEC 651]. The minimum volume $V_{\mathrm{min}}$ and maximum net weight $m_{\mathrm{UF_6}}$ for the 30B-10 and the 30B-20 cylinder are derived from table 1-13. The densities of $UF_6$ for the temperatures $T_1 = 68\,°\mathrm{F}\ (20\,°\mathrm{C})$ and $T_2 = 267.8\,°\mathrm{F}\ (131\,°\mathrm{C})$ are derived from table 1-1.

$$\rho_{\mathrm{UF_6,1}} = 317.8\ \frac{\mathrm{lb}}{\mathrm{ft^3}}$$ solid, at 68 °F (20 °C)

$$\rho_{\mathrm{UF_6,2}} = 198.8\ \frac{\mathrm{lb}}{\mathrm{ft^3}}$$ liquid, at 267.8 °F (131 °C)

According to [USEC 651], the pressure inside an empty 30B cylinder is assumed to be 5 psi or less. This is valid for the empty 30B-X cylinder, too:

$$p_{\mathrm{Air,0}} = 5\ \mathrm{psi}$$

For the temperature $T_1$, the volume of $UF_6$ and air inside the 30B-X cylinder for a filling ratio $r_\mathrm{f}$ are calculated as:

$$V_{\mathrm{UF_6,1}} = \frac{r_\mathrm{f} \cdot m_{\mathrm{UF_6}}}{\rho_{\mathrm{UF_6,1}}}$$

$$\mathrm{V_{Air,1}} = \mathrm{V_{30B-X}} - \mathrm{V_{UF_6,1}}$$

The air pressure for the temperature $T_1$ is then:

$$\mathrm{p_{Air,1}} = \frac{\mathrm{p_{Air,0}} \cdot \mathrm{V_{30B-X}}}{\mathrm{V_{Air,1}}}$$

The vapor pressure of liquid $UF_6$ for the temperature $T_2$ is linearly interpolated from the data listed in table 2-23.

$$p_{\mathrm{UF_6},2} = 123.53\ \mathrm{psi}$$

The volume and pressure of the air inside the 30B-X cylinder for the temperature $T_2$ are:

$$V_{\mathrm{Air},2} = V_{\mathrm{30B-X}} - \frac{r_\mathrm{f} \cdot m_{\mathrm{UF_6}}}{\rho_{\mathrm{UF_6},2}}$$

$$p_{\mathrm{Air},2} = p_{\mathrm{Air},1} \cdot \frac{V_{\mathrm{Air},1} \cdot T_2}{V_{\mathrm{Air},2} \cdot T_1}$$

The total pressure for the temperature $T_2$ is the summation of the partial pressures:

$$p_{\mathrm{Total},2} = p_{\mathrm{UF_6},2} + p_{\mathrm{Air},2}$$

The results for filling ratios of 50 % and 100 % for the 30B-10 and 30B-20 cylinder are listed in table 2-24. These are compared to the results for the standard 30B cylinder determined in [DNT 2019].

**Table 2-24 Total pressure inside 30B and 30B-X cylinders for filling ratios of 50 % and 100 %**

| Parameter | Temperature in °F (°C) | 30B cylinder filling ratio | | 30B-10 cylinder filling ratio | | 30B-20 cylinder filling ratio | |
|---|---|---|---|---|---|---|---|
| | | 50 % | 100 % | 50 % | 100 % | 50 % | 100 % |
| $m_{\mathrm{UF_6}}$ in lb | - | 5020 | | 3219 | | 2802 | |
| $V_{\mathrm{min}}$ in ft³ | - | 26.0 | | 19.2 | | 17.4 | |
| $V_{\mathrm{UF_6}}$ in ft³ | 68 (20) | 7.90 | 15.80 | 5.06 | 10.13 | 4.41 | 8.82 |
| | 267.8 (131) | 12.35 | 25.25 | 8.10 | 16.19 | 7.05 | 14.10 |
| $V_{\mathrm{Air}}$ in ft³ | 68 (20) | 18.10 | 10.20 | 14.14 | 9.07 | 12.99 | 8.58 |
| | 267.8 (131) | 13.37 | 0.75 | 11.10 | 3.01 | 10.35 | 3.30 |
| $p_{\mathrm{Air}}$ in psi | 68 (20) | 7.18 | 12.74 | 6.79 | 10.58 | 6.70 | 10.14 |
| | 267.8 (131) | 13.40 | 239.83 | 11.92 | 43.99 | 11.59 | 36.30 |
| $p_{\mathrm{Total}}$ in psi (MPa) | 267.8 (131) | 136.93 (0.94) | 363.36 (2.51) | 135.45 (0.93) | 167.52 (1.16) | 135.12 (0.93) | 159.83 (1.10) |

The maximum total pressure at a temperature of 267.8 °F/131 °C is well below the admissible pressure of 2.74 MPa/397.36 psig for the 30B-X cylinder. The resulting safety margins calculated with the admissible pressure are listed in table 2-25.

**Table 2-25 Safety margins for the pressure build-up inside the 30B-X cylinder**

| | 30B-10 cylinder | | 30B-20 cylinder | |
|---|---|---|---|---|
| Filling ratio in % | 50 | 100 | 50 | 100 |
| Safety margin | 2.93 | 2.37 | 2.94 | 2.49 |

Because of the large minimum ullage of the 30B-10 and 30B-20 cylinder of 17.6 % and 20.8 %, respectively, the maximum pressure at a temperature of 267.8 °F/131 °C is even below the MAWP (1.38 MPa/200 psig) of the 30B cylinder that also applies to the 30B-X cylinder.

Therefore, the admissible temperature for the 30B-X cylinder is set to 131 °C/267.8 °F. This admissible temperature is below the allowable temperatures defined in standards or the hot-working temperatures and liquidus temperatures/melting points of the materials being part of the pressure-containment of the 30B-X cylinder. The admissible temperatures for the cylinder shells, valve and plug are listed in detail in [DNT 2019]. The additional components of the 30B-X cylinder compared to the standard 30B cylinder are the lattice holders, the CCRs, and the neutron absorbing material. The material specifications for the lattice holders and the CCRs comply to the 30B cylinder and, therefore, exceed the admissible temperature as well. With 2763 °C/5005 °F, the melting point of the neutron absorbing material in the form of $B_4C$ is far above the admissible temperature.

Furthermore, there is no danger of rupture because of a possible pressure build-up caused by melted $UF_6$ contents for temperatures above the triple point. Since the same DN30 PSP is used for the DN30 and the DN30-X package, the admissible component temperatures for the DN30 package established in [DNT 2019] are also applicable to the DN30-X package. The admissible temperatures are summarized in table 2-26 below.



**Table 2-26 Admissible component temperatures of the DN30-X package**

| Component | Material | Admissible temperature in °C | |
|---|---|---|---|
| | | RCT / NCT | HAC |
| DN30 PSP | | | |
| Outer shell | Type 304/1.4301 | 70 / 100 1) | 900 6) |
| Inner shell | Type 304/1.4301 | 60 1) | 900 6) |
| Foam | PIR foam | 60 2) | - |
| Thermal insulation | Microporous material (see table 1-12) | 60 2) | 1000 |
| Intumescent material | Intumescent material (see table 1-12) | 150 3) | 600 |
| 30B-X cylinder | | | |
| Shells | Pressure vessel steel | | |
| Lattice Holder/CCRs | Pressure vessel steel | 64 4) | 131 5) |
| Neutron absorber | Boron carbide | | |
| Valve / plug | | | |
| Body | Aluminum bronze | | |
| Stem | Nickel copper alloy | 64 4) | 131 5) |
| Solder | Tin lead alloy | | |

1) Calculation temperature: 70 °C for handling / RCT and 100 °C for lifting lugs at the top half
2) Identical to temperature of shells
3) Temperature where the expansion of the intumescent material begins
4) Triple point temperature of $UF_6$
5) Covering maximum temperature for the components of the 30B cylinder (see calculations above)
6) The hot forming of material Type 304/1.4301 is carried out at temperatures of 950 to 1200 °C. At 900 °C a sufficient strength remains and, thus, a deformation by own weight is not expected. The strength of the outer shell is neither relevant for the containment system nor for shielding and criticality safety.

### 2.3.2 Thermal Analysis of the DN30-X Package under HAC

#### 2.3.2.1 Software

The thermal analysis is carried out with [ANSYS] Workbench 2021 R1, which is a software environment for performing linear and non-linear structural, thermal, and electromagnetic analyses using the finite element method (FEM). The capabilities of ANSYS Workbench encompass geometry creation and optimization, meshing, preparing the finite element model, solving and post-processing of results. For thermal problems, ANSYS Workbench can solve steady-state as well as transient problems using two- or three-dimensional models. A model may include multiple materials, and the thermal conductivity, density and specific heat of each material may be temperature-dependent. Materials may undergo change of phase. Thermal properties of materials may be entered as data or may be extracted from a material properties library. The boundary conditions that may be surface-to-environment or surface-to-surface, may be specified temperatures or any combination of prescribed heat flux, forced convection, natural convection and radiation. The boundary condition parameters may be time- and/or temperature-dependent. General grey body radiation problems may be modelled with user-defined factors for radiant exchange. Heat generation rates and boundary temperatures may be time- and position dependent, respectively. Coupled-physics analysis are supported, e.g. structural-thermal, thermal-electric or thermal-diffusion. Additional functions that are not available via the Workbench user interface can be included in the model using command scripts and the ANSYS parametric design language (APDL).

#### 2.3.2.2 Calculation Model

For the thermal analysis of the DN30-X package, an axisymmetric two-dimensional model is used. It is based on the thermal model of the DN30 package that is detailed in [DNT 2019] and was validated and benchmarked using two real-world thermal tests with DN30 prototypes. Compared to the calculation model of the DN30 package, only the 30B cylinder is replace by the 30B-X cylinder in the calculation model of the DN30-X package. The model of the DN30 PSP remains the same. The calculation model of the DN30 PSP is shown in figure 2-64.

The skirts, mantle, and ellipsoidal heads of the 30B-X cylinder are identical to the standard 30B cylinder. The only difference in the two thermal models is the internal CCS that is built in the cavity of the 30B-X cylinder. The geometry of the CCS is adapted to the two-dimensional environment so that the weight of the CCS, the radial positions of the CCRs and the lateral positions of the lattice holders are equivalent to the model used for the structural analyses (see section 2.2.6). Between the CCRs and the ellipsoidal heads, a small gap is present on both sides. The influence of a direct contact between the CCRs and the ellipsoidal heads is investigated in a sensitivity analysis in section 2.3.2.5. The calculation model of the 30B-X cylinder in comparison to the 30B cylinder is shown in figure 2-65.

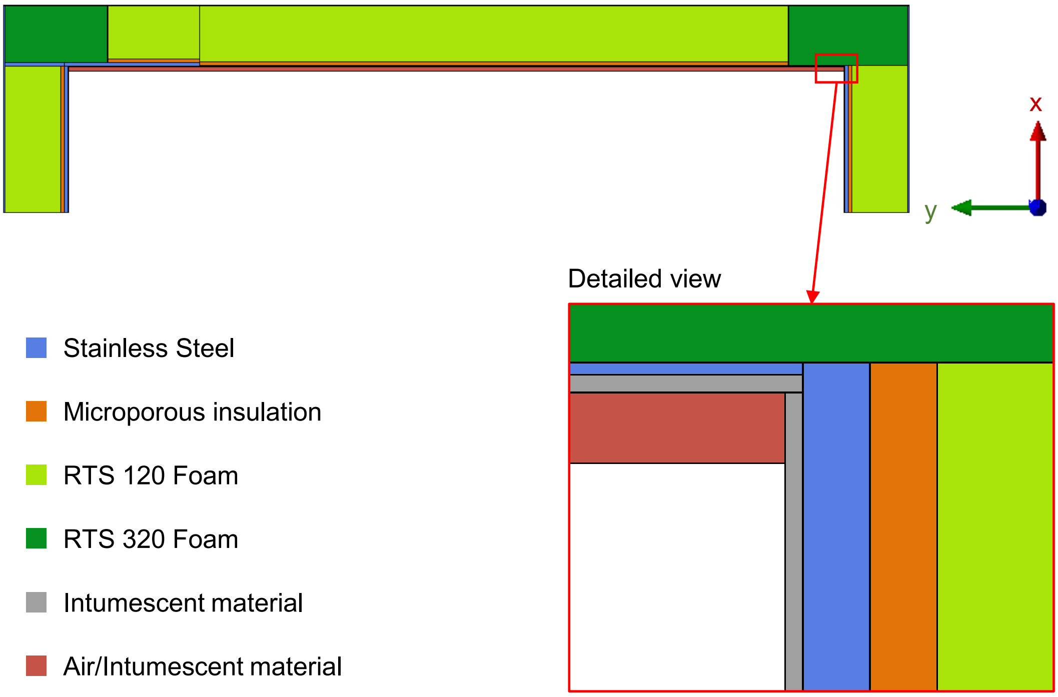


**Figure 2-64 DN30-X thermal model – Geometry of the DN30 PSP**

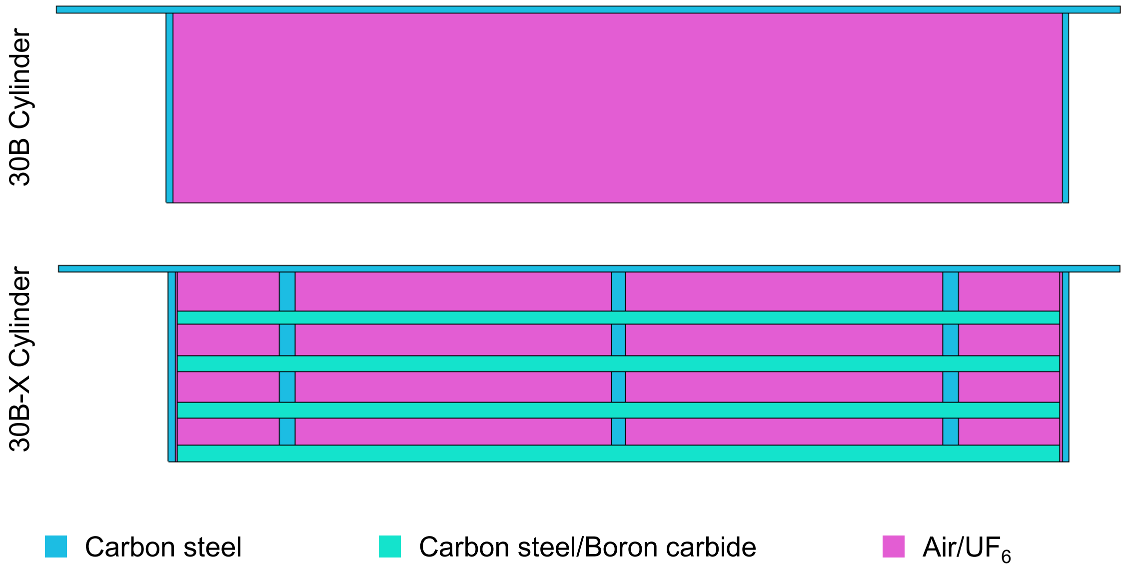


**Figure 2-65 DN30-X thermal model – Geometry of the 30B-X compared to the 30B cylinder**

### 2.3.2.3 Boundary Conditions and Heat Exchange

Initial temperatures, ambient temperatures and heat transfer to the ambient or in gaps via solar insolation, radiation and convection are the same as in the model used for the DN30 package in [DNT 2019]. The heat generation because of incineration of the foam is identical as well.

The maximum heat generation of the radioactive content is the identical to the DN30 package with a thermal power of 3 W. Due to the additional CCS, the remaining free volume inside the 30B-X cylinder is smaller, resulting in a higher heat generation per volume:

$$Q = \frac{P_{\text{th}}}{V_{\text{free}}} = \frac{3\ \text{W}}{0.538\ \text{m}^3} = 5.58\ \frac{\text{W}}{\text{m}^3}$$

#### 2.3.2.4 Calculations for the DN30-X Package under HAC

The calculations for the DN30-X package under HAC are performed with the following boundary conditions (see [DNT 2019] as well):

- The fire temperature is set to 800 °C/1475 °F, the fire duration is 30 min.
- During the cooling phase, the ambient temperature is set to 38 °C/100 °F, solar insolation is considered as defined in [DNT 2019].

The maximum component temperatures for different filling ratios are listed in table 2-27 compared to the temperatures calculated for the DN30 package in [DNT 2019].

**Table 2-27 Thermal test under HAC – Maximum component temperatures for the DN30-X package in comparison to the DN30 package for different filling ratios**

| Component | Temperature in °C | | | | | |
|---|---|---|---|---|---|---|
| | Empty cylinder | | Partially filled cylinder (50 %) | | Filled cylinder (100 %) | |
| | 30B | 30B-X | 30B | 30B-X | 30B | 30B-X |
| Cylinder | | | | | | |
| Valve | 122.2 | 113.5 | 113.4 | 105.9 | 110.3 | 104.2 |
| Plug | 120.4 | 110.4 | 110.6 | 102.9 | 107.2 | 101.1 |
| Mantle | 124.5 | 120.7 | 119.5 | 116.7 | 117.9 | 115.8 |
| DN30 PSP | | | | | | |
| Inner shell | 187.7 | 187.7 | 187.6 | 187.6 | 187.6 | 187.6 |
| Outer shell | 785.4 | 785.4 | 785.4 | 785.4 | 785.4 | 785.4 |

Compared to the 30B cylinder loaded into the DN30 PSP (for a detailed discussion of the results see [DNT 2019]), the maximum temperatures calculated for the thermal test under HAC are significantly lower for the 30B-X cylinder loaded into the same DN30 PSP because of the increased heat sink of the CCS. For the bounding case considering an empty cylinder, the maximum temperatures are about 9-10 °C lower at the valve and plug for the 30B-X than for the 30B cylinder. For the partially filled and filled cylinder, the effect of the increased heat sink is slightly lower, but the maximum temperatures for the 30B-X cylinder are still significantly lower for the valve and plug by 6-8 °C.

For all calculated cases and components, the maximum temperatures are not only below the admissible temperatures defined in Table 2-26 but even below the design limit of 121 °C/250 °F as specified in [ANSI N14.1].

Figure 2-66 shows the maximum temperatures at the DN30-X package during the fire phase and the cooling phase, which are reached for an empty 30B-X cylinder.

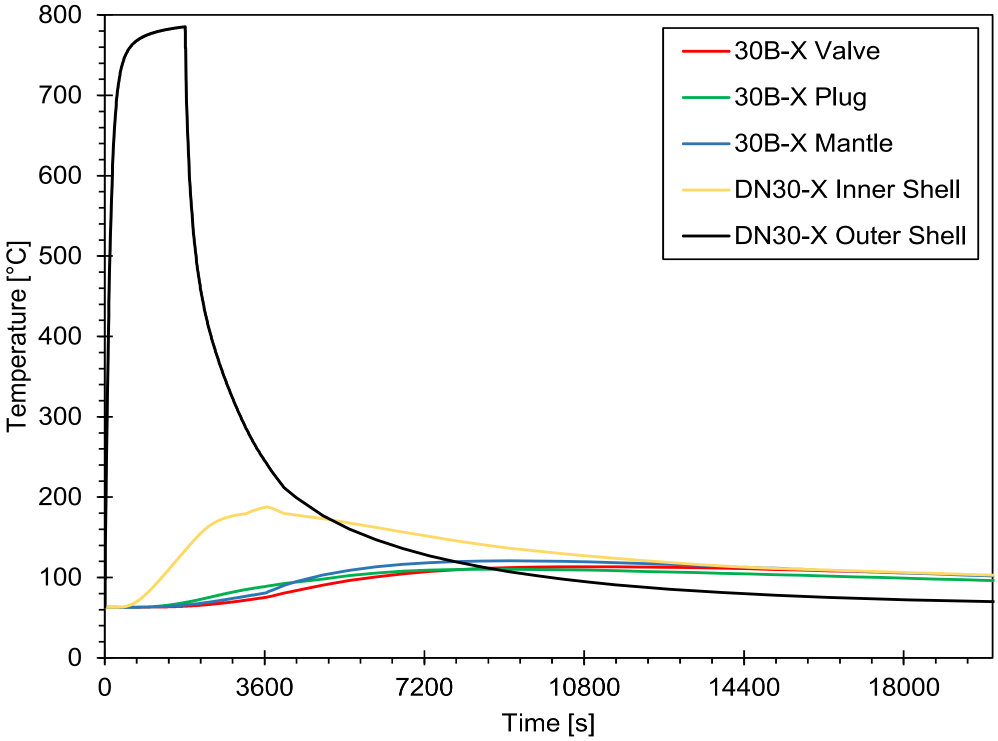


**Figure 2-66 Thermal test under HAC – Calculated temperatures at the DN30-X package considering an empty 30B-X cylinder for the fire phase and 5 hours of cooling down**

The calculated temperature distribution for the DN30-X package loaded with an empty 30B-X cylinder is shown in figure 2-67 for the time at the end of the fire (t = 1810 s) and in figure 2-68 for the time of the maximum temperature of the valve (t = 10910 s).

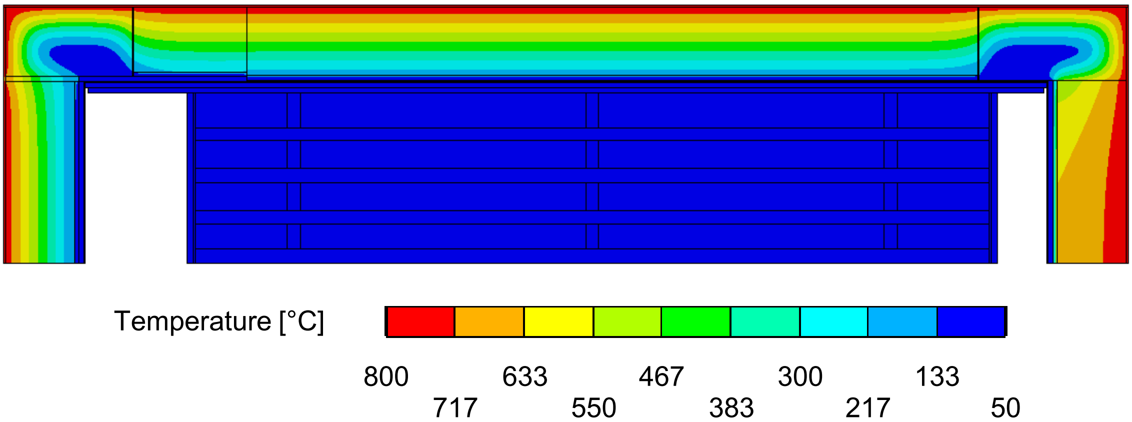


**Figure 2-67 Thermal test under HAC – Temperature distribution at the DN30-X package considering an empty 30B-X cylinder at the end of the fire (t = 1810 s)**

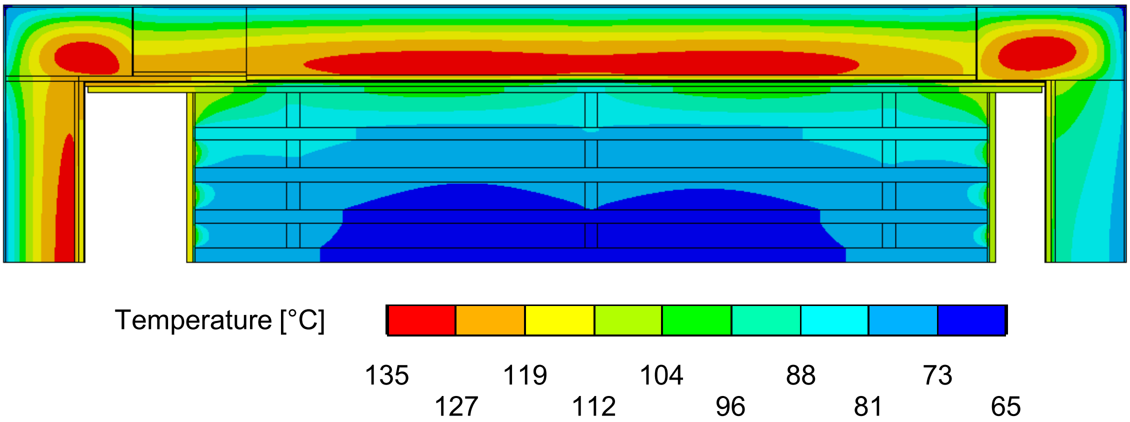


**Figure 2-68 Thermal test under HAC – Temperature distribution at the DN30-X package considering an empty 30B-X cylinder at the time of maximum valve temperature (t = 10910 s)**

A comparison between the calculated temperatures for an empty 30B-X and an empty 30B cylinder is shown in figure 2-69. The maximum temperatures calculated for the empty 30B-X cylinder are generally lower than for the empty 30B cylinder. Furthermore, they are reached in a shorter time.

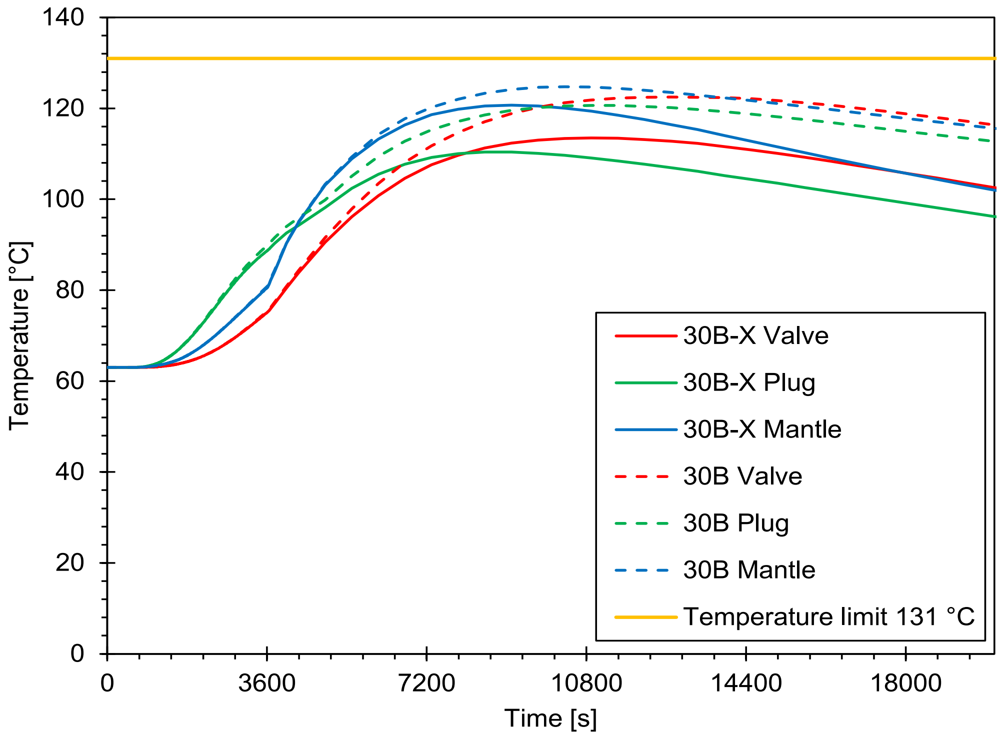


**Figure 2-69 Thermal test under HAC – Calculated temperatures at the empty 30B-X compared to the empty 30B cylinder during the fire phase and 5 hours of cooling down**

This is the case for the partially filled and filled cylinders, too. The increased heat sink of the 30B-X cylinder leads to lower maximum temperatures for the components of the pressure envelope which are reached in less time. The corresponding temperature curves for the comparison of partially filled and filled cylinders are shown in Figure 2-70 resp. Figure 2-71.

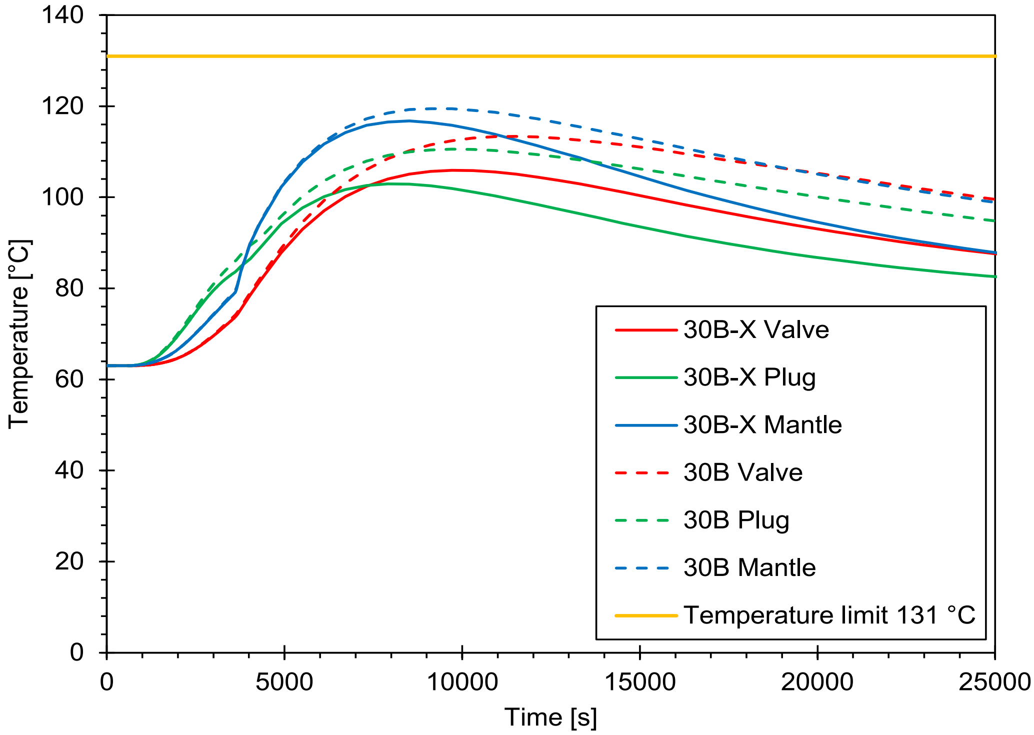


**Figure 2-70 Thermal test under HAC – Calculated temperatures at the partially filled 30B-X compared to the partially filled 30B cylinder during the fire phase and 5 hours of cooling down**

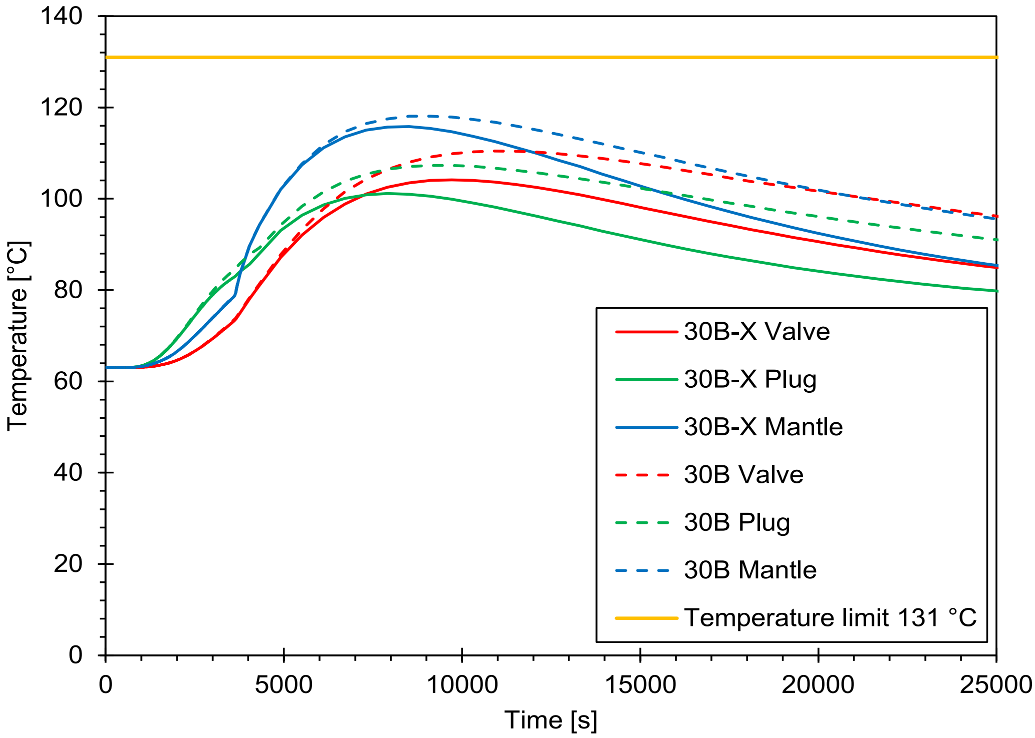


**Figure 2-71 Thermal test under HAC – Calculated temperatures at the filled 30B-X compared to the filled 30B cylinder during the fire phase and 5 hours of cooling down**

In summary, the maximum temperatures calculated for the 30B-X under HAC are lower than the maximum temperatures calculated for the 30B cylinder for empty, partially filled, and filled

cylinders. The maximum temperatures of the 30B-X cylinder are also significantly below the admissible temperatures defined in Table 2-26.

#### 2.3.2.5 Sensitivity Analysis for the CCS

In the calculations presented in this section, the influence of a direct contact between the CCRs and the ellipsoidal head on the valve or plug side of the 30B-X cylinder is investigated. Figure 2-72 shows the calculated temperatures at an empty 30B-X cylinder for the base model that has a small gap between the CCRs and the 30B-X cylinder shell in comparison to the modified model for the sensitivity analysis that simulates a direct contact between the CCRs and the 30B-X cylinder shell at the head and bottom of the cylinder. The corresponding maximum component temperatures of the DN30-X package are listed in table 2-28.

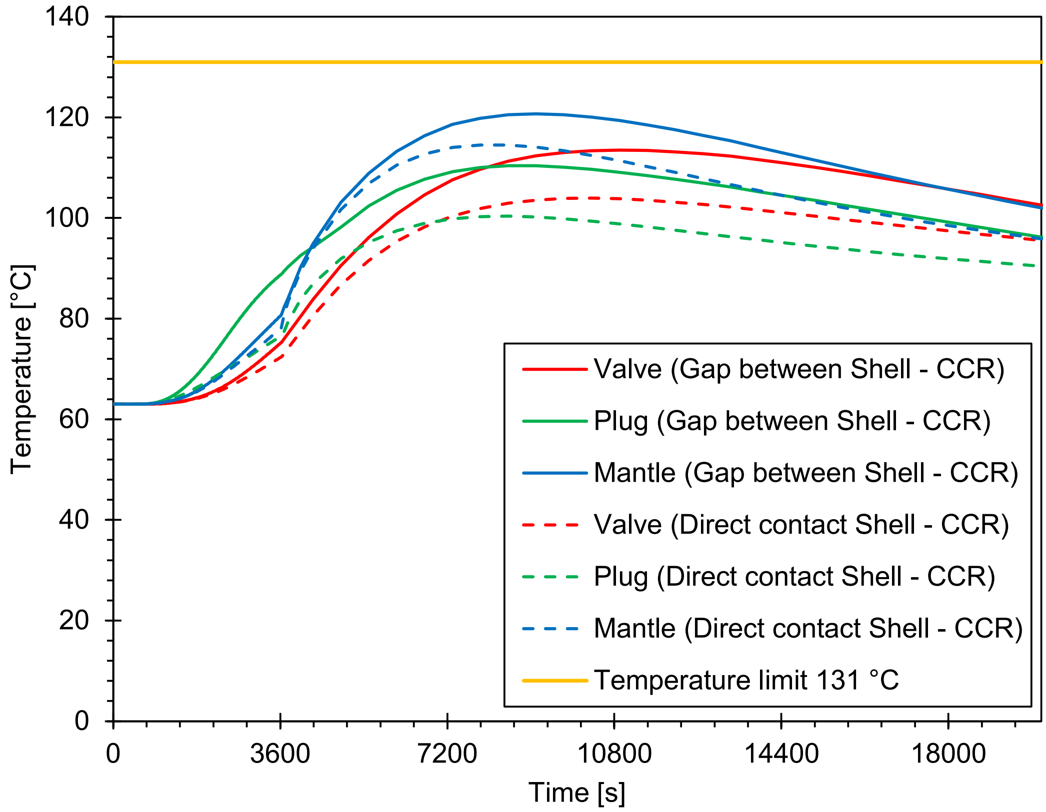


**Figure 2-72 Thermal test under HAC – Sensitivity analysis for CCS – Calculated temperatures at the 30B-X cylinder**

The sensitivity analysis shows that the impact of the increased heat sink of the CCS on the temperatures at the 30B-X cylinder is even more significant with a direct contact between the CCRs and the cylinder shells of the 30B-X cylinder. The calculated temperatures obtained with the modified calculation model for the sensitivity analysis are significantly lower than for the base model with a gap between the CCRs and the 30B-X cylinder shell. Consequently, they are even further below the admissible temperatures.

**Table 2-28 Thermal test under HAC – Sensitivity analysis for CCS – Maximum component temperatures**

| Component | Temperature in °C | |
|---|---|---|
| | Standard model | Modified model |
| 30B-X cylinder | | |
| Valve | 113.5 | 103.9 |
| Plug | 110.4 | 100.4 |
| Mantle | 120.7 | 114.5 |
| DN30 PSP | | |
| Inner Shell | 187.7 | 187.6 |
| Outer Shell | 785.4 | 785.4 |

1) The standard model considers a gap between the CCRs and the 30B-X cylinder shell.
2) The new model simulates a direct contact between the CCRs and the 30B-X cylinder shell

## 2.3.3 Proof for the DN30-X Package to Meet the Regulatory Requirements

### 2.3.3.1 Ambient Temperatures and Pressures

For the analysis, an ambient temperature of 38 °C is considered (see [DNT 2019]). Pressures that are likely to be encountered under RCT and NCT have no effect on the results of the thermal analysis. Consequently, the requirements of [10 CFR Part 71] §71(c)(1)-(4) or [SSR-6 2018] para. 616 are met.

### 2.3.3.2 Component Temperatures of the DN30-X Package

In the thermal analysis for the DN30 package in [DNT 2019], the maximal component temperatures during RCT and NCT are at their maximum 63 °C for the DN30 PSP and 53 °C for the 30B cylinder and its contents. As explained in the introduction to section 2.2, these temperatures are also covering for the DN30-X packaging because of the increased heat sink provided by the interior CCS of the 30B-X cylinder. Therefore, the maximal component temperatures of the DN30-X packaging during RCT and NCT are lower than the admissible values specified in table 2-26.

In the thermal analysis of the DN30 package in [DNT 2019], the maximal component temperatures of the DN30 PSP reached during the thermal test under HAC are close to the admissible temperatures defined in table 2-26. However, tests with a prototype of the DN30 package showed that these temperatures do not affect the function of the inner and outer shells of the DN30 PSP with respect to shielding and criticality safety.

As shown in section 2.3.3.3, the maximum temperature of the 30B-X cylinder are significantly below the maximum temperatures calculated for the DN30 package for an empty, partially filled (50 %) and filled cylinder.

The maximum temperature calculated for the 30B-X cylinder shell is below the admissible temperature defined in table 2-26. The temperatures of the valve and plug thread are below the admissible temperature defined in table 2-26 as well. The maximum temperatures calculated for the components of the 30B-X cylinder are even below the design limit specified in [ANSI N14.1] of 121 °C/250 °F.

#### 2.3.3.3 Rupture of the Containment System

Regarding a rupture of the containment system, an empty and a full cylinder define the two bounding cases. For an empty cylinder, the temperatures during the thermal test under HAC are maximized as the 30B-X cylinder provides the lowest possible heat sink. For a full cylinder, the temperatures are generally lower, but the significant volume expansion of the $UF_6$ content during its solid-to-liquid phase change potentially causes a pressure build-up with increasing temperatures.

The maximum temperatures reached during the thermal test under HAC required for the evaluations in this section are taken from the thermal analysis of the DN30-X package in section 2.3.2.

For an empty 30B-X cylinder and filling ratios up to 50 %, a maximum temperature of 120.7 °C is reached at its components and its cavity during the thermal test under HAC. This maximum temperature is at least 10 °C below the admissible temperature for the containment system of the DN30-X of 131 °C listed in table 2-26. For a 100 % filled and 50 % partially filled 30B-X cylinder, the maximum temperature reached during the thermal test under HAC are even lower with a maximum of 115.8 °C resp.116.7 °C. Therefore, the maximum temperatures do not exceed the design limit of 121 °C (250 °F) as specified in [ANSI N14.1] and, thus, are at least 10 °C below the admissible temperature for the containment system of the DN30-X of 131 °C listed in table 2-26.

Additionally, the safety ratios calculated for a pressure build-up caused by melted $UF_6$ contents is significantly higher for the admissible temperature of 131 °C for the 30B-X cylinder compared to the 30B cylinder because of the increased ullage (see Table 2-25).

As proven by the above evaluation, all admissible temperatures are met for the containment system of the DN30-X packaging. In the determination of these admissible temperatures, a possible pressure build-up in the 30B-X cylinder due to melted $UF_6$ contents was considered. As the admissible internal pressure, the hydrostatic test pressure of 2.76 MPa (400 psig) specified in [ANSI N14.1] was assumed. Furthermore, it was shown in the thermal analysis of the DN30 package in [DNT 2019] that the wall thicknesses of the cylinder shell and heads are above the required wall thicknesses calculated according to [ASME BPVC]. As the pressure-containment of the 30B-X cylinder is identical to the 30B cylinder, all requirements of [49 CFR Part 173] §420(a)(3) or [SSR-6 2018] para. 632(c) are met.

#### 2.3.3.4 Influence of the Thermal Test on the Criticality Safety Analysis

The thermal analysis for the DN30 package in [DNT 2019] proves that the stainless-steel shells of the DN30 PSP as well as the carbon steel shell of the 30B cylinder are not affected by the thermal test in such a way that their thickness and density is reduced. As the pressure-containment of the 30B-X cylinder is identical to the 30B cylinder, it is verified in section 2.6 that criticality safety is ensured when taking into account these results. In the criticality safety analysis, a complete loss of the foam is considered.

The requirements of [10 CFR Part 71] §55(d), §55(e) and §59(a)(2) or [SSR-6 2018] para. 682 and 685 with respect to the thermal test under HAC are met.

## 2.4 Containment Design Analysis

As described in the guideline through the technical analyses in section 2.1.1.3, the containment design analysis of the DN30-X package, consisting of the DN30 PSP and the 30B-X cylinder, is carried out in the same manner as for the already licensed DN30 package [CoC 9362], consisting of the DN30 PSP and the 30B cylinder. This is possible due to:

- The pressure envelope of the 30B-X and the standard 30B cylinder including the valve and the plug being identical
- The fact that both the DN30 and the DN30-X package are a Type AF package

The containment design analysis of the DN30 package in [DNT 2019] covers enriched uranium specified in [ASTM C996] and all filling ratios from cylinders containing heel quantities up to cylinders filled with the maximum amount of $UF_6$ of 2227 kg (see table 1-13). As applicable to a Type AF package, RCT and NCT are considered, as there is no restriction on the radioactivity release under HAC, which is due to the limit of 1 $A_2$ for the radioactive content of Type A packages.

In the following, it is shown for the DN30-X package that the objective of verification as laid down in section 2.4.1 is met, by appropriately adopting the results of the containment design analysis of the DN30 package in [DNT 2019] to the DN30-X package.

### 2.4.1 Objective of verification

It is verified that the DN30-X package complies with the requirements under NCT according to [10 CFR Part 71] §43(f) and [49 CFR Part 173] §412(j) or [SSR-6 2018] para. 648(a) when submitted to the tests under NCT according to [10 CFR Part 71] §71(c)(7) and §71(c)(9) and [49 CFR Part 173] §465(c) and §465(d) or [SSR-6 2018] para. 722 and 723:

**Prevent loss or dispersal of the radioactive content**

Identical to the safety analysis of the DN30 package in [DNT 2019], the following allowable release rate is defined under NCT:

$$R_{\mathrm{N}} \leq 10^{-6} \frac{A_2}{\mathrm{h}}$$

For Type AF packages, there is no restriction on the radioactivity release under HAC due to the limit of 1 $A_2$ for the whole content.

### 2.4.2 Calculation Method

The containment design analysis for the DN30-X package is performed in the same manner as for the DN30 package in [DNT 2019]. Only the required standard helium leakage rates differ from the DN30 package, which is solely due to the differences in the content weight and the certified minimum volume of the 30B-X and the standard 30B cylinder. All other aspects of the analysis like possible leakage paths etc. are identical.

### 2.4.3 Package Data Used for the Analysis

In the thermal analysis of the DN30-X package in section 2.2, a maximum temperature of 64 °C has been determined at the DN30 PSP shells under NCT. This temperature is assumed for the entire DN30-X package in the containment design analysis so that the $UF_6$ content just remains in solid form having the lowest possible density of $\varrho_{UF_6} = 4.88\,g/cm^3$ in that state (see [USEC 651]). Then, the free volume $V_N$ inside the containment system of a filled cylinder that is available under NCT is calculated by:

$$V_N = V_{min} - \frac{m_{UF_6}}{\varrho_{UF_6}}$$

The certified minimum volume $V_{min}$ of each cylinder design is listed in table 1-13. For cylinders containing heel quantities, the free volume of the inner cavity is assumed to be the certified minimum volume $V_{min}$. The resulting free volumes for each cylinder design and fill condition are listed in table 2-29. The allowable leakage rate of the 30B-X cylinder in table 2-29 is specified in section 1.2.9 with reference to [ANSI N14.1].

**Table 2-29 Package data used for the containment design analysis under NCT**

| Item | Condition | Value | | |
|---|---|---|---|---|
| | | 30B cylinder | 30B-10 cylinder | 30B-20 cylinder |
| Temperature | Filled<br>Heels | 64 °C | | |
| Free volume of cavity | Filled | 0.2694 m³ | 0.2448 m³ | 0.2325 m³ |
| | Heels | 0.736 m³ | 0.544 m³ | 0.493 m³ |
| Allowable leakage rate | Filled<br>Heels | $1.0 \cdot 10^{-4}\ Pa \cdot m^3/s$ | | |

### 2.4.4 Determination of Radioactive Inventory

The allowable radioactive inventory for the DN30-X package (Type AF package) is 1 $A_2$ (see the content specification in section 1.3). According to [10 CFR Part 71], Appendix A or [SSR-6 2018] Table 2, the $A_2$ values of natural uranium U(nat), enriched uranium with natural isotopic composition U (enriched to 20 % or less) and depleted uranium U(dep) are unlimited. Hence, all amounts of contents, ranging from 0 kg up to the specific fill limits of the 30B-10 and 30B-20 cylinder listed in table 1-4 and complying with the content specifications in section 1.3, can be transported in the DN30-X package. For the containment analysis, the maximal admissible radioactive inventory of 1 $A_2$ is assumed for both the filled cylinder and cylinders containing heel quantities.

### 2.4.5 Radioactive Inventory, Releasable Radioactive Inventory and Activity Concentration in the Cavity Atmosphere

The radioactive inventory, the derived releasable inventory, and the activity concentration in the cavity atmosphere for the 30B-X cylinder are listed in table 2-30.

**Table 2-30 Radioactive inventory, releasable radioactive inventory, and activity concentration in the cavity atmosphere**

| Item | Condition | Value | | |
|---|---|---|---|---|
| | | 30B cylinder | 30B-10 cylinder | 30B-20 cylinder |
| Radioactive inventory in $A_2$ | Filled | | 1 | |
| | Heels | | | |
| Releasable activity in $A_2$ | Filled | 0.0023 | 0.0032 | 0.0035 |
| | Heels | | 1 | |
| Activity concentration in $A_2/\mathrm{m}^3$ | Filled | 0.0084 | 0.0131 | 0.0150 |
| | Heels | 1.36 | 1.84 | 2.03 |

The determination of these values follows the same approach that is used in the safety analysis of the DN30 package in [DNT 2019]. Therefore, the corresponding values of the standard 30B cylinder are listed as well providing a reference. Details on the determination of each item in table 2-30 are given in the following subsections.

### 2.4.5.1 Filled Cylinder

For the determination of the releasable inventory of a filled 30B-X cylinder under NCT, it is assumed that the pressure in the cavity is equal to the pressure $p_{\mathrm{cav}} = 152\ \mathrm{kPa}$ at the triple point of $UF_6$ (64.1 °C) (see table 1-1). Furthermore, it is assumed that the gaseous $UF_6$ is an ideal gas so that the amount of substance of gaseous $UF_6$ is determined by:

$$n_{\mathrm{UF_6,gas}} = \frac{p_{\mathrm{cav}} \cdot V_{\mathrm{N}}}{R \cdot T_{\mathrm{N}}}$$

In the above equation, the free volume of the cavity at the temperature $T_{\mathrm{N}} = 64\ °\mathrm{C}$ is taken from table 2-29. Furthermore, the gas constant $R = 8.3143\ \mathrm{J/mole\ K}$ is used.

The amount of substance of the $UF_6$ gas corresponds to a mass of:

$$m_{\mathrm{UF_6,gas}} = n_{\mathrm{UF_6,gas}} \cdot M_{\mathrm{UF_6}} \qquad \text{with} \qquad M_{\mathrm{UF_6}} = 352\ \mathrm{g/mole}$$

Assuming that the radioactivity is homogeneously distributed in the $UF_6$ and that the gaseous $UF_6$ contains the same mass concentration of radioactivity as the solid $UF_6$, the activity in the gaseous $UF_6$, which is equivalent to the releasable radioactivity, is calculated by:

$$R_{\mathrm{N,avail}} = A_{\mathrm{UF_6,gas}} = \frac{m_{\mathrm{UF_6,gas}}}{m_{\mathrm{UF_6}}} \cdot 1\ A_2$$

The activity concentration under NCT is determined based on the free volume of the cavity:

$$C_{\mathrm{N}} = \frac{R_{\mathrm{N,avail}}}{V_{\mathrm{N}}}$$

The resulting radioactive inventory, the derived releasable inventory, and the activity concentration in the cavity atmosphere for the filled 30B-X cylinder are listed in table 2-30 and compared to the standard 30B cylinder.

#### 2.4.5.2 Cylinders Containing Heel Quantities

The maximum heel quantities for the 30B-10 and 30B-20 cylinder are specified in table 1-4. These form the basis to determine the releasable inventory of a heels cylinder under NCT. For both cylinders, maximum heel quantities of 11.3 kg are permissible, which is equivalent to:

$$n_{\mathrm{UF_6}} = \frac{m_{\mathrm{UF_6}}}{M_{\mathrm{UF_6}}} = 32.386\ \mathrm{mol} \qquad \text{with} \quad M_{\mathrm{UF_6}} = 352\ \mathrm{g/mol}$$

Assuming that the temperature is equal to the triple point of $UF_6$ (64.1 °C) (see table 1-1) and that the gaseous $UF_6$ is an ideal gas, the pressure in the cylinder cavity is determined by:

$$p = \frac{n_{\mathrm{UF_6}} \cdot R \cdot T_{\mathrm{TP}}}{V_{\mathrm{N}}}$$

In the above equation, the free volume of the cavity under NCT is taken from table 2-29 and the gas constant is $R = 8.3143\ \mathrm{J/mole\ K}$. The resulting pressure values for the standard 30B and the 30B-X cylinder are given in table 2-31.

**Table 2-31 Pressure in the cavity for cylinders containing heel quantities**

| Item | Condition | Value | | |
|---|---|---|---|---|
| | | 30B cylinder | 30B-10 cylinder | 30B-20 cylinder |
| Pressure in the cavity in kPa | Heels | 123 | 167 | 184 |

In case of the standard 30B, the pressure in the cavity is below the gas pressure of the $UF_6$ of $p = 152\ \mathrm{kPa}$, meaning the whole content is indeed in gaseous form. For the 30B-10 and 30B-20 cylinder, the resulting pressure is above the gas pressure so that the content is partially in solid form. Nevertheless, the covering assumption is made that the whole content contributes to the releasable radioactivity. Then, using the same assumptions regarding the distribution of the radioactivity in the $UF_6$, the releasable radioactivity is in all cases:

$$R_{\mathrm{N,avail}} = 1A_2$$

The activity concentration is again determined based on the free volume of the cavity:

$$C_{\mathrm{N}} = \frac{R_{\mathrm{N,avail}}}{V_{\mathrm{N}}}$$

The resulting radioactive inventory, the derived releasable inventory, and the activity concentration in the cavity atmosphere for the 30B-X cylinder containing heel quantities are listed in table 2-30 and compared to the standard 30B cylinder.

### 2.4.6 Required Standard Helium Leakage Rates

The determination of the required standard helium leakage rates for the 30B-X cylinder is performed in the same manner as in the safety analysis of the DN30 package in [DNT 2019]. In the following subsections, the corresponding results for filled cylinders and cylinders containing heel quantities are given.

#### 2.4.6.1 Filled Cylinder

For the determination of the required helium leakage rate under NCT of a filled 30B-X cylinder, it is assumed that the pressure in the cavity is equal to the pressure $p = 152\ \mathrm{kPa}$ at the triple point of $UF_6$ (64.1 °C) (see table 1-1). Then, the allowable leakage rate of $UF_6$ is given by

$$L_{\mathrm{N,UF_6}} = \frac{(R_\mathrm{N} - P_\mathrm{N}) \cdot p_\mathrm{cav}}{C_\mathrm{N}}$$

where $R_\mathrm{N}$ is the allowable release rate under NCT defined in section 2.4.1 and $C_\mathrm{N}$ is the activity concentration in the cavity atmosphere of a filled cylinder under NCT as listed in table 2-30. The allowable release rate by permeation is $P_\mathrm{N} = 0$ because there are no elastomeric gaskets. The results are given in table 2-32.

**Table 2-32 Allowable leakage rates of $UF_6$ under NCT for filled cylinders**

| Item | Condition | Value | | |
|---|---|---|---|---|
| | | 30B cylinder | 30B-10 cylinder | 30B-20 cylinder |
| Allowable leakage rate in $\mathrm{Pa \cdot m^3/s}$ | Filled | $5.04 \cdot 10^{-3}$ | $3.23 \cdot 10^{-3}$ | $2.81 \cdot 10^{-3}$ |

The corresponding capillary diameter is determined by taking into account laminar flow and molecular flow. Since the pressure envelope of the 30B-X cylinder is identical to the standard 30B cylinder, the same leakage paths apply, and the same capillary lengths are investigated as in the safety analysis of the DN30 package in [DNT 2019]. The capillary diameter is obtained by solving the following fourth-order equation:

$$L_{\mathrm{N,UF_6}} = 0.0123 \frac{D^4}{\mu_{\mathrm{UF_6}} \cdot a} (p_\mathrm{u}^2 - p_\mathrm{d}^2) + 1.204 \frac{D^3}{a} \sqrt{\frac{T}{M_{\mathrm{UF_6}}}} (p_\mathrm{u} - p_\mathrm{d}) \qquad (12)$$

In equation (12), the following input data are used:

- Allowable leakage rate $L_{\mathrm{N,UF_6}}$ of $UF_6$ (see table 2-32)
- Viscosity of the $UF_6$ gas $\mu_{\mathrm{UF_6}} = 1.91 \cdot 10^{-3}\ \mathrm{Pa \cdot s}$ (see [DeWitt 1960])
- Molecular mass of $UF_6$ $M_{\mathrm{UF_6}} = 0.352\ \mathrm{kg/mol}$
- Capillary lengths of $a = 1 \cdot 10^{-4}\ \mathrm{m}$, $1 \cdot 10^{-3}\ \mathrm{m}$, $2 \cdot 10^{-3}\ \mathrm{m}$ and $1 \cdot 10^{-2}\ \mathrm{m}$
- Pressure in the cavity $p_\mathrm{u} = 1.52 \cdot 10^5\ \mathrm{Pa}$ (triple point of $UF_6$)
- Ambient pressure $p_\mathrm{d} = 2.5 \cdot 10^5\ \mathrm{Pa}$ according to [10 CFR Part 71] §71(b)(3)
- Gas temperate in the capillary $T = 337\ \mathrm{K}$

*Note: Values have to be used in the given units to obtain correct results by equation (12).*

The resulting capillary diameter for the 30B-X cylinder in comparison to the 30B cylinder is listed in table 2-33. Only the result for the shortest leakage path (capillary length) is given that also results in the lowest required standard helium leakage rate.

With the calculated capillary diameter, the required standard helium leakage rates under NCT can be calculated using equation (12) with the parameters of the helium leakage test:

$$L_{\mathrm{N,He}} = 0.0123 \frac{D^4}{\mu_{\mathrm{He}} \cdot a} \left(p_{\mathrm{u}}^2 - p_{\mathrm{d}}^2\right) + 1.204 \frac{D^3}{a} \sqrt{\frac{T}{M_{\mathrm{He}}}} \left(p_{\mathrm{u}} - p_{\mathrm{d}}\right) \quad (13)$$

In equation (13), the following input data are used:

- Viscosity of Helium at 298 K $\mu_{\mathrm{He}} = 19.6 \cdot 10^{-3}\ \mathrm{Pa \cdot s}$
- Molecular mass of Helium $M_{\mathrm{He}} = 0.004\,\mathrm{kg/mol}$
- Capillary diameter D in m as determined from equation (13)
- Capillary lengths of $a = 1 \cdot 10^{-4}\ \mathrm{m},\ 1 \cdot 10^{-3}\ \mathrm{m},\ 2 \cdot 10^{-3}\ \mathrm{m}$ and $1 \cdot 10^{-2}\ \mathrm{m}$
- Pressure in the cavity at standard conditions $p_{\mathrm{u}} = 1.01325 \cdot 10^5\ \mathrm{Pa}$
- Ambient pressure at standard conditions $p_{\mathrm{d}} = 0\ \mathrm{Pa}$
- Standard temperate $T = 298\ \mathrm{K}$

*Note: Values have to be used in the given units to obtain correct results by equation (13).*

The resulting required standard helium leakage rates under NCT for the 30B-X cylinder in comparison to the 30B cylinder are listed in table 2-33. Again, only the result for the shortest leakage path (capillary length) is given that results in the lowest required standard helium leakage rate.

#### 2.4.6.2 Cylinders Containing Heel Quantities

For the determination of the required helium leakage rate under NCT of a 30B-X cylinder containing heel quantities, the same approach as in section 2.4.6.1 is used. The pressure in the cavity is taken from table 2-31, resulting in the following allowable leakage rate of $UF_6$ that is identical to the standard 30B and the 30B-X cylinder:

$$L_{\mathrm{N,UF_6}} = \frac{\left(R_{\mathrm{N}} - P_{\mathrm{N}}\right) \cdot p_{\mathrm{cav}}}{C_{\mathrm{N}}} = 2.523 \cdot 10^{-5}\ \mathrm{Pa \cdot m^3/s}$$

The results given in table 2-32 are calculated with the allowable release rate $R_{\mathrm{N}}$ as defined in section 2.4.1 and with the activity concentration $C_{\mathrm{N}}$ as listed in table 2-30. The release rate by permeation is again $P_{\mathrm{N}} = 0$.

The resulting capillary diameter and required standard helium leakage rate under NCT for the 30B-X cylinder in comparison to the 30B cylinder are listed in table 2-33. Only the result for the shortest leakage path (capillary length) is listed that also results in the lowest required standard helium leakage.

### 2.4.7 Summary and Evaluation of Results

The lowest values of the required standard helium leakage rates for the 30B-X cylinder and the corresponding capillary diameters are summarized in table 2-33. As a reference, the standard 30B cylinder is listed as well.

**Table 2-33 Capillary diameter and required standard helium leakage rates under NCT**

| Item | Condition | Value | | |
|---|---|---|---|---|
| | | 30B cylinder | 30B-10 cylinder | 30B-20 cylinder |
| Capillary diameter in m | Filled | $3.92 \cdot 10^{-5}$ | $3.46 \cdot 10^{-5}$ | $3.33 \cdot 10^{-5}$ |
| | Heels | $0.94 \cdot 10^{-5}$ | $0.79 \cdot 10^{-5}$ | $0.75 \cdot 10^{-5}$ |
| Required standard helium leakage rate in $Pa \cdot m^3/s$ | Filled | $1.72 \cdot 10^{-1}$ | $1.06 \cdot 10^{-1}$ | $0.92 \cdot 10^{-1}$ |
| | Heels | $7.72 \cdot 10^{-4}$ | $4.06 \cdot 10^{-4}$ | $3.37 \cdot 10^{-4}$ |

The containment design analysis of the DN30-X package shows that the allowable release rate under NCT defined in section 2.4.1 is met for the contents specified in section 1.3. To comply with the allowable release rate under NCT, the standard helium leakage rates listed in table 2-33 are required. In all cases, these are more than a factor of 3 below the allowable leakage rate of $1.0 \cdot 10^{-4}\ \mathrm{Pa} \cdot \mathrm{m}^3/s$ that is specified in section 1.2.9 for the 30B-X cylinder.

Even after HAC, which is not to be considered for a Type AF package, the actual helium leakage rates, measured at standard 30B cylinders after the regulatory tests performed with the DN30 package, were well below $1 \cdot 10^{-6}\ \mathrm{Pa} \cdot \mathrm{m}^3/s$ (see [DNT 2019]).

## 2.5 External Dose Rates Analysis

In [DNT 2019], Appendix 2.5, a detailed analysis of the external dose rates at the DN30 package loaded with filled standard 30B cylinders as well as 30B cylinders containing heels under RCT and NCT has been performed. This analysis covers Commercial Grade and Reprocessed $UF_6$ with an enrichment up to 5 wt.-% $^{235}U$ in uranium.

The external dose rates analysis for the DN30-X package is strongly based on the analysis for the DN30 package with the following main differences:

- The internal CSS of the 30B-X cylinder is taken into account
- The analysis covers $UF_6$ grade HALEU 10 and HALEU 20
- For the 30B-X cylinder, a minimal wall thickness of 1.1 cm is considered (see table 1-13)

### 2.5.1 Objective of Verification

#### 2.5.1.1 Verification for all Types of Packages

For DN30-X packages loaded with 30B-X cylinders that are either filled with $UF_6$ complying with the compositions in table 1-2 or that contain heel quantities of $UF_6$ complying with the composition in table 1-3, it has to be verified that the limit value for RCT specified in [10 CFR Part 71] §47(a) and [49 CFR Part 173] §441(a) or [SSR-6 2018] para. 526 is not exceeded:

$$\mathrm{TI} \leq 10$$

A transport index $\mathrm{TI} \leq 10$ is equivalent to:

$$\mathrm{DL} \leq 0.1\ \frac{\mathrm{mSv}}{\mathrm{h}}$$ at a distance of 1 m from the external surface of the package

It has to be verified that the limit value for RCT specified in [10 CFR Part 71] §47(a) and [49 CFR Part 173] §441(a) or [SSR-6 2018] para. 527 is not exceeded:

$$\mathrm{DL} \leq 2\ \frac{\mathrm{mSv}}{\mathrm{h}}$$ at the surface of the package

It has to be verified that the limit values for RCT specified in [10 CFR Part 71] §47(b) or [SSR-6 2018] para. 566(b) are not exceeded:

$$\mathrm{DL} \leq 2\ \frac{\mathrm{mSv}}{\mathrm{h}}$$ at any point on the external surface of the vehicle

$$\mathrm{DL} \leq 0.1\ \frac{\mathrm{mSv}}{\mathrm{h}}$$ at any point 2 m from the vertical planes represented by the outer lateral surfaces of the vehicle, or, if the load is transported in an open vehicle, at any point 2 m from the vertical planes projected from the outer edges of the vehicle

Whenever calculations are performed for the vehicle, it is assumed that the external surface of the package coincides with the external surface of the vehicle. The package might be oriented with its longitudinal axis parallel or perpendicular to the longitudinal axis of the vehicle. In case of

parallel orientation, two adjacent packages positioned face-to-face along their symmetry axis are considered. In case of perpendicular orientation four adjacent packages positioned side-by-side are considered.

For the dose rate in 2 m distance from the vehicle, the dose rate in 2 m distance from the packages is multiplied by a factor of 1.5 derived in [DNT 2019]. This factor conservatively covers all possible arrangements of packages oriented with their longitudinal axis either parallel or perpendicular to the longitudinal axis of the vehicle.

#### 2.5.1.2 Verification for Type AF Packages

It has to be verified that, the package complies with the requirements according to [10 CFR Part 71] §43(f) and [49 CFR Part 173] §412(j) or [SSR-6 2018] para. 648(b), when submitted to the tests under NCT according to [10 CFR Part 71] §71(a)(6)-(10) and [49 CFR Part 173] §465(a)-(e) or [SSR-6 2018] para. 719-724:

$\Delta DL \leq 20\ \%$ (no significant increase in external surface radiation)

$\Delta DL$ is the increase in the maximal radiation level at any external surface of the package.

### 2.5.2 Assumptions for the Calculations

The calculations of dose rates at the DN30 package and at the vehicle are based on the assumptions listed in sections 2.5.2.1 to 2.5.2.3.

#### 2.5.2.1 Assumptions Valid for all Calculations

The following assumptions are valid for all calculations carried out throughout this chapter:

- The treated contents comply with the content description in section 1.3.
- The same maximal outer dimensions are used for the calculation model of the 30B-X cylinder as are defined for the standard 30B cylinder in [ANSI N14.1]. Conservatively, a minimal wall thickness of 1.1 cm is assumed (see table 1-13).
- Axial and radial dimensions of the 30B-X cylinder are identical under RCT and NCT.
- The skirts of the 30B-X cylinder are neglected for the considered calculation models and all 30B-X cylinders are assumed to have flat heads.
- The DN30 PSP is taken into account in the calculations.
- The CCS is considered by modelling 37 CCRs, which is an approximation for the 30B-10 and for the 30B-20 cylinder.
- For filled 30B-X cylinders, no ullage is considered so that the $UF_6$ fills whole cavity.
- For 30B-X cylinders containing heel quantities, a puddle at the bottom of the cylinder is assumed, covering all other credible arrangements of the heels (see [DNT 2019]). This also covers an arrangement with heels on the surface of the CCRs, as the distance between the heels and the surface of the DN30-X package is increased.

#### 2.5.2.2 Assumptions for Routine Conditions of Transport

As in the safety analysis of the DN30 package in [DNT 2019], a conservative density of 0.1 g/cm$^3$ is assumed for the polyisocyanurate rigid foam (PIR foam). In reality, the PIR foam used in the manufacturing of the DN30 PSP has a higher density than 0.1 g/cm$^3$.

#### 2.5.2.3 Assumptions for Normal Conditions of Transport

As in the safety analysis of the DN30 package in [DNT 2019], the following assumptions are made regarding the tests under NCT that are prescribed in [10 CFR Part 71] §71(a)(6)-(10) and [49 CFR Part 173] §465(a)-(e) or [SSR-6 2018] para. 719-724:

- Neither the shape of the $UF_6$ inside the 30B-X cylinder nor the dimensions of the 30B-X cylinder are affected by the tests.
- A maximum admissible deformation is assessed for the DN30 PSP, up to which the dose rate increase remains below the admissible limit value.

### 2.5.3 Calculation Method, its Verification and Validation

The calculation of dose rates at the DN30-X package is carried out by means of the program system SCALE 6.2.3/6.2.4 [SCALE 2020] (in [DNT 2019], SCALE 6.1 [SCALE 2011] has been used). The gamma and neutron source terms are determined by means of the depletion analysis sequence ORIGEN in the v7-27n-19g energy-group structure. The dose rates are calculated by means of the analysis sequence MAVRIC.

### 2.5.4 Gamma and Neutron Source Terms

In the safety analysis of the DN30 package in [DNT 2019], it was shown that the neutron dose rates are negligibly small and can be accounted for by multiplying the gamma dose rates by a factor of 1.05. The same applies for HALEU 10 and HALEU 20 and, thus, only the gamma source terms are given here.

#### 2.5.4.1 Gamma Source for Filled Cylinders

In the same way as in the safety analysis of the DN30 package in [DNT 2019], the gamma terms needed for subsequent dose rate calculations are determined over a period of up to 10 years. This particular period is considered because of the source intensity of $^{232}U$ and its decay products that reach their maximum within this period. Hence, arbitrary periods are covered by the analysis.

The considered nuclides as well as the contribution of their daughter nuclides are identical to the nuclides considered in [DNT 2019] and, therefore, are not repeated here. The gamma source terms for HALEU 10 and HALEU 20 are given in table 2-34.

**Table 2-34 Gamma source terms of HALEU 10 and HALEU 20 for filled cylinders**

| Energy boundaries in MeV | Gamma source term in $s^{-1}$ | | |
|---|---|---|---|
| | Enriched Commercial Grade[1)] | HALEU 10 | HALEU 10 |
| Enrichment in wt.-% $^{235}U$ in U | 5 | 10 | 20 |
| Mass of $UF_6$ in kg | 2277 | 1460 | 1271 |
| 2.000E+01 - 1.000E+01 | 1.6564E+00 | 1.0093E+00 | 7.8515E-01 |
| 1.000E+01 - 8.000E+00 | 2.2657E+01 | 1.3828E+01 | 1.0800E+01 |
| 8.000E+00 - 6.500E+00 | 1.0569E+02 | 6.4659E+01 | 5.0819E+01 |
| 6.500E+00 - 5.000E+00 | 5.4374E+02 | 3.3378E+02 | 2.6470E+02 |
| 5.000E+00 - 4.000E+00 | 1.3377E+03 | 8.2426E+02 | 6.6000E+02 |
| 4.000E+00 - 3.000E+00 | 7.5323E+03 | 9.2792E+03 | 1.5818E+04 |
| 3.000E+00 - 2.500E+00 | 4.1391E+07 | 7.9703E+07 | 1.6177E+08 |
| 2.500E+00 - 2.000E+00 | 7.0689E+04 | 4.5773E+04 | 4.1195E+04 |
| 2.000E+00 - 1.660E+00 | 1.7352E+07 | 1.0776E+07 | 8.7463E+06 |
| 1.660E+00 - 1.330E+00 | 1.8416E+07 | 1.3885E+07 | 1.5669E+07 |
| 1.330E+00 - 1.000E+00 | 1.8893E+08 | 1.1603E+08 | 9.1846E+07 |
| 1.000E+00 - 8.000E–01 | 9.4203E+07 | 6.5309E+07 | 6.5239E+07 |
| 8.000E–01 - 6.000E–01 | 2.4884E+08 | 1.6472E+08 | 1.5199E+08 |
| 6.000E–01 - 4.000E–01 | 3.5701E+08 | 2.7821E+08 | 3.2739E+08 |
| 4.000E–01 - 3.000E–01 | 3.9967E+08 | 2.5390E+08 | 2.1635E+08 |
| 3.000E–01 - 2.000E–01 | 1.0492E+09 | 9.9052E+08 | 1.4166E+09 |
| 2.000E–01 - 1.000E–01 | 6.6449E+09 | 7.4255E+09 | 1.2016E+10 |
| 1.000E–01 - 4.500E–02 | 5.6865E+09 | 4.5813E+09 | 5.6669E+09 |
| 4.500E–02 - 1.000E–02 | 3.8080E+10 | 4.4634E+10 | 7.8279E+10 |
| Total | 5.2826E+10 | 5.8614E+10 | 9.8417E+10 |

1) For information purposes only and as specified in [ASTM C996]

### 2.5.4.2 Gamma Source for Cylinders Containing Heel Quantities

For cylinders containing heel quantities, the source term is calculated as follows:

- The amount of all decay products present in a filled cylinder is calculated for a period of 10 years (this corresponds to the gamma source terms given table 2-34).
- The amount of these decay products is added to the maximum heel quantity of 11.3 kg of $UF_6$ for the 30B-X cylinder (see table 1-4).
- Then, the source term for the heels is evaluated after a very short decay time of one day as the source term decreases with time.

**Table 2-35 Gamma source terms of HALEU 10 and HALEU 20 for cylinders containing heel quantities**

| Energy boundaries in MeV | Gamma source term in $s^{-1}$ | | |
|---|---|---|---|
| | Enriched Commercial Grade[1)] | HALEU 10 | HALEU 10 |
| Enrichment in wt.-% $^{235}U$ in U | 5 | 10 | 20 |
| Mass of $UF_6$ in kg | 11.3 | 11.3 | 11.3 |
| 2.000E+01 - 1.000E+01 | 8.3138E-03 | 7.8993E-03 | 7.0779E-03 |
| 1.000E+01 - 8.000E+00 | 1.1380E-01 | 1.0837E-01 | 9.7648E-02 |
| 8.000E+00 - 6.500E+00 | 5.3144E-01 | 5.0780E-01 | 4.6142E-01 |
| 6.500E+00 - 5.000E+00 | 2.7383E+00 | 2.6294E+00 | 2.4182E+00 |
| 5.000E+00 - 4.000E+00 | 6.7482E+00 | 6.5147E+00 | 6.0688E+00 |
| 4.000E+00 - 3.000E+00 | 3.6333E+03 | 6.9629E+03 | 1.4121E+04 |
| 3.000E+00 - 2.500E+00 | 4.2267E+07 | 8.1296E+07 | 1.6514E+08 |
| 2.500E+00 - 2.000E+00 | 6.1493E+04 | 4.0084E+04 | 3.6264E+04 |
| 2.000E+00 - 1.660E+00 | 1.6875E+07 | 1.0491E+07 | 8.5377E+06 |
| 1.660E+00 - 1.330E+00 | 1.8004E+07 | 1.3687E+07 | 1.5625E+07 |
| 1.330E+00 - 1.000E+00 | 1.8364E+08 | 1.1286E+08 | 8.9478E+07 |
| 1.000E+00 - 8.000E–01 | 9.2059E+07 | 6.4168E+07 | 6.4691E+07 |
| 8.000E–01 - 6.000E–01 | 2.4241E+08 | 1.6108E+08 | 1.4974E+08 |
| 6.000E–01 - 4.000E–01 | 3.4888E+08 | 2.7419E+08 | 3.2619E+08 |
| 4.000E–01 - 3.000E–01 | 3.8290E+08 | 2.3983E+08 | 1.9835E+08 |
| 3.000E–01 - 2.000E–01 | 6.3144E+08 | 4.6818E+08 | 5.1677E+08 |
| 2.000E–01 - 1.000E–01 | 1.6526E+09 | 1.0762E+09 | 9.6075E+08 |
| 1.000E–01 - 4.500E–02 | 4.4063E+09 | 3.0031E+09 | 2.9178E+09 |
| 4.500E–02 - 1.000E–02 | 1.0946E+10 | 8.5588E+09 | 1.0130E+10 |
| Total | 1.8964E+10 | 1.4064E+10 | 1.5543E+10 |

1) For information purposes only and as specified in [ASTM C996]

## 2.5.5 Model Specification

### 2.5.5.1 Geometrical Model for the DN30-X Packaging

#### 2.5.5.1.1 30B-X Cylinder

The calculation model of the 30B-X cylinder is based on the dimensions of the standard 30B cylinder as specified in [ANSI N14.1]. Throughout the external dose rates analysis of the DN30-X package, the following conservative assumptions are made for the calculation model:

- The 30B-X cylinder is simplified to a cylinder with flat heads.
- The modeled 30B-X cylinder is compliant with the maximal dimensions specified for the standard 30B cylinder in [ANSI N14.1].

- The modeled 30B-X cylinder considers the minimal wall thickness of 1.1 cm as specified in table 1-13.
- The skirts, valve, plug and nameplate of the 30B-X cylinder are neglected.
- The CCS is modelled by 37 CCRs having a diameter of 6.03 cm and a wall thickness of 0.315 cm. The CCRs are arranged in a hexagonal pitch of 5 cm.

2.5.5.1.2 DN30 PSP

The DN30 PSP is modelled as described in the safety analysis of the DN30 package in [DNT 2019]. Consequently, neither the feet nor the six closure devices are modeled.

### 2.5.5.2 Geometrical Models for the Content

2.5.5.2.1 Filled Cylinder under RCT and NCT

The calculation model used for the filled 30B-X cylinder under RCT and NCT is a cylinder filled with $UF_6$ having no ullage. The source is homogeneously distributed within the $UF_6$.

The materials and material densities for $UF_6$, carbon steel, stainless steel and foam are the same as used in the safety analysis of the DN30 package in [DNT 2019]. Conservatively, a density of 1.2 g/cm$^2$ is assumed for the $B_4C$.

Figure 2-73 and figure 2-74 show the calculation model. The $UF_6$ is shown in red, $B_4C$ in blue, carbon steel in green, stainless steel in magenta and foam in yellow.

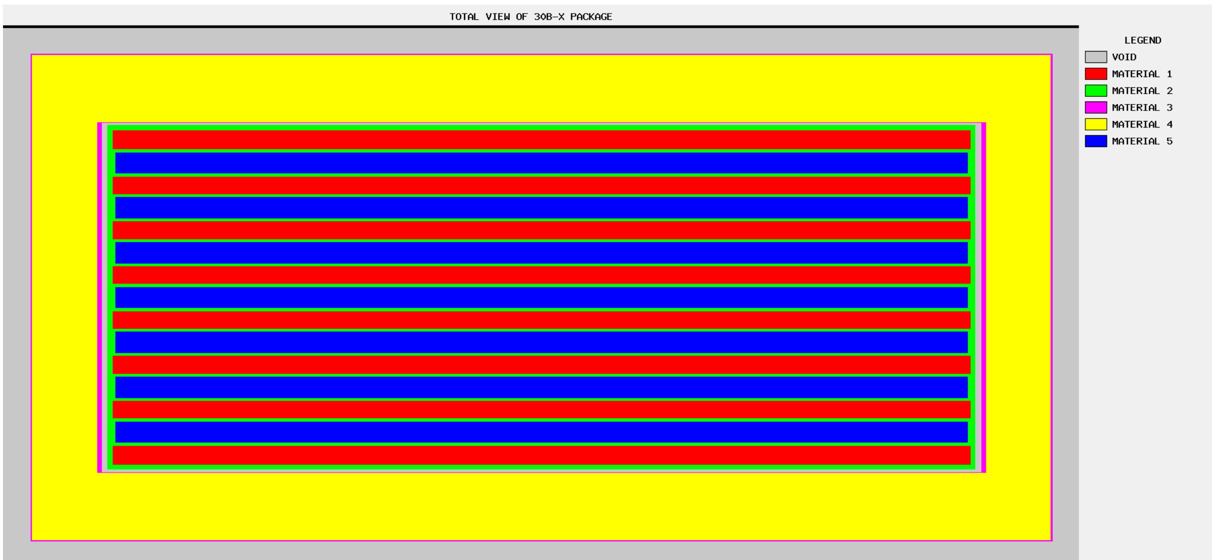


**Figure 2-73 Cross section of the calculation model along the longitudinal axis**

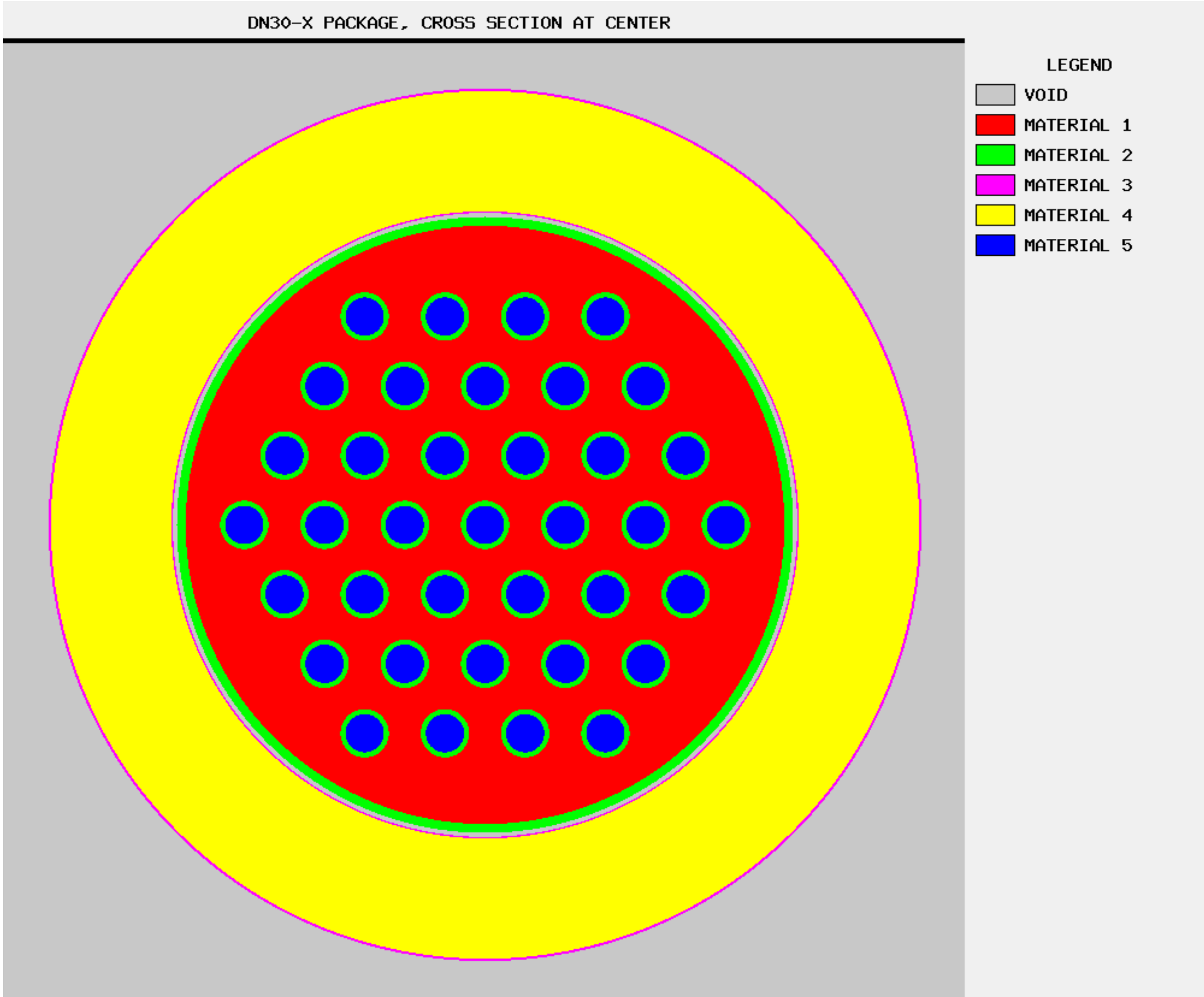


**Figure 2-74 Cross section of the calculation model perpendicular to the longitudinal axis**



#### 2.5.5.2.2 Cylinder Containing Heel Quantities under RCT and NCT

Based on the experience from the external dose rates analyses performed for the DN30 package in [DNT 2019], a calculation model with the following properties is used:

- The heels material is accumulated at the bottom of the cylinder in form of a puddle.
- The puddle is modelled with a height of 3 cm and the $UF_6$ has a density corresponding to 20 % of the density used for the filled cylinder.

### 2.5.6 Dose Rate Profiles

In order to assess the maximum dose rates at the DN30-X package, dose rate profiles are calculated showing the levels of dose rate around the package. Figure 2-75 shows the dose rate profile for the cross section along the longitudinal axis for a single DN30-20 package containing a cylinder completely filled with HALEU 20. This profile shows that the maximum radiation level is to be expected at the lateral center of the package. The axial dose rate is lower than the radial dose rate.

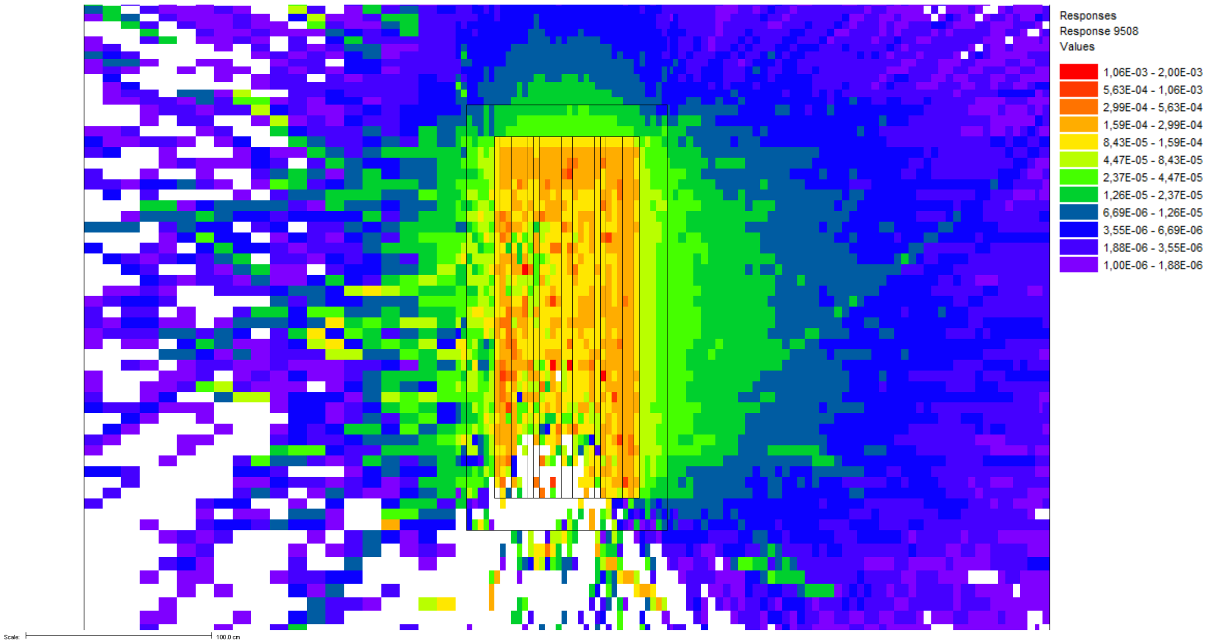


**Figure 2-75 Gamma dose rate profile – DN30-X package loaded with a 30B-X cylinder 100 % filled with HALEU 20 (cross section along the longitudinal axis)**

Figure 2-76 shows the corresponding dose rate profile for the cross section perpendicular to the longitudinal axis through the center of the DN30-X package. This figure shows that there is no influence of the CCS on the circumferential distribution of the dose rates, which are the same all around the package.

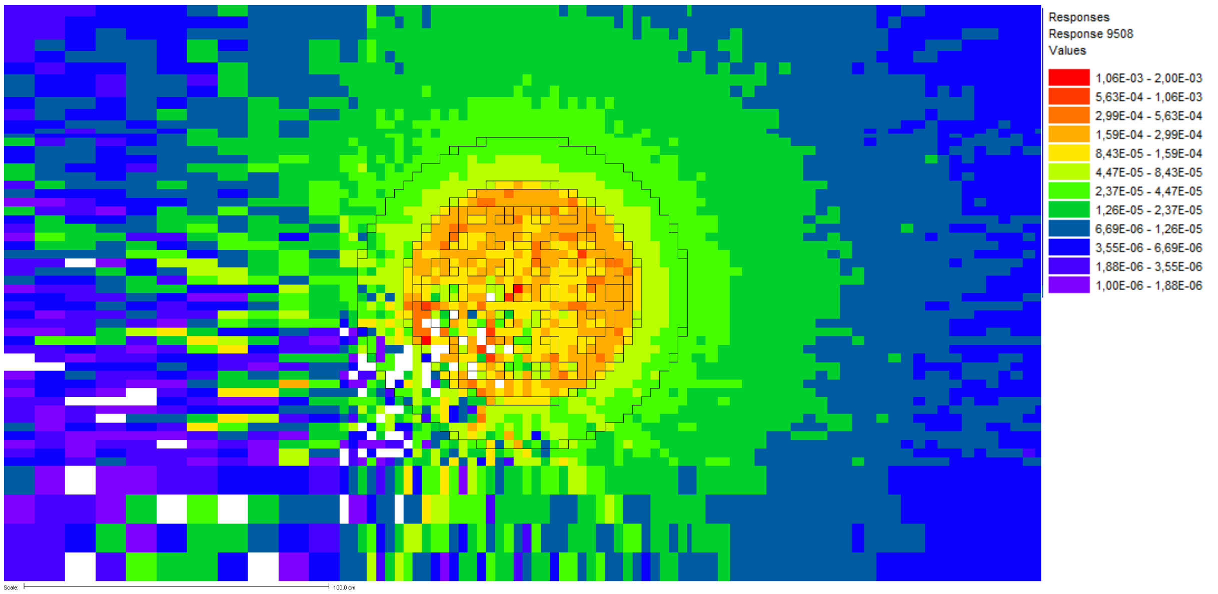


**Figure 2-76 Gamma dose rate profile – DN30-X package loaded with a 30B-X cylinder 100 % filled with HALEU 20 (cross section perpendicular to the longitudinal axis)**

### 2.5.7 Calculation of the Dose Rates

Only gamma dose rates are calculated. Based on the results of the safety analysis of the DN30 package in [DNT 2019], neutron dose rates are taken into account by multiplying the gamma dose rates with a factor of 1.05.

#### 2.5.7.1 Dose Rates for the DN30-X Package Loaded with a Filled Cylinder

For the DN30-X package loaded with a filled cylinder, dose rates were calculated by applying the gamma source terms in table 2-34. The results in radial and axial direction at the surface of the package and at distances of 1 m and 2 m from the external surface of the package are given in table 2-36.

The resulting total (gamma and neutron) dose rates are given in table 2-37. Here, for the arrangement of DN30-X packages on a trailer or flat-rack, the maximum dose rate at a distance of 2 m from the external surface of the package is multiplied by a factor of 1.5 according to [DNT 2019] to assess the dose rates at a distance of 2 m from the vehicle.

**Table 2-36 Maximal gamma dose rates under RCT – DN30-X package loaded with a 30B-X cylinder containing HALEU 10 or HALEU 20 – Results at the surface as well as at distances of 1 m and 2 m from the external surface of the package**

| Item | HALEU 10 | | | HALEU 20 | | |
|---|---|---|---|---|---|---|
| | Surface | 1 m 1) | 2 m 1) | Surface | 1 m 1) | 2 m 1) |
| Gamma dose rate in radial direction in µSv/h | 19.5 | 4.3 | 1.7 | 31.6 | 7.0 | 2.8 |
| Gamma dose rate in axial direction in µSv/h | 11.7 | 1.4 | 0.4 | 20.2 | 2.3 | 0.7 |

1) Distance measured from the external surface of the DN30-X package

**Table 2-37 Maximal total (gamma and neutron) dose rates under RCT – DN30-X package loaded with a 30B-X cylinder containing HALEU 10 or HALEU 20 – Results at the surface as well as at distances of 1 m from the external surface of the package and 2 m from the vehicle**

| Item | HALEU 10 | | | HALEU 20 | | |
|---|---|---|---|---|---|---|
| | Surface | 1 m 1) | 2 m 2) | Surface | 1 m 1) | 2 m 2) |
| Gamma dose rate in radial direction in µSv/h | 20.4 | 4.5 | 2.7 | 33.2 | 7.4 | 4.4 |
| Gamma dose rate in axial direction in µSv/h | 12.3 | 1.4 | 0.7 | 21.2 | 2.4 | 1.2 |

1) Distance measured from the external surface of the DN30-X package
2) Distance measured from the external surface of the vehicle

#### 2.5.7.2 Dose Rates for the DN30-X Package Loaded with a Cylinder Containing Heel Quantities

For the DN30-X package loaded with a cylinder containing heel quantities, dose rates are calculated by applying the gamma source terms in table 2-35. The results in radial and axial direction at the surface of the package and at distances of 1 m and 2 m from the external surface of the package are given in table 2-38.

The total (gamma and neutron) dose rates are given in table 2-39. Here, for the arrangement of DN30-X packages on a trailer or flat-rack, the maximum dose rate at a distance of 2 m from the package is multiplied by a factor of 1.5 according to [DNT 2019] to assess the dose rates at a distance of 2 m from the vehicle.

**Table 2-38 Maximal gamma dose rates under RCT – DN30-X package loaded with a 30B-X cylinder containing heel quantities of HALEU 10 or HALEU 20 – Results at the surface as well as at distances of 1 m and 2 m from the external surface of the package**

| Item | HALEU 10 | | | HALEU 20 | | |
|---|---|---|---|---|---|---|
| | Surface | 1 m 1) | 2 m 1) | Surface | 1 m 1) | 2 m 1) |
| Gamma dose rate in radial direction in µSv/h | 356 | 42.1 | 14.6 | 453 | 52.6 | 18.2 |
| Gamma dose rate in axial direction in µSv/h | 18.1 | 4.8 | 1.9 | 24.2 | 6.6 | 2.7 |

1) Distance measured from the external surface of the DN30-X package

**Table 2-39 Maximal total (gamma and neutron) dose rates under RCT – DN30-X package loaded with a 30B-X cylinder containing heel quantities of HALEU 10 or HALEU 20 – Results at the surface as well as at distances of 1 m from the external surface of the package and 2 m from the vehicle**

| Item | HALEU 10 | | | HALEU 20 | | |
|---|---|---|---|---|---|---|
| | Surface | 1 m 1) | 2 m 2) | Surface | 1 m 1) | 2 m 2) |
| Gamma dose rate in radial direction in µSv/h | 374 | 44.2 | 23.1 | 476 | 55.2 | 28.7 |
| Gamma dose rate in axial direction in µSv/h | 19.0 | 5.1 | 3.1 | 25.4 | 6.8 | 4.2 |

1) Distance measured from the external surface of the DN30-X package
2) Distance measured from the external surface of the vehicle

## 2.5.8 Verification of Compliance with Dose Rate Limits

### 2.5.8.1 Verification of the Dose Rates according to 10 CFR §71.47(a) and 49 CFR §173.441(a) or SSR-6 para. 526

The maximal total dose rates at a distance of 1 m from the surface of the DN30-X package loaded with a 30B-X cylinder filled with $UF_6$ or containing heel quantities of $UF_6$ complying with table 1-2 and table 1-3, respectively, are listed in table 2-40.

For the DN30-X package loaded with a filled 30B-X cylinder, the transport index is $\mathrm{TI} = 0.8$. Hence, the transport of the DN30-X package loaded with a 30B-X cylinder containing $UF_6$ complying with the composition in table 1-2 may be carried out under non-exclusive use.

For the DN30-X package loaded with a 30B-X cylinder containing heel quantities, the transport index is $\mathrm{TI} = 5.6$. Hence, the transport of the DN30-X package loaded with a 30B-X cylinder containing heel quantities of $UF_6$ complying with the composition in table 1-3 may be carried out under non-exclusive use.

**Table 2-40 Maximal total dose rates under RCT at a distance of 1 m from the external surface of the package – DN30-X package loaded with a 30B-X cylinder filled with HALEU 10 or HALEU 20 or containing heel quantities of HALEU 10 or HALEU 20**

| $UF_6$ composition | Total dose rate in µSv/h |
|---|---|
| HALEU 10 | 5 |
| HALEU 20 | 8 |
| Heels of HALEU 10 | 45 |
| Heels of HALEU 20 | 56 |
| Limit value (for non-exclusive use) | 100 |

### 2.5.8.2 Verification of the Dose Rates according to 10 CFR §71.47(a) and 49 CFR §173.441(a) or SSR-6 para. 527

The maximal total dose rates at the surface of the DN30-X package loaded with a 30B-X cylinder filled with $UF_6$ or containing heel quantities of $UF_6$ complying with table 1-2 and table 1-3, respectively, are listed in table 2-41. The calculated dose rates are below the limit value and, thus, the objective of verification is met.

**Table 2-41 Maximal total dose rates under RCT at the surface of the package – DN30-X package loaded with a 30B-X cylinder filled with HALEU 10 or HALEU 20 or containing heel quantities of HALEU 10 or HALEU 20**

| $UF_6$ composition | Total dose rate in µSv/h |
|---|---|
| HALEU 10 | 21 |
| HALEU 20 | 34 |
| Heels of HALEU 10 | 375 |
| Heels of HALEU 20 | 476 |
| Limit value (for non-exclusive use) | 2000 |

### 2.5.8.3 Verification of the Dose Rates according to 10 CFR §71.47(b) or SSR-6 para. 566(b)

Maximal total dose rates at the external surface of the vehicle (equivalent to the dose rate at the external package surface) loaded with DN30-X packages each loaded with a 30B-X cylinder filled with $UF_6$ or containing heel quantities of $UF_6$ are listed in table 2-42. The dose rates are below the limit of 2000 µSv/h and, thus, the objective of verification is met.

**Table 2-42 Maximal total dose rates under RCT at the external surface of a vehicle loaded with DN30-X packages each loaded with a 30B-X cylinder filled with HALEU 10 or HALEU 20 or containing heel quantities of HALEU 10 or HALEU 20**

| $UF_6$ composition | Total dose rate in µSv/h |
|---|---|
| HALEU 10 | 21 |
| HALEU 20 | 34 |
| Heels of HALEU 10 | 375 |
| Heels of HALEU 20 | 476 |
| Limit value | 2000 |

Maximal total dose rates at a distance of 2 m from the external surface of a vehicle transporting four DN30-X packages each loaded with a 30B-X cylinder filled with $UF_6$ or containing heel quantities of $UF_6$ are given in table 2-43. The dose rates are below the limit of 100 µSv/h and, thus, the objective of verification is met.

**Table 2-43 Maximal total dose rates under RCT at a distance of 2 m from the external surface of a vehicle transporting four DN30-X packages each loaded with a 30B-X cylinder filled with HALEU 10 or HALEU 20 or containing heel quantities of HALEU 10 or HALEU 20**

| $UF_6$ composition | Total dose rate in µSv/h |
|---|---|
| HALEU 10 | 3 |
| HALEU 20 | 5 |
| Heels of HALEU 10 | 24 |
| Heels of HALEU 20 | 29 |
| Limit value | 100 |

#### 2.5.8.4 Verification according to 10 CFR §71.43(f) and 49 CFR §173.412(j) or SSR-6 para. 648(b)

The increase of the dose rate after the tests simulating NCT was analyzed in the safety analysis of the DN30 package in [DNT 2019]. Even under very pessimistic assumptions, an increase of 19.7 % was determined for the dose rate at the surface of the DN30 package, which is still below the admissible limit of 20 %.

As proven by the analyses in section 2.2.6.2.5, this result also applies to the DN30-X package. This is due to both packages consisting of the same DN30 PSP as well as the 30B-X and standard 30B cylinder having the same gross weight. Hence, the deformations of the DN30 PSP under NCT are essentially identical.

### 2.5.9 Summary and Evaluation of Results

The dose rate analysis shows that the dose rate limits as listed in section 2.5.1 and prescribed in [10 CFR Part 71] and [49 CFR Part 173] or [SSR-6 2018] are met for the contents specified in table 1-2 and table 1-3.

The calculated dose rates at the DN30-X package containing filled 30B-X cylinders or 30B-X cylinders containing heel quantities are in all cases less than the dose rates limits. The assessment also covers multiple refilling of 30B-X cylinders containing heel quantities with new product.

## 2.6 Criticality Safety Analysis

The criticality safety analysis for the DN30-X package, documented in full in Appendix 2.6, covers RCT, NCT and HAC, taking into account the maximal enrichment of 10 wt.-% $^{235}U$ for the DN30-10 and 20 wt.-% $^{235}U$ for the DN30-20. It is valid for all filling ratios from $UF_6$ heels up to the maximum amount of $UF_6$ defined in section 1.3.2.1, and covers $UF_6$ containing up to 0.5 wt.-% volatile impurities (HF) and additional hydrogenated uranium residues from the reaction of humidity with $UF_6$ accumulated during the time period between recertifications.

Due to maximal $UF_6$ enrichments above 5 wt.-% $^{235}U$, the analysis has to take into account optimal moderation of the $UF_6$ for the single package. The exclusion of water inleakage allowed in [10 CFR Part 71] §55(g) or [SSR-6 2018], para. 680 (b)(i), is only applicable for packages with $UF_6$ enriched to a maximum of 5 wt.-% $^{235}U$ and cannot be credited for higher enrichments.

The drop tests for the mechanical analysis demonstrate that any damage to the cylinder valve and plug can be excluded even under HAC, so that water ingress can be excluded for the package arrays under NCT and HAC.

### 2.6.1 Objective of Proof

Criticality safety is proven according to the requirements for fissile material packages in [10 CFR Part 71] §55 or [SSR-6 2018], para. 673. For RCT, NCT and HAC the following criticality safety criterion is applied:

$$k_{\text{eff}} + 3\sigma + \Delta k \leq 0.95$$

For the proof, systematical deviations $\Delta k$ of the calculation method are taken into account. They are determined by comparison of calculation results with benchmark experiments. This analysis, summarized in section 2.6.3.2, results in a covering estimate of the systematical bias:

$\Delta k = 0.0077$ for the DN30-10

$\Delta k = 0.0070$ for the DN30-20

It is shown that the DN30-X package fulfills the criticality safety criterion, taking into account all manufacturing tolerances, credible and hypothetical conditions of the arrangement of the $UF_6$ and inleaked water in the 30B-X cylinder, as well as all deformations of the package and especially the CCS due to RCT, NCT and HAC:

### 2.6.2 Assumptions for the Proof of Criticality Safety

The proof of criticality safety for the DN30-X package is based on the assumptions detailed in sections 2.6.2.1 through 2.6.2.4.

#### 2.6.2.1 Assumptions Valid for all Calculations

The following assumptions are valid for all calculations:

- The admissible number is N = infinite (CSI = 0).
- The content is enriched $UF_6$ with an enrichment of 10 wt.-% $^{235}U$ in uranium for the DN30-10, and 20 wt.-% $^{235}U$ in uranium for the DN30-20.

- The density of $UF_6$ is conservatively assumed at a theoretical density of 5.5 g/cm$^3$ extrapolated to -40°C from given data at different temperatures (see [DNT 2019], section 6.1 of Appendix 2.2.5).
- Axial and radial dimensions of the 30B cylinder are identical under RCT, NCT and HAC.
- For the representation of the 30B cylinder in the calculation model, the skirts and the shape of the cylinder heads are taken into account.
- The valve and plug as well as the name plate are neglected in all calculation models.
- Water might penetrate arbitrarily into the foam of the PSP.

#### 2.6.2.2 Assumptions for the single package under RCT, NCT and HAC

The proof for the single package under RCT, NCT and HAC is carried out under the assumption of optimal moderation of the contents with water and a full water reflector:

- The DN30 PSP is conservatively neglected
- The 30B-X cylinder is surrounded by a 30 cm water reflector.
- Optimal moderation of the $UF_6$ contents with water is assumed.
- All deformations of the package and especially the CCS due to HAC are considered.
- Additional calculations are performed for the pessimistic assumption that the $UF_6$ contents form a heterogeneous lattice with water or transform into the uranium compound $UO_2F_2$.

#### 2.6.2.3 Assumptions for 5 x N Packages under NCT

The proof for 5 x N = infinite number of packages under NCT is covered by the proof for an infinite number of packages under HAC according to section 2.6.2.4.

#### 2.6.2.4 Assumptions for 2 x N Packages under HAC

The proof is carried out for 2 x N = infinite number of packages under HAC. The proof is based on the conditions of the packages after the tests required to demonstrate their ability to withstand HAC. Ingress of large water volumes into the cavity of the 30B-X cylinder is not assumed as the mechanical analysis shows that the integrity of the cylinder is not compromised under HAC.

- The $UF_6$ contains the maximum of 0.5 wt.-% volatile impurities (HF), as well as 11.3 kg of hydrogenated uranium residues (HUR) concentrated in a sphere.
- Moderation from water ingress due to the immersion under a head of 15 m water for 8 hours is negligible compared to the hydrogen in HF and HUR (see [DNT 2019], section 6.7 of Appendix 2.2.5).
- The 30B-X cylinder is completely filled with $UF_6$. The HUR sphere can be placed anywhere within the cylinder cavity.
- The total thickness of the DN30 PSP around the 30B-X cylinder is reduced to 10 cm in radial direction (around the mantle) and 8 cm in axial direction (on the valve/plug ends), conservatively covering all deformations due to HAC impacts.
- Additional calculations are performed for the hypothetical assumption that the PSP is completely compacted around the cylinder, taking only the steel of the shells into account.

### 2.6.3 Calculation Method, Verification and Validation

All criticality safety calculations in this document are performed by means of the sequence CSAS6 of the criticality safety code KENO VI from version 6.1.2 of the SCALE package [SCALE 2011].

All calculations use the multi-group cross section library v7-238 based on ENDB/B-VII data.

#### 2.6.3.1 Verification

The verification consists of the installation and functional verification of the SCALE 6.1.2 program system. The functional verification is carried out by the editor of the program system on the basis of the appropriate verification plan. For the individual user, the verification of the program system SCALE 6.1.2 consists of the installation verification on the basis of case studies delivered by the editor. The case studies were calculated successfully and compared with the likewise delivered reference output files. There were no differences in the output files which exceeded the range of admissible deviations mentioned in the installation guide accompanying the code package. Thus, successful installation verification is given.

#### 2.6.3.2 Validation

The calculation method (code and cross-section data) used to establish criticality safety must be validated against measured data (e.g. criticality benchmark experiments) that could be applicable to the package design characteristics. The validation process provides a basis for the reliability of the calculation method and should justify that the calculated $k_{eff}$, plus bias and uncertainties (if necessary) for the actual package conditions will ensure the compliance with the criticality safety criterion.

The ICSBEP (International Criticality Safety Benchmark Evaluation Project) [NEA 2019] contains a large number of evaluated criticality safety benchmark experiments which can be used for validation purposes. Applicable benchmarks should be selected based on their similarity to the application case. For the DN30-X package under covering assumptions, consisting of a large mass of optimally moderated $UF_6$ reflected by water and interspersed by $B_4C$ rods, there are no obviously similar benchmark experiments. Accordingly, applicable benchmarks are selected via a sensitivity analysis using the TSUNAMI module of the SCALE 6.1.2 package [SCALE 2011].

TSUNAMI provides a quantitative measure of the degree of similarity between an experiment and an application by comparing the sensitivity of $k_{eff}$ to changes in the underlying cross-section data. The degree of similarity is expressed in the correlation coefficient $c_k$. Applicable benchmarks must have a correlation coefficient of $c_k \geq 0.90$.

Investigation of several benchmark series, described in detail in section 4.2.1 of Appendix 2.6, resulted in a total of 31 applicable benchmarks for the DN30-10 and 37 applicable benchmarks for the DN30-20. The determination of the calculational bias $\Delta k$ from these benchmarks, taking into account the bias uncertainty, results in a covering estimate of $\Delta k = 0.0077$ for the DN30-10 and $\Delta k = 0.0070$ for the DN30-20.

Apart from being carefully checked with TSUNAMI sensitivity calculations, the selection of benchmark experiments covers a range of $^{235}U$ enrichments and EALF (energy of the average lethargy of fission) values that includes the values of the applications DN30-10 and DN30-20, making any extrapolation of the results unnecessary.

### 2.6.4 Material Compositions

#### 2.6.4.1 $UF_6$

For the $UF_6$, a maximal density of 5.5 g/cm³ is assumed. This conservative assumption is derived from an extrapolation of tabulated $UF_6$ density values to -40 °C and covers the density of 5.1 g/cm³ at room temperature by a large margin (see [DNT 2019], section 6.1 of Appendix 2.2.5).

##### 2.6.4.1.1 $UF_6$ impurities

In the proof for the single package, optimal moderation of the $UF_6$ with water is assumed. Accordingly, the assumption of pure $UF_6$ is covering and neither HF impurities nor hydrogenated uranium residues (HUR) need to be taken into account in the calculations.

In the proof for arrays of packages, the maximal amount of 0.5 wt.-% volatile impurities is taken into account. These are assumed as HF, using the standard material „hfacid“ in SCALE. The 5.5 g/cm³ density of $UF_6$ is used for the mixture of $UF_6$ and HF.

In addition to these volatile impurities, the moderation from hydrogenated uranium residues is taken into account with conservative assumptions based on [MILIN 2016]: The enveloping composition of HUR is $UO_2F_2$-$2H_2O$-2HF, and the mass of HUR is assumed to be equivalent to the maximal allowable heels mass of 11.3 kg. In the calculations, this compound is replaced by $UO_2F_2$-$3H_2O$ with a density of 4.317 g/cm³ (see [DNT 2019], section 6.3.3 of Appendix 2.2.5).

#### 2.6.4.2 Carbon steel (30B-X cylinder and CCS)

For the carbon steel of the 30B-X cylinder and the CCS, the standard material „carbonsteel“ of the SCALE library with a density of 7.8212 g/cm$^3$ is used.

#### 2.6.4.3 Boron carbide ($B_4C$)

The neutron absorber $B_4C$ in the CCRs is taken into account with a density of 1.2 g/cm³. This is equivalent to 88.9% of the specified $B_4C$ density of 1.35 g/cm³, and thus slightly below the maximal 90% credit applied to solid homogeneous boron-based neutron absorbers (see section 7.4.7.2 of [NUREG 2216]).

#### 2.6.4.4 Stainless steel (DN30 PSP)

For calculations where the stainless steel walls of the DN30 PSP are taken into account, the standard material „ss304“ of SCALE library with a density of 7.94 g/cm$^3$ is used.

#### 2.6.4.5 Water

For the water used as a reflector and moderator in the proof for the single package, and as interstitial moderation in the proof for package arrays, a covering density of 1.0 g/cm³ is taken into account in the calculations.

#### 2.6.4.6 $UO_2F_2$

For the single package, a comparison calculation is performed for the pessimistic assumption that $UF_6$ mixed with water will completely transform into the compound $UO_2F_2$. For this compound, the maximal theoretical density of 6.37 g/cm³ is taken into account.

### 2.6.5 Calculation Models

Since the outer cylinder shell is identical for the DN30-10 and DN30-20, and the CCS only differs in the number and distribution of CCRs, the criticality calculation models for both versions of the DN30-X are mostly identical and will be presented here together.

Section 2.6.5.1 presents the calculation model of the 30B-X cylinder itself, including the CCS. The calculation model for the single package in isolation, taking into account unlimited water moderation of the $UF_6$ content, is described in section 2.6.5.2. The calculation model for the infinite array of packages under HAC, where moderation is provided only by the HF and HUR impurities in the $UF_6$, is described in section 2.6.5.3.

#### 2.6.5.1 30B-X cylinder

For the outer parts (walls and skirts) of the 30B-X cylinder, the domed heads are modeled in an ellipsoidal shape. Both skirts are modeled straight and without any bends at their ends. The outer diameter is 76.8 cm, and the outer length is 207.5 cm over the skirts and 193.5 cm over the ends of the domed heads. Using maximal values for the diameter and the length is conservative, since it maximizes the amount of $UF_6$ in general and, more importantly, in regions not directly adjacent to the CCRs.

Valve, plug, and nameplate of the cylinder are completely neglected. The domed head at the plug end is modeled in such a way that its outer surface is in line with the end of the skirt, i.e. moved 1.3 cm outwards. This is conservative since it allows for smaller distances between the fissile contents in adjacent packages.

The wall thickness is assumed at its nominal value of 13 mm. An overview of the dimensions of the walls and skirts of the 30B-X cylinder in the calculation model is shown in Figure 2-77.

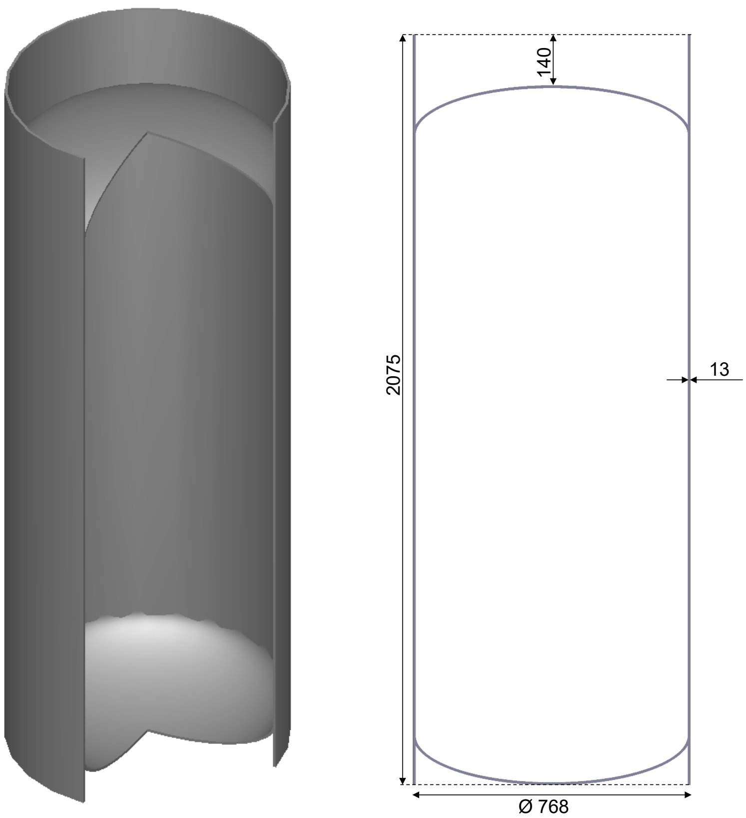


**Figure 2-77 Calculation model of the 30B-X cylinder calculation model (without CCS)**

For the CCS, the CCRs are modelled with their nominal dimensions (outer Ø 60.3 mm, wall thickness 5.5 mm, lengths see table 2-44) and positions. Manufacturing tolerances and CCS deformations under HAC are evaluated with variational calculations. The lattice holders and all other structural parts of the CCS are conservatively neglected.

The criticality calculation models for the 30B-10 and the 30B-20 are shown in Figure 2-78. The cross section along the cylinder axis shows the shortened CCRs in front of the valve and the plug.

**Table 2-44 CCR numbers, ring diameters and lengths for the 30B-10 and the 30B-20**

| CCR ring | ring radius | CCR length | number of CCRs 30B-10 | number of CCRs 30B-20 |
|---|---|---|---|---|
| central CCR | 0 cm | 185 cm | 1 | 1 |
| 1st ring | 10 cm | 183 cm | 6 | 7 |
| 2nd ring | 19 cm | 178 cm | 10 | 12 |
| 2nd ring[1)] | 19 cm | 172 cm | 2 | 2 |
| 3rd ring | 28 cm | 170 cm | 14 | 21 |

1) shortened CCRs in front of the valve / plug

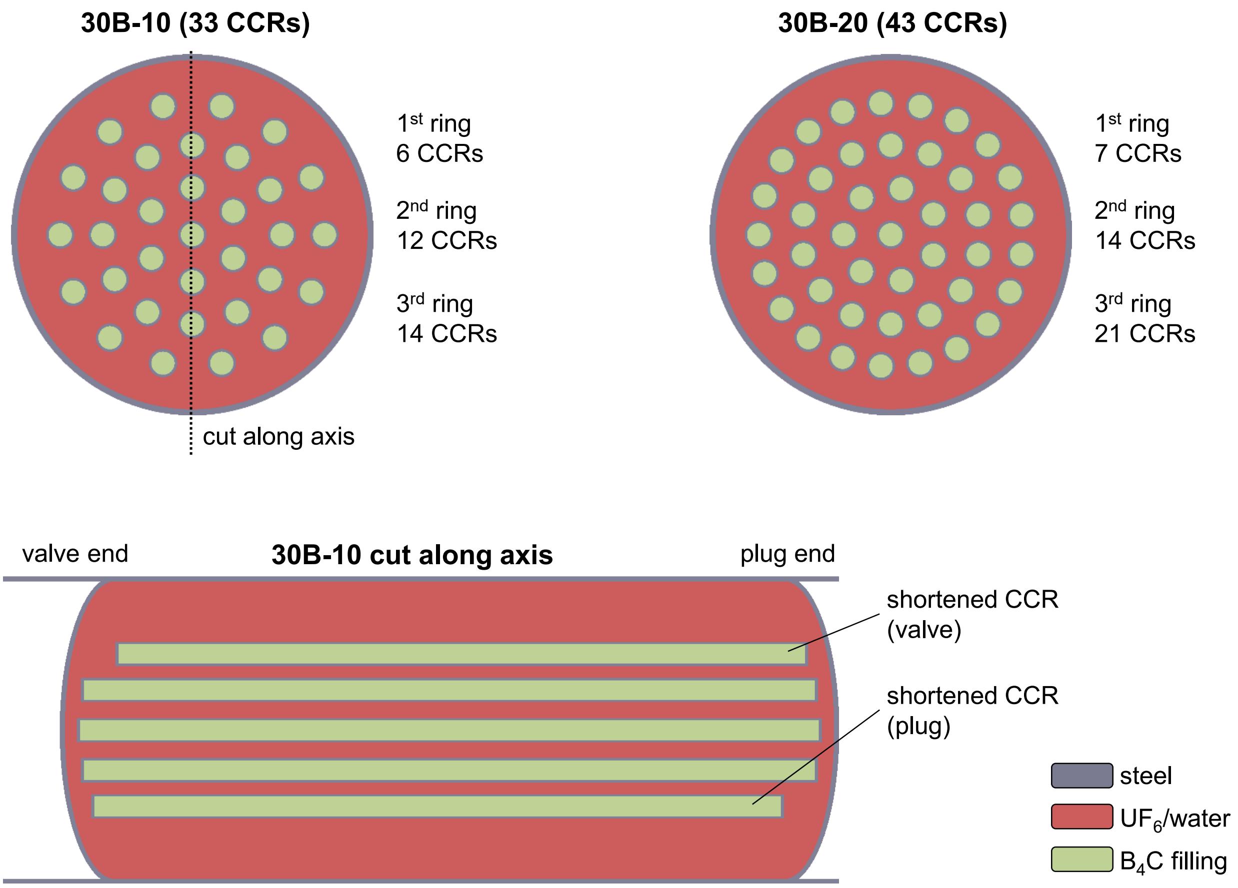


**Figure 2-78 Calculation models for the 30B-10 and 30B-20 cylinder**

### 2.6.5.2 Single package in isolation

For the single package with unlimited water moderation of the $UF_6$ content, the 30B-X cylinder is assumed to be completely filled with a mixture of $UF_6$ and water. The point of optimal moderation is determined through variation of the water/$UF_6$ ratio. The $UF_6$ fill limit is not taken into account, so that there is an overestimation of the fissile content for low amounts of water moderator.

On the outside, the 30B cylinder is surrounded by 30 cm of water reflector on all sides. The basic calculation model for the single package in isolation is shown in Figure 2-79.

Additional calculations are performed with a simplified representation of the DN30 PSP to show that the assumption of a bare 30B-X cylinder is the covering case. In this simplified representation, only the steel walls of the PSP are taken into account and assumed to be compacted around the cylinder, with a total thickness of 5 mm in radial direction and 14 mm in axial direction. The foam insulation as well as the distance between inner and outer shell is completely neglected.

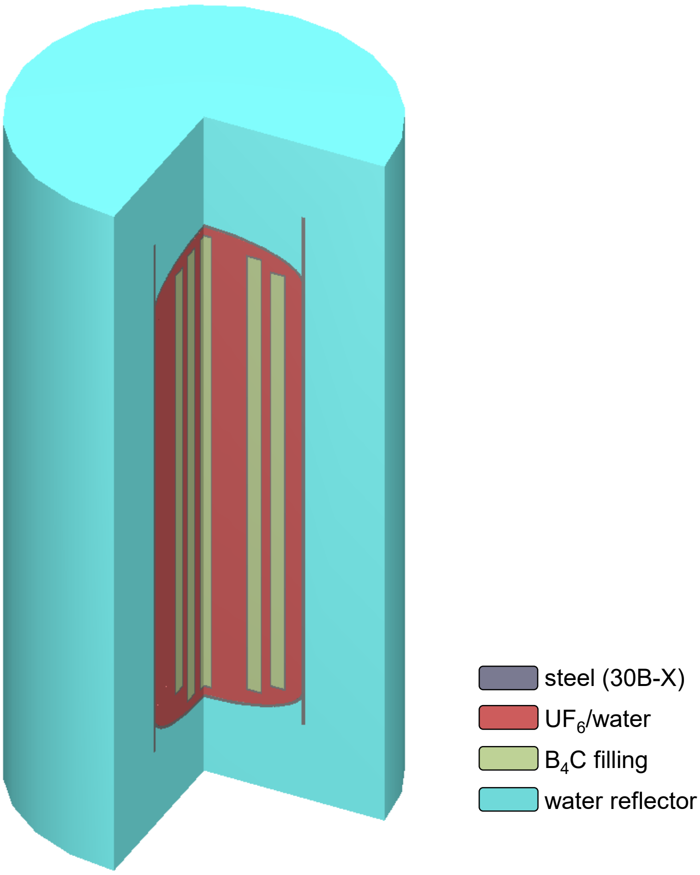


**Figure 2-79 Calculation model for the single package in isolation**

#### 2.6.5.3 Infinite array of packages

For the array of packages under HAC, an infinite three-dimensional array is achieved by enclosing the DN30-X package in a hexagonal prism with mirror reflection on all surfaces. External water moderation is investigated by adding water layers with varying thickness between packages.

The total thickness of the DN30 PSP around the 30B-X cylinder is assumed to be reduced to 10 cm in radial direction (around the mantle) and 8 cm in axial direction (on the valve/plug ends), conservatively covering all deformations due to HAC impacts. The foam material is neglected.

Moderation of the $UF_6$ is provided by the maximum of 0.5 wt.-% volatile impurities (HF), and the additional assumption of 11.3 kg HUR. Since the valve and plug retain their function under HAC, the ingressing water due to the immersion under a head of 15 m water for 8 hours only amounts to < 3 g and can be neglected.

The covering assumption for the distribution of these impurities in $UF_6$ cylinders is given in [MILIN 2016]: the HF is dispersed evenly within the $UF_6$, but the HUR is assumed to be concentrated in a sphere. To maximize the reactivity, the well-moderated HUR spheres in adjacent packages are brought closely together by placing them at the wall of the domed plug head (where the shorter skirt makes for a small distance to the next cylinder). Furthermore, the sphere is placed close to the CCR that is shortened at the plug end. The covering calculation model for a cylinder within the infinite package array is shown in Figure 2-80.

Additional calculations are performed for the assumption that the PSP is completely compacted around the 30B-X cylinder, taking only the steel material of the inner and outer shell into account.

It should be noted that even with these pessimistic assumptions regarding $UF_6$ impurities and the deformations of the DN30 PSP, the $k_{eff}$ result for the infinite array is below the result for the optimally moderated single package.

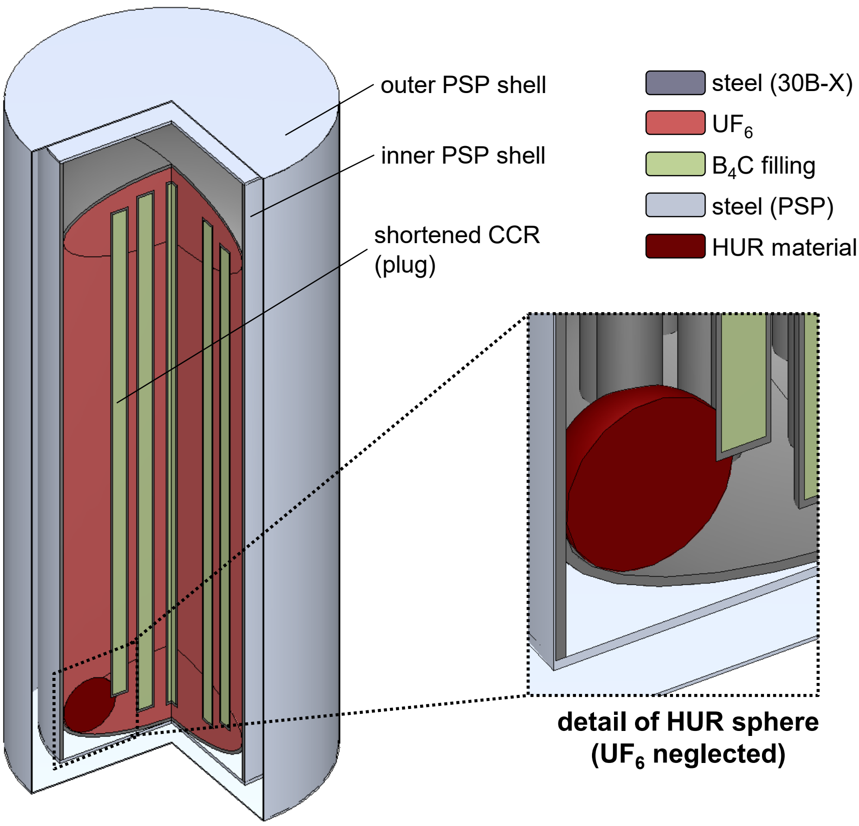


**Figure 2-80 Calculation model for the infinite package array**

### 2.6.6 Proof of Criticality Safety for the Single Package in Isolation

Safe subcriticality for the single package under all conditions of transport is proven according to [10 CFR Part 71] §55 or [SSR-6 2018], para. 682.

The covering calculation models for the DN30-10 and the DN30-20 take into account optimal moderation of the $UF_6$ contents with water, manufacturing tolerances and the deformations of the package under HAC. The most penalizing assumptions for these parameters are derived via variation calculations described in detail in chapter 7 of Appendix 2.6.

The results for the covering calculation model are:

**$k_{eff} + 3\sigma + \Delta k$ = 0.9058** for the DN30-10

**$k_{eff} + 3\sigma + \Delta k$ = 0.9130** for the DN30-20

For the covering calculation model, the criticality safety criterion is met with a large margin to the limit of safe subcriticality.

Comparison calculations with the hypothetical assumption of heterogeneous $UF_6$/water mixtures with the optimal size of the $UF_6$ particles give maximal results of:

**$k_{eff} + 3\sigma + \Delta k$ = 0.9185** for the DN30-10

**$k_{eff} + 3\sigma + \Delta k$ = 0.9192** for the DN30-20

Comparison calculations with the pessimistic assumption that the $UF_6$ contents will completely transform into the compound $UO_2F_2$ give maximal results of:

**$k_{eff} + 3\sigma + \Delta k$ = 0.9389** for the DN30-10

**$k_{eff} + 3\sigma + \Delta k$ = 0.9411** for the DN30-20

The results from these comparison calculations demonstrate that the criticality safety criterion is met even when taking into account additional pessimistic assumptions about the $UF_6$ contents.

### 2.6.7 Proof of Criticality Safety for the Infinite Array of Packages

The criticality safety proof for the array of packages under HAC according to [10 CFR Part 71] §59(a)(2) or [SSR-6 2018], para. 685 is carried out for an infinite number of packages in an infinite quadratic and hexagonal lattice with axial infinite stacking.

Since calculation assumptions under HAC are more restrictive than assumptions for NCT, the proof for the package array under NCT according to [10 CFR Part 71] §59(a)(1) or [SSR-6 2018], para. 684 is covered by the proof for the array of packages under HAC.

In addition to the most penalizing assumptions regarding manufacturing tolerances and the deformations of the package under HAC, the covering calculation model for the package array takes into account internal moderation from $UF_6$ impurities: 0.5 wt.-% volatile impurities (HF), and the additional assumption of 11.3 kg HUR. The HF is dispersed evenly within the $UF_6$, while the well-moderated HUR impurities are assumed to be concentrated in a sphere.

Optimum interspersed hydrogenous moderation is achieved with a water layer on the 30B-X cylinder with maximal water density. The optimal thickness of this water layer is derived from variation calculations presented in chapter 8 of Appendix 2.6.

With these covering assumptions, the maximal results for the array of packages are:

**$k_{eff} + 3\sigma + \Delta k = 0.7207$** for the DN30-10

**$k_{eff} + 3\sigma + \Delta k = 0.8777$** for the DN30-20

For the covering calculation model, the criticality safety criterion is met with a large margin to the limit of safe subcriticality. Especially for the DN30-10, the results are lower than for the single package in isolation.

Comparison calculations with the additional extremely pessimistic assumption of the DN30 PSP being completely compacted around the 30B-X cylinder give maximal results of:

**$k_{eff} + 3\sigma + \Delta k = 0.7731$** for the DN30-10

**$k_{eff} + 3\sigma + \Delta k = 0.9109$** for the DN30-20

The results from these comparison calculations demonstrate that the criticality safety criterion is met even when taking into account additional extremely pessimistic assumptions about the deformations of the DN30-X package under HAC.

### 2.6.8 Summary and Evaluation of Results

The criticality safety for the DN30-10 package loaded with $UF_6$ with a maximal enrichment of 10 wt.-% $^{235}U$ in uranium and the DN30-20 package loaded with $UF_6$ with a maximal enrichment of 20 wt.-% $^{235}U$ in uranium is proven in accordance with the requirements of [10 CFR Part 71] §55 and §59 or [SSR-6 2018], para. 673 under all credible considerations, including pessimistic or hypothetical assumptions about the packaging and the $UF_6$ contents:

1. Flooding with water is taken into account for the single package in isolation under all conditions of transport. There is no credit taken from [10 CFR Part 71] §55(g) or [SSR-6 2018] para. 680(b)(i).
2. For the content the most reactive arrangement in the packaging is determined. Any credible rearrangement of contents and the inleaked water in the package is taken into account in the analyses.
3. Based on results of analyses and drop tests described in the mechanical analysis, no release of contents from the package needs to be assumed.
4. Water around the package is considered in the analysis of an array of packages with variation of the water layer thickness at maximal water density.
5. Temperature changes are taken into account by assuming a conservatively high density for $UF_6$ and a theoretical maximal water density of 1 g/cm$^3$.
6. For the 30B-X cylinder, the most penalizing assumptions about manufacturing tolerances and deformations under HAC are taken into account in the analysis.
7. The DN30 PSP is completely neglected in the criticality analysis for the single package and assumed to be compacted to a thickness of 10 cm in radial direction (around the mantle) and 8 cm in axial direction (on the valve/plug ends), conservatively covering all deformations due to HAC impacts.
8. The neutron absorber $B_4C$ in the CCRs is taken into account with 88.9 % of its specified density. This is slightly below the maximal 90 % credit applicable to solid homogeneous boron-based neutron absorbers (see section 7.4.7.2 of [NUREG 2216]).

The analysis, described in detail in Appendix 2.6, covers the following arrangements:

- Single package under all conditions of transport
- Arrangement of an infinite number of packages under NCT
- Arrangement of an infinite number of packages under HAC.

The results of the analysis demonstrate that the criticality safety criterion is met with a large safety margin for the covering calculation models for the single package and the infinite array of packages.

For the single package in isolation, the analysis is extended by comparison calculations with pessimistic assumptions about the $UF_6$ contents, i.e. heterogeneous $UF_6$/water mixtures and transformation into the denser compound $UO_2F_2$.

For the infinite array of packages under HAC, the analysis is extended by comparison calculations for the hypothetical assumption of a completely compacted DN30 PSP. The results of these comparison calculations demonstrate safe subcriticality even with these additional pessimistic assumptions.

**For both the DN30-10 and the DN30-20 package, the calculated $k_{eff}$-values are in all cases lower than the value defined as objective of proof in section 2.6.1. The criticality safety requirements for the transport of a package for fissile material according to [10 CFR Part 71] §55 and §59 or [SSR-6 2018], para. 673 are fulfilled.**

# Appendix 1.1 (List of Applicable Documents)

Applicable Documents
List 0045-LST-2021-001

Proprietary Information

Not to be published

# Appendix 1.4.1A (Drawings 30B-X Cylinder)

1) "30B-10 Cylinder", Parts List 0045-STL-1000-000
2) "30B-20 Cylinder", Parts List 0045-STL-2000-000

Proprietary Information

Not to be published

# Appendix 1.4.1B (Drawings DN30 PSP)

Parts List 0023-STL-1000-000

Proprietary Information

Not to be published

## Appendix 1.7.1 (Handling Instruction)

“Use and handling of the DN30-X package”, Handling Instruction 0045-HA-2021-001

## Appendix 1.7.2 (Contamination and Dose Rate Measurements)

"Contamination and dose rate measurement at the DN30-X package", Test Instruction 0045-PA-2021-002

## Appendix 1.8 (Inspections of 30B-X Cylinders)

"Periodic inspections of the 30B-X cylinder", Test Instruction 0045-PA-2021-001

## Appendix 1.9.1 (IMS)

1) Quality Management Handbook of company Orano NCS GmbH, 2020
2) DIN EN ISO 9001
3) Confirmation on quality assurance according to nuclear standard KTA 1401
4) Confirmation of the Qualification for the development, manufacturing and operation of packagings of packages requiring approval for the transport of radioactive material

Proprietary Information

Not to be published

## Appendix 1.9.2 (Manufacturing Specification 30B-X Cylinder)

“Specification 30B-X cylinder”, Specification 0045-SPZ-2021-001

Proprietary Information

Not to be published

## Appendix 1.9.3 (Quality Assurance Program)

1) U.S. NRC Quality Assurance Program Approval #0951, Rev. 1, July 6, 2018
2) Quality Assurance Program 0023-QAP-2017-001

Proprietary Information

Not to be published

# Appendix 2.6 (Criticality Safety Analysis)

“Criticality Analysis of the DN30-X Package with 10 wt.-% or 20 wt.-% $^{235}U$”

Proprietary Information

Not to be published